MOLECULAR MECHANISMS OF TOUCH SENSORY TRANSDUCTION IN *C. elegans* : STRUCTURE/ACTIVITY RELATIONSHIPS OF DEGENERATION CHANNELS IN TOUCH PERCEPTION IN *C. elegans*

by

WEI-HSIANG LEE

A Dissertation submitted to the

Graduate School-New Brunswick

Rutgers, The State University of New Jersey and

The Graduate School of Biomedical Sciences

University of Medicine and Dentistry of New Jersey

in partial fulfillment of the requirements

for the degree of Doctor of Philosophy

Graduate Program in Neuroscience

written under the direction of

Dr. Monica Driscoll

and approved by

_____

_____

_____

_____

New Brunswick, New Jersey

[May, 2009]

ABSTRACT OF THE DISSERTATION

STRUCTURE/ACTIVITY RELATIONSHIPS OF DEGENERIN CHANNELS IN *C. elegans* TOUCH PERCEPTION

by

WEI-HSIANG LEE

Dissertation Director:

Dr. Monica Driscoll

Mechanical signaling plays an important role in cell shape and volume regulation, touch sensation, hearing, proprioception, gravitaxis, and turgor regulation. *C. elegans* provides a powerful model for elaborating mechanisms of eukaryotic mechanotransduction. Genetic screening identified candidate touch-transducing channels (DEG/ENaCs and TRP channels). In *C. elegans*, six touch neurons (ALML/R, AVM, PLML/R, PVM) are located in specific places in the body, optimized to detect forces delivered to those parts of the body. MEC-4 is expressed in six gentle touch sensory neurons. MEC-10, on the other hand, is expressed in these six neurons, as well as in two extra pairs of neurons, PVDL/R and FLPL/R. Laser ablation studies showed that the six touch neurons respond to gentle and harsh body touch and suggested that FLP and PVD neurons are responsible for the harsh touch response.

MEC-10 encodes a component of the core gentle touch sensory channel that is expressed in both gentle touch and harsh touch neurons. I studied the first *mec-10*

null mutant and showed that MEC-10 is required for both gentle and harsh touch sensation in *C. elegans* since the *mec-10* null mutant is gentle touch insensitive and reduces harsh touch responses. We also used the intracellular calcium reporter cameleon to show that responses of gentle touch neurons and PVD/FLP to touch stimuli decreased in *mec-10* null mutant. However, *mec-10* null mutation has no significant impact on proprioception and *mec-10(d)*-induced neurodegeneration. I also made *mec-4* and *mec-10* hybrid proteins by switching their extracellular and transmembrane domains and checked their function by rescuing assay. Failure to complement the touch sensation function suggested that specific sequences are required for the normal functions of *mec-4* and *mec-10*; smaller perturbation may be needed to recover protein function in chimeras.

Based on the solved MEC-4 N-terminal NMR structure prediction, I introduced point mutations into this domain and studied biological consequences in genetic rescue assays and by monitoring dominant negative effects normally seen when the N-terminal is expressed alone. I found that generally, the amino acid substitutions predicted to perturb structure disrupt channel function as predicted. The disrupted mutant strains can also exhibit a significantly decreased density of immuno-stained channel punctae distributed along touch neuron processes. However, the rescue of channel function and the dominant negative effects are not well correlated. Overall, my data advance understanding of MEC-10 and MEC-4 function on mechanosensation.

ACKNOWLEDGEMENT

I would like to thank my thesis advisor, dr. Monica Driscoll. She is always very patient and positive thinking to help me working on my projects. She always provides very useful suggestions and a good lab environment for my work. I would also like to thank my committee members, Dr. Chris Rongo, Dr. William Wadswarth, and Dr. Cathy Savage-Dunn for their suggestions on my thesis, and further thoughts for these projects. I also want to thank Dr. Laura Bianchi, Dr. Gabriel Tsechpenakis, Dr. John Everett, Dr. Montelione, and Dr. Schafer lab for their collaborations on my projects. I also need to say thank you to all current and previous members in Driscoll lab. It's very nice to work with you.

I also need to thank my parents and sisters for their supporting and encouraging me to pursue Ph.D. degree aboard. Finally, I am grateful to my friend, YuhRu. We spend the time together to work on both of our theses, and help and encourage each other.

LIST OF CONTENTS

LIST OF TABLES

LIST OF FIGURES

Introduction

Mechanosensory signaling constitutes the basis for the senses of touch, hearing and proprioception. Cellular mechanotransduction is also very important for development and homeostasis. Sensory mechanotransduction depends on specialized receptor cells to generate electrical signals in response to physical stimuli. Specialized molecules can sense the stimuli and change the permeability of the cellular membrane.

Two types of mechanosensory ion channel

There are two known ways for a membrane protein to sense mechanical stimulation. A protein might be directly mechanosensitive, and be sensitive to a stimulus that changes with mechanical pressure, like the tension of the membrane. For example, the bacterial membrane tension sensory channel MscL (mechanosensitive channels), is the only well understood mechanically-gated channel (Martinac et al., 1987; Sukharev et al., 1994; Sukharev et al., 1997). This channel is known to be directly gated by stretch of the membrane. In response to the tension conveyed via the lipid bilayer, MscL increases its open probability by several orders of magnitude.

For the other kind of channel, the open and closed conformation can be caused by changes of cell membrane bilayer thickness, tension, local curvature or direct tethering to intracellular cytoskeleton or extracellular proteins. A typical example of the second kind of channel is the model of hair cells in the hearing system

(Hudspeth, 1997). This model proposes that extracellular “tip links” connecting stereocilia tips act as external gating springs for mechanosensory channels. Two cadherins, cadherin 23 and protocadherin 15, are reported to form the tip-link filaments (Kazmierczak et al., 2007). However, the cloning of the hair cell mechanotransducing channel has been challenging due to the small number of hair cells and the low number of transduction channels. Several TRP (transient receptor potential) channels, TRPN1, TRPV4, TRPML3 and TRPA1, are thought to be candidates for this ion channel (Corey, 2006; Kwan et al., 2006). However, there is no convincing evidence for any of these candidates in hair-cell transduction yet.

Genetic analyses in *C. elegans* and *Drosophila* provided a breakthrough in understanding eukaryotic mechanotransduction by identifying candidate touch-transducing channels (DEG/ENaCs and TRP channels). The DEG/ENaC and TRP channel proteins are members of large gene families found in worms, flies, and mammals. These channels are cation-selective and insensitive to membrane voltage.

The DEG/ENaC family channels are identified by two founding member classes: the degenerins (unusual mutations affecting the *C. elegans* proteins can cause cell degeneration) and epithelial Na^+ channels in mammals. The third branch of the DEG/ENaC family is the ASIC (acid-sensitive ion channels) which are H^+-gated Na^+/Ca^{2+}-channels in vertebrate neurons. One common characteristic of the

DEG/ENaC family is that these ion channels are blocked by the diuretic amiloride. DEG/ENaCs share a common topology although only a few regions of the proteins show sequence similarity. DEG/ENaCs have short intracellular N and C termini, two membrane-spanning sequences that form the channel pore, and a large extracellular loop. The large extracellular loop of DEG/ENaCs has some cysteine-rich domains that may participate in contacts with extracellular proteins (Jasti et al., 2007; Kellenberger and Schild, 2002). In terms of secondary structure and membrane topology, but not primary sequence, the DEG/ENaC family members are similar to MscL from bacteria.

One of the well-known DEG channels is the channel in the six gentle touch neurons in *C. elegans*. Six gentle touch neurons (ALML, ALMR, AVM, PLML, PLMR, and PVM) are required for responses to gentle mechanical stimuli on anterior and posterior part of worm body (Chalfie et al., 1985). Screening for mutants that are defective in the response to the gentle stroke of an eyelash hair dragged across the body identified several *mec* (mechanosensory abnormal) genes, including *mec-4* and *mec-10* (Chalfie and Au, 1989; Chalfie and Sulston, 1981). MEC-4 and MEC-10 proved to be among founding members of the DEG/ENaC ion channel superfamily, which are co-expressed exclusively in the six gentle touch neurons (Chalfie et al., 1993; Hong and Driscoll, 1994; Mitani et al., 1993). MEC-4 and MEC-10 are postulated to constitute the heteromeric ion channel. Gating tension is thought to be applied on the channel by tethering the large extracellular MEC-4 and MEC-10 channel domains to a specialized

extracellular matrix that surrounds the touch receptor neurons and anchoring intracellular channel domains to a 15-protofilament microtubule (MT) network (Cueva et al., 2007). Candidate extracellular matrix proteins are the MEC-5 collagen and MEC-1 and MEC-9 proteins (Du et al., 1996; Emtage et al., 2004). Two other MEC proteins, MEC-7 β-tubulin and MEC-12 α-tubulin, are the components which form ~~of~~ the 15-protofilament microtubules (Fukushige et al., 1999; Savage et al., 1994). The channel contact to the cytoskeleton is thought to involve MEC-2, a stomatin-related protein that might associate with lipid rafts. The stomatin-like domain in MEC-2 can be immunoprecipitated by MEC-4 (Huang et al., 1995; Zhang et al., 2004).

mec-10 is expressed in the six gentle touch neurons and in other two pairs of neurons (PVDL, PVDR, FLPL, and FLPR). The two PVD neurons, which do not express *mec-4* but only *mec-10*, have an extensive branching pattern and covers most of the body, and also have been implicated in responses to harsh touch (Way and Chalfie, 1989). The FLP neurons have been implicated in harsh touch responses in studies in which *mec-3*, a transcription factor needed for touch-cell-specific features is lacking. *mec-3* mutants do not respond to gentle touch but do respond to harsher touches, which are delivered by pick prodding (Way and Chalfie, 1989).

In my study, I have investigated the role of MEC-10 in gentle and harsh touch sensation. Functional assay of a *mec-10* null mutant shows MEC-10 is required for harsh touch sensation in *C. elegans*.

Structure and function analysis of DEG/ENaC channels

Four ASIC genes (ASIC1-4) were identified based on their homology to DEG/ENaC channels (Waldmann et al., 1997). They show high expression in the mammalian central nervous system. AISCs are also found in the peripheral nervous system, especially in the small-diameter sensory neurons involved in pain sensation. ASIC channels are activated by a drop in extracellular pH and can generate proton-gated cation currents. However, the physiological role of ASICs remains uncertain. The expression in sensory neurons suggests a role in pain perception following tissue acidosis (Krishtal, 2003). The presence of ASICs in the brain, which lacks nociceptors, suggests that these channels have functions beyond nociception (Waldmann and Lazdunski, 1998). Recent research shows that ASICs play a critical role in Ca^{2+}-dependent neuronal injury. Acidosis of ischemia activates Ca^{2+}-permeable ASICs and induces glutamate receptor-independent Ca^{2+} overload in ischemia brain that causes neuronal injury (Xiong et al., 2004). ASIC1a knock-out mice exhibit deficits in multiple fear behaviors. Restoring ASIC1a in the amygdala of knock-out mice can only rescue context-dependent fear memory, but not all fear behaviors (Coryell et al., 2008).

The first structure of the DEG/ENaC family proteins was solved recently on chicken ASIC1 (Jasti et al., 2007). The central region of the protein including the two transmembrane domains and the extracellular domain was crystallized at low pH after the removal of 25 N-terminal and 64 C-terminal residues. The requirement of removal N- and C-termini supports our finding that transmembrane domain and intracellular N-terminal all together are not stable *in vitro*. The solved channel structure is a chalice-shaped homotrimer with dimensions 130 Å long and 85 Å wide. Detailed structure confirmed that the extracellular domain contains a bound chloride ion and ~~a~~ disulfide-rich, multidomain regions enriched in acidic residues and carboxyl-carboxylate pairs within 3 Å. Many cysteine residues in the extracellular domain are conserved throughout ASIC, DEG, ENaC, and FaNaCh proteins. The ASIC1 contains seven disulfide bonds in this region, five of them are located in a nearly straight line point to the highly conserved Trp288 residue. This structure may provide structural integrity and facilitate faithful transduction of conformational changes (Jasti et al., 2007).

John Everett solved the structure of the MEC-4's N-terminal, which had not yet been analyzed in the ASIC1 structure paper (it was removed from the crystal). I introduced dozens of mutations in the N terminal domain and analyzed the function of these proteins to test structural predictions. Gentle touch function was disturbed in many of the sites we predicted. This study supported the prediction of MEC-4 structure and may also suggest the importance of protein-protein interaction domains in this region.

Chapter I: Analysis of the Contributions of DEG/ENaC subunit MEC-10 to Mechanical Perception in Different Specialized Mechanosensory Neurons

Introduction

Mechanosensory ion channels are gated in response to mechanical stimuli (Bianchi and Driscoll, 2002; Sukharev et al., 1994). Such channels are under-studied and thus structure/function analyses on these mechanically-gated channels can provide ground-breaking insights into mechanotransduction. In this chapter, I focus on my analyses of the role of the MEC-10 DEG/ENaC in mechanical signaling in distinct neuronal types.

MEC-4 and MEC-10 are thought to be core subunits of a mechanotransducing ion channel complex in gentle touch neurons.

The nematode *C. elegans* has proved a facile model system for the identification of molecules involved in touch transduction. Wild type nematodes respond to gentle touch by moving away from the stimulus. Mutations affecting *mec-4* and *mec-10* (mechanosensory abnormal) were isolated in a screen for touch-insensitive mutants specifically defective in the response to the gentle stroke of an eyelash hair dragged across the body (Chalfie and Au, 1989; Chalfie and Sulston, 1981). MEC-4 and MEC-10 proved to be among founding members of the DEG/ENaC ion channel superfamily, which are co-expressed exclusively in the six nematode neurons that sense gentle touch (ALML/R, AVM, PLML/R, PVM) (Hong and

Driscoll, 1994; Huang and Chalfie, 1994; Mitani et al., 1993). Unlike MEC-4, MEC-10 is also expressed in two other neurons, pairs postulated to be involved in harsh touch sensation (Huang and Chalfie, 1994; Way and Chalfie, 1989). Note that lack of *mec-4* also appears to impact swimming coordination, implicating the MEC channel in proprioception (Tsechpenakis et al., 2008).

A genetic paradox regarding *mec-10* mutations.

The genetics of *mec-10* are interesting in that they are strikingly different from *mec-4* genetics. For *mec-4*, many alleles were isolated in the screen for touch-insensitive mutants (Chalfie and Au, 1989; Chalfie and Sulston, 1981). In general, these *mec-4* mutations are distributed over the coding sequence (although they are clustered in the conserved MEC-4(N) domain, in and around one CRD, and in the pore-lining domain), and there are several null alleles in the collection. By contrast, *mec-10* alleles isolated in the screen for specific gentle touch mutants are rare (listed in Table 1 below) and encode point mutations that, when present at analogous positions in other DEG/ENaCs such as *mec-4* and *unc-8*, cause a dominant-negative impact on channel activity (note that it was not known whether these mutant MEC-10 subunits actually do act as dominant-negatives for channel activity, a possibility I addressed using electrophysiological approaches and report on in this chapter).

When I began my work, there were no known *mec-10* null mutations. Why there should be so many alleles of *mec-4* (including null alleles) and so few *mec-10*

alleles (and no null alleles) seems paradoxical, and suggests that *mec-10* null mutants might either lack a phenotype for gentle touch, or might have a second phenotype (perhaps uncoordination) that would have limited the isolation of *mec-10* alleles in a screen for specific touch insensitivity. Goals of the work in this chapter were to isolate and characterize null mutants of *mec-10* to address how the lack of a MEC-10 subunit impacts gentle touch sensation, MEC-4(d)-induced neurodegeneration, and harsh touch sensation.

Position	N-terminal	C-terminal			
Allele	*e1515*	*u20*	*u390*	*u332*	*e1715*
AA change	S105F	G676R	L679R	G680E	G684R

Table 1. *mec-10* alleles.
Six mutant alleles of *mec-10* have a recessive phenotype and no detectable touch-cell morphology abnormality (Huang and Chalfie, 1994). Five *mec-10* alleles specify changes in the coding region near or in the second transmembrane domain (gray shadow marks the changes inside transmembrane domain II (Figure 3 Panel a)). S105F is defective in a highly conserved region; the identical mutation in *mec-4* eliminates *mec-4* function (Hong and Driscoll, 1994); mutations affecting this site in *unc-8* have dominant-negative effects on channel function (Shreffler et al., 1995).

MEC-4 and MEC-10 channel subunits serve different functions in gentle touch neurons.

MEC-4 and MEC-10 channel subunits are homologous, but encode distinct activities in gentle touch transduction—*mec-4* and *mec-10* alleles complement each other and over-expression of the *mec-4* gene cannot compensate for the loss of *mec-10* and *visa versa*, supporting that MEC-4 and MEC-10 are not functionally redundant in gentle touch sensation (Huang and Chalfie, 1994). MEC-4 is known to be required for the touch neurons to respond to *gentle* touch stimuli. However, a MEC-4-independent harsh touch response was found in touch neurons with the

cameleon-reported activity assay (Suzuki et al., 2003), and this response does not depend on MEC-4, so another mechanosensitive channel, gated in response to more extreme stimuli, exists in the touch neurons. Although MEC-4 appears uninvolved in harsh touch, when I began my work, it remained possible that MEC-10 might form distinct channels in gentle touch neurons that function in harsh touch sensation or might contribute to harsh touch sensation by the harsh touch sensory neurons PVD and FLP.

MEC-10 does impact the touch receptor complex implicated in gentle touch perception.

MEC-4 and MEC-10 are postulated to form a heteromeric channel that makes up the core of the mechanosensory ion channel in the six gentle touch neurons.

The model for the MEC complex:

Gating tension is thought to be applied on the channel by tethering the large extracellular MEC-4 and MEC-10 channel domains to a specialized extracellular matrix that surrounds the touch receptor neurons and anchoring intracellular channel domains to a 15-protofilament microtubule (MT) network. Candidate extracellular matrix proteins are the MEC-5 collagen and MEC-1 and MEC-9 proteins, which contain EGF and Kunitz protease inhibitor type repeats and are also expressed in, and secreted by, the touch neurons (Du et al., 1996; Emtage et al., 2004). Touch neurons are filled with unique large-diameter 15-protofilament microtubules, their distal ends are close to the cell membrane (Chalfie and

Thomson, 1982). Null mutations in either *mec-7* β-tubulin or *mec-12* α-tubulin eliminate the production of the 15-protofilament microtubules and disrupt touch sensitivity (Fukushige et al., 1999; Savage et al., 1994). Although a previous model suggested microtubules contact the channel to confer gating tension, recent immuno-EM studies do not support that the channel directly contacts microtubule ends (Cueva et al., 2007). The channel contact to intracellular proteins is proposed to involve MEC-2, a stomatin-related protein that might associate with lipid rafts. MEC-6 is a single transmembrane component need for channel function and related to paraoxanases (Goodman et al., 2002). MEC-14 and MEC-18 are possible channel regulators. MEC-14 is a protein of 453 amino acids that exhibits some similarity to aldo-keto reductases and the β-subunit of Shaker-type potassium channels. Genetic interactions between *mec* genes have suggested that *mec-14* encodes a protein that may modulate the proposed mechanosensory apparatus (Caldwell et al., 1998). Genetic analysis also showed that *mec-18* mutations enhanced the *mec-10(gof)*-induced degenerations, implying that MEC-18 might be a negative regulator of channel activity (Huang and Chalfie, 1994).

Interaction genetics of mec-10.

mec-10 mutations do show genetic interactions with other *mec* genes encoding other parts of the mechanotransducing MEC complex. Mutations in all *mec-10* alleles but *mec-10(u20)* increase the frequency of *mec-10*-induced (*mec-10(A673V)*) neuronal degeneration, while *mec-10*-induced (*mec-10(A673V)*)

neuronal degeneration is partially suppressed by alleles of *mec-2, mec-4, mec-6, mec-12, mec-14,* and *mec-15* and enhanced by mutations in *mec-18* (Huang and Chalfie, 1994). *mec-10(e1515)* and *mec-10(e1715)* also enhance the touch-insensitive phenotype of temperature-sensitive *mec-4* and *mec-5* mutants (Gu et al., 1996). Overall, the genetic data support that MEC-10 is a component of the MEC channel in gentle touch neurons, although by itself the genetic data is not definitive on this issue. Note also data from our NMR work that show that the MEC-10 N terminus can associate with the MEC-4 N terminus under NMR assay conditions, further supporting their capacity to interact in a heteromeric channel. Since in the recently published crystal structure of the mammalian neuronal ASIC1a channel there are three DEG/ENaC subunits in the channel (Jasti et al., 2007), with one subunit in a different configuration than the other two, and since some genetic data support at least two MEC-4 subunits present in the channel (Hong and Driscoll, 1994; Huang and Chalfie, 1994), we envision the MEC channel as having one MEC-10 and two MEC-4 subunits.

Electrophysiological data from channel expression in Xenopus oocytes.

Unlike MEC-4, which can assemble into homomeric channels, the MEC-10 channel subunit cannot form a channel on its own (or with MEC-2 and /or MEC-6) in *Xenopus oocytes* (Brown et al., 2007; Chelur et al., 2002; Goodman et al., 2002). MEC-10 does appear to associate with MEC-4 to form a heteromeric channel, and

modestly influences channel properties (amiloride sensitivity) as assayed in *Xenopus* oocytes (Brown et al., 2007; Goodman et al., 2002).

MEC-4(d) (A713V, the degeneration position mutation) with different sizes of bulky residues (larger than alanine), can increase the whole cell amiloride-sensitive current in *Xenopus* oocytes. This is a result of increasing single channel steady-state open probability (P_0) but not the conductance in the mutated MEC-4(d) ion channels specifying A713C, A713T, A713D, and A713V (Brown et al., 2008). Certain mutations (A713G, A713T, and A713D) also alter the affinity and voltage dependence of amiloride blockade. Mutating the *d* residue of MEC-10 to cysteine, aspartate, and valine can enhance or suppress the current of MEC-4(d) when co-expressed in oocytes. This suggests that MEC-4 and MEC-10 interact near the *d* position to regulate channel activity (Brown et al., 2007).

In general, the presence of the MEC-10 subunit seems to dampen MEC-4(d) channel currents (Goodman, 2002, Goodman, 2007; Brown et al., 2007). When I began my work, the effects of mutant *mec-10* subunits on channel activity had not been tested; I report on that study as part of this chapter.

Not all touch sensation by the gentle touch neurons is specific to the gentle touch stimuli and the MEC channel.

Using the touch neuron cameleon reporter (p_{mec-4}YC2.12) we can record the changing of intracellular calcium concentration in the gentle touch receptor neurons during mechanical stimulation (Kerr et al., 2000; Suzuki et al., 2003).

Cameleons are multidomain proteins that include YFP and CFP moieties linked by calmodulin and a calmodulin binding peptide; when Ca^{2+} binds the calmodulin domain, conformational changes allow fluorescence resonance energy transfer (FRET) between YFP and CFP such that ratios of fluorescence signals reflect intracellular Ca^{2+} changes (Miyawaki et al., 2000). Comparing the results of WT and the *mec-4* null mutant in touch neurons, we found the *mec-4* null strain (*mec-2* null strain, too) did not respond to gentle touch but did still respond to a different harsh touch stimulus. This suggests a previously unsuspected capacity for sensation of a harsher touch stimulus in touch neurons that acts without MEC-4 and MEC-2. One possibility we considered is that the harsh touch sensation might require MEC-10 activity.

Dr. Laura Bianchi also found a stretch-activated Na^{+} channel activity that is MEC-4-independent in cultured touch neurons. The only other known Na^{+} channel expressed in touch neurons is MEC-10. Possibly, the stretch channel she found in cultured neurons mediates harsh touch *in vivo* and includes MEC-10.

The two other neuronal types that express *mec-10,* PVD and FLP, have been suggested to function in harsh touch sensation.

Like *mec-10* (Huang and Chalfie, 1994), the homeo-box-containing gene *mec-3* is expressed in the gentle touch neurons and the FLP and PVD neurons (Way and Chalfie, 1989). The ultrastructure of PVDs reveals that the neuronal endings are

highly branched to send web-like structures along the body, suggestive of roles in mechano-perception (Figure 2 Panel b and c).

mec-3 is necessary for the differentiation of the six gentle touch receptors, because in the *mec-3* mutant, the touch receptors do not function and have none of their distinguishing features, such as 15-pf microtubules (Way and Chalfie, 1989). *mec-3* is also needed for PVD function: the PVD neurons no longer mediate a response to harsh mechanical stimuli in *mec-3* mutants that lack functional gentle touch receptors (Way and Chalfie, 1989). It is unclear whether FLP also mediates a response to a mechanical stimulus. *unc-86* animals, which lack FLP, respond when prodded on the pharynx, in the region of the FLP sensory process. Because a number of additional putative mechanosensory neurons exist in the head, any of these could mediate a response in the absence of FLP.

To summarize, currently *mec-10* is the only DEG/ENaC that we know is expressed in PVD and FLP, two neurons implicated in behavioral responses to harsh touch. One hypothesis I set out to test in work outlined in this chapter is whether *mec-10* is needed for FLP and PVD function in harsh touch perception.

Wondering about touch perception coding.

MEC-4 and MEC-10 are homologous. In fact, there are about two dozen *C. elegans* degenerin DEG/ENaCs and several have been implicated in touch perception and/or proprioception. Our preliminary observations suggest that these channel subunits are expressed in a range of cell types with a variety of overlap.

One working hypothesis is that these subunits come together in distinct heteromeric complexes that have different mechanical gating sensitivities—these combinations might encode perceptory range.

If gating sensitivity is encoded in part in DEG/ENaC subunits, and if MEC-4 and MEC-10 participate in channels that sense distinct forces, chimeric subunits might be used to identify functional domains critical for gentle vs. harsh touch. For this reason, I also constructed molecular hybrids having combinations of MEC-4 and MEC-10 domains and tested these for the ability to complement *mec-4* and *mec-10* mutations.

Working hypotheses on MEC-10.

Due to the lack of a null mutant, the role of MEC-10 in touch perception has not been clearly experimentally determined. The neuronal expression pattern and the somewhat unusual allele isolation statistics led us to wonder:

-Are existing *mec-10* alleles dominant-negative on MEC channel function? -What is the gentle touch phenotype of the *mec-10* null mutation? -What is the harsh touch phenotype of the *mec-10* null mutation? -Does *mec-10* impact swimming behavior? -How does *mec-10* impact cameleon-reported responses of touch neurons and PVD/FLP? -Can chimeras of *mec-4* and *mec-10* complement either *mec-4* or *mec-10* null alleles *in vivo* for gentle or harsh touch perception?

Addressing these questions probes the working hypotheses:

1) MEC-10 forms a channel without MEC-4 in touch neurons that participates in harsh touch perception. 2) MEC-10 is an essential subunit in a harsh touch-sensing channel in PVD and FLP neurons.

In sum, in this chapter I address the role of MEC-10 in gentle and harsh touch sensation.

Results

The first *mec-10* deletion allele

mec-4(null) mutants do not respond to gentle touch stimuli but do respond to harsher touch. *mec-10* is the only DEG/ENaC gene that we know of other than *mec-4* that is expressed in the six gentle touch neurons. *mec-10* is also expressed in other harsh touch neurons (PVD, FLP). Therefore, DEG/ENaC *mec-10* is proposed to play critical roles in gentle touch and harsh touch transduction, yet its actual contributions to these functions had not been clearly determined due to the lack of a *mec-10* null allele. I sought a *mec-10* deletion by PCR-based screening in EMS-induced mutant pools in our own lab and by petitioning two *C. elegans* gene knockout consortia (the *C. elegans* Gene Knockout Consortium, OK and National Bioresource Project for the Experimental Animal "Nematode *C. elegans*", Japan) to prioritize screens for *mec-10* deletions.

I first checked the *mec-10(ok1104)* from the Oklahoma knockout consortium. *mec-10(ok1104)* has a deletion from intron 4 to part of exon 16 which encodes most of the MEC-10 extracellular domain. However, this strain did not show any phenotype (touch-sensitive). After carefully checking the sequence, I found another partial deletion in this deletion strain suggesting a complex rearrangement. I recovered this sequence by using several primers inside the deletion paired with outer primers. The *mec-10* sequence after this deletion is in-frame. Furthermore, the RT-PCR product from a pair of primers also showed that a partially substituted

mec-10 mRNA is expressed (Figure 4 Panel d). Overall, my data suggests that *mec-10(ok1104)* includes a complex rearrangement of partial deletion and duplication. A functional MEC-10 protein might still be produced in the touch neurons in this mutant.

I then obtained *mec-10(tm1552)* from the Japanese knockout consortium. *mec-10(tm1552)* has a deletion of 448 basepairs (from base 1112 @ intron 4 to1559 @ exon 6, Figure 4 Panel b) that disrupts coding sequences for exon 5 and part of exon 6, which encode part of the MEC-10 extracellular domain. The deletion induces a frameshift that would create three premature stop codons close to the deletion site. Thus, the prediction is that if the *mec-10(tm1552)* allele were transcribed and translated, it would specify the first 189 MEC-10 amino acids, including the intracellular N terminus, the first transmembrane domain and extracellular residues up to amino acid 195 (last 6 amino acids are frame-shifted with a stop codon). Most of the MEC-10 extracellular domain and part of the 2nd transmembrane domain would be physically missing, as would the rest of MSDII and C-terminal residues that follow the new in-frame stop codons.

It seems that allele *tm1552* may be a functional null mutation for the following reasons: 1) We know that the transmembrane domain 2 and other sequences missing are critical to DEG/ENaC functions. 2) The *tm1522* is fully recessive, such that *tm1522*/+ has normal touch sensitivity. The N-termini of several other DEG/ENaCs exert dominant-negative effects on channel function (Hong et al., 2000). This is not true for *mec-10(tm1522)*. Although this is negative evidence, the

lack of dominant-negative activity would be consistent with the absence of demonstrable N-terminal protein product from this allele. 3) I tried to detect the remnant *mec-10* cDNA in this strain using RT-PCR with the same pair of primers mentioned above, but was unable to detect a *mec-10* transcript in the *mec-10(tm1522)* background. Previous work has shown that the *smg* genes in *C. elegans* are responsible for rapid turnover of nonsense mutant mRNAs. The *smg* system would be predicted to degrade mRNAs containing premature stop codons that could encode potentially toxic protein fragment (Pulak and Anderson, 1993). In sum, the N-terminal MEC-10 protein seems unlikely to be significantly produced in this mutant.

Gentle touch sensitivity phenotype of *mec-10(tm1552)*.

Since no candidate null mutations in *mec-10* had been isolated in screens for gentle touch-insensitive mutants, we wondered if a likely null mutation would have a gentle touch phenotype. I examined touch responses to eyelash stroke for 5 continuous times on the anterior and posterior worm bodies. Counting the total responding times and dividing by total touches gives the response ratio. I found that *mec-10(tm1552)* mutants were, in fact, gentle touch insensitive (Figure 5). The *mec-10(tm1552)/+* worms are touch sensitive, indicating that *mec-10(tm1552)* is a recessive mutation.

Harsh touch assays

A. Focus on FLP and PVD.

One of our key hypotheses is that *mec-10* contributes to harsh touch sensation by FLP and PVD. Harsh touch is difficult to execute without activating gentle touch receptors, complicating behavioral analysis. Thus, to test for MEC-10 contributions to harsh touch perception, I constructed strains that were *mec-10(tm1552) mec-4(d)* so that gentle touch receptor neurons would be absent, and harsh touch receptors would still be present but would lack MEC-10. I compared responses to posterior prodding (PVD assay) in *mec-10(tm1552) mec-4(d)* and *mec-4(d)* lines. I compared harsh touch responses to those in the *mec-3* null mutant, in which both harsh and gentle touch receptors are thought to fail to differentiate to perform either sensory function. I found that *mec-10(tm1552) mec-4(d)* exhibits significantly decreased responses to harsh touch (Figure 6). This suggests that *mec-10* does contribute to harsh touch sensation mediated by PVD.

B. Focus on touch receptor neurons defective in gentle touch sensation.

As described in the introduction, our previous work with cameleon revealed that the gentle touch receptors could respond to harsh touch when the gentle touch response was inactivated by *mec-4* or *mec-2* mutation (Suzuki et al., 2003). Since *mec-10* was expressed in harsh touch neurons, I considered the possibility that *mec-10* might contribute to harsh touch sensation in the gentle touch neurons. To

address this at the behavioral level, I compared behavioral responses to harsh touch stimuli in a *mec-4(null*) mutant strain to a *mec-10(tm1552) mec-4(null)* double mutant null strain (Figure 6). I found that the *mec-10(tm1552) mec-4(null)* shows significantly decreased responses to harsh touch. My data is consistent with the possibility that the MEC-10 channel might contribute to harsh touch sensation by specialized touch receptor neurons.

C. Analysis of swimming phenotype.

i. human observation.

We had also previously showed that the *mec-4* null mutant has a modest defect in swimming, suggesting that the gentle touch channel might also function in proprioception (Tsechpenakis et al., 2008). I therefore tested how the *mec-10(tm1552)* mutant performed in swimming assays. I manually scored the number of body bends for 30 seconds beginning one minute after animals were transferred into 50 μl of M9 buffer. Worms with gentle touch defects, such as *mec-4(u253), mec-4(d), mec-3(e1338)*, and *mec-10(e1515)* have a higher bend frequency (Figure 7). *mec-10(tm1552)* alone did not show a significant difference compared to wild type N2 worms, suggesting that *mec-10* activity is not critical for this proprioception-like property. Double mutant strains with *mec-10(tm1552)* added to the background – *mec-10(tm1552) mec-4(u253)* and *mec-10(tm1552) mec-4(d)* also show a similar bend frequency as compared with *mec-4(u253)* and *mec-4(d)*, consistent with the conclusion that MEC-10 is not centrally involved in modulating swimming behavior.

ii. Automated observation.

Human observation can only grossly quantitate bending frequency and does not allow detection of more subtle changes. Our previous automated observations indicate that the bending amplitudes, moving distance, and even the symmetry during swimming are distinctive phenotypes that show differences among mutants. Our automated tracking system helped to gain insight into these differences in body bending. Figure 8 shows the average motion and distance covered by animals in each frame. Even though most *mecs* have higher bending frequency, only *mec-3(e1338)* shows significantly higher swimming performance than wild type. Our program also analyzed animals' locomotion by extracting deformation, symmetry, and shape to better evaluate precise differences between all strains. In Figure 9, panel a shows most strains have similar magnitude of deformation from frame to frame, suggesting there are limitations in the animals' anatomy and physiology of movement. Moreover, although most tested *mecs* have similar bending frequencies, only *mec-4(u253)* has a bigger bending amplitude. *mec-4(u253); Ex[mec-4]* also has a bigger bending amplitude—so not all functions can be fully rescued by injection of wild type extrachromosomal array. *mec-10(tm1552)* does not have a higher bending frequency or larger bending amplitude than wild type, although it does show lower symmetry (Figure 9 Panel c) than other tested strains. This has also been confirmed in Figure 10 which shows that *mec-10(tm1552)* has a much higher probability of staying in the asymmetric C and O shapes as compared to wild type. Overall, my results indicate that the specific features in animals' swimming behavior are complicated and may be

genetically regulated independently from each other. To understand the whole picture we probably need to assay several representative *mec* mutants with attention to multiple parameters. My results indicate that *mec-10* mutants do exhibit some subtle locomotory differences from wild type and *mec-4* in swimming behavior. Gentle and harsh touch sensation may be two of the parameters that have influences on the swimming behavior of *C. elegans*.

Contributions of *mec-10* to *mec-4(d)*-induced necrosis

How *mec-10* contributes to *mec-4(d)* toxicity

Previous work suggested that *mec-10* point mutations did not block *mec-4(d)*-induced necrosis, suggesting that *mec-10* might not be required for hyperactivated MEC-4(d) channel activity. However, as I emphasized above, all existing *mec-10* mutations were point mutations, and thus the *mec-10 mec-4(d)* lines tested still had MEC-10 subunits in the background, even though the MEC-10 subunits were defective. These MEC-10 subunits might have been necessary to support mutant MEC-4(d) channel activity. To ask whether neurodegeneration could occur in the absence of *mec-10*, I constructed double mutant *mec-10(tm1552) mec-4(d)* by recombination (both are on the right arm of the X chromosome) and I assayed the extent of neurodegeneration in the double mutant strain. I monitored two touch neurons near the tail, the PLMs, to score cell death. I also scored newly hatched (within 4 hours) L1 worms using a high power microscope to count the vacuoles in the tail (Figure 11 Panel d). I find that *mec-4(d)*

kills touch receptor neurons to the same extent whether *mec-10* is present or not (Figure 11 Panel a). Thus, the MEC-10 DEG/ENaC subunit is not needed for the hyperactivated MEC-4(d) channel to be neurotoxic.

Contributions of *mec-10* to *mec-10(d)*-induced necrosis

If *mec-10* is engineered to encode the amino acid substitution analogous to the *mec-4(d)* A713V subunit, the MEC-10(A673V) channel (which I will refer to as *mec-10(d)*) is very weakly neurotoxic (Huang and Chalfie, 1994; Zhang et al., 2008). This engineered mutation was originally introduced into nematodes as a transgene, and was thus expressed in the presence of wild type *mec-10* subunits. What might happen to *mec-10(d)* toxicity when *mec-10* is absent? There are two possibilities. First, if *mec-10(+)* is essential for toxicity, necrosis would be eliminated in the Ex[p*mec-10(d)*] background if the *mec-10(tm1552)* allele was present. Alternatively, if MEC-10(+) normally limits the extent of neurodegeneration (possibly by limiting channel currents), neurotoxicity of the introduced *mec-10(d)* channel might increase in the *mec-10* null mutant background. To distinguish between these possibilities, I compared lines that were Ex[p*mec-10(d)*]; *mec-10(tm1552*) to Ex[p*mec-10(d)*] alone. I counted necrosis by scoring the vacuoles in the tails of newly hatched (within 4 hours) L1 worms under high power microscope (Figure 11 Panel a). We also introduced the *uIs22*[*mec-3::gfp*] (Toker et al., 2003; Wu et al., 2001) into these strains so we could also count the living PLMs at the L4 stage (Figure 11 Panel b). I find that the *mec-10(+)* gene has no influence on the necrosis induced by Ex[p*mec-10(d)*]. The

over-expressed *mec-10(d)* seems sufficient to induce necrosis on its own. This is consistent with a model in which a single MEC-10 subunit is present in the touch sensing channel.

Finally, the *mec-10(tm1552)* mutants harboring the integrated *mec-10(d)* point mutation (*bzIs75[P_{mec-4}mec-10(d)::GFP + unc-119(+) IV]*) show the minor necrosis phenotype, but they do not have a mechanosensory abnormal phenotype. This suggests that *mec-10* elimination does not enhance activity of the *mec-10(d)* channel to impact toxicity. Another possibility is that *mec-10(d)* maintains a negative effect on the channel. The double mutant strain *mec-10(tm1552);P_{mec-4}mec10(d)GFP* shows no significant difference in extent of necrosis when compared to the *mec-10(tm1552)* strain. *mec-10(tm1552);P_{mec-4}mec10(d)GFP* has a necrosis ratio similar to the *P_{mec-4}mec10(d)GFP* worms even though the latter strain has endogenous *mec-10*. Thus wild type *mec-10* is neither needed for *mec-10(d)*-induced necrosis nor does it appear to act as a negative regulator for the weak *mec-10(d)* necrosis inducer. There may be one MEC-10 subunit set channel complex.

Electrophysiology--testing for mutant MEC-10 impact on mec-4(d) channel activity

Testing whether previously existing *mec-10* alleles have dominant-negative impact on channel activity.

Five initially reported *mec-10* alleles encoded substitutions near or in the two MEC-10 transmembrane domains (1st TMD: *e1515*(S105F); 2nd TMD: *u20*(G676R), *u390*(L679R), *u332*(G680E) and *e1715*(G684R)) (Huang and Chalfie, 1994). Analogous substitutions in other *C. elegans* DEG/ENaCs had dominant-negative effects on channel activity (Hong et al., 2000; Schafer et al., 1996), and we therefore wondered if the only *mec-10* mutations that could be isolated might be those that act semi-dominantly to disrupt function of the MEC channel complexes. One approach toward addressing this is to determine the consequences of the MEC-10 substitutions on channel activity in a heterologous expression system.

To test the impact of *mec-10* mutations on MEC channel activity, I collaborated with Dr. Laura Bianchi to assay channels in the *Xenopus* oocyte heterologous expression assay. In this assay we expressed *mec-4(d)*, *mec-6* and *mec-2* cRNAs together with various *mec-10*s. Standardly, the *mec-10(d)* subunit is used in the channel assays. However the *mec-10(+)* subunit can also be used in channel assays (Brown et al., 2007; Goodman et al., 2002). Adding either *mec-10(+)* or *mec-10(d)* cRNA into the *mec-4(d)*, *mec-6* and *mec-2* cRNA combination can decrease the whole cell current. However, the wild type *mec-10* cDNA shows a more significant negative effect on this expression system.

I constructed *mec-10* cDNAs encoding *e1515*(S105F), *u20*(G676R), *u390*(L679R),

u332(G680E) and *e1715*(G684R). The *mec-10* cDNA I used as a template included a GFP tag at the C-terminus that enabled me to track the mutant proteins produced. I transcribed these *in vitro* and injected into oocytes together with *mec-4(d)*, *mec-2* and *mec-6*.

I found that all the *mec-10* mutations originally identified *in vivo* as deficient in gentle touch produced MEC-10 subunits that reduced the MEC channel conductance in oocytes (Figure 12 Panel a). In all cases, although currents are very small, the mutant MEC-10 subunits appear associated with lower currents than wild type currents. The mutant MEC-10 subunits do appear to make it to the oocyte plasma membrane, as visualized by my staining of sections of injected oocytes with GFP antibodies (Figure 5 Panel b). I conclude that mutant MEC-10 subunits corresponding to previously isolated *mec-10* point mutations can have a negative impact on MEC channel function. These data support that touch-insensitive phenotypes of *mec-10* mutations *in vivo* might result from general channel disruption.

Cameleon FRET assay provide higher sensitivity on touch sensation

The engineered genetically-encoded molecule “cameleon” is a calcium-indicator. “Cameleon” includes calmodulin with cyan fluorescent protein (CFP) and yellow fluorescent protein (YFP) linked by this calcium binding domain. When Ca^{2+} is bound, a conformational change brings CFP and YFP close enough to let fluorescence resonance energy transfer (FRET) occur (Miyawaki et al., 1997). Recording the change of absorbance ratios at different wavelengths can reflect the

change of intracellular Ca^{2+} concentration. We reasoned that cameleon could provide higher resolution information on consequence of *mec-10* elimination. I constructed strains that had the cameleon reporter. I used the *mec-4* promoter (expressed in ALMs, AVM, PLMs and PVM) and got the *egl-46* promoter (expressed in FLPs, PVDs and other neurons) strain from Dr. Shafer's lab, so that we could visualize response in touch receptor neurons and in harsh touch receptor neurons.

We had collaborators in Dr. Shafter lab perform imaging assays. With the touch-neuron-specific *mec-4* promoter in ALM, they observed the magnitude of the gentle-touch-evoked calcium influx was significantly reduced in a *mec-10(tm1552)* background, consistent with a role of MEC-10 in gentle touch perception.

In addition to the gentle body touch receptors, two other pairs of mechanosensory neurons, the FLPs and the PVDs, that also express MEC-10 were tested by using the calcium-sensitive fluorescent protein YCD3 under the control of the *egl-46* promoter. In wild type animals, FLP neurons respond to nose touch, and a robust calcium transient can be monitored in these cells in response to nose touch. In *mec-10 null* allele, partial reductions of touch-evoked calcium transient were observed. In addition to the MEC-10 protein, the TRPV channel OSM-9, is the other mechanotransduction channel expressed in the FLPs. The *osm-9 null* mutant also exhibited a significant reduction of touch-evoked calcium transients in FLPs. Moreover, the *mec-10 osm-9* double mutant allele showed virtually no

significant calcium increase in response to mechanosensory stimulation in FLPs. Thus it appears that in FLPs, MEC-10 and OSM-9 function together, possibly independently, to mediate nose touch mechanosensation. In PVD neurons, *mec-10 null,* but not *osm-9* loss-of-function animals, fail to provide detectable calcium transients after harsh touch stimulation of PVD. MEC-10 is therefore essential for harsh touch sensation in PVD. If a theme in mechanosensory transduction is that a DEG/ENaC and a TRP channel work together, a channel other than OSM-9 provides this function in PVD.

Specific domains in *mec-4* and *mec-10* that influence perception?

MEC-4 and MEC-10 channel subunits are approximately the same size and are encoded by similar genes (Figure 4 Panel a). I hypothesize that elements in the primary sequence of subunits *mec-4* and *mec-10* are critical for differences in touch sensation (harsh vs. gentle). If so, domain swap and site-directed mutagenesis may identify elements that mediate perception. I constructed chimeric MEC-4 and MEC-10 proteins by switching specific domains in MEC-4 with MEC-10's to determine the critical parts of the channel sequence. Here I made two chimeric proteins by switching the extracellular domain with the two membrane-spanning domains between MEC-4 and MEC-10. DNA sequences were cut and re-ligated after the two transmembrane domains, which are very conserved in these two proteins (Figure 13). In other words, chimeras differ in two transmembrane domains and extracellular domain, intracellular domains was kept as a unit. Microinjection of the constructs into *mec-4(null)* and *mec-10(null)*

backgrounds was followed by testing for the restoration of gentle touch sensation in each. *mec-4* and *mec-10* wild type DNA were also injected into null strains as a positive control. A hybrid MEC-10 protein with GFP at the C-terminal was used to make the chimeras, so chimeras with intracellular (N- and C-terminals) MEC-10 domains could be tracked by GFP expression. GFP images in Figure 14 panel b indicate that MEC-10longGFP and chimeras can be expressed in touch cells.

My results from the gentle touch assay (Figure 14 Panel a) show that neither of the chimeras can totally restore the gentle touch sensory function of mutant touch neurons. MEC-4 deficiency cannot be complemented at all; on the other hand MEC-10 deletion can be partially complemented by the chimera with the *mec-4extra/mec-10intra* variant to a degree better than the *mec-4intra/mec-10extra*. Thus, MEC-10's critical function in touch sensation may be conferred by the transmembrane and intracellular domains. However, the weakness of the complementation suggests both extracellular and intracellular components are required for normal function.

In general, MEC-4/MEC-10 chimeras introduced into the *mec-10(tm1552)* background did not show significant differences in swimming. Only m*ec-4(u253); Ex[mec-4extra+mec-10intra]* has a bending frequency close to N2's. Possibly, the *mec-4* extracellular domain is important for the role of regulating body bend rate during swimming.

Discussion

The null phenotype of *mec-10*

MEC-10 and MEC-4 are thought to be core proteins of a mechanosensory ion channel in *C. elegans*. *mec-10* and *mec-4* genes were found by screening for a defect in sensing a gentle touch stimulus. However, the numbers of mutations found in these two genes were very different. The *mec-4* mutations are basically distributed over the coding sequence, and there are also several null alleles. By contrast, *mec-10* alleles isolated in the screen for specific gentle touch mutants are rare, and they are all point mutations; no *mec-10* null allele was found during the extensive screen. This raised the question as to whether the *mec-10* null mutant might not have a touch-insensitive phenotype.

mec-10(null) is gentle touch insensitive.

mec-10(tm1552) is the first null allele to be generated and characterized. My work showed that this allele is a recessive mutation. Because the *mec-10(tm1552)* mutation disrupts the C-terminal domains of the MEC-10 subunit and because I did not detect *mec-10* mRNA in this strain, *mec-10(tm1552)* may be a functional null. It appears then, that a true MEC-10 deficiency is touch-insensitive. This leaves a mystery about the few *mec-10* mutations identified in screens. The touch sensitivity in the deletion mutant is not hard to assay – thus it is not clear why more alleles of *mec-10*, including those that are null, were not found. Possibly this was a chance fluctuation.

mec-10 impacts harsh touch sensation.

The double mutant *mec-10(tm1552) mec-4(u253)* and *mec-10(tm1552) mec-4(d)* strains also show significantly decreased harsh touch response ratios. The gentle and harsh touch assays indicate that MEC-10 is essential for gentle and harsh touch sensation. MEC-10 might act in the gentle touch neurons to confer this phenotype. Preliminary data on cameleon-reported responses in FLPs and PVDs support a role in those touch sensors (see below) as does genetic testing in the *mec-10(tm1552) mec-4(d)* mutant which lacks gentle touch neurons.

mec-10 and touch receptor neurodegeneration

We also made an engineered *mec-10(d)* gene and integrated into a strain and measured touch neuron degeneration. *mec-10(d)* alone can induce a weak degeneration phenotype (Huang and Chalfie, 1994; Zhang et al., 2008). How does *mec-10* influence *mec-4(d)* degeneration? Although MEC-10(d) can decrease the whole cell current of the MEC-4(d) ion channel in oocytes, we do not see any significant degeneration rate changes when I introduced *mec-10(d)* or *mec-10(0)* into a *mec-4(d)* strain. Thus, *mec-4(d)* is a necrosis inducer strong enough on its own that no enhancement can be detected and *mec-10* status does not change the potency for death. *mec-4(d)* channels that are homomeric must be able to efficiently induce death. The presence of endogenous *mec-10* also did not alter the level of degeneration induced by *mec-10(d)*. Thus the MEC-10(d) channels can be homomeric and lack MEC-10(+) to still induce neurodegeneration.

mec-10 impacts swimming behavior in a subtle way

We also developed a new assay to monitor the swimming behavior changes in *mec* worms. Our results show that the gentle and harsh touch MEC channel might also function in proprioception. The basic concept is to score the number of body bends in a certain period of time. This can be done easily manually. However, this level of analysis is not enough to show all the features of swimming behavior that may be influenced by mechanosensory neurons. Our system also monitored the amplification, shape, and symmetry of body bends. Worms with gentle touch defects (*mec-4(null)* for example) show increased body bending number. The differences between control and mutant strains vary according to mutants studied. *mec-10(tm1552)* and double mutants containing *mec-10(tm1552)* do not show any difference from wild type. This result suggests that *mec-10* does not influence the swimming frequency although *mec-4* does. We also monitored the shape and symmetry of each body bend. *mec-10(tm1552)* shows the highest ratio of animals appearing in the C and O shapes. The low symmetry score for *mec-10(tm1552)* also confirmed this. These results suggest *mec-10* has a subtle impact on swimming and proprioception. I also found that *mec-10(0) mec-4(0)* did not change swimming frequency (compared to *mec-4(0)*), suggesting harsh touch disruption does not have a major impact on swimming frequency.

mec-3(e1338), the mutant that lacks differentiated touch neurons, has a significantly higher body bend frequency than all other *mec* strains. Since *mec-3*

worms without good touch neuron functions have higher body bend frequency than other *mecs*, additional factors other than the gentle touch channel may contribute to swimming impact via touch neurons. The *mec-3* differences are also comparable from the computerized analyses; *mec-3(1338)* exhibits a larger moving distance than most strains.

MEC-10 influences calcium transients in gentle and harsh touch neurons

Cameleon-integrated *mec-10* strains that I constructed were tested and imaged by our collaborator Dr. Schafer's lab. With a touch-neuron-specific promoter in ALM, they observed the magnitude of the touch-evoked calcium influx was significantly reduced in a *mec-10(tm1552)* background, consistent with a role of MEC-10 in gentle touch perception. Note that this is different from *mec-4 null* which eliminates the calcium transient (Bianchi et al., 2004). In addition to the gentle body touch receptors, two other pairs of mechanosensory neurons, the FLPs and the PVDs, express MEC-10. The calcium indicator YCD3 under the control of the *egl-46* promoter is expressed in both FLP and PVD neurons. FLP neurons respond to nose touch. In *mec-10* null and *mec-10 osm-9* double mutant alleles, partial and total reductions of touch-evoked calcium transient were observed. In PVD neurons, *mec-10 null* but not *osm-9* loss-of-function animals, showed no detectable calcium transients after harsh touch stimulation of PVD. Thus it appears that in FLPs, MEC-10 and OSM-9 function together to mediate nose touch mechanosensation. MEC-10 is essential for harsh touch sensation in PVD. (A paper reporting this data

was reviewed at *Neuron*, and we are currently revising the paper for resubmission. See appendix I).

MEC-10 mutant subunits do interfere with channel activity in oocyte expression systems

mec-4(d) is a degeneration-inducing mutation found from screening procedures. MEC-4(d) (A713V) with a bulky residue (larger than alanine) can increase the whole-cell amiloride-sensitive current in *Xenopus* oocytes. I found that expressing the mutant MEC-10 subunits that correspond to genetically isolated amino acid changes with MEC-4(d) in oocytes inhibits the current more than the wild type MEC-10 or the MEC-10(d) subunits. The mutant MEC-10 subunits do have somewhat of a negative impact on channel conductance, and they do appear to make it to the oocyte plasma membrane, as visualized by my staining of sections of injected oocytes with GFP antibodies. This suggests that touch-insensitive phenotypes *in vivo* for these *mec-10* alleles might result from general channel disruption.

Small perturbations impair MEC-4 and MEC-10 functions

MEC-4 and MEC-10 are encoded by similar genes. I hypothesized that elements in the primary sequence of subunits *mec-4* and *mec-10* are critical for differences in touch sensation (harsh vs. gentle). Here I made two chimeric proteins by switching the extracellular domain and the two transmembrane domains, which are very conserved in these two proteins, from the intracellular domains. A rescuing assay

in *mec-4(null)* and *mec-10(null)* background strains showed partial function restored only in *mec-10(null)* strains, MEC-4 deficiency cannot be complemented at all. The *mec-4extra/mec-10intra* variant can complement a little better than the *mec-4intra/mec-10extra*. Thus, MEC-10's critical function in touch sensation may be conferred by the intracellular domains. I also tested the swimming function on these chimeras. In general, MEC-4/MEC-10 chimeras introduced into the *mec-10(tm1552)* background did not show significant differences in swimming. Only *mec-4(u253); Ex[mec-4extra+mec-10intra]* has a bending frequency close to N2's. Possibly, the *mec-4* extracellular domain is important for the role in regulating body bend rate during swimming. Overall, the chimeras cannot function as well as the normal proteins. My results indicate that even though MEC-4 and MEC-10 have very similar structures, functions of the proteins can be impaired by small perturbations. Smaller modifications might increase the chance to maintain the overall function of the chimeras. The extracellular domains of MEC-4 and MEC-10 have some small specific domains. Chimeras that only switch one or some of these domains should be a good approach in the future to reveal more about structure/function.

My results indicate that MEC-10 contributes the function of gentle touch and is required for harsh touch in FLPs and PVDs. MEC-10 also plays a role in proprioception. More detailed studies in the furture, including electrophysiology and genetics may add details to understanding of how MEC-10 executes those functions. Some genetics that remain for the future: Does the MEC-4/MEC-10

channel have a Trp channel partner for gentle touch? Does the FLP channel use another Degenerin for harsh touch sensation? Does the PVD MEC-10 channel use another DEG/ENaC channel? Do MEC-2 + MEC-6 act in other touch sensing channels? What are the structural elements of the primary sequence that code the range of stimuli that gate the channels?

Chapter II: Structure and function of MEC-4

Introduction

Electrophysiological studies have suggested that mechanosensory ion channels are gated in response to mechanical stimuli to initiate a cellular response (Bianchi and Driscoll, 2002; Sukharev et al., 1994). A key goal in the area of mechanotransduction is to elaborate the structure/function relationships of mechanically gated ion channels. My work presented in this chapter has focused on structure/function of MEC-4, a touch-transducing, mechanosensitive ion channel.

MEC-4 and MEC-10 are core subunits of a mechanotransducing ion channel complex.

The nematode *C. elegans* has proved a facile model system for the identification of molecules involved in touch transduction. Wild type nematodes respond to gentle touch by moving away from the stimulus. Mutations affecting *mec-4* and *mec-10* (mechanosensory abnormal) were isolated in a screen for touch-insensitive mutants specifically defective in the response to the gentle stroke of an eyelash hair dragged across the body (Chalfie and Au, 1989; Chalfie and Sulston, 1981). MEC-4 and MEC-10 proved to be among founding members of the DEG/ENaC ion channel superfamily, which are co-expressed exclusively in the six nematode neurons that sense gentle touch (ALML/R, AVM, PLML/R, PVM) (Chalfie et al., 1993; Hong and Driscoll, 1994; Mitani et al., 1993). All members of the DEG/ENaC

superfamily have two membrane-spanning domains and an extracellular region with Cysteine-rich domains (CRDs, the most conserved is designated CRD3) situated between the transmembrane segments. N- and C-termini project into the intracellular cytoplasm, whereas most of the protein, including the CRDs, is extracellular.

MEC-4 and MEC-10 form a heteromeric channel postulated to constitute the core of the long-sought mechanosensory ion channel. Gating tension is thought to be applied on the channel by tethering the large extracellular MEC-4 and MEC-10 channel domains to a specialized extracellular matrix that surrounds the touch receptor neurons and anchoring intracellular channel domains to a 15-protofilament microtubule (MT) network. Alternative models that rely more on extracellular tethering and membrane interaction have been suggested (Chalfie, 2009). Candidate extracellular matrix proteins are the MEC-5 collagen and MEC-1 and MEC-9 proteins, which contain EGF and Kunitz protease inhibitor type repeats and are also expressed in, and secreted by, the touch neurons (Du et al., 1996; Emtage et al., 2004). Null mutations in either *mec-7* β-tubulin or *mec-12* α-tubulin eliminate the production of the 15-protofilament microtubules and disrupt touch sensitivity (Fukushige et al., 1999; Savage et al., 1994).

The channel contact to the cytoskeleton is thought to involve MEC-2, a prohibitin (PHB)-domain protein. MEC-2 and Podocin, a similar protein from the mammalian kidney, bind to cholesterol and affect the lipid environment of the channel. This

binding requires the PHB domain and increases the activity of DEG/ENaC (for MEC-2) and TRPC (for podocin) ion channel (Brown et al., 2008; Huber et al., 2006). MEC-2 was previously referred as a stomatin-related protein. The newly defined PHB domain (AA 139-300) and the old stomatin-like domain (AA 114-363) are basically referred to the same domain. The central MEC-2 domain (AA 114-363) includes a hydrophobic domain and a cytoplasmic hydrophilic domain, that together exhibit 65% identity to human red blood cell protein stomatin. This stomatin-like domain can be immunoprecipitated by MEC-4. *lacZ* fusion proteins with at least 118 amino acids of MEC-2 produce β-galactosidase activity in both cell bodies and the processes of the six touch cells. The fusion protein with only 42 N-terminal amino acids exhibits staining in cell bodies only (Huang et al., 1995; Zhang et al., 2004). This suggests that a MEC-2 N-terminal region (including AA 42-118) is sufficient for the proper localization of MEC-2. Moreover, the GST-MEC-4(1-108) can pull down full-length MEC-2 and the MEC-2(88-375) stomatin-like region (Zhang et al., 2004). The MEC-2 stomatin-like domain includes a hydrophobic region thought to be situated in the membrane in a hairpin configuration such that most of the protein faces the cytoplasm. This suggests that MEC-2 is more likely to interact with the cytoplasmic and/or membrane spanning regions of MEC-4. GFP-labeled MEC-4 puncta form along the process in the absence of MEC-2, so MEC-2 does not initiate or drive channel complex assembly (MEC-4, MEC-10 and MEC-6) at sites along the neuronal process. However, the MEC-2 punctate pattern does require other proteins of the degenerin complex (MEC-4, MEC-10 and MEC-6), suggesting that MEC-2 may be recruited late in the

formation of the channel complex (Zhang et al., 2004). Co-expression of MEC-2 with MEC-4 and MEC-10 in *Xenpopus* oocytes has demonstrated that MEC-2 can increase the permeability of the mechanosensory ion channel (MEC-4(d) and MEC-10) ~ten-fold (Goodman et al., 2002). For this reason, MEC-2 appears to be a direct contributor to MEC channel function.

In vivo structure/function on MEC-4

a. Conserved regions are important for function.

EMS-induced MEC-4 mutations were identified at high frequency in screens for touch-insensitive mutants (Chalfie and Au, 1989; Chalfie and Sulston, 1981). Sequence analysis revealed that EMS-induced *mec-4* single amino acid substitutions that cause loss-of-function cluster in 4 regions along the *mec-4* coding sequence (Hong et al., 2000). These channel-inactivating substitutions cluster in: In91-95, intracellular amino acids 91-95; Ex533–542, extracellular amino acids 533–542; ExCRDIII595–601, extracellular residues 595–601 within the Cys-rich domain III; and MSDII713–739, membrane-spanning domain II residues 713–739 which is the pore-inning domain. The majority of channel-disrupting amino acid substitutions affect conserved residues.

b. The conserved region of the intracellular N terminus.

This large-scale analysis was a good genetic approach to structure-function studies in that it identified substitutions with clear physiological consequences. The

highly conserved intracellular amino acids 91-95 in the N terminus fall within a short region near MSDI (Hong et al., 2000)(see Figure 15). The amino acid substitutions T91I, S92E, and G95E affect the highly conserved region. Transgenic *mec-4 null* mutants harboring reintroduced MEC-4 substitutions T91I, S92F, and G95E exhibit behavioral defects identical to those in EMS-induced genomic mutants, whereas the wild type *mec-4* gene can rescue mutant defects, confirming the feasibility of using transformation rescue in channel structure/function assays (Hong et al., 2000).

What is the biological function of the conserved region of N terminus? In the mammalian epithelial Na^+ channel (α-ENaC), one missense mutation substituting for a glycine (G95S) that is completely conserved throughout the DEG/ENaC ion channel family, reduced α-ENaC open probability (Gründer et al., 1999). Electrophysiological data show a significant decrease in Na^+ current for alanine substitutions not only for G95 but also for two highly conserved amino acids H94 and R98. Thus a working model is that the conserved region regulates channel opening in some way. We hypothesized that knowledge of the N terminal structure might provide some insight into how this region functions.

At the more C-terminal end of the protein, MEC-4 A713 is situated adjacent to the extracellular face of channel pore made from MSDII. Large side chain amino acid substitutions for MEC-4 A713 induce necrotic-like death of the touch receptor neurons - *mec-4(d)* alleles encoding A713V or A713T are dominant mutations

(Driscoll and Chalfie, 1991). Studies of MEC-4(d) and related channels from *C. elegans*, flies and mammals with analogous substitutions at this position support that steric hindrance conferred by large amino acid sidechains “locks” the channel in the open conformation, creating a hyperactive channel (Brown et al., 2007; Goodman et al., 2002; O'Hagan et al., 2005). MEC-4 substitutions T91I, S92F, and G95E encoded in transgenes also specifiying A713V can block this channel hyperactivation and prevent the neurodegeneration (Hong et al., 2000). Since the T91I, S92F, and G95E substitutions in an otherwise wild type MEC-4 generate a mutant subunit that fails to function but does not hyperactive the channel, it appears that the conserved domain is not a required negative regulator of channel function (if this domain did negatively regulate, that channel might also conduct excess current, but it does not). Rather, the conserved region appears required to activate or allow MEC-4 channel opening, and is required even in the presence of the A713V substitution.

c. The MEC-4 N terminal domain can exert dominant negative effects on channel activity.

Over-expression of the wild type MEC-4 in the *mec-4(+)* background can partially negatively regulate touch sensitivity (Hong et al., 2000). This dominant-negative effect is thought to occur by disrupting assembly of the channel complex. Moreover, the N-terminal domain (1-109) expressed from a transgene interferes *in trans* with the function of the MEC-4 channel, and this fragment by itself exerts a dominant-negative effect. Interestingly, however, the N-terminal fragment

containing T91I, S92F or G95E substitutions looses the capacity for interference. This suggests that the conserved domain might be critical for inter-subunit interactions in assembly for normal channel function. Note that the dominant negative effects of the N-terminal domain expressed on its own suggest the N-terminal domain folds and functions *in vivo* to form a domain that might participate in protein-protein interactions. The dependence on the conserved N-terminal residues for function implies that these might be required in the dominant negative mechanism--one possibility is that this conserved domain might be required for proper folding of the N terminus.

What are the structure/function relationships in the rest of the N-terminus?

The non-conserved region of the N-terminus has also been shown to be required for MEC-4 function (Hong et al., 2000). A constructed *mec-4* deletion MEC-4(Δ22-86), which eliminated most of the nonconserved N-terminus, fails to complement a *mec-4(-)* mutation (Hong et al., 2000). Immunocytochemistry confirms that mutant MEC-4(Δ22-86) protein is produced from the transgene and suggests that the deletion mutant channel is able to initiate channel assembly, i.e, cause dominant negative interference (Hong et al., 2000). However, it is striking that in EMS mutant screens no *mec-4*-inactivating mutations were found to induce substitutions in the MEC-4 N-terminal intracellular domain in this non-conserved region (exon 1 and part of exon 2). One possibility is that EMS has a limited capacity to induce disrupting substitutions based on EMS specificity for GC-AT transitions. However, when I looked at potential EMS-induced changes for MEC-4

N terminus amino acids, I did find several possible changes (refer to Table 2). Alternatively, multiple amino acids might need to be changed in order to disrupt N terminal function over much of the N-terminus. In sum, relatively little is understood about how MEC-4 N contributes to channel function.

Thinking about N-terminal cysteines:

Work on DEG/ENaC family member ENaC α, β, γ suggested that multiple Cys residues in the N- and C- termini can interact with metal

The mammalian ENaC channel is probably a heterotrimer, and made of one α, one β, and one γ ENaC subunit arranged around the channel pore in an βαγ configuration (Canessa et al., 1994; Firsov et al., 1998; Jasti et al., 2007). The amino termini of αβγ ENaC subunits contain 8 cysteine residues, and 5 of them are conserved among family members. Electrophysiological study shows that ENaC is highly sensitive to intracellular thiol reagents and thiol oxidation, suggesting these Cys residues are available for interaction (Kellenberger et al., 2005). ENaC can be blocked from the cytosolic side by sulfhydryl-reactive methanethiosulfonate (MTS) derivatives, the transition metal cations Cd^{2+} and Zn^{2+} reacting with thiol groups of cysteine residues, and $Cu(Phe)_3$, a mild oxidizing agent that promotes the formation of disulfide bonds (Kellenberger et al., 2005).

Substitutions of individual or multiple cysteine residues in the same domain in either the N- or C-terminus or TM1 or TM2 of ENaC were not sufficient to abolish the channel sensitivity to intracellular MTSEA, a MTS reagent. However, the

mutant channel with substitutions in all N- and C-termini cysteine residues of the all three αβγ ENaC subunits abolishes the effect from intracellular MTSEA. ENaC is relatively insensitive to externally applied thiol-modifying reagents, which excludes the possibility of effects on extracellular cysteine residues. Overall this study was the first to reveal a role for accessible intracellular Cys residues in DEG/ENaC channel complexes. Work I describe in this chapter tested the function of intracellular MEC-4 Cys residues.

We collaborated to solve the NMR structure of the MEC-4 N terminus

When we started our work there was no structural information on any of the proteins of the core DEG/ENaC channel. For his thesis project, John Everett determined the NMR structure of the MEC-4 N terminus *(Everett et al. in preparation).* MEC-4 N was expressed in recombinant *E. coli* and purified in the presence of detergent micelles. Circular dichroism, 2D HSQC, and HetNOE spectra confirmed that MEC-4 N was folded within our *in vitro* system. He used ^{2}H-decoupled triple resonance NMR spectroscopy techniques to determine the three-dimensional structure of MEC-4N. The structure indicates that MEC-4N features a five-helix bundle topology (helix α4 is quite short), with a large transiently ordered region situated between helixes α4 and α5 (Figure 16 Panel a).

The global fold is a four helix bundle with a small single turn helix that associates with α3. Five helical bundles are rare in solved structures while four helical bundles are much more common. Interestingly, the highly conserved DEG/ENaC

consensus sequence is situated in a fairly disordered region of the N-terminal fragment (Figure 16 Panel a).

The structure features regions of an acidic concentration surface and a basic concentration surface (Figure 16 Panel b). The basic surface is markedly smaller than the acidic surface. The structure possess a large negatively charged face, arising from negatively charged residues within its transiently structured region, and a smaller positively charged face on the nearly opposite side of the protein. There is also an unusual high hydrophobicity on the surface. On the charged surface representations of MEC-4 N, the white surfaces are hydrophobic or polar. These hydrophobic regions may be participated in protein interactions or membrane associations *in vivo*.

We find that Cys residues are situated together in the three dimensional structure in a manner that might support metal binding. Addition of equal molar amounts of Zn^{2+} or Cu^{2+} to MEC-4 N induces comparable ^{15}N HSQC peak perturbations that suggest that the introduction of metals induces a structural shift. The perturbations primarily correspond to MEC-4 N's transiently ordered region and $\alpha 5$ (Figure 16 Panel c).

Our determination of MEC-4N backbone atom resonance assignments also allowed us to map interfaces between MEC-4N and co-expressed channel subunit MEC-10N (Figure 16 Panel d), as well as the binding interface with stomatin

MEC-2 (Figure 16 Panel d). The conserved disordered region is only significantly impacted by the addition of MEC-10. MEC-2 domains other than MEC-2 S (stomatin-like domain of MEC-2, residues 141-361) are required to up-regulate MEC-4 / MEC-10 channel activity. MEC-2 S has been shown to interact with MEC-4 N *in vitro* via GST (glutathione S-transferase) pulldown experiments (Goodman et al., 2002). The stomatin-like domain of MEC-2 is responsible for recruiting MEC-2 to MEC-4.

Testing novel structural relationships suggested by NMR.

We wanted to test whether amino acids predicted to be important for MEC-4N structure were in fact critical for function. We used our MEC-4N structure to predict amino acids that should be critical for structural maintenance and tested these for NMR-reported structural perturbations as well as for disruption of MEC-4 function *in vivo*. Here I summarize my work on design, mutagenesis and *in vivo* testing, along with a discussion of significance of this work. Deciphering structure–activity relationships in mechanically gated channels is essential for elaborating molecular mechanisms of mechanotransduction. Our results provide the first structure/function insights into the tertiary and quaternary structure of the cytosolic face of a DEG/ENaC channel complex and hold novel implications for mechanotransduction mechanisms.

Results

My molecular constructions had two purposes: 1) I constructed mutations in the *mec-4N* cDNA plasmid that would be used to express the MEC-4 N terminal domain protein fragment to test how a given amino acid substitution disrupted the NMR structure; 2) I constructed mutations that changed MEC4 N-terminal amino acids in a *mec-4* genomic clone. Such plasmids could be used to test the impact of MEC-4 substitutions in channel function in a genetic complementation assay. I assayed these *mec-4* mutant alleles for function *in vivo* by assaying for complementation of the touch-insensitive phenotype conferred by the *mec-4*(*u253*) deletion allele. I also tested whether genomic *mec-4* clones maintained a dominant negative characteristic in wild type worms. The dominant negative feature suggests the mutant protein is made and can at least initiate channel complex assembly enough to compete. This suggests basic folding *in vivo* occurs despite the substitutions I introduce.

Design of MEC-4 N mutations to test NMR findings

We examined the NMR structure to test residues predicted to be important for N-terminal structural integrity. In the figures that follow, the mutations of interest are represented as sticks while MEC-4 N's backbone is depicted with colored ribbon. Here I summarize the rationale and results.

V23E & I65E: substitutions predicted to be non-disrupting.

One way to probe the structure is to make substitutions that are predicted to have

little impact on structure. Here I describe two such substitutions.

V23

V23 resides at the beginning of the helix-2 :: helix-3 turn. V23's methyl protons posses very distinct, yet degenerate, chemical shifts, suggesting a unique chemical environment and a potentially structurally important role. However, the structure does not place V23 in a structurally critical position. The unique chemical shift may arise from the neighboring aromatic group of Y24. We predicted that changing V23 should *not* have a major impact on the MEC-4 N structure.

I constructed an N terminal expression vector encoding MEC-4N(V23E). NMR data from the MEC-4N(V23E) fragments revealed minimal structural perturbation (Figure 19 & Table 3). I constructed an allele encoding full length MEC-4(V23E) and tested for function in transgenic animals. My *in vivo* touch test on *mec-4 null* mutant worms express transgenic MEC-4(V23E) show nearly normal touch sensitivity. Most worms respond to stimuli more than 3 times of a total 5 times stimuli (Figure 17 Panel a). Transgenic worms of MEC-4(V23E) with wild type background also show the same level of dominant negative effect as MEC-4N (Figure 18 Panel a), which is consistent with our structure prediction. I conclude that the V23E MEC-4 substitution does not impact NMR structure or native MEC-4 function, thus V23 does not play a critical structural role in MEC-4, consistent with our NMR model. In addition V23 does not appear to be essential for function.

I65

The delta methyl protons of MEC-N's three iso-leucines exhibit degenerate NMR signals, suggesting that they are not buried and consequently not required for the stability of the MEC-4 N structure. We predicted that changing I65 should have a negligible impact on the MEC-4 N structure.

I constructed an N terminal expression vector encoding MEC-4N(I65E). NMR data from the MEC-4N(I65E) fragments also revealed minimal structural perturbation (see Table 3). I constructed an allele encoding full length MEC-4(I65E) and tested for function in transgenic animals. My *in vivo* touch tests on the *mec-4 null* mutant worms that express transgenic MEC-4(I65E) reveals that they are touch sensitive. Most worms respond to stimuli at least 3 times in a total 5 times stimulus (Figure 17 Panel a). Transgenic worms that express MEC-4(I65E) in the wild type background show the same level of dominant negative effect as MEC-4N (Figure 18 Panel a). Thus, the I65E substation does not appear to disrupt channel subunit interactions or MEC-4 functions, consistenet with structural predictions. I conclude that I65 is not critical to MEC-4 N structure and function.

Testing Substitutions Predicted to Disrupt MEC-4 structure

Helix 1

L7

L7 is the most hydrophobic reside of helix-1's hydrophobic face (residues 3-9). The L7 side chain orients towards the hydrophobic face of amphipathic helix-2. We predicted that changing L7 to a charged residue should have a major impact on the MEC-4 N structure.

I made an expression construct to test impact on N terminal fragment NMR structure. John Everett found that: The structure of the L7E fragment exhibits a moderate structure perturbation (see Figure 21 & Table 3), suggesting a significant contribution to structural integrity. I constructed an allele encoding full length MEC-4(L7E) and tested for function in transgenic animals. My *in vivo* touch test on the *mec-4 null* mutants harboring transgenic MEC-4(L7E) shows decreased responses compared to wild type--most worms respond for the first or first two stimuli (Figure 17 Panel b). It might be noteworthy that touch responsiveness of the L7E mutant appears higher than negative control, so there may be some function. Wild type worms that express MEC-4N(L7E) show a reduced level of dominant negative effect as MEC-4N. I conclude that the L7 hydrophobic residue is important for normal touch sensitivity and MEC-4 function, and contributes in part by maintaining the N terminal structure.

Helix 2

Y19

Y19 is the only aromatic residue in helix-2 (residues 17-22) and contacts between Y19 and helix-1 are the major contacts used to orient helix 1 in the structure. The hydroxyl group of Y19 points towards the helix-1 :: helix-2 turn. We predicted that changing Y19 would have a major impact on the MEC-4 N structure.

I constructed an N terminal expression vector encoding MEC-4N(Y19E). The structure of the L7E fragment exhibits a moderate structure perturbation (see Figure 22 & Table 3), suggesting a significant contribution to structural integrity. I constructed an allele encoding full length MEC-4(Y19E) and tested for function in transgenic animals. My *in vivo* touch test on *mec-4* null mutant transgenic MEC-4(Y19E) shows a severely decreased touch response ratio. Most worms do not respond to the stimulus or respond to the first stimulus only (Figure 17 Panel b). Transgenic worms with wild type background show the same level of dominant negative effect as MEC-4N, and thus the mutant protein appears expressed. I conclude that Y19 plays an important role in MEC-4 function, and it may do this by maintaining the structural integrity of the MEC-4 N terminus.

M20

There are no long-range contacts orienting M20. Since M20 is the only residue in helix-2 with a fully hydrophobic side chain, it is predicted to play a role in MEC-4's hydrophobic core. We predicted that changing M20 to a charged residue should have a major impact on the MEC-4 N structure.

I constructed an N terminal expression vector encoding MEC-4N(M20E) fragement. The NMR structure of the M20E fragment exhibits a major structural perturbation (see Table 3), suggesting a significant contribution to structural integrity. I constructed an allele encoding full length MEC-4(M20E) and tested for function in transgenic animals. My *in vivo* touch test on the *mec-4 null* mutant transgenic MEC-4(M20E) shows a severely decreased touch response ratio. The majorities of worms do not respond to the stimulus or respond to the first stimulus only (Figure 17 Panel b). I also tested the MEC-4(M20E) variant for impact in *mec-4(+)* background. Transgenic worms of the *mec-4(+)* show the same level of dominant negative effect as MEC-4N, so the protein appears expressed and able to interrupt the complex assembly. I conclude that M20 plays an important role in MEC-4 function, and that it may do so by contributing to structural integrity of the N terminal domain. However, structures required for dominant negative effect must be maintained.

Helix 3

L28

L28 is the first helical residue of helix-3 (residues 28-38) following P27. The methyl protons of L28 possess unique chemical shifts suggesting a unique chemical environment. There are no long-range contacts to these distinct methyls, suggesting that they are not part of the hydrophobic core but rather project away

from the protein. We predicted that changing L28 should *not* have a major impact on the MEC-4 N structure, although it is possible that these methyls might be functionally important for protein-protein interactions.

I constructed an N terminal expression vector encoding MEC-4N(L28E). The L28E fragment exhibits a minor structure perturbation (see Table 3). I constructed a full length mutant *mec-4* gene encoding MEC-4(L28E) and introduced this into the *mec-4* null mutant and *mec-4(+)* background strains and then tested for function in transgenic animals. My *in vivo* touch test on the transgenic MEC-4(L28E) mutant reveals a severely decreased touch response ratio. Most worms do not respond to the stimulus or respond to the first stimulus only (Figure 17 Panel b). Transgenic worms of the *mec-4(+)* background show an enhanced level of dominant negative effect as compare to MEC-4N. This suggests both that the protein folds *in vivo* and that some essential interactions might disrupted by the substitution. I conclude that L28 plays an important role in MEC-4 function, although it does not impact structure in our prediction.

Y30

Y30 is the first residue of helix-3's hydrophobic face (Y30 L31 Q32) and makes contacts with V23, Y19 and possibly with L7 and C88 as well. We predicted that changing Y30 should have a major impact on the MEC-4 N structure.

I constructed a plasmid to express the MEC-4N(Y30E) fragment for NMR studies. The NMR structure of the Y30E fragment exhibits a moderate structural

perturbation (see Figure 25 & Table 3), suggesting a significant contribution of Y30 to structural integrity. I also constructed a transgene to express MEC-4(Y30E) in the *mec-4* null mutant to test for function. My *in vivo* touch test on the transgenic MEC-4(Y30E) mutant shows a decreased response ratio compared to wild type--most worms respond only to the first or first two stimuli (Figure 17 Panel b). It might be noteworthy that touch responsiveness of the Y30E mutant appears slightly higher than the negative control. When I introduced MEC-4N(Y30E) into the *mec-4(+)* background, I found a significant dominant negative impact. This MEC-4N(Y30E) maintains domains that are needed for dominant negative effect and may enhance the action by disrupting required interaction. I conclude that the Y30 is important for normal touch sensitivity and MEC-4 function, and that part of its role may be to maintain structural integrity.

L31

If L28 is mostly exposed to the solvent, then L31 (3 residues away in a helix) cannot be fully buried. Weak contacts show that L31 interacts with helix-2 via interactions with Y19 and M20. We thus predicted that changing L31 should have an impact on the MEC-4 N structure.

I constructed a L31E mutant to test for structural impact. NMR analysis revealed that the structure of the L31E fragment exhibits a major perturbation (see Figure 26 & Table 3), suggesting a significant contribution to structural integrity. I also constructed a full length MEC-4(L31E) transgene and introduced this into the

mec-4 null mutant to test for function in touch sensitivity. My *in vivo* touch test on the transgenic MEC-4(L31E) mutant shows a decreased touch response ratio, although the response is still higher than the negative control. Most worms respond for no more than two times (Fig. 21b). I also introduced the L31E mutant into the *mec-4(+)* background to test for dominant negative effects. Worms show an enhanced level of dominant negative effect as compared to MEC-4N. I conclude that L31 is important to MEC-4 function and maintaining MEC-4 structural integrity.

F37

F37 resides at the end of helix-3 and is responsible for orienting the small single turn helix-4 (residues 41-44) to the end of helix-3 as well as orienting elements of MEC-4 N's transiently ordered region. We predicted that changing F37 should have a major impact on the MEC-4 N structure.

I constructed a gene to express the F37E N terminal fragment. This study reveals a major structure perturbation for the F37E mutant (see Table 3), suggesting a significant contribution to structural integrity. I also constructed a genomic clone encoding MEC-4N(F37E) to test for *in vivo* function by introducing into a *mec-4 null* mutant background. My *in vivo* touch test on the transgenic MEC-4(F37E) mutant shows a severely decreased touch response ratio. Most worms do not respond for the stimulus or respond to the first stimulus only (Figure 17 Panel b). I also introduced the MEC-4(F37E) transgene into *mec-4(+)* background to test for

dominant negative impact. Transgenic worms with wild type background show an enhanced level of dominant negative effect as compared to MEC-4N. I conclude that F37 plays an important role in MEC-4 function, and it may do this by maintaining structural integrity of the N terminus. However, the F37E dominant negative substitution does not disrupt function, so some structure must be maintained.

Helix 4

Y43

Y43 resides in the center of the small single turn helix-4. The existence of this small helix is supported by Wishart and Talos analyses. This small helix is predicted to be involved with MEC-4 N's interaction with MEC-2. Y43 is responsible for orienting helix-4 to helix-3. We predicted that changing Y43 should have an impact on the orientation of helix-4 and interaction with MEC-2 and should therefore disrupt touch sensation.

I introduced the Y43E substitution into the construct encoding the MEC-4N fragment for NMR study. John Everett found that the structure of the Y43E fragment exhibits a moderate structural perturbation (see Figure 28 & Table 3), suggesting that Y43 makes a significant contribution to structural integrity. I also constructed a genomic clone encoding Y43E for functional test in the *mec-4* null mutant background. My *in vivo* touch test on the transgenic MEC-4(Y43E) mutant

shows a severely decreased touch response ratio. Most worms respond for no more than one time (Figure 17 Panel b). I also introduced the genomic clone encoding MEC-4(Y43E) into the *mec-4(+)* background to test its dominant negative properties. Transgenic worms of Y43E in the wild type background show a reduced level of dominant negative effect as compared to MEC-4N. I conclude that V43 is required for MEC-4 function, and it might do this by providing structural integrity.

Helix 4 :: Helix 5 transient

F69

F69 is situated near the end of MEC-4 N's transiently ordered region and is responsible for structuring this region. We predicted that changing F69 should disrupt MEC-4 N's transiently ordered region.

I constructed a plasmid to express the MEC-4N(F69E) fragment for NMR studies. The structure of the F69E fragment exhibits a major structural perturbation (see Table 3), suggesting a significant contribution to structural integrity. I also constructed a transgene to express MEC-4(F69E) in the *mec-4* null mutant to test for function. My *in vivo* touch test on the transgenic MEC-4(F69E) mutant shows a decreased response ratio compared to wild type-most worms respond for the first or first two stimuli (Figure 17 Panel b). It might be noteworthy that touch responsiveness of the F69E mutant appears higher than negative control. I also

introduced the genomic clone encoding MEC-4(F69E) into the *mec-4(+)* background to test its dominant negative properties. Transgenic worms with wild type background show a reduced level of dominant negative effect as compared to MEC-4N. I conclude that the F69 hydrophobic residue is important for normal touch sensitivity and MEC-4 function and maintaining MEC-4 structural integrity.

71 PKLL 74 deletion

Immediately before helix-5 (residues 77-88), there is an interesting stretch of residues, 71 PKLL 74, which orients the end of MEC-4 N's transiently ordered region, ordered by F69, with the beginning of helix-5. We predicted that deleting these residues should disrupt MEC-4 N's transiently ordered region and possibly disrupt helix-1 and helix-5.

I constructed a gene to express the 71PKLL74 N terminal fragment. This study reveals a minor structure perturbation (see table 3), suggesting a contribution to structural integrity. I also constructed a genomic clone encoding ∆71PKLL74 for functional test in the *mec-4* null mutant background. My *in vivo* touch test on the transgenic MEC-4(∆71PKLL74) mutant shows a significantly decreased touch response ratio, only it is still a little bit higher than negative control (Figure 17 Panel b). I also introduced the genomic clone encoding MEC-4(∆71PKLL74) into the *mec-4(+)* background to test its dominant negative properties. Transgenic worms with wild type background show the same level of dominant negative effect as MEC-4N. I conclude that the PKLL region is important for MEC-4 *in vivo* function.

Helix 5

W82

W82 resides in the first half of helix 5. Helix-5 is strictly amphipathic except for W82 which resides squarely in the center of its hydrophilic face rather than its hydrophobic face. The HN group of W82's side chain interacts with the backbone HNs of I99 and G100 as well as residues in MEC-4 N's transiently ordered region. W82 may be responsible for orienting MEC-4 N's conserved DEG/ENaC sequence prior to I99. Thus, we predicted it should be functionally important.

To test this hypothesis I construct a gene encoding MEC-4N(W82E). John Everett's NMR analysis revealed a minor structural perturbation as a consequence of the W82E substitution (see Figure 31 & Table 3). I also constructed a genomic clone encoding MEC-4N(W82E). I introduced into the *mec-4* null mutant to test for function. My *in vivo* touch test on the transgenic MEC-4(W82E) mutant shows a severely decreased touch response ratio. Most worms respond to the stimulus for no more than one time (Figure 17 Panel b). I also tested for dominant negative activity of MEC-4N(W82E) in a wild type background. I found that transgenic worms in the wild type background show a reduced level of dominant negative effect as compared to MEC-4N. This suggested that the protein may be degraded or may lack an essential structure that mediates interaction. Even though hydrophic W82 projects from an amphipathic helix, it might be involved in

interactions in the complex. I conclude that W82 is critical for MEC-4 function and possibly structure.

F84

Helix 5 is the least well oriented helix due to a lack of contacts, partially accounting for the unusual weakness of helix-5 spin systems. F84 is believed to be a major component of Helix-5's hydrophobic face. We predicted that changing F84 should have a major impact on the MEC-4 N structure.

I constructed a MEC-4N fragment mutant that harbored the F84E substitution. John Everett found that this change conferred a moderate structural perturbation (see Figure 32 & Table 3), suggesting a significant contribution to structural integrity. I constructed a genomic *mec-4* clone that encodes MEC-4(F84E) and tested for *in vivo* function by introducing it into the *mec-4* null background. My *in vivo* touch test on the transgenic MEC-4(F84E) mutant shows a decreased response ratio that is comparable to the negative control. Most worms respond to touch stimulus for no more than one time (Figure 17 Panel b). I also tested for dominant negative activity in the *mec-4(+)* background. Transgenic worms in the wild type background show an enhanced level of dominant negative effect as compared to MEC-4N. This suggests the structural perturbation disrupts assembly in a significant way. I conclude that F84 makes a critical contribution to MEC-4 function, and makes this by disrupting structure, but not in a way that disrupts all interactions.

F87

Like F84, F87 also contributes to Helix-5's hydrophobic face and is believed to contribute to MEC-4 N's hydrophobic core. We predicted that changing F87 to a charged residue should have a major impact on the MEC-4 N structure.

I constructed a MEC-4N clone encoding F87E. John Everett contributed NMR studies on this fragment and found that the structure of the F87E fragment exhibits a minor structural perturbation (see Figure 33 & Table 3), suggesting a change in structural integrity. I also constructed *mec-4* genomic clone encoding substitution F87E and tested for function by introducing into the *mec-4* null mutant background. My *in vivo* touch test on the transgenic MEC-4(F87E) mutant shows a severely decreased touch response ratio. Most worms do not respond to the stimulus or respond to the first stimulus only (Figure 17 Panel b). I also introduced the MEC-4(F87E) mutant into the wild type *mec-4(+)* background to test for dominant negative activity. I found that transgenic worms in the wild type background show an enhanced level of dominant negative effect as compared to MEC-4N. I conclude that F87 plays an important role in MEC-4 function, perhaps by maintaining core structure. The F87E substitution does not change structure enough to change all assembly interactions.

The Cysteines

C52, C62, and C88

As noted above, intracellular cysteines in the ENaC channel have been implicated in channel regulation and metal binding (Kellenberger et al., 2005). Nothing is known of the biological function of these cysteine residues. A very interesting result from our NMR structure is that MEC-4 N's three cysteines spatially co-localize suggesting potential for disulfide bridges or a metal-binding site. Bioinformatic prediction tools predict that C52 and C62 are involved in a disulfide bridge but their C^{β} shifts do not support this for our NMR model. Since addition of divalent metals induces a structural shift (see below), the presence of a metal-binding site comprised of cysteine residues is more probable. We predicted that if interactions with metals, or not-yet-detected disulfide bridges, are important to channel function, then mutating the cysteines should interrupt channel function.

I constructed a mutant fragment in which the cysteine residues C52, C62, and C88 were switched to Ala. When John Everett expressed the cys-mutant fragment, he observed a minor structural perturbation (see Figure 34 and Table 3). I also constructed *mec-4* alleles in which individual cysteine residues were changed to Ala. I tested these for function in a *mec-4* null background. All these mutant alleles showed decreased touch sensitivity as compared to wild type, with C88A appearing most severely defective. I also tested the C52AC62A double mutant and found it is defective for gentle touch. I also tested Cys mutants for ability to confer dominant negative effects on *mec-4(+)* activity by introducing Cys mutant gene into the wild type background. I find that C52A, C62A and the C52AC62A double

are somewhat reduced in the dominant negative effect, suggesting they could disrupt normal interactions in the channel complex or could be somewhat unstable as subunits. The C88A mutant is mildly increased for its dominant negative impact, suggesting it can still interact in complex formation. Generally, I conclude that each Cys is critical for MEC-4 function, data consistent with the working hypothesis that Cys52, Cys62 and Cys88 might participate in metal binding. The presence of Cys residues is important for structural integrity.

The Highly Conserved Histidine

H94

His 94 is one of the most conserved amino acids among DEG/ENaC members in the N-terminal conserved region. Previous studies showed that alanine substitution for H94 of αENaC can suppress amiloride-sensitive Na^+ current dramatically (Gründer et al., 1999). Analogous substitution in DEG-1 can disrupt channel function (Shreffler et al., 1995). We predicted that changing H94 should have a major impact on the MEC-4 function. However, we have no idea if H94 substitution (which is in a disoriented region) alters MEC-4N structure. Thus we probed structure/function of the MEC-4N(H94A) mutant.

I constructed a gene encoding MEC-4N(H94A). John Everett's structural analysis suggested only a minor structure perturbation. I also constructed a genomic mutant clone encoding MEC-4(H94A) and tested for function by introducing into

mec-4 null mutants. My *in vivo* touch test on the transgenic MEC-4(H94A) mutant shows a severely decreased touch response ratio. Most worms do not respond to the stimulus or respond to the first stimulus only (Figure 17 Panel c). I also tested MEC-4(H94A) for dominant negative activity in the wild type background. Transgenic worms in the wild type background show an enhanced level of dominant negative effect as compared to MEC-4N. I conclude that H94 plays an important role in MEC-4 function, but that it does this by altering the specific function rather than the structure.

Puncta measurement in touch neuron processes by MEC-2 antibody staining.

MEC-2 stomatin-like domain (AA 141-361) has been shown to interact with MEC-4 N *in vitro* via GST (glutathione S-transferase) pulldown experiments (Goodman et al., 2002). The stomatin-like domain of MEC-2 is responsible for recruiting MEC-2 to MEC-4. I use the MEC-2 antibody to stain the puncta in touch neuron processes. Pictures were taken by fluorescent microscope and analyzed by ImageJ. Wild type animal has around 250 puncta per mm in touch neuron processes while *mec-4* null has much less (~180/mm). *mec-4(d)* and the double mutant, *mec-10(tm1552) mec-4(u253),* also have much lower puncta density (~170/mm and ~140/mm) than wild type worms. Note that the *mec-10(tm1552) mec-4(u253)* also has lower density than mec-4 *null* worms. I measured some MEC-4 N-terminal mutants that disrupted the touch sensation function, L7E, Y19E, M20E, Y30E, Y43E, F69E, and W82E. All of them have significant lower puncta density than wild type worms. All

of them failed to rescue the *mec-4* null phenotype. I also measured the cysteine mutants, C52A, C62A, C52AC62A, and C88A. C62A and C88A have similar phenotype with previous mutants, but the C52A mutant has no significant difference. The C52AC62A double mutant is the only one that can rescue the mec-4 *null* phenotype and has a little bit higher density (but not statistically significant) than wild type animals. I also measured the average length of each punctum and the blank area between them. My results show that the average length of each punctum was shorten in most mutants. The blank areas between puncta were longer in most of the mutants, except C52AC62A, which has higher puncta density than wild type.

DISCUSSION

I have tested 20 point mutations that change MEC-4N based on the predictions from our structural data. In the *mec-4* null mutant background, I used the transform assay to test the ability of each substitution to recover touch neuron function. Most of our transgenic mutants show touch sensory defects at different levels. I also tested for dominant negative effects by MEC-4 mutant expression in wild type worms. Mutants showed variable effects on the dominant negative property on MEC-4 expression.

Structure predicting function

I tested amino acid substitutions that were predicted to perturb protein structure, including L7E, Y19E, M20E, Y30E, L31E, F37E, Y43E, F69E, W82E, F84E, F87E, and C88A. All these substitution mutants show defects in the touch sensation rescue assay confirming the predicted functional importance of residues that appear important for structure. Other mutants not predicted for structural changes but exhibiting functional defects are L28E, C52A, C62A, 71PKLL74 deletion, and H94A. H94A is one of the most conserved amino acids in the DEG/ENaC superfamily. It was previously shown that substitution of the amino acids in this conserved region disturbed the function of the MEC-4 ion channel. My results confirmed this, and showed this is the effect of amino acid function rather than a major structural change. In fact, the highly conserved region is not highly structured in solution, the H94 substitution may interfere with protein-protein

interaction function of MEC-4N that causes a functional defect of the ion channel.

L28E has no effect on structure and L28 is exposed on the outside of the MEC-4N domain. Cysteines (C52, C62, and C88) in MEC-4N domain have been implicated in metal binding by our structural studies. My result suggests these sites are also required for channel function *in vivo*.

However, there are also two mutants V23E and I65E that show NMR ^{15}N HSQC perturbations but with no major defect on mechanosensory function. Transgenic mutants of these two amino acids in the wild type background also show no difference from the wild type MEC-4N dominant negative effect, consistent with the prediction that these two substitutions should not have major impacts on ion channel function. In general, the prediction that specific amino acids are important for function based on the NMR structure was borne out by my studies. Why these substitutions were not identified in genetic screens is not clear. One possibility is that this was simply due to chance, and not enough MEC-4 mutants were isolated. However, it might also be possible that the identified substitutions do not impact touch as much as true nulls. For example, their effects might be minimized by assembly of the MEC channel complex.

Dominant negative activities of MEC-4

Over-expression of the MEC-4 in the wild type background can partially negatively regulate touch sensitivity (Hong et al., 2000). Moreover, expressing only the

N-terminal domain (1-109) of MEC-4 can also interfere the function of the wild type MEC-4 channel. Previous studies also showed the substitutions T91I, S92F and G95E, which are all in a conserved domain, could destroy this dominant negative effect. Transgenic worms with the same substitutions in the wild type background show very different effects for each mutant compared with those in *mec-4* null worms. I identified them into different classes. Group I is the two predicted non-structure perturbations, V23E and I65E, that show no significant differences from wild-type *mec-4* in both *mec-4* null rescue and *mec-4(+)* dominant negative assays. This suggests that they are basically normal in structure and function. Group II contains L7E, Y43E, F69E, and W82E in our predicted structure perturbation group and two cysteine substitutions, C52A and C62A. These all show functional defects in touch sensation and a significantly reduced dominant negative effect. This suggests that these substitutions disrupt the structure of MEC-4 and/or the possible protein-protein interaction domain in the N-terminal. Group III includes Y19E, M20E, and the 71PKLL74 deletion. These have touch sensation defects but show no difference from *mec-4(+)* in dominant negative effect. This suggests that even though the structure has a major perturbation (M20E) or the touch sensation function is disrupted, the protein-protein interaction domain that is required for dominant negative effect may not be disrupted. Group IV contains L28E, Y30E, L31E, F37E, F84E, F87E, C88A, Y49A, and H94A. These failed to rescue the touch sensation defects in *mec-4* null worms but enhanced the dominant-negative effect in wild type background. L31E and F37E have major structure perturbations that could destroy the MEC-4 channel function easily. This

might prompt degradation of other subunits in the channel complex. Other substitutions only have moderate or minor structure perturbations, but they may disrupt the structure of the whole MEC-4 channel complex through the protein-protein interaction domains. These results may indicate that the rescue of channel function and the dominant negative effects can act by very different ways.

MEC-4 N-terminal mutants have lower puncta density in touch neuron processes

mec-4(u253) has much lower puncta density in touch neuron processes than wild type (~250 vs ~180). I also measured some mutants that failed to rescue the abnormal touch sensation function, L7E, Y19E, M20E, Y30E, Y43E, F69E, and W82E. All of them failed to rescue the less puncta phenotype in *mec-4* null. This may indicate that the localization of the channel complexes in these mutants are disrupted. Since I labeled MEC-2 but not MEC-4, the results may also caused by disruption of protein-protein interaction between MEC-4 (possible the MEC-4 N terminal) and MEC-2, and the channel complex might have normal localization but without MEC-2. Both possibilities can result decreased ion channel activities in touch neuron and thus disturb the touch sensation function in touch neurons. The cysteine mutants C62A and C88A have similar phenotype with previous mutants. However, the C52A and the double mutant C52AC62A did not show significant differences with wild type worms. But all of them disrupt the normal function of touch sensation in touch neurons. This results show that not all cysteines may disrupt the protein-protein interactions and cause the abnormal function of touch

sensation. The Cys52 might only participate in metal binding and abnormal metal alone could also disrupt the function of mechanosensory ion channel. My results may indicate that MEC-4 N-terminal is important in protein-protein interaction and the integrality of ion channel complex.

Summary

I studied the first *mec-10* null mutant and found:

1) The *mec-10(tm1552)* null mutant is gentle touch insensitive. *mec-10* null shows dramatically decreased response ratio on my gentle touch test, although it still has higher touch ratio than *mec-4* null.

2) *mec-10(tm1552)* impacts harsh touch sensation. Both double mutants *mec-10(0) mec-4(0)* and *mec-10(0) mec-4(d)* show a decreased response ratio for harsh touch stimuli as compared to *mec-4(0)* and *mec-4(d)* alone. These data support our hypothesis that *mec-10* is required for harsh touch sensation.

3) *mec-10* null is a recessive mutation. Heterozygous *mec-10/+* is touch sensitive, establishing that *mec-10* null is a recessive mutation.

4) *mec-10(tm1552)* does not change *mec-4(d)* and *mec-10(d)* toxicity. I introduced *mec-10* null into *mec-4(d)* and *mec-10(d)* strains and the level of neurodegeneration caused by these two mutations did not change.

5) The *mec-1(tm1552*) mutant does not have a higher bending frequency or larger amplitude, but has lower symmetry of motion. In a swimming assay, the *mec-10* null did not affect the bending frequency and amplitude. These observations suggest that *mec-10* null mutation has no significant impact on proprioception. The asymmetry in swimming assay may correlate with the asymmetric response along touch neuron processes, although further work is needed to confirm this possibility.

6) The existing *mec-10* alleles are dominant-negative on MEC channel function in heterologous expression assay. Five *mec-10* point mutations found by touch

screening are all have dominant-negative effect on our oocyte assay. All of them show decreased whole cell current than ion channel complexes with *mec-10* or *mec-10(d)*.

7) *mec-10(tm1552)* exhibits decreased cameleon-reported responses of gentle touch neurons and PVD/FLP, suggesting roles in both gentle and harsh touch sensation

8) Chimeric MEC-4 MEC-10 channels do not function well in touch assays. The chimeras of *mec-4* and *mec-10* cannot complement either *mec-4* or *mec-10* null alleles *in vivo* for gentle or harsh touch perception. My extracellular and transmembrane domain exchanging chimeras do not function well. We may need smaller and more specific domain exchanges to have better functional protein and thus be able to locate the domains which make MEC-4 and MEC-10 functionally different.

Based on the solved MEC-4 N-terminal NMR structure prediction, I introduced point mutations into this domain and studied biological consequences in genetic rescue assays and by monitoring dominant negative effects normally seen when the N-terminal is expressed alone. V23E and I65E, which are predicted to exert no structural perturbation, show no changes on rescue and dominant-negative effect assays. The amino acid substitutions predicted to perturb structure disrupt channel function supporting the validity of the structure. One substitution that needs to be mentioned is the L28E, which has no structure perturbation, but is predicted to be exposed outside the MEC-4N helix bundle structure. My data suggests this residue might contribute to an important protein-protein interaction,

as the substitution does have significant influence on rescue activity and dominant-negative effects. The disrupted mutant strains also exhibit a significantly decreased density of immuno-stained channel puncta distributed along touch neuron processes. However, the rescue of channel function and the dominant negative effects are generally not well correlated. Overall, my results support that our structure prediction is reasonable and supported by genetic data; novel findings also came of analysis of NMR structure relative to *in vivo* function.

Materials and methods

C. elegans strains and growth

Nematode strains were maintained at 20^{o}C on standard nematode growth medium (NGM) seeded with *Escherichia coli* strain OP50 as food source.

The crosses to make the *mec-4 mec-10* double mutant rely on recombination because these two genes are on the same chromosome. I used two linked mutations with obvious phenotypes: *unc-7* (uncoordinated) and *dpy-6* (dumpy) as markers, *dpy-6* located next to *mec-10*, and *unc-7* is near to *mec-4*. So I first made double mutants of *mec-10 unc-7* and *dpy-6 mec-4*. Then I could cross these two strains, and pick the progeny without *unc* and *dpy* phenotypes to identify double *mec* recombinants. The distances between these two genes (*mec-10* and *dpy-6*, *mec-4* and *unc-7*) are much longer then distances between *mecs* (~20 centiMorgans vs <1 and ~2 cM), so it is relatively easier to have the recombination between the two *mec* genes is more frequent. Finally, I used PCR to confirm the *mec-10* deletion allele.

Primers used to confirm *mec-10* deletion alleles: 1) For *mec-10(tm1552)*: 5'-GTAGGGTCTGCAACTAGCTC-3' and 5'-TGCTTGGGCAAGCTCC AAAC-3' 2) For *mec-10(ok1104)*: 5'-TCATTTGCAGCATTTTCTCG-3' and 5'-ATTTATCAATCAGGCGGT CG-3'; inside deletion: 5'-CGCAAAAGGAAAATTCCAAA-3', 5'-ACGCGCAAGCCTAGAAAAT A-3',

5'-GCTTTGGTGTATTCCGCCTA-3', and 5'-GACGGAAATCGTGGATCACT-3' 3) For RT-PCR: 5'-AAATTATCTCGCAAGTGACACTAACTTTCT-3' and 5'-CCAAAGTATTCCCA TAAATTCAATACCATT-3'

Hybrid proteins with MEC-4 and MEC-10 domains

Chimeric proteins for MEC-4 and MEC-10 were engineered on two plasmids by swapping extracellular domains. In other words, chimeras differ in two transmembrane domains and extracellular domain, intracellular domains was kept as a unit. Constructs for MEC-4 were in pBluescript KS(-) plasmid with a 6.1 kb genomic *mec-4(+)* clone (that contains ~1.9 kb upstream of the predicted *mec-4* initiation codon including the final coding exons of the gene 5' to *mec-4*, all introns, and ~0.5 kb of 3'-flanking sequence). Constructs for MEC-10 were in pPD95.77 plasmid with a 6.1 kb genomic *mec-10(+)longGFP* clone. The following primers were used for making chimeric constructs: MEC-4 N-terminal: 5'ATATACGTTTGGAGCTTCACCAATCATGGG3'; MEC-4 TMD1: 5'TATCGAGCAGTTTGGGTCGTACT TTTTCTT3'; MEC-4 TMD2: 5'CATGTAGGCAGTTTCCAAGAAAAGGAACAC3'; MEC-4 C-terminal: 5'AGTGCCG AACATAACTACTCTCTGTACAAA3'; MEC-10 N-terminal: 5'TAAACTGTTTGGAGCTTGCCCAAGCATTGG3'; MEC-10 TMD1: 5'TACAGGTAATAGGCATATTGGGAGGGAGCT3'; MEC-10 TMD2: 5'CATGTATATCAGCTCAAAGGCTA GACACAC3'; MEC-10 C-terminal: 5'GCAATTGCACATCACATAAACCAGCAGAGA3'. Primers were synthesized, 5'-phosphorylated, and PAGE purified by Integrated DNA technologies, Inc.

(Coralville, IA). Ligations were done by QuickLigase (New England Biolabs, Inc. Ipswich, MA). All constructs were confirmed by sequence analysis. Two chimeric constructs were made: mec4extra+mec10intra: This construct contains the whole mec-4 extracellular domain and two mec-10 intracellular domains including N- and C-terminus. mec-4 extracellular domain was made by primers MEC-4 TMD1+MEC-4 TMD2 on pBluescript KS(-) plasmid with a genomic *mec-4(+)* clone. mec-10 intracellular domains were made by primers MEC-10 N-terminal+ MEC-10 C-terminal on pPD95.77 plasmid with a genomic *mec-10(+)longGFP* clone. These two PCR products were ligated by QuickLigase. mec4intra+mec10extra: This construct contains two mec-4 intracellular domains including N- and C- terminus and the whole mec-10 extracellular domain. mec-4 intracellular domains were made by primers MEC-4 N-terminal+ MEC-4 C-terminal on pBluescript KS(-) plasmid with a genomic *mec-4(+)* clone. mec-10 extracellular domains were made by primers MEC-10 TMD1+ MEC-10 TMD2 on pPD95.77 plasmid with a genomic *mec-10(+)longGFP* clone. These two PCR products were ligated by QuickLigase.

Generating and scoring of transgenic animals

Plasmid DNAs (50 mg/ml) were co-injected with co-transformation marker DNA (50 mg/ml) for all the samples tested. Chimeric *mec-4* and *mec-10* constructs were introduced into recessive *mec-4(u253)* and *mec-10(tm1552)* mutants. *mec-4(u253)* has a partial deletion of *mec-4*-coding sequences and is a likely functional null allele (Hong et al., 2000). *myo-2::GFP* expressed in pharynx was co-injected with both constructs to facilitate the identification of GFP transformants.

Harsh and gentle touch assay

For each allele tested, I scored 5 sequential gentle touches on anterior and posterior worm bodies (Chalfie and Sulston, 1981). At least 50 young adult worms with GFP were assayed for touch sensitivity. Gentle and harsh stimuli were delivered by eyelash and wire. Mean value was determined by averaging response ratios from all worms tested.

Automated swimming analysis

To analyze *C. elegans* swimming I transferred 5 to 10 nematodes to a 50 μl drop of M9 buffer on a glass coverslip at room temperature. I recorded swimming behavior for 30 seconds at a rate of 18 frames/sec, beginning 1 minute after transfer to liquid. I then analyzed videos to extract locomotion features, determining mean values by averaging results obtained from 10 videos that simultaneously score 5 to 10 animals per video (Tsechpenakis et al., 2008).

Neurodegeneration scoring assay

I scored for PLM GFP signals by observing the tails of L4 stage larvae with fluorescence dissection microscopy. I scored for swollen necrotic-like PLM touch neurons by examining tails of L1 stage larvae with DIC microscopy as previously described (Maricq et al., 1995).

Generating and recording of cameleon strains

We used the cameleon reporter with cell-specific *C. elegans* promoters. Using the touch neuron cameleon reporter (P_{mec-4}YC2.12) and a promoter expressed in PVDs and FLPs (P_{egl-46}YCD3), we can record the changing of intracellular calcium concentration during mechanical stimuli (Suzuki et al., 2003). Single and double mutants were crossed with reporters to perform the tests.

Oocyte expression and immunocytochemistry

The *mec-2, mec-4(d),* and *mec-10* expression clones were prepared in bacterial strain SMC4. We cloned *mec-6* into pGEM. EGFP sequences were introduced to the 5'- or 3'-end of *mec-10.* Mutations at second sites introduced by PCR were confirmed by sequencing.

Capped RNAs were synthesized using a T7 mMESSAGE mMACHINE kit (Ambion, CA), purified on RNAeasy columns (Qiagen, CA), and checked for size, integrity and concentration. Stage V-VI oocytes were manually defolliculated after 2 h of collagenase treatment (2 mg/ml in Ca^{2+}-free OR2 solution) of *Xenopus laevis* ovaries (NASCO, WI). Oocytes were injected with 52 nl of complementary RNA (cRNA) mix to a final amount of 5 ng per oocyte of each cRNA except for *mec-6*, which was injected at 1 ng per oocyte. We incubated oocytes in OR2 (82.5mM NaCl, 2.5 mM KCl, 1mM $CaCl_2$, 1mM $MgCl_2$, 1mM Na_2HPO_4, 0.5g/l polyvinyl pyrolidone, 5mM HEPES (pH 7.2), 2mM Na-pyruvate, penicillin and streptomycin (0.2 mg/ml)) at 20 °C for at least 4 d before fixing.

For immunohistochemistry, oocytes were fixed in 4% paraformaldehyde in PBS and sliced by vibrotome. Oocyte slices were stained with antibody to GFP (Invitrogen, CA) diluted 1:200 in 1% bovine serum albumin in PBS plus 0.1% Tween 20. The secondary antibody was Cy3-conjugated donkey anti-rabbit (diluted 1:200). After staining, slices were mounted with Vectorex medium (Vector, CA) and photographed with an Axiplan 2 microscope (Zeiss, NY) equipped with a digital camera.

Site-Directed Mutagenesis

Single or multiple amino acid substitutions or deletions in the MEC-4 N-terminal were engineered on two plasmids by using Site-directed mutagenesis kits from New England Biolabs or Stratagene. Constructs for protein production for NMR studies contained the first 309 bps of *mec-4* 5'-end cDNA in plasmid pET-23(+). Constructs for tests of MEC-4 function were pBluescript SK(-) plasmid with a 6.1 kb genomic *mec-4(+)* clone (that contains ~1.9 kb upstream of the predicted *mec-4* initiation codon including the final coding exons of the gene 5' to *mec-4*, all introns, and ~0.5 kb of 3'-flanking sequence). Primers used for both are listed in Table 2. Phusion sit-directed mutagenesis kit (New England Biolabs, Inc. Ipswich, MA) required special modified 5'-phosphorylated primers. Primers were synthesized, modified, and PAGE purified (if required) by Integrated DNA technologies, Inc. (Coralville, IA). Double mutant strain (C52AC62A) was made by applying the

site-directed mutagenesis procedure twice on the same plasmid. All mutations were confirmed by sequence analysis.

Generation and scoring of transgenic animals

Plasmid DNAs (50 mg/ml) were coinjected with cotransformation marker DNA (50 mg/ml) for all the samples tested. *mec-4* alleles encoding single or multiple amino acid substitutions or deletions were introduced into recessive *mec-4(u253)* mutants. *mec-4(u253)* has a partial deletion of *mec-4*-coding sequences and is a likely functional null allele (Hong et al., 2000). Plasmid pRF4, which carries the dominant marker *rol-6(su1006)* (Kramer et al., 1990), was coinjected with *mec-4* alleles to facilitate the identification of roller transformants. For each *mec-4* allele tested, I scored 5 sequential touches, and at least 50 rollers were assayed for touch sensitivity (Chalfie and Sulston, 1981).

Methods and details of NMR structural studies are in (Everett, Lee et al, in preparation).

References

Bianchi, L., and Driscoll, M. (2002). Protons at the gate: DEG/ENaC ion channels help us feel and remember. Neuron *34*, 337-340.
Bianchi, L., Gerstbrein, B., Frøkjaer-Jensen, C., Royal, D.C., Mukherjee, G., Royal, M.A., Xue, J., Schafer, W.R., and Driscoll, M. (2004). The neurotoxic MEC-4(d) DEG/ENaC sodium channel conducts calcium: implications for necrosis initiation. Nat Neurosci *7*, 1337-1344.
Brown, A.L., Fernandez-Illescas, S.M., Liao, Z., and Goodman, M.B. (2007). Gain-of-Function Mutations in the MEC-4 DEG/ENaC Sensory Mechanotransduction Channel Alter Gating and Drug Blockade. J Gen Physiol *129*, 161-173.
Brown, A.L., Liao, Z., and Goodman, M.B. (2008). MEC-2 and MEC-6 in the Caenorhabditis elegans Sensory Mechanotransduction Complex: Auxiliary Subunits that Enable Channel Activity. J Gen Physiol *131*, 605-616.
Caldwell, G.A., L, C., N, H., S, G., Y, T., MX, H., and M, C. (1998). MEC-14 May Modulate Mechanosensory Channels. In East Coast Worm Meeting.
Canessa, C.M., Schild, L., Buell, G., Thorens, B., Gautschi, I., Horisberger, J.D., and Rossier, B.C. (1994). Amiloride-sensitive epithelial Na+ channel is made of three homologous subunits. Nature *367*, 463-467.
Chalfie, M. (2009). Neurosensory mechanotransduction. Nat Rev Mol Cell Biol *10*, 44-52.
Chalfie, M., and Au, M. (1989). Genetic control of differentiation of the Caenorhabditis elegans touch receptor neurons. Science *243*, 1027-1033.
Chalfie, M., Driscoll, M., and Huang, M. (1993). Degenerin similarities. Nature *361*, 504.
Chalfie, M., and Sulston, J. (1981). Developmental genetics of the mechanosensory neurons of Caenorhabditis elegans. Dev Biol *82*, 358-370.
Chalfie, M., Sulston, J.E., White, J.G., Southgate, E., Thomson, J.N., and Brenner, S. (1985). The neural circuit for touch sensitivity in Caenorhabditis elegans. J Neurosci *5*, 956-964.
Chalfie, M., and Thomson, J.N. (1982). Structural and functional diversity in the neuronal microtubules of Caenorhabditis elegans. J Cell Biol *93*, 15-23.
Chelur, D.S., Ernstrom, G.G., Goodman, M.B., Yao, C.A., Chen, L., O' Hagan, R., and Chalfie, M. (2002). The mechanosensory protein MEC-6 is a subunit of the C. elegans touch-cell degenerin channel. Nature *420*, 669-673.

Corey, D.P. (2006). What is the hair cell transduction channel? J Physiol *576*, 23-28.
Coryell, M.W., Wunsch, A.M., Haenfler, J.M., Allen, J.E., McBride, J.L., Davidson, B.L., and Wemmie, J.A. (2008). Restoring Acid-sensing ion channel-1a in the amygdala of knock-out mice rescues fear memory but not unconditioned fear responses. J Neurosci *28*, 13738-13741.
Cueva, J.G., Mulholland, A., and Goodman, M.B. (2007). Nanoscale Organization of the MEC-4 DEG/ENaC Sensory Mechanotransduction Channel in Caenorhabditis elegans Touch Receptor Neurons. J Neurosci *27*, 14089-14098.
Driscoll, M., and Chalfie, M. (1991). The mec-4 gene is a member of a family of Caenorhabditis elegans genes that can mutate to induce neuronal degeneration. Nature *349*, 588-593.
Du, H., Gu, G., William, C.M., and Chalfie, M. (1996). Extracellular proteins needed for C. elegans mechanosensation. Neuron *16*, 183-194.
Emtage, L., Gu, G., Hartwieg, E., and Chalfie, M. (2004). Extracellular proteins organize the mechanosensory channel complex in C. elegans touch receptor neurons. Neuron *44*, 795-807.
Firsov, D., Gautschi, I., Merillat, A.-M., Rossier, B.C., and Schild, L. (1998). The heterotetrameric architecture of the epithelial sodium channel (ENaC). The EMBO Journal *17*, 344–352.
Fukushige, T., Siddiqui, Z.K., Chou, M., Culotti, J.G., Gogonea, C.B., Siddiqui, S.S., and Hamelin, M. (1999). MEC-12, an alpha-tubulin required for touch sensitivity in C. elegans. J Cell Sci *112 (Pt 3)*, 395-403.
Goodman, M.B., Ernstrom, G.G., Chelur, D.S., O'Hagan, R., Yao, C.A., and Chalfie, M. (2002). MEC-2 regulates C. elegans DEG/ENaC channels needed for mechanosensation. Nature *415*, 1039-1042.
Gründer, S., Jaeger, N.F., Gautschi, I., Schild, L., and Rossier, B.C. (1999). Identification of a highly conserved sequence at the N-terminus of the epithelial Na+ channel alpha subunit involved in gating. Pflugers Arch *438*, 709-715.
Gu, G., Caldwell, G.A., and Chalfie, M. (1996). Genetic interactions affecting touch sensitivity in Caenorhabditis elegans. Proc Natl Acad Sci U S A *93*, 6577-6582.
Hong, K., and Driscoll, M. (1994). A transmembrane domain of the putative channel subunit MEC-4 influences mechanotransduction and neurodegeneration in C. elegans. Nature *367*, 470-473.
Hong, K., Mano, I., and Driscoll, M. (2000). In vivo structure-function analyses of Caenorhabditis elegans MEC-4, a candidate mechanosensory ion channel subunit. J Neurosci *20*, 2575-2588.
Huang, M., and Chalfie, M. (1994). Gene interactions affecting mechanosensory transduction in Caenorhabditis elegans. Nature *367*, 467-470.

Huang, M., Gu, G., Ferguson, E.L., and Chalfie, M. (1995). A stomatin-like protein necessary for mechanosensation in C. elegans. Nature *378*, 292-295.
Huber, T.B., Schermer, B., M 羹 ller, R.U., H 繹 hne, M., Bartram, M., Calixto, A., Hagmann, H., Reinhardt, C., Koos, F., Kunzelmann, K.*, et al.* (2006). Podocin and MEC-2 bind cholesterol to regulate the activity of associated ion channels. Proceedings of the National Academy of Sciences *103*, 17079-17086.
Hudspeth, A. (1997). Mechanical amplification of stimuli by hair cells. Curr Opin Neurobiol *7*, 480-486.
Hudspeth, A.J. (2008). Making an Effort to Listen: Mechanical Amplification in the Ear. Neuron *59*, 530-545.
Jasti, J., Furukawa, H., Gonzales, E.B., and Gouaux, E. (2007). Structure of acid-sensing ion channel 1 at 1.9[thinsp]A resolution and low pH. Nature *449*, 316-323.
Kazmierczak, P., Sakaguchi, H., Tokita, J., Wilson-Kubalek, E.M., Milligan, R.A., Muller, U., and Kachar, B. (2007). Cadherin 23 and protocadherin 15 interact to form tip-link filaments in sensory hair cells. Nature *449*, 87-91.
Kellenberger, S., Gautschi, I., Pfister, Y., and Schild, L. (2005). Intracellular thiol-mediated modulation of epithelial sodium channel activity. J Biol Chem *280*, 7739-7747.
Kellenberger, S., and Schild, L. (2002). Epithelial sodium channel/degenerin family of ion channels: a variety of functions for a shared structure. Physiol Rev *82*, 735-767.
Kerr, R., Lev-Ram, V., Baird, G., Vincent, P., Tsien, R.Y., and Schafer, W.R. (2000). Optical Imaging of Calcium Transients in Neurons and Pharyngeal Muscle of C. elegans. Neuron *26*, 583-594.
Kramer, J.M., French, R.P., Park, E.C., and Johnson, J.J. (1990). The Caenorhabditis elegans rol-6 gene, which interacts with the sqt-1 collagen gene to determine organismal morphology, encodes a collagen. Mol Cell Biol *10*, 2081-2089.
Krishtal, O. (2003). The ASICs: signaling molecules? Modulators? Trends Neurosci *26*, 477-483.
Kwan, K.Y., Allchorne, A.J., Vollrath, M.A., Christensen, A.P., Zhang, D.S., Woolf, C.J., and Corey, D.P. (2006). TRPA1 contributes to cold, mechanical, and chemical nociception but is not essential for hair-cell transduction. Neuron *50*, 277-289.
Maricq, A.V., Peckol, E., Driscoll, M., and Bargmann, C.I. (1995). Mechanosensory signalling in C. elegans mediated by the GLR-1 glutamate receptor. Nature *378*, 78-81.
Martinac, B., Buechner, M., Delcour, A.H., Adler, J., and Kung, C. (1987). Pressure-sensitive ion channel in Escherichia coli. Proc Natl Acad Sci U S A *84*, 2297-2301.

Mitani, S., Du, H., Hall, D.H., Driscoll, M., and Chalfie, M. (1993). Combinatorial control of touch receptor neuron expression in Caenorhabditis elegans. Development *119*, 773-783.
Miyawaki, A., Llopis, J., Heim, R., McCaffery, J.M., Adams, J.A., Ikura, M., and Tsien, R.Y. (1997). Fluorescent indicators for Ca2+ based on green fluorescent proteins and calmodulin. Nature *388*, 882-887.
Miyawaki, A., Tsien, R.Y., and Jeremy Thorner, S.D.E.a.J.N.A. (2000). Monitoring protein conformations and interactions by fluorescence resonance energy transfer between mutants of green fluorescent protein. In Methods in Enzymology (Academic Press), pp. 472-500.
O'Hagan, R., Chalfie, M., and Goodman, M.B. (2005). The MEC-4 DEG/ENaC channel of Caenorhabditis elegans touch receptor neurons transduces mechanical signals. Nat Neurosci *8*, 43-50.
Pulak, R., and Anderson, P. (1993). mRNA surveillance by the Caenorhabditis elegans smg genes. Genes Dev *7*, 1885-1897.
Savage, C., Xue, Y., Mitani, S., Hall, D., Zakhary, R., and Chalfie, M. (1994). Mutations in the Caenorhabditis elegans beta-tubulin gene mec-7: effects on microtubule assembly and stability and on tubulin autoregulation. J Cell Sci *107 (Pt 8)*, 2165-2175.
Schafer, W.R., Sanchez, B.M., and Kenyon, C.J. (1996). Genes affecting sensitivity to serotonin in Caenorhabditis elegans. Genetics *143*, 1219-1230.
Shreffler, W., Magardino, T., Shekdar, K., and Wolinsky, E. (1995). The unc-8 and sup-40 Genes Regulate Ion Channel Function in Caenorhabditis elegans Motorneurons. Genetics *139*, 1261-1272.
Sukharev, S.I., Blount, P., Martinac, B., Blattner, F.R., and Kung, C. (1994). A large-conductance mechanosensitive channel in E. coli encoded by mscL alone. Nature *368*, 265-268.
Sukharev, S.I., Blount, P., Martinac, B., and Kung, C. (1997). Mechanosensitive channels of Escherichia coli: the MscL gene, protein, and activities. Annu Rev Physiol *59*, 633-657.
Suzuki, H., Kerr, R., Bianchi, L., Frøkjaer-Jensen, C., Slone, D., Xue, J., Gerstbrein, B., Driscoll, M., and Schafer, W.R. (2003). In vivo imaging of C. elegans mechanosensory neurons demonstrates a specific role for the MEC-4 channel in the process of gentle touch sensation. Neuron *39*, 1005-1017.
Toker, A.S., Teng, Y., Ferreira, H.B., Emmons, S.W., and Chalfie, M. (2003). The Caenorhabditis elegans spalt-like gene sem-4 restricts touch cell fate by repressing the selector Hox gene egl-5 and the effector gene mec-3. Development *130*, 3831-3840.
Tsechpenakis, G., Bianchi, L., Metaxas, D., and Driscoll, M. (2008). A Novel Computational Approach for Simultaneous Tracking and Feature Extraction of C. elegans Populations in Fluid Environments. IEEE Transactions on Biomedical Engineering.

Vollrath, M.A., Kwan, K.Y., and Corey, D.P. (2007). The Micromachinery of Mechanotransduction in Hair Cells. Annual Review of Neuroscience *30*, 339-365.
Waldmann, R., Champigny, G., Bassilana, F., Heurteaux, C., and Lazdunski, M. (1997). A proton-gated cation channel involved in acid-sensing. Nature *386*, 173-177.
Waldmann, R., and Lazdunski, M. (1998). H(+)-gated cation channels: neuronal acid sensors in the NaC/DEG family of ion channels. Curr Opin Neurobiol *8*, 418-424.
Way, J.C., and Chalfie, M. (1989). The mec-3 gene of Caenorhabditis elegans requires its own product for maintained expression and is expressed in three neuronal cell types. Genes Dev *3*, 1823-1833.
Wu, J., Duggan, A., and Chalfie, M. (2001). Inhibition of touch cell fate by egl-44 and egl-46 in C. elegans. Genes Dev *15*, 789-802.
Xiong, Z.G., Zhu, X.M., Chu, X.P., Minami, M., Hey, J., Wei, W.L., MacDonald, J.F., Wemmie, J.A., Price, M.P., Welsh, M.J.*, et al.* (2004). Neuroprotection in ischemia: blocking calcium-permeable acid-sensing ion channels. Cell *118*, 687-698.
Zhang, S., Arnadottir, J., Keller, C., Caldwell, G.A., Yao, C.A., and Chalfie, M. (2004). MEC-2 is recruited to the putative mechanosensory complex in C. elegans touch receptor neurons through its stomatin-like domain. Curr Biol *14*, 1888-1896.
Zhang, W., Bianchi, L., Lee, W.H., Wang, Y., Israel, S., and Driscoll, M. (2008). Intersubunit interactions between mutant DEG/ENaCs induce synthetic neurotoxicity. Cell Death Differ *15*, 1794-1803.

Table Legends

Table 2: EMS-inducible point mutations in the MEC-4 N-terminal intracellular domain. I first list (left columns) the possible EMS-induced mutations that could affect the intracellular MEC-4 amino terminal structure and indicated what amino acid substitutions they would be expected to induce. The right column indicates site-directed substitutions I tested. Only a few of our predicted function-perturbed sites could have been generated as GC to AT transitions as expected for EMS mutagenesis.

Table 3: *in vitro* structural and *in vivo* functional consequences of MEC-4 N mutants. Based on insights from the MEC-4 N structure, substitutions predicted to perturb or maintain the MEC-4 N structure were tested *in vitro* and *in vivo*. Predicted structure perturbing mutations involved buried hydrophobic residues or residues may actual contact while predicted non- structure perturbing mutations involved solvent exposed hydrophobic residues.

Table 4: Primers for site-directed mutagenesis. Listed are primers used for sited-directed mutagenesis. Two kits from NEB and Stratagene were used to make mutations on *mec-4* cDNA (N-terminal fragment) and *mec-4* genomic DNA. Mutations close to intron 1 required separate primers for cDNA and genomic DNA

(for injection, labeled as *in vivo* above). Two kits have different strategies for primer design. Mutation sites were located in the center of both sense and antisense primers (overlapped) for the Stratagene kit and in the center of sense primer (non-overlapped with antisense primer) for the NEB kit. NEB Phusion site-directed mutagenesis kit also required 5'-Phosphorylated modified primers*.

Figure Legends

Figure 1: Hair Cells and the tip links. a) A single hair bundle array of stereocilia, some remain connected by tip links (arrowhead) (Hudspeth, 2008). b) Two stereocilia and the tip link extending between them (scale bar=0.1 μm). c) Deflection of hair bundle. Stereocilia tips remain in contact. d) Model of transduction. Shearing with positive deflection increases tension in tip links, which pull open a transduction channel at each end. Myosin motors slip or climb to restore resting tension. An elastic gating spring likely exists between a channel and the actin cytoskeleton (Vollrath et al., 2007). e) Model of CDH23 and PCDH15 localization at tip links (Kazmierczak et al., 2007).

Figure 2: Touch neurons in *C. elegans.* a) There are six gentle touch neurons: PLMs, ALMs, AVM, and PVM (pink); and two pairs of harsh touch neurons (blue): FLPs and PVDs. Cameleon data show that the gentle touch neurons also respond to harsh touch (two colors) using a mechanism that does not require MEC-4 and MEC-2. b) Cartoon diagram of FLP position near the *C. elegans* head; green indicates the pharynx. FLP has been suggested to respond to harsh touch. Diagram is from WormAtlas (http://www.wormatlas.org). c) Cartoon diagram of PVD. The PVD cell bodies are located in the posterior, but note the extensive branching of the process that might enable the sensory field of the neuron to be

over most of the body surface. PVDL and PVDR are symmetric, figure shows PVDL only. Diagram is from WormAtlas (http://www.wormatlas.org).

Figure 3: Summary of MEC-10 mutant subunits previously identified in genetic screens. a) Schematic representation of a MEC-10 subunit showing the position of the EMS mutations precisely analyzed with respect to the subunit structure. TM and CRD stand for transmembrane domain and cysteine-rich domain. Mutation *e1715* (S105F) is within a conserved N-terminal region: residue corresponding to MEC-10 S105 is either an S or a T in most family members across species. b) Sequence alignment of the second transmembrane domain of MEC-10 with other DEG/ENaCs. The positions of the MEC-10 amino acid substitutions encoded by point mutations are shown by the arrows; skull and crossbones indicates the "d" position where large sidechain amino acid substitutions can be neurotoxic.

Figure 4: The extracellular loop and 2nd transmembrane domain of MEC-10 are truncated in the *mec-10(tm1552)* deletion strain. a) *mec-10(tm1552)* has a deletion that removes sequences of exon 5 and part of exon 6. The deletion is 448 bp and impacts the extracellular part of MEC-10. Predicted sequence shows a frameshift with three premature stop codons (the first one is TAA at the end of the sequence below) very close to the deletion site

(……tctattcatattttt-deletion-TTTATGCAGCAAAAAAAGCTAA). This suggests that most of the extracellular part and 2nd transmembrane domain of MEC-10 is missing in this mutant strain. Red arrows indicate the region corresponding to primer pair for RT-PCR. Primers were designed to avoid the homologous sequences between *mec-4* and *mec-10*. Purple arrow shows the region corresponding to one of the primers used to identify the deletion, another primer is inside the intron 2. Blue underline indicates the region corresponding to deleted sequence. Green underlines indicate the 1st and 2nd transmembrane domain. Star indicates the MEC-4(d) (MEC-4(A713V)) and MEC-10(d) (MEC-10(A673V)) amino acid change. b) A pair of primers with sequence 5'-GTAGGGTCTGCAACTAGCTC-3' and 5'-TGGGAGGGAGCTTCATCTTA-3' were used to identify the deleted gene from the wild type. Blue arrows indicate the position of primers. Blue rectangle shows the deleted sequence. c) Single-worm PCR from *mec-10(tm1552)* and wild type strains gives products with length of 1644 and 2092 bps respectively. d) Primer pair with sequence 5'-AAATTATCTCGCAAGTGACACTAACTTTCT-3' and 5'-CCAAAGTATTCCCATAAATTCAATACCATT-3' were used for RT-PCR to amplify the mRNA in both strains. No specific cDNA can be recovered from the mutant strain, the wild type strain produces a detectable band. RT-PCR products with length 824 and 936 bps from *mec-10(ok1104)* and N2 total RNA. *mec-10(tm1552)* did not give any significative RT-PCR products.

Figure 5: The *mec-10* deletion mutant is strongly insensitive to gentle touch. The bars indicate the percentage of responses to 5 continuous gentle touch tests for each strain indicated. Most *mec-10(tm1552)* worms only respond about once during the test. Note that the *mec-10(tm1552)* strain is not as defective in touch response as is the *mec-4(d)* strain in which touch receptor neurons become necrotic and die. *mec-10(tm1552)* is touch-insensitive. Point mutant *mec-10(e1515)* is only modestly less sensitive. I conclude that the paucity of *mec-10* alleles identified in genetic screens cannot be explained by suggesting that *mec-10* null mutants have no touch phenotype. Statistical significances were tested by t-test. * $p < 0.05$ versus *mec-3(e1338)*, ** $p < 0.005$ versus *mec-3(e1338)*, + $p < 0.05$ versus N2, ++ $p < 0.005$ versus N2.

Figure 6: The *mec-10* deletion mutant decreases, but does not eliminate sensitivity to harsh touch. Harsh touch tests were delivered 5 times on each worm by platinum wire. *mec-3(e1338)* and N2 were used as negative and positive controls. Mutant strains insensitive to gentle touch respond to harsh touch at different level. *mec-4* and *mec-10* single mutant strains do respond to harsher stimuli. *mec-10(null)* background decreases the sensitivity of *mec-4(null)* and *mec-4(d)* significantly. Statistical significance was respecting tested by t-test. ** $p < 0.005$.

Figure 7: Body bend frequency for swimming. I manually scored the number of body bends beginning one minute after animals were transferred into 50 μl of M9 buffer, room temperature. Each bar represents the average from at least 30 individually scored animals. Worms with gentle touch defect, such as *mec-4(u253),* *mec-3(e1338)*, and *mec-10(e1515)* have higher bend frequency, as do the double mutants *mec-10(tm1552) mec-4(u253)* and *mec-10(tm1552) mec-4(d)*. *mec-10(tm1552)* alone did not show a significant difference compared to wild type N2 worms. Null *mec-4* strain with normal extrachromosome *mec-4 (mec-4(u253); Ex[mec-4])*, can be recovered for changes in body bend frequency. The chimeria *mec-4extra+mec-10intra* can also lower the bend frequency to close to the bend frequency of N2, but the *mec-4intra+mec-10extra* can not. Statistical significance was tested by t-test. * $p < 0.05$ versus N2, ** $p < 0.005$ versus N2.

Figure 8: Computer generated comparison of position changes relative to the plate for swimming animals. Average distance covered (a) and motion (b) per frame by swimming animals. *mec-3(e1338)* has a larger moving distance than most strains. These data support *mec-3(e1338)* is a hyperactive swimmer and suggest that overexpression of *mec-4* can hyperactivate motion/prove. Number of videos used for each genotype was 6 to 10 (30 to 100 animals). Statistical significance was tested by t-test. * $p < 0.05$ versus N2, ** $p < 0.005$ versus N2.

Figure 9: Comparison of local deformation. a) Scores for average animal deformation per frame. We extracted the deformation from frame to frame and converted pixel scores to μm. b) Scores for absolute animal deformation per frame. We scored deformation as compared to a straight-line connecting head and tail. These data suggest that *mec-10 mec-4* doubles exhibit uncoordinated swimming and again suggest that overexpression of *mec-4* can change swimming behavior. Number of videos used for each genotype was 6 to 10 (30 to 100 animals). Statistical significance was tested by t-test. * $p < 0.05$ versus N2, ** $p < 0.005$ versus N2.

Figure 10: Comparison of body shape profiles of wild type and mutants. We monitored the body shape during the swimming. Both symmetric (I and O) and asymmetric (S and C) shape were recorded. *mec-10(tm1552)* shows the highest ratio appearing in C and O shape. The lowest symmetry of *mec-10(tm1552)* also confirmed this. However, none of these strains show statistically significant differences in symmetry. Number of videos used for each genotype was 6 to 10 (30 to 100 animals).

Figure 11: MEC-10(d) induces a minor necrosis phenotype with or without *mec-10* wild type in the background. Worms with integrated *mec-10(d)* point mutation (P_{mec-4}*mec-10(d)GFP*) show a minor necrosis phenotype. Crossing with

the *mec-10* deletion strain eliminated the endogenous *mec-10* wild type gene from the *mec-10(d)* background, leaving *mec-10(d)* only. However, no significant changes in the extent of *mec-10(d)*-induced neurodegeneration were observed. Each bar represents the average number of live PLM cells. a) Live cells were counted as the # of neurons without necrotic vacuoles during L1 stage. The p-value between *mec-10(tm1552);*P_{mec-4}*mec-10(d)GFPIs22* and P_{mec-4}*mec-10(d)GFPIs22* is 0.91329, which is not significant. b) Cells were counted as live PLMs expressing GFP (*uIs22*[*mec-3::gfp dpy-20*(+)] (Toker et al., 2003; Wu et al., 2001)) during the L4 stage. p-value is 0.608755. I conclude *mec-10(+)* neither enhances nor suppresses *mec-10(d)*-induced neurodegeneration. c) The p-value between *mec-10(tm1552) mec-4(d)* and *mec-4(d)* is 0.734387, which is not significant. This also shows that *mec-10(tm1552)* neither enhances nor suppresses *mec-4(d)*-induced neurodegeneration. d) A typical vacuole caused by degenerating PLMs in a *mec-4(d)* L1 worm's tail.

Figure 12: MEC-10 mutant subunits suppress MEC-4(d) currents more than WT. a) Average Na+ current at −100 mV was recorded from oocytes injected with *mec-4(d)*, *mec-2* and *mec-6* plus the *mec-10* subunit type indicated on the x axis, and from non-injected oocytes. n is 5 to 27. Data are the mean ± s.e.m. The dashed line indicates the current level that is obtained when oocytes are injected with *mec-4(d)*, *mec-2* and *mec-6* (Bianchi et al., 2004; Goodman et al., 2002). The

mutant MEC-10 subunits appear to inhibit current more than the wt MEC-10 or the MEC-10(d) subunits. Thus, at this level of analysis, the mutant MEC-10 subunits do have somewhat of a negative impact on channel conductance. b) Fluorescent photographs of oocytes expressing MEC-4(d), MEC-2, MEC-6 plus either wild type MEC-10::GFP or MEC-10::GFP point mutations (S105F, G676R, L679R, G680E, G684R), stained with antibody to GFP. A non-injected oocyte serves as negative control. Pictures were taken under the same magnification and use the same exposure time. Materials inside oocytes did not reflect UV-light homogeneously. At least 3 oocytes were sliced and checked for each mutation. I conclude that the MEC-10 subunits do make it to the oocyte surface with the possible exception of L679R and therefore mutant subunits are unlikely to disrupt conductance by preventing surface expression.

Figure 13: Sequence structures of *mec-10*, *mec-4*, and chimeric proteins. Two chimeras were made by switching the extracellular domain and transmembrane domains between MEC-4 and MEC-10. DNA sequences were cut and re-ligated at the two transmembrane domains (darker green and red boxes), which are very conserved in these two proteins. Three Cys-rich domains (CRDs, light blue boxes), extracellular regulator domain (ERD, blue box), and neurototoxin-related domain (NTD, blue box) in MEC-4 extracellular domain are also shown.

Figure 14: Chimeric MEC proteins do not fully restore MEC-4 or MEC-10 defects. Chimeras made by switching extracellular and transmembrane domains of MEC-4 and MEC-10 were injected into *mec-4(u253)* and *mec-10(tm1552)* background respectively. *mec-4* and *mec-10* wild type DNA were injected into null strains as positive control. a) None of the chimeras can totally recover the gentle touch sensory function of touch neurons. MEC-4 deficiency cannot be complemented at all; on the other hand MEC-10 deletion can be partially complemented by the chimera with the *mec-4extra/mec-10intra* variant. Thus, MEC-10's critical function in touch sensation may be conferred by the transmembrane and intracellular domains. b) I used a hybrid protein MEC-10 with GFP at C-terminal. Chimeras with intracellular (N- and C-terminals) MEC-10 domain also contain the GFP. GFP expression indicates that MEC-10long GFP and chimeras can be expressed normally in touch cells. Statistical significance was tested by t-test. * $p < 0.05$, ** $p < 0.005$.

Figure 15: Protein sequence of the first 106 amino acids in MEC-4. Red bars indicate five α-helix structures. Different colors indicate how each structural domain correlates to following ribbon diagrams.

Figure 16: a) Ribbon diagram of MEC-4 N with W82 depicted with orange sticks and DEG/ENaC conserved residues (91 – 99) depicted with red sticks. Note that

the conserved region is situated in a non-structured loop. There are two small (2-3 residue) beta elements in the last quarter of the conserved sequence that appear to form a *very* small anti-parallel sheet. Five helices are numbered. b) Predicted MEC-4 N electrostatic potential surfaces. Negatively charged surfaces are colored red and positively charged surfaces are colored blue. MEC-4 N is a polar molecule with one side possessing a large negatively charged face while the nearly opposing face is positively charged. c) Ribbon diagram highlighting MEC-4 N's three cysteines (shown as sticks) and the metal perturbed residues (highlighted blue). Their positioning in proximity in 3-D space suggests they might act together in metal binding. d) Addition of the stomatin-related domain of MEC-2 and the amino terminal domain of MEC-10 induce distinct sets of ^{15}N HSCQ peak perturbations. Addition of MEC-2 S induces peak perturbations corresponding to residues of the α1 – α2 loop, α3 – α4 loop, and α4 (A, blue surface). Addition of MEC-10 N induces peak perturbations corresponding to the residues of MEC-4 N's transiently ordered domain and its conserved DEG/ENaC sequence (B, red surface).

Figure 17: *in vivo* touch sensitivity assays for *mec-4* mutations that might perturb structure (and therefore function). Worms with the defective null *mec-4(u253)* deletion mutation are touch-insensitive and this strain was host for one transgene. Injections with wild type and *mec-4* genomic DNA bearing engineered test mutations partially rescued responses during 5 continuous gentle touch tests. Wild type strains *mec-4(+)* and *rol-6* strain (pRF 4 bearing the

dominant allele of *rol-6(su1006)* which causes animals to roll when moving (Kramer et al., 1990) are positive and negative controls, respectively.) a. Assays of MEC-4 mutants harboring substitutions predicted not to perturb structure. b. Assays of MEC-4 mutants harboring substitutions predicted to perturb structure. c. Substitutions for three cysteines and the conserved residue H94 on the MEC-4 N-terminal. Statistical significances were tested by t-test. * $p < 0.05$ versus *rol-6*, ** $p < 0.005$ versus *rol-6*, + $p < 0.05$ versus *mec-4(+)*, ++ $p < 0.005$ versus *mec-4(+)*.

Figure 18: *in vivo* touch sensitivity assays for *mec-4* mutations that might perturb structure (and therefore function). Over-expression of the wild type MEC-4 in the *mec-4(+)* background can partially negatively regulate touch sensitivity (Hong et al., 2000), and the wild type N2 strain was used for all assays .Injections with *mec-4* genomic DNA bearing engineered test mutations showed different levels of dominant negative regulation during 5 continuous gentle touch tests. Wild type strains *mec-4(+)* and *rol-6* strain (pRF 4 bearing the dominant allele of *rol-6(su1006)* which causes animals to roll when moving (Kramer et al., 1990) are positive and negative controls respectively.) a. Test for dominant negative action - MEC-4 mutants predicted not to perturb structure. b. Test for dominant negative action of MEC-4 mutants predicted to change structure. c. Test for dominant negative action of substitutions for three cysteines and H94 on mec-4 N-terminal. * $p < 0.05$ versus *rol-6*, ** $p < 0.005$ versus *rol-6*, + $p < 0.05$ versus *mec-4(+)*, ++ $p < 0.005$ versus *mec-4(+)*.

Figure 19: Ribbon diagram of MEC-4N(V23) and ^{15}N HSQC spectrum of MEC-4N(V23E).

Figure 20: Ribbon diagram of MEC-4N(I65).

Figure 21: Ribbon diagram of MEC-4N(L7) and ^{15}N HSQC spectrum of MEC-4N(L7E).

Figure 22: Ribbon diagram of MEC-4N(Y19) and ^{15}N HSQC spectrum of MEC-4N(Y19E).

Figure 23: Ribbon diagram of MEC-4N(M20).

Fig. 24. Ribbon diagram of MEC-4N(L28).

Figure 25: Ribbon diagram of MEC-4N(Y30) and ^{15}N HSQC spectrum of MEC-4N(Y30E).

Figure 26: Ribbon diagram of MEC-4N(L31) and ^{15}N HSQC spectrum of MEC-4N(L31E)

Figure 27: Ribbon diagram of MEC-4N(F37).

Figure 28: Ribbon diagram of MEC-4N(Y43) and ^{15}N HSQC spectrum of MEC-4N(Y43E).

Figure 29: Ribbon diagram of MEC-4N(F69).

Figure 30: Ribbon diagram of MEC-4N(71PKLL74) and ^{15}N HSQC spectrum of MEC-4N(Δ71PKLL74).

Figure 31: Ribbon diagram of MEC-4N(W82) and ^{15}N HSQC spectrum of MEC-4N(W82E).

Figure 32: Ribbon diagram of MEC-4N(F84) and ^{15}N HSQC spectrum of MEC-4N(F84E).

Figure 33: Ribbon diagram of MEC-4N(F87) and ^{15}N HSQC spectrum of MEC-4N(F87E).

Fig. 34. Ribbon diagram of MEC-4N(C52), MEC-4N(C62), and MEC-4N(C88) and ^{15}N HSQC spectrum of MEC-4N(C52A), MEC-4N(C62A), and MEC-4N(C88A).

Figure 35: ^{15}N HSQC spectrum of MEC-4N(H94A).

Figure 36: Puncta number and length changes in MEC-4 N-terminal mutant worms. a) Worms were whole mount fixed and labeled by MEC-2 antibody. Pictures were analyzed by the software ImageJ (http://rsbweb.nih.gov/ij/). The numbers of puncta in touch neuron processes were measured and the average numbers per mm were calculated. *mec-4(u253)* has significant decreased number

of puncta versus the wild type worms and is used as negative control. Most mutants expected C52A and C52AC62A have lower puncta density in neuron processes. b) Average length of puncta and blank areas between puncta were measured. The length of puncta is not the only factor that changes the average number per mm. Blank areas between puncta show more significant changes between mutants. Statistical significances were tested by t-test. * $p < 0.05$ versus *mec-4(u253)*, ** $p < 0.005$ versus *mec-4(u253)*, + $p < 0.05$ versus N2, ++ $p < 0.005$ versus N2.

Figure 37: Sequence alignment of 3 Cysteine regions in MEC-4 and other DEG/ENaC superfamily members. The amino termini of $\alpha\beta\gamma$ mammalian ENaC channel subunits contain 8 cysteine residues, and 5 of them are conserved among family members (not all shown here). Cys residues are highlighted by red. C52 and C62 (numbered by MEC-4) are not highly conserved in the primary sequence. C88 is conserved in C. elegans degenerins and mammalian ENaCs family. Histine (H94) is highly conserved through all family members. Dark blocks indicate the identical amino acids among all or part of the proteins. Gray blocks indicate the homologous ones.

Table 2: EMS-inducible point mutations in the MEC-4 N-terminal intracellular domain.

Mutation Site	Base change	Code change	EMS Alteration	Site-directed substitution
19	C-T	CTG-tTG	Silent	
21	G-A	CTG-CTa	Silent	
19, 21	C-T, G-A	CTG-tTa	Silent	
19, 20	C-G, T-A	CTG-gaG		L7E
57	C-T	TAC-TAt	Silent	
55, 57	T-G, C-A	TAC-gAa		Y19E
60	G-A	ATG-ATa	M20I	
58, 59	A-G, T-A	ATG-gaG		M20E
67	G-A	GTT-aTT	V23I	
68,69	T-A,T-A	GTT-Gtt		V23E
82, 83	T-G, T-A	TTA-gaA		L28E
90	C-T	TAC-TAt	Silent	
88, 90	T-G, C-A	TAC-gAa		Y30E
91, 92	T-G, T-A	TTA-gaA		L31E
127,129	T-G, T-A	TAT-gAa		Y43E
155	G-A	TGT-TaT	C52Y	
154, 155	T-G, G-C	TGT-gcT		C52A
185	G-A	TGT-TaT	C62Y	
184, 185	T-G, G-C	TGT-gcT		C62A
193, 194, 195	A-G, T-A, T-A	ATT-gaa		I65E
245	G-A	TGG-TaG	W82Stop	
246	G-A	TGG-TGa	W82Stop	
245, 246	G-A, G-A	TGG-Taa	W82Stop	
244, 245	T-G, G-A	TGG-gaG		W82E
252	C-T	TTC-TTt	Silent	
250, 251, 252	T-G, T-A, C-A	TTC-gaa		F84E
259, 260, 261	T-G, T-A, T-A	TTT-gaa		F87E
263	G-A	TGC-TaC	C88Y	
264	C-T	TGC-TGt	Silent	
263, 264	G-A, C-T	TGC-Tat	C88Y	
262, 263	T-G, G-C	TGC-gcC		C88A
280	C-T	CAC-tAC	H94Y	
282	C-T	CAC-CAt	Silent	
280, 282	C-T, C-T	CAC-tAt	H94Y	
280, 281	C-G, A-C	CAC-gcC		H94A

Table 3: *in vitro* structural and *in vivo* functional consequences of MEC-4 N mutants.

AA substitution	Location	Structure perturbation prediction[1]	^{15}N HSQC perturbations[2]	Touch perception defect assay result	Dominant negative effect
L7E	α1	Yes	moderate	- -	- -
Y19E	α2	Yes	moderate	- - -	+
M20E	α2	Yes	**major**	- -	+
V23E	α2 - α3 loop	No	moderate	+	+
L28E	α3	No	minor	- - -	+ + +
Y30E	α3	Yes	moderate	- -	+ +
L31E	α3	Yes	**major**	- -	+ + +
F37E	α3	Yes	**major**	- - - -	+ +
Y43E	α4	Yes	moderate	- -	-
C52A	TOR	No	minor	- -	- -
C62A	TOR	No	minor	- -	-
I65E	TOR	No	minor	- -	+
F69E	TOR	Yes	**major**	+	- -
PKLL del[4]	TOR	No	minor	- -	+
W82E	α5	Yes	minor	- -	- -
F84E	α5	Yes	moderate	- - -	+ +
F87E	α5	Yes	moderate	- - -	+ +
C88A	α5	Yes	minor	- - -	+ +
H94A[6]	conserved[5]	No	minor	- - -	+ + +

1. Prediction of whether or not the mutation would perturb the MEC-4 N structure, measured via ^{15}N HSQC perturbations, beyond the site of the mutation. 2. Number of ^{15}N HSQC perturbations peak perturbations greater or equal one half peak width. 3. TOR: Transiently ordered region (res 45-75) 4. Deletion of residues 71-74 (PKLL). 5. Transiently ordered carboxy terminal residues (res 89-103). 6. Previously published touch-inhibiting substitution.

Table 4: Primers for site-directed mutagenesis.

Substitution site	5' Primer (sense)	3' primer (antisense)
NEB kit*		
L7E	CTTCGGGACCCATCCGAGTACATG	GTGTTGGTAGTTTTTCTCGTTTTGCATCCA
Y19E	GACCCATCCGAGGAAATGTCCCAGGTTTAT	CCGAAGGTGTTGGTAGTTTTTCAGGTTTTG
M20E	GACCCATCCGAGTACGAGTCCCAGGTTTAT	CCGAAGGTGTTGGTAGTTTTTCAGGTTTTG
L28E	TGGAGACCCGGAAGCGTACTTACAAGAGACGA	TAAACCTGGGACATGTACTCGGATGGGTCC
Y30E	TGGAGACCCGTTAGCGGAATTACAAGAGACGA	TAAACCTGGGACATGTACTCGGATGGGTCC
Y31E	TGGAGACCCGTTAGCGTACGAACAAGAGACGA	TAAACCTGGGACATGTACTCGGATGGGTCC
F84E	AGCCTGGCATGAAAAAGAGTTTTGCTACAAAA	AGACGTTTGTCATAGGGTAGCAATTTTGGA
F87E	AGCCTGGCATTTCAAAGAGGAATGCTACAAAA	AGACGTTTGTCATAGGGTAGCAATTTTGGA
C52A	GGTTATGGCGAAGCTTTCAACTCTACAGAA	AAAATCTTCATAATATTCTCTTTCTGTCACAAA
C62A *in vivo*	ATTTCCGAATTTCAGGCTGAACTTATTACG	GTTAGATTACTCAGCTGCGACTTTTTGCAA
71-PKLL-74	CCCTATGACAAACGTCTAGCCTGGCATTTC	ATCGAATTCTCCCGTAATAAGTTCACATTG
Stratagene kit		
V23E	CCATCCGAGTACATGTCCCAGGAATATGGAGACCCGTTAGCGTAC	GTACGCTAACGGGTCTCCATATTCCTGGGACATGTACTCGGATGG
Y43E	CTAAATTTGTGACAGAAAGAGAAGAATATGAAGATTTTGGTTATGGC	GCCATAACCAAAATCTTCATATTCTTCTCTTTCTGTCACAAATTTAG
C62A	CTCTACAGAATCAGAAGTACAAGCTGAACTTATTACGGGAGAATTC	GAATTCTCCCGTAATAAGTTCAGCTTGTACTTCTGATTCTGTAGAG
I65E	CAGAAGTACAATGTGAACTTGAAACGGGAGAATTCGATCCAAAATTG	CAATTTTGGATCGAATTCTCCCGTTTCAAGTTCACATTGTACTTCTG
I65E *in vivo*	CCGAATTTCAGTGTGAACTTGAAACGGGAGAATTCGATCCAAAATTG	CAATTTTGGATCGAATTCTCCCGTTTCAAGTTCACACTGAAATTCGG
C88A	GCCTGGCATTTCAAAGAGTTTGCCTACAAAACATCTGCTCACGG	CCGTGAGCAGATGTTTTGTAGGCAAACTCTTTGAAATGCCAGGC
W82E	CCCTATGACAAACGTCTAGCCGAGCATTTCAAAGAGTTTTGCTAC	GTAGCAAAACTCTTTGAAATGCTCGGCTAGACGTTTGTCATAGGG
H94A	GTTTTGCTACAAAACATCTGCTGCCGGAATTCCCATGATTGGTGAAG	CTTCACCAATCATGGGAATTCCGGCAGCAGATGTTTTGTAGCAAAAC

Figure 1: Hair Cells and the tip links.

a)

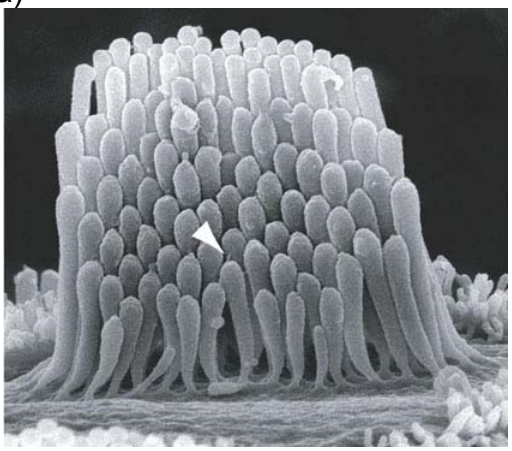

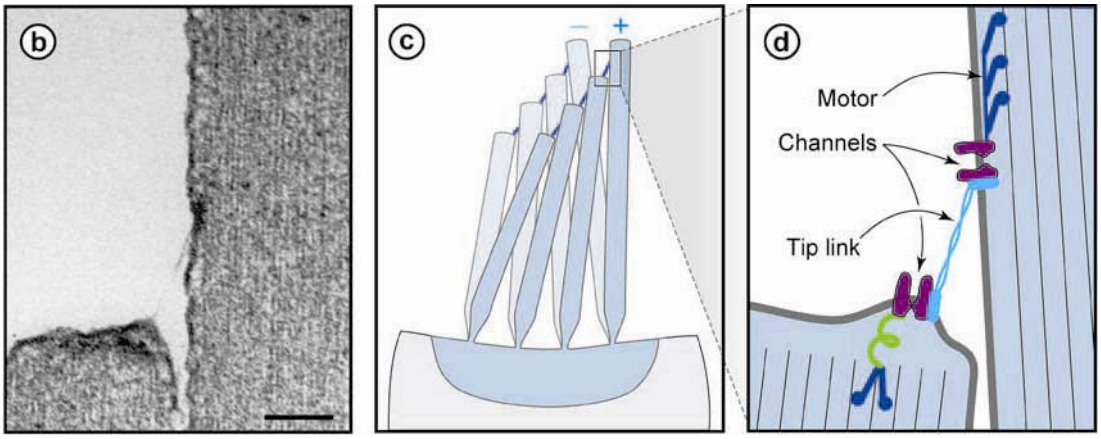

e)

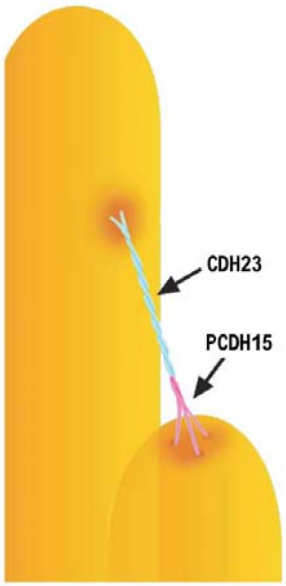

Figure 2: Touch neurons in *C. elegans.*

a)

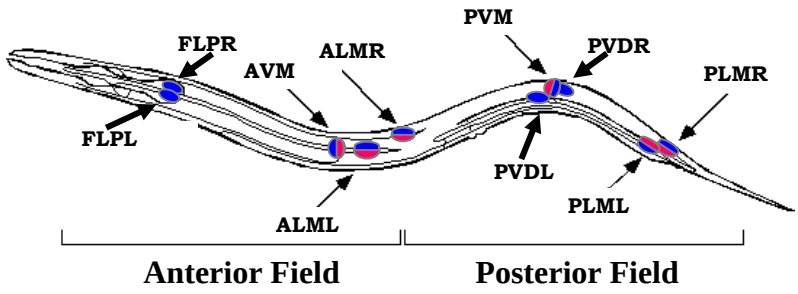

- Gentle touch
Harsh touch

b)

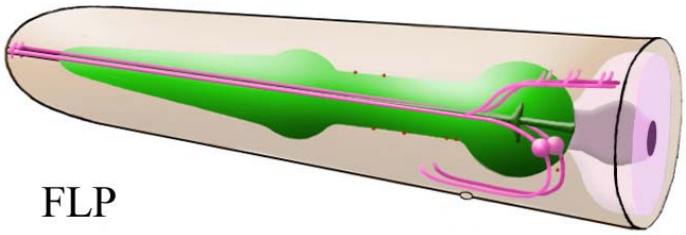

c)

Figure 3: Summary of MEC-10 mutant subunits previously identified in genetic screens.

a)

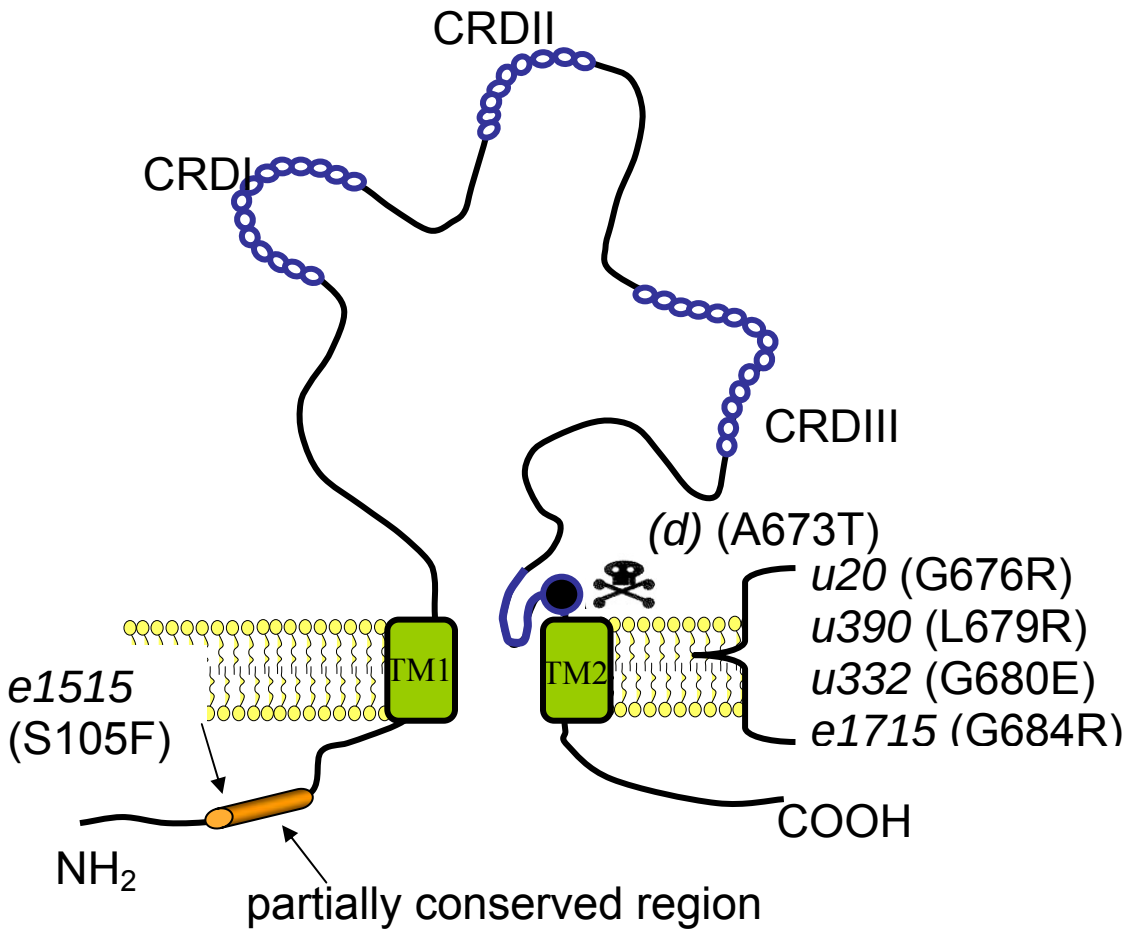

b)

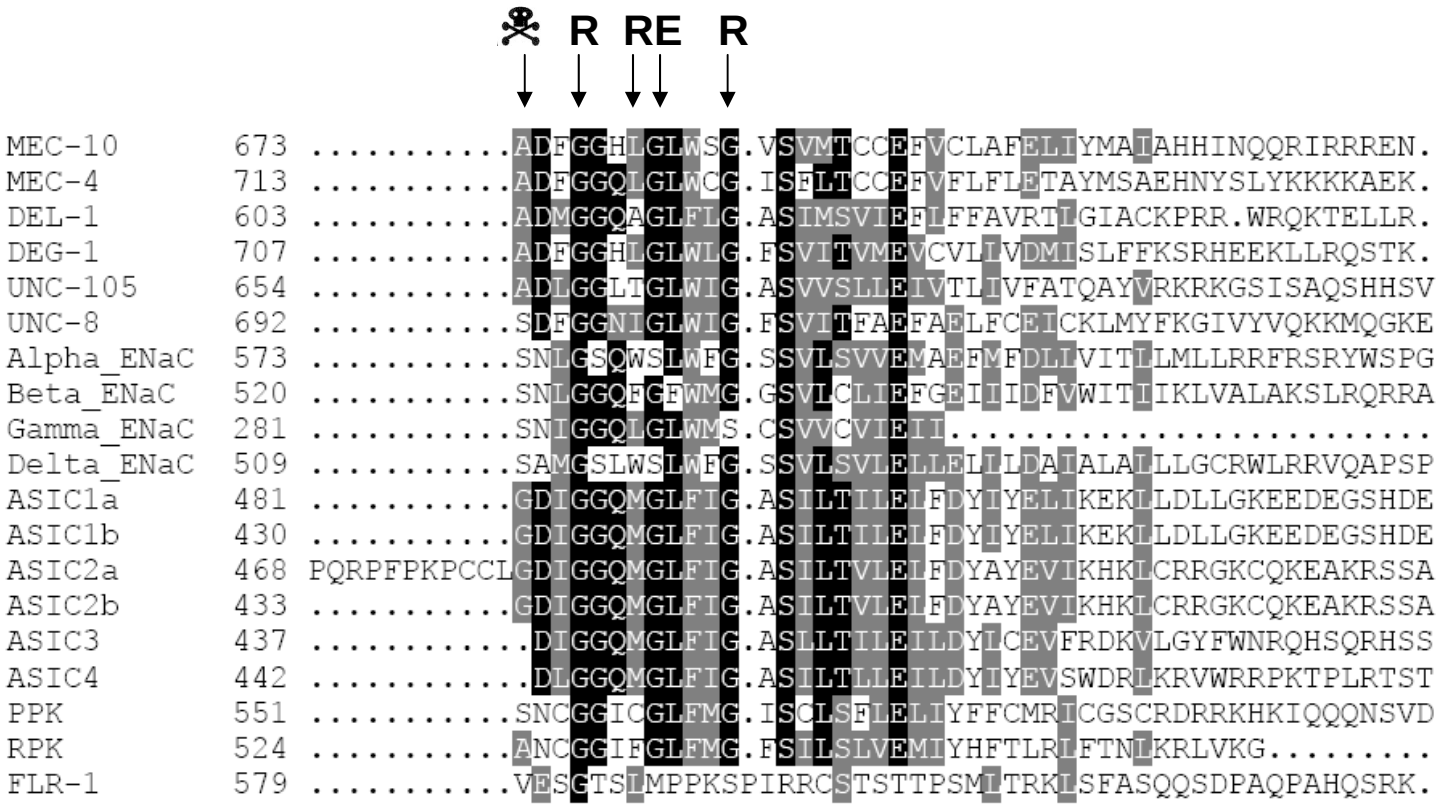
R
RE
R
MEC-10 673 ..........ADFGGHLGLWSG.VSVMTCCEFVCLAFELIYMAIAHHINQQRIRRREN.
MEC-4 713 ..........ADFGGQLGLWCG.ISFLTCCEFVFLFLETAYMSAEHNYSLYKKKKAEK.
DEL-1 603 ..........ADMGGQAGLFLG.ASIMSVIEFLFFAVRTLGIACKPRR.WRQKTELLR.
DEG-1 707 ..........ADFGGHLGLWLG.FSVITVMEVCVLLVDMISLFFKSRHEEKLLRQSTK.
UNC-105 654 ..........ADLGGLTGLWIG.ASVVSLLEIVTLIVFATQAYVRKRKGSISAQSHHSV
UNC-8 692 ..........SDFGGNIGLWIG.FSVITFAEFAELFCEICKLMYFKGIVYVQKKMQGKE
Alpha_ENaC 573 ..........SNLGSQWSLWFG.SSVLSVVEMAEFMFDLLVITLLMLLRRFRSRYWSPG
Beta_ENaC 520 ..........SNLGGQFGFWMG.GSVLCLIEFGEIIIDFVWITIIKLVALAKSLRQRRA
Gamma_ENaC 281 ..........SNIGGQLGLWMS.CSVVCVIEII..........
Delta_ENaC 509 ..........SAMGSLWSLWFG.SSVLSVLELLELLLDAIALALLLGCRWLRRVQAPSP
ASIC1a 481 ..........GDIGGQMGLFIG.ASILTILELFDYIYELIKEKLLDLLGKEEDEGSHDE
ASIC1b 430 ..........GDIGGQMGLFIG.ASILTILELFDYIYELIKEKLLDLLGKEEDEGSHDE
ASIC2a 468 PQRPFPKPCCLGDIGGQMGLFIG.ASILTVLELFDYAYEVIKHKLCRRGKCQKEAKRSSA
ASIC2b 433 ..........GDIGGQMGLFIG.ASILTVLELFDYAYEVIKHKLCRRGKCQKEAKRSSA
ASIC3 437 ....DIGGQMGLFIG.ASLLTILEILDYLCEVFRDKVLGYFWNRQHSQRHSS
ASIC4 442 ....DLGGQMGLFIG.ASILTLLEILDYIYEVSWDRLKRVWRRPKTPLRTST
PPK 551 ..........SNCGGICGLFMG.ISCLSFLELIYFFCMRICGSCRDRRKHKIQQQNSVD
RPK 524 ..........ANCGGIFGLFMG.FSILSLVEMIYHFTLRLFTNLKRLVKG.....
FLR-1 579 ..........VESGTSLMPPKSPIRRCSTSTTPSMLTRKLSFASQQSDPAQPAHQSRK.

Figure 4: The extracellular loop and 2nd transmembrane domain of MEC-10 are truncated in the *mec-10(tm1552)* deletion strain.

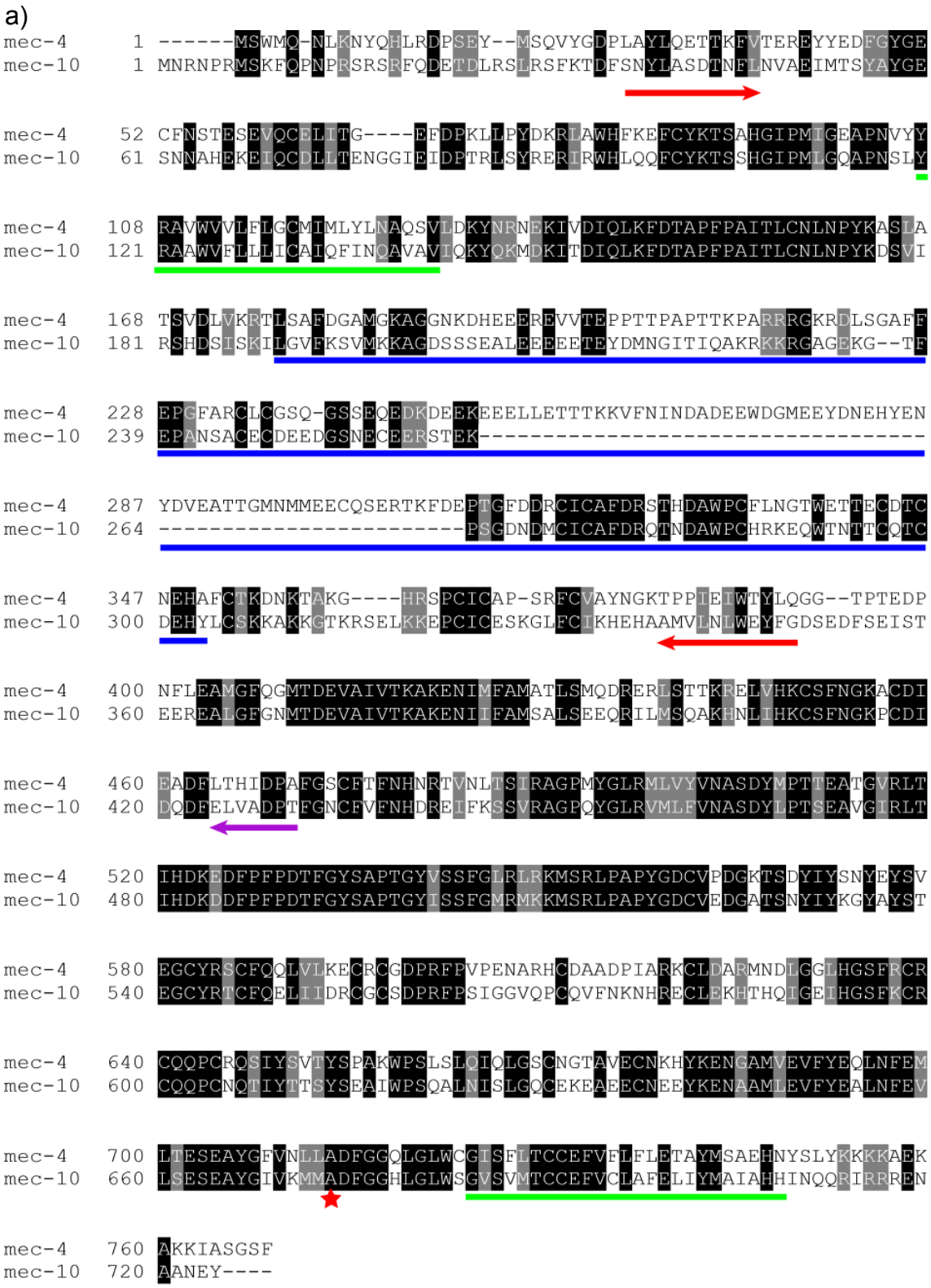

b) mec-10 (F16F9.5)

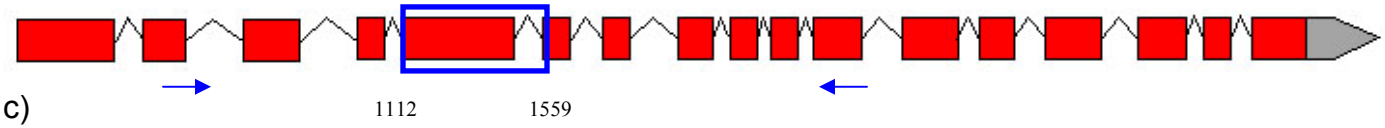

c)

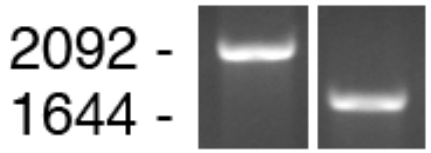

d)

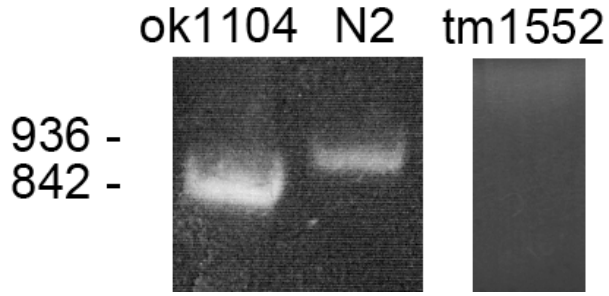

Figure 5: The *mec-10* deletion mutant is strongly insensitive to gentle touch.

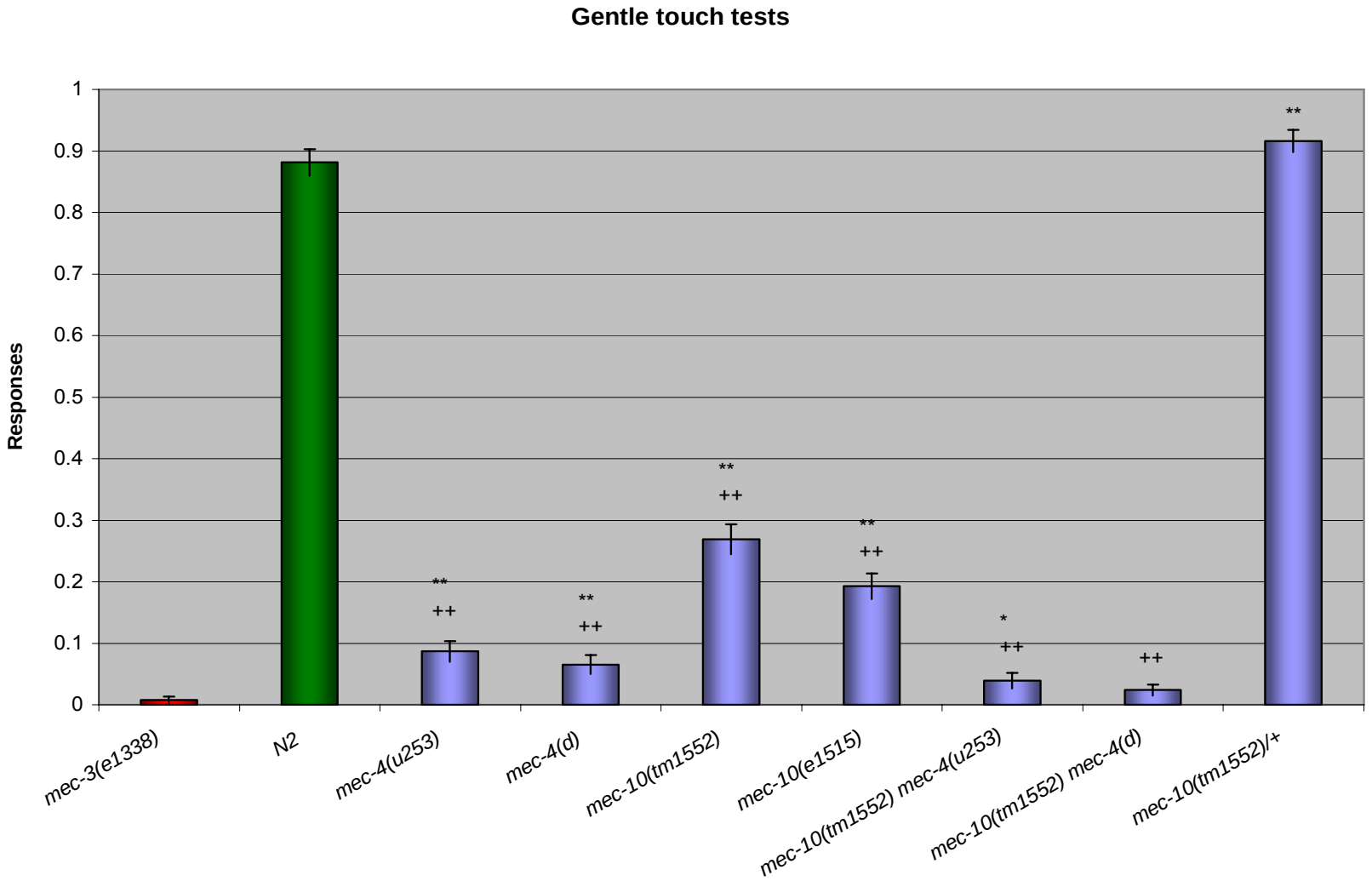

Figure 6: The *mec-10* deletion mutant decreases, but does not eliminate sensitivity to harsh touch.

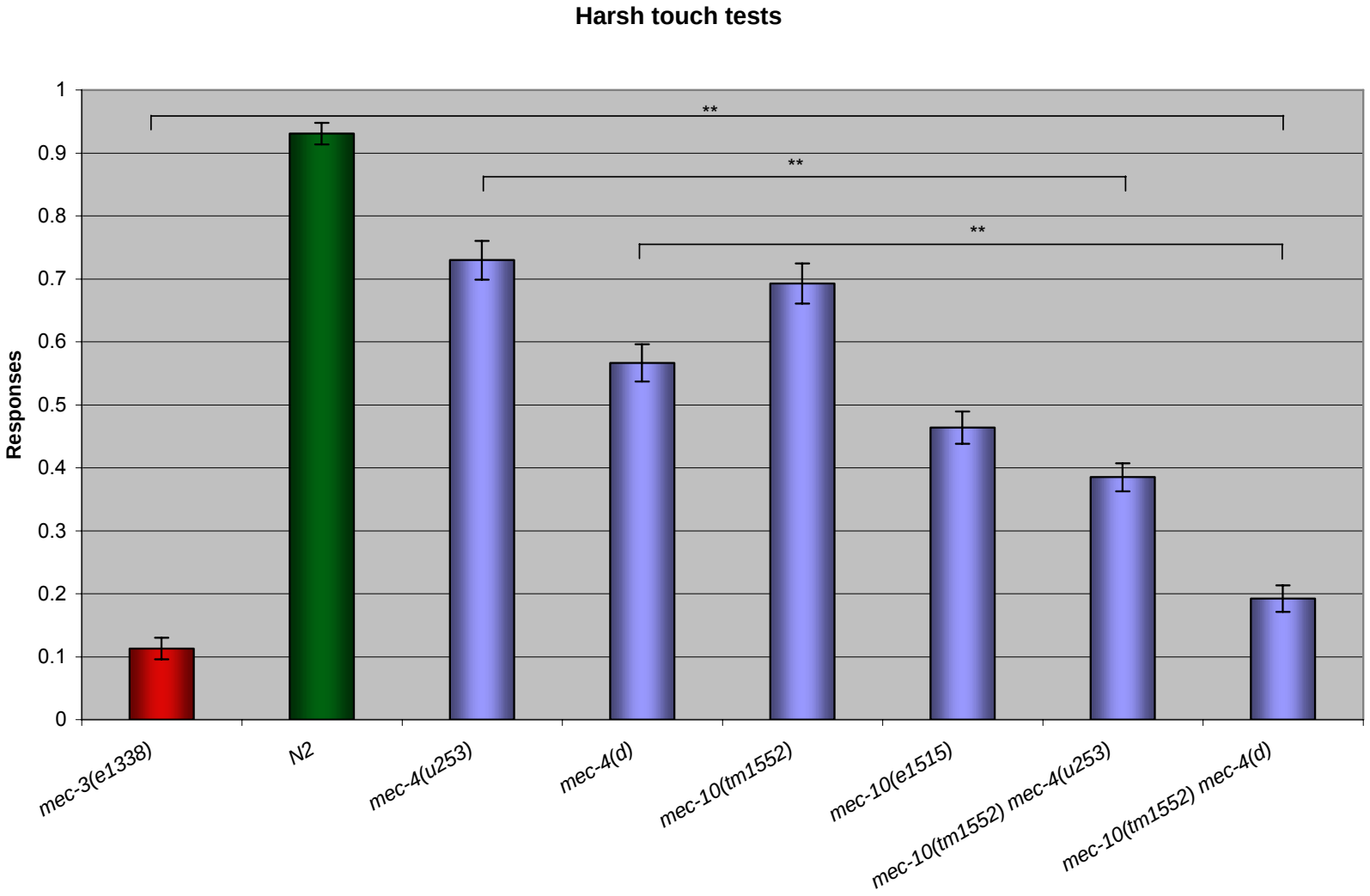

Figure 7: Body bend frequency for swimming.

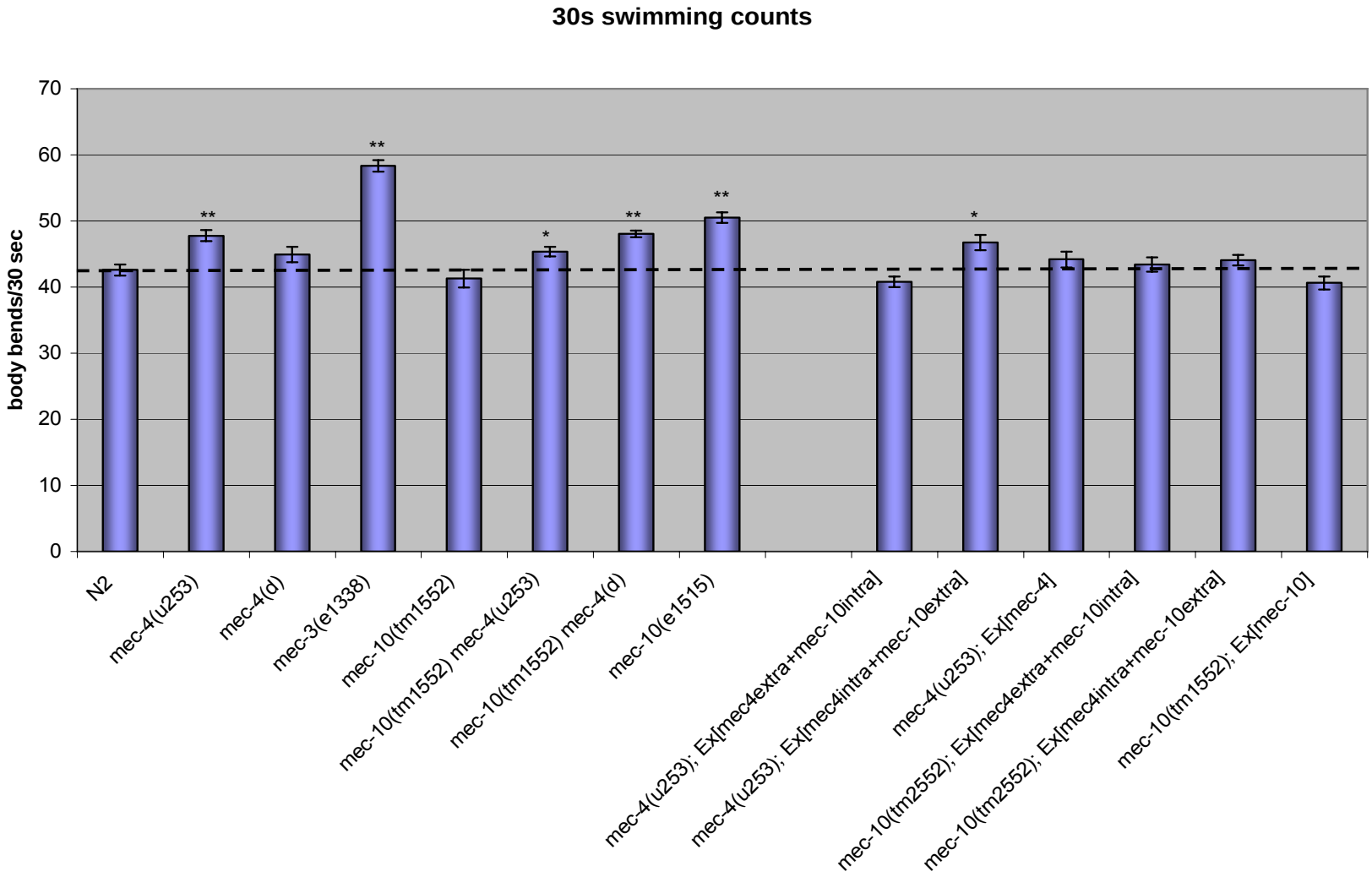

Figure 8: Computer generated comparison of position changes relative to the plate for swimming animals.

a)

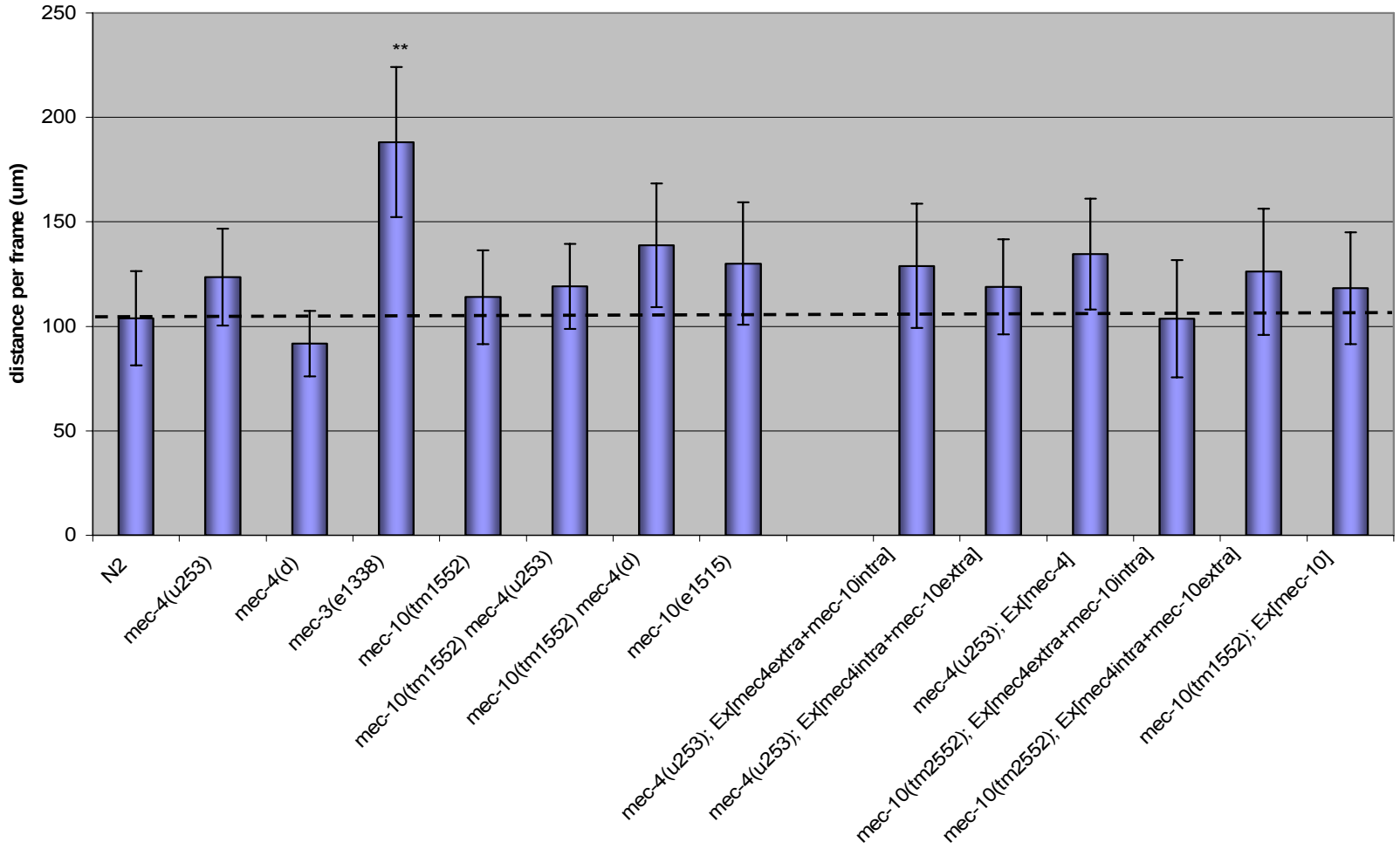

b)

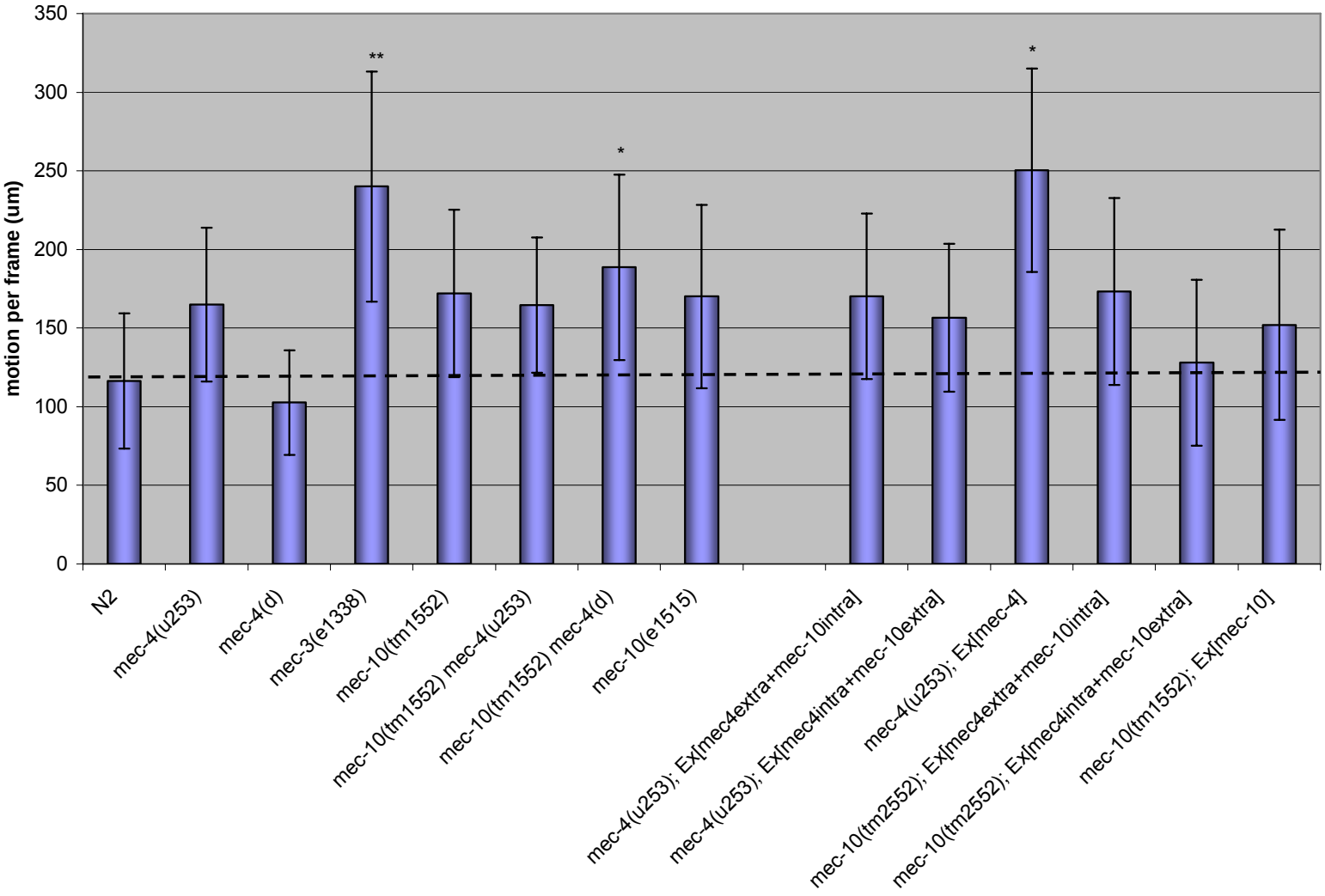
motion per frame (um)
350
300
250
200
150
100
50
0
**
*
*
N2
mec-4(u253)
mec-4(d)
mec-3(e1338)
mec-10(tm1552)
mec-10(tm1552) mec-4(u253)
mec-10(tm1552) mec-4(d)
mec-10(e1515)
mec-4(u253); Ex[mec4extra+mec-10intra]
mec-4(u253); Ex[mec4intra+mec-10extra]
mec-4(u253); Ex[mec-4]
mec-10(tm2552); Ex[mec4extra+mec-10intra]
mec-10(tm2552); Ex[mec4intra+mec-10extra]
mec-10(tm1552); Ex[mec-10]

Figure 9: Comparison of local deformation.

a)

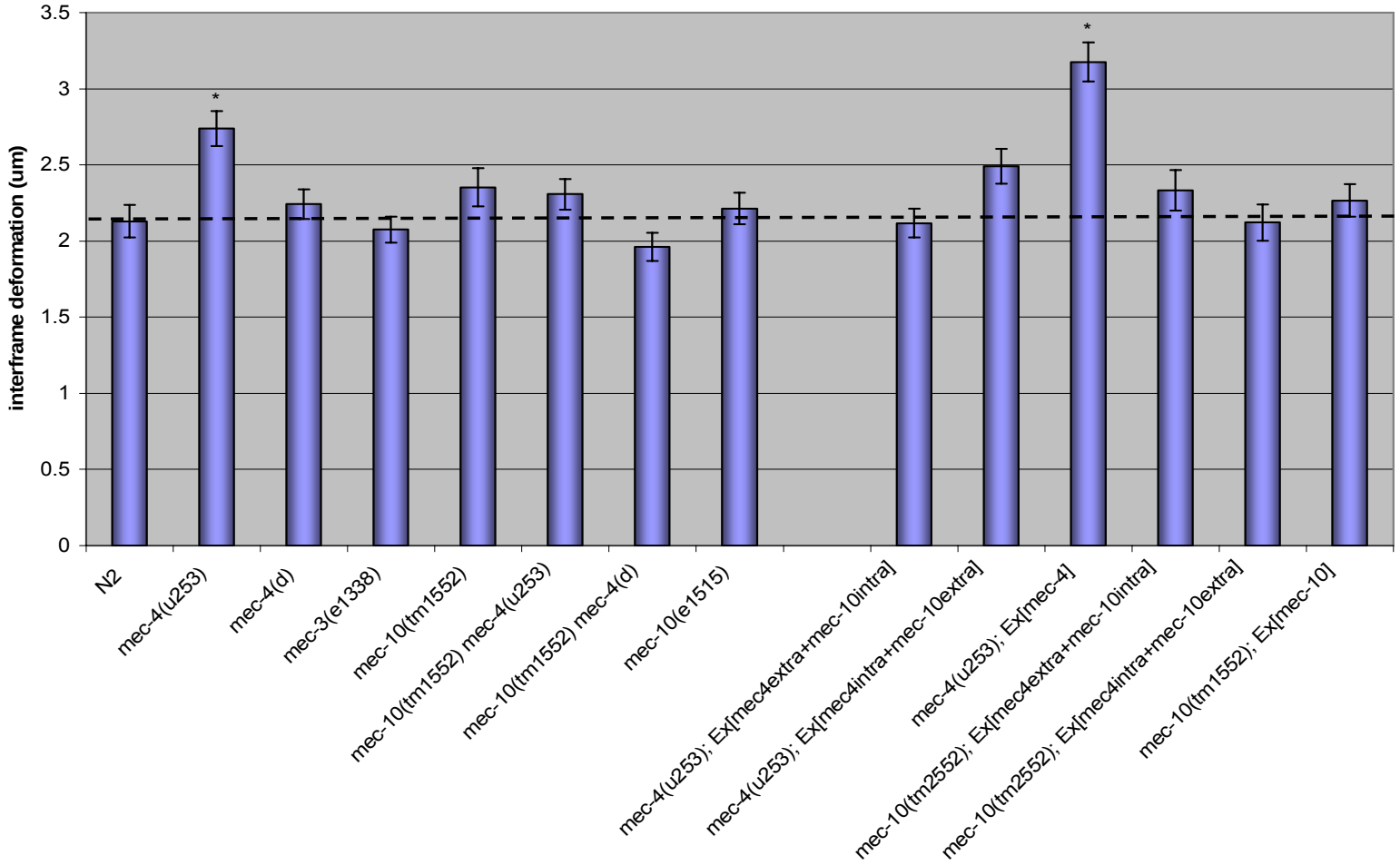

b)

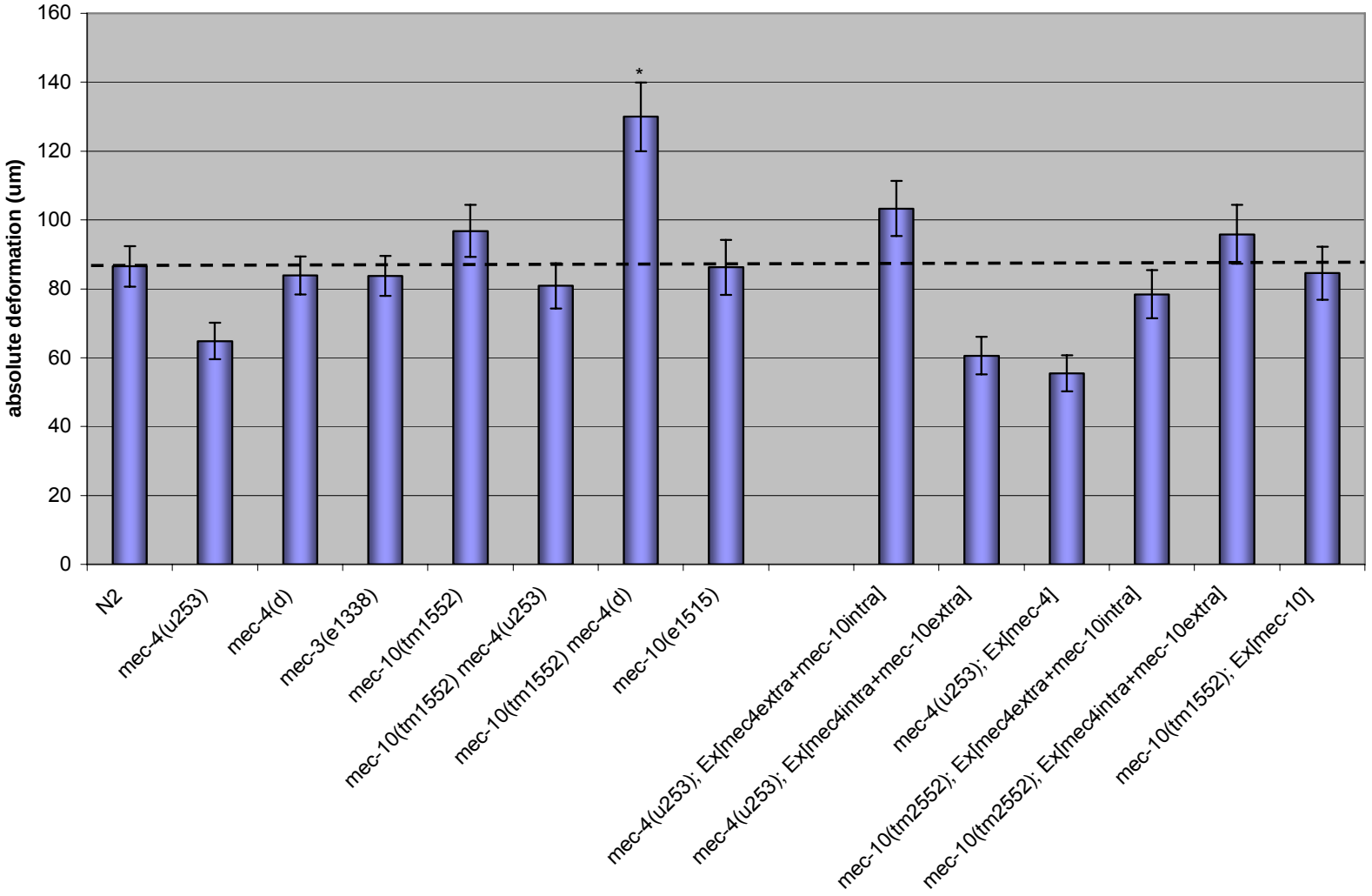
absolute deformation (um)
160
140
120
100
80
60
40
20
0
*
N2
mec-4(u253)
mec-4(d)
mec-3(e1338)
mec-10(tm1552)
mec-10(tm1552) mec-4(u253)
mec-10(tm1552) mec-4(d)
mec-10(e1515)
mec-4(u253); Ex[mec4extra+mec-10intra]
mec-4(u253); Ex[mec4intra+mec-10extra]
mec-4(u253); Ex[mec-4]
mec-10(tm2552); Ex[mec4extra+mec-10intra]
mec-10(tm2552); Ex[mec4intra+mec-10extra]
mec-10(tm1552); Ex[mec-10]

Figure 10: Comparison of body shape profiles of wild type and mutants.

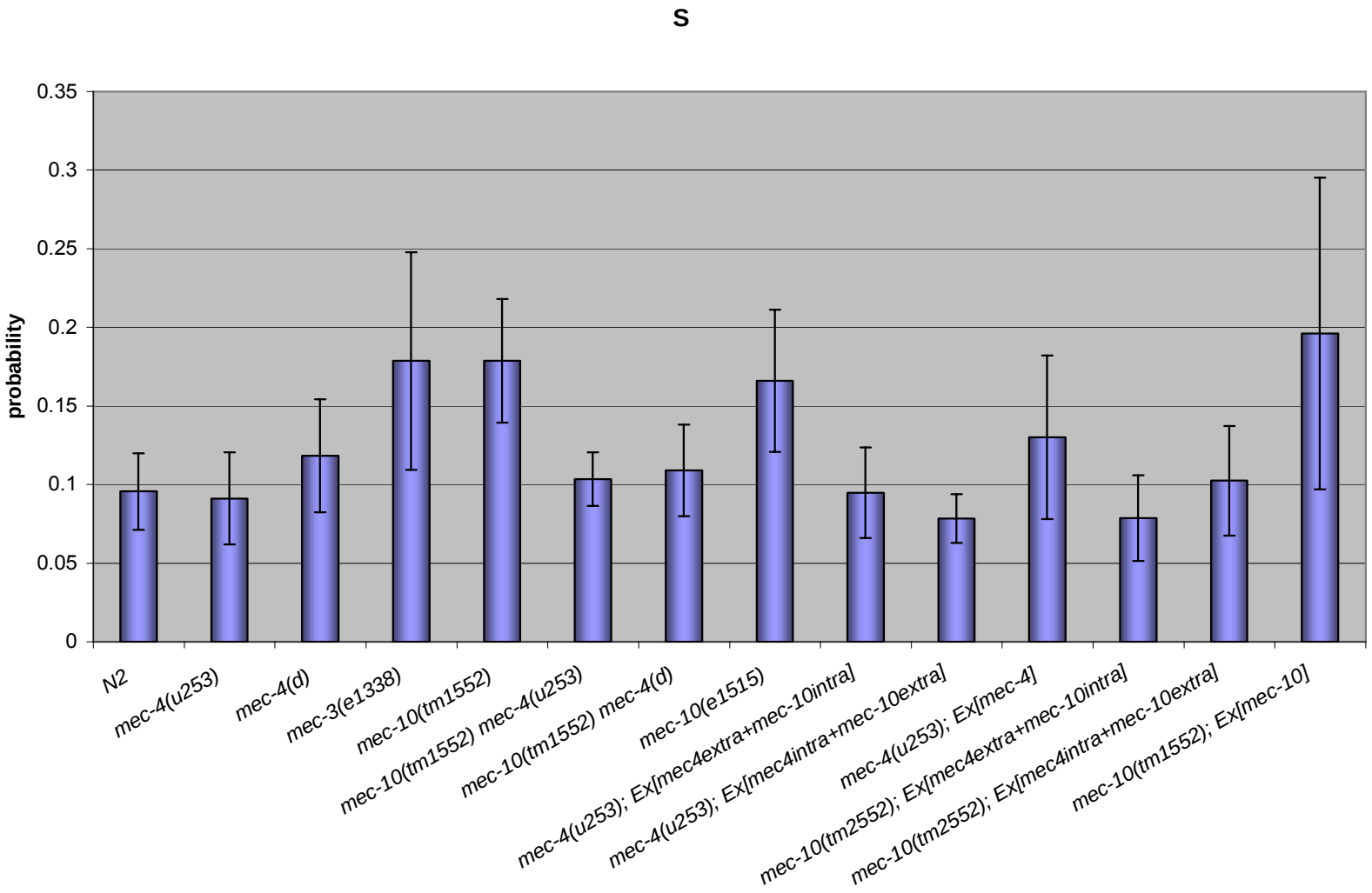

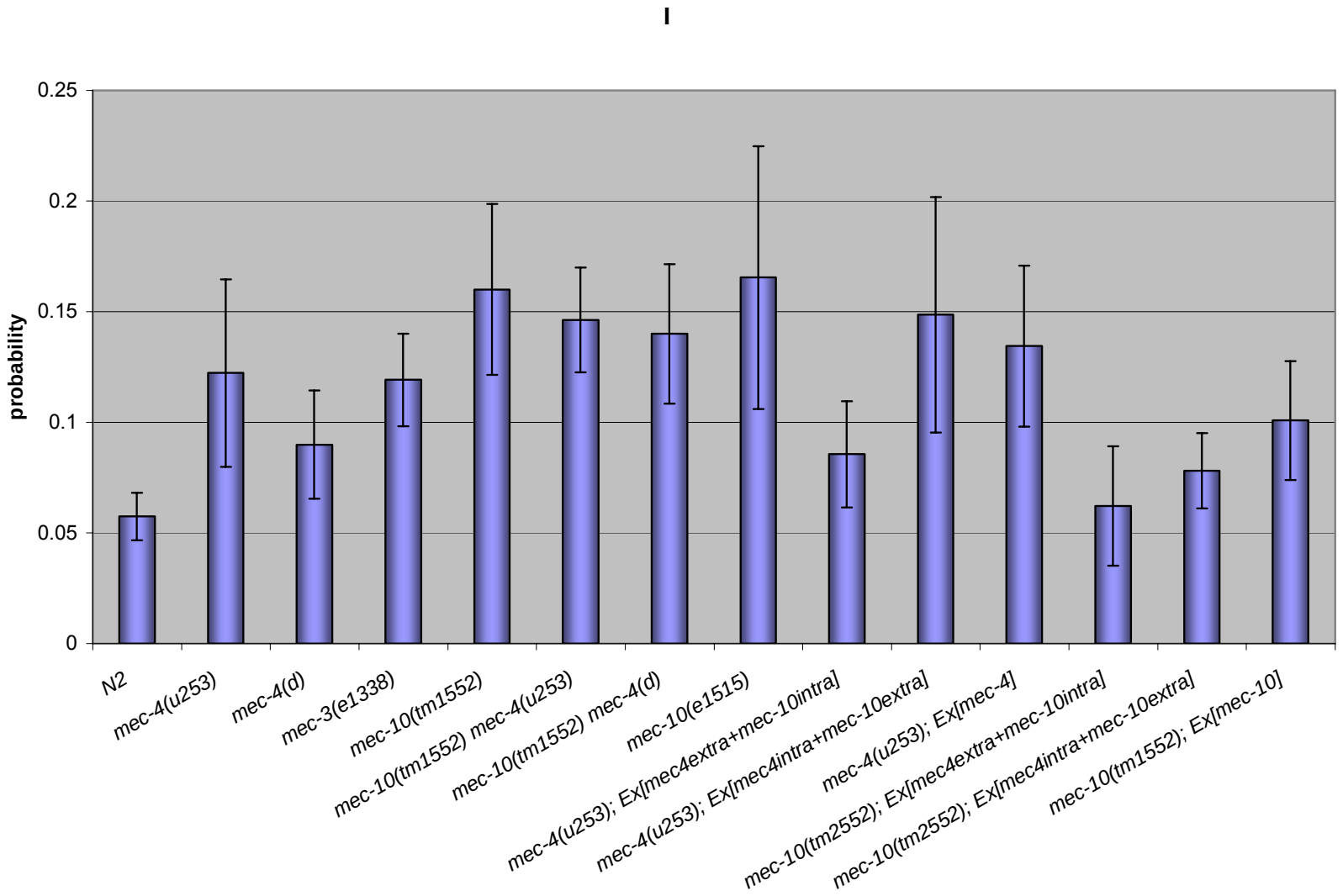
I
probability
0.25
0.2
0.15
0.1
0.05
0
N2
mec-4(u253)
mec-4(d)
mec-3(e1338)
mec-10(tm1552)
mec-10(tm1552) mec-4(u253)
mec-10(tm1552) mec-4(d)
mec-10(e1515)
mec-4(u253); Ex[mec4extra+mec-10intra]
mec-4(u253); Ex[mec4intra+mec-10extra]
mec-4(u253); Ex[mec-4]
mec-10(tm2552); Ex[mec4extra+mec-10intra]
mec-10(tm2552); Ex[mec4intra+mec-10extra]
mec-10(tm1552); Ex[mec-10]

C

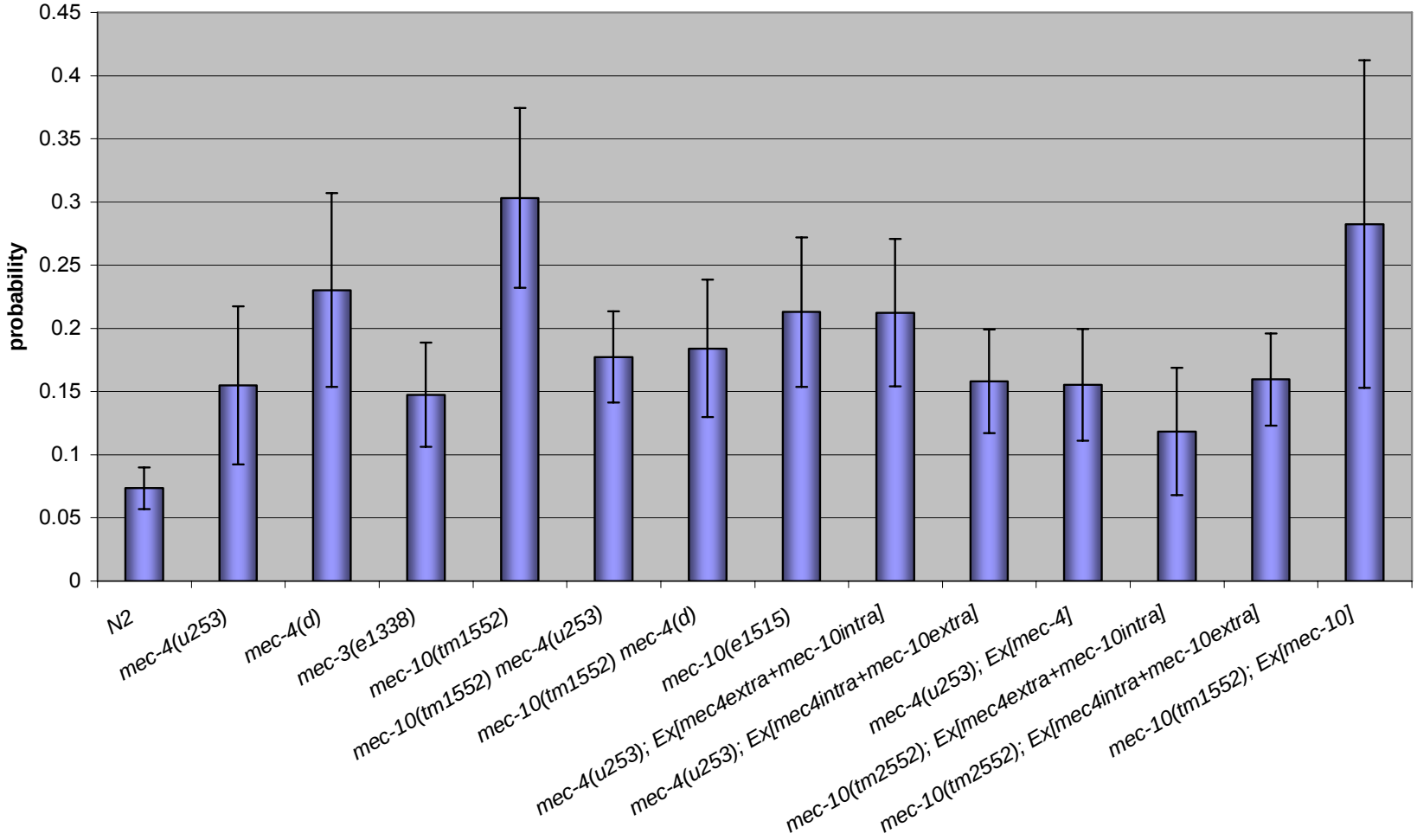
probability
0.45
0.4
0.35
0.3
0.25
0.2
0.15
0.1
0.05
0
N2
mec-4(u253)
mec-4(d)
mec-3(e1338)
mec-10(tm1552)
mec-10(tm1552) mec-4(u253)
mec-10(tm1552) mec-4(d)
mec-10(e1515)
mec-4(u253); Ex[mec4extra+mec-10intra]
mec-4(u253); Ex[mec4intra+mec-10extra]
mec-4(u253); Ex[mec-4]
mec-10(tm2552); Ex[mec4extra+mec-10intra]
mec-10(tm2552); Ex[mec4intra+mec-10extra]
mec-10(tm1552); Ex[mec-10]

O

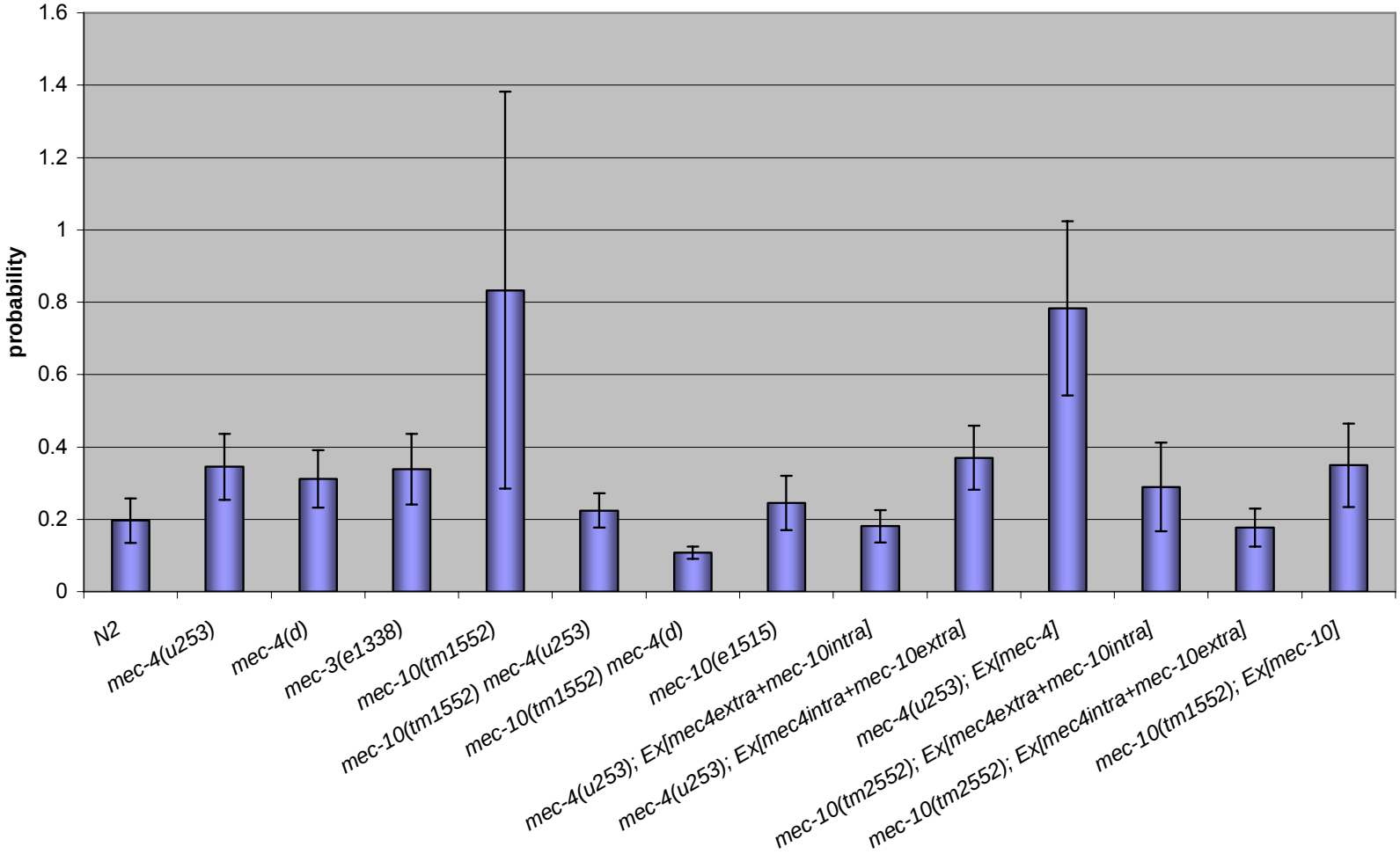
probability
1.6
1.4
1.2
1
0.8
0.6
0.4
0.2
0
N2
mec-4(u253)
mec-4(d)
mec-3(e1338)
mec-10(tm1552)
mec-10(tm1552) mec-4(u253)
mec-10(tm1552) mec-4(d)
mec-10(e1515)
mec-4(u253); Ex[mec4extra+mec-10intra]
mec-4(u253); Ex[mec4intra+mec-10extra]
mec-4(u253); Ex[mec-4]
mec-10(tm2552); Ex[mec4extra+mec-10intra]
mec-10(tm2552); Ex[mec4intra+mec-10extra]
mec-10(tm1552); Ex[mec-10]

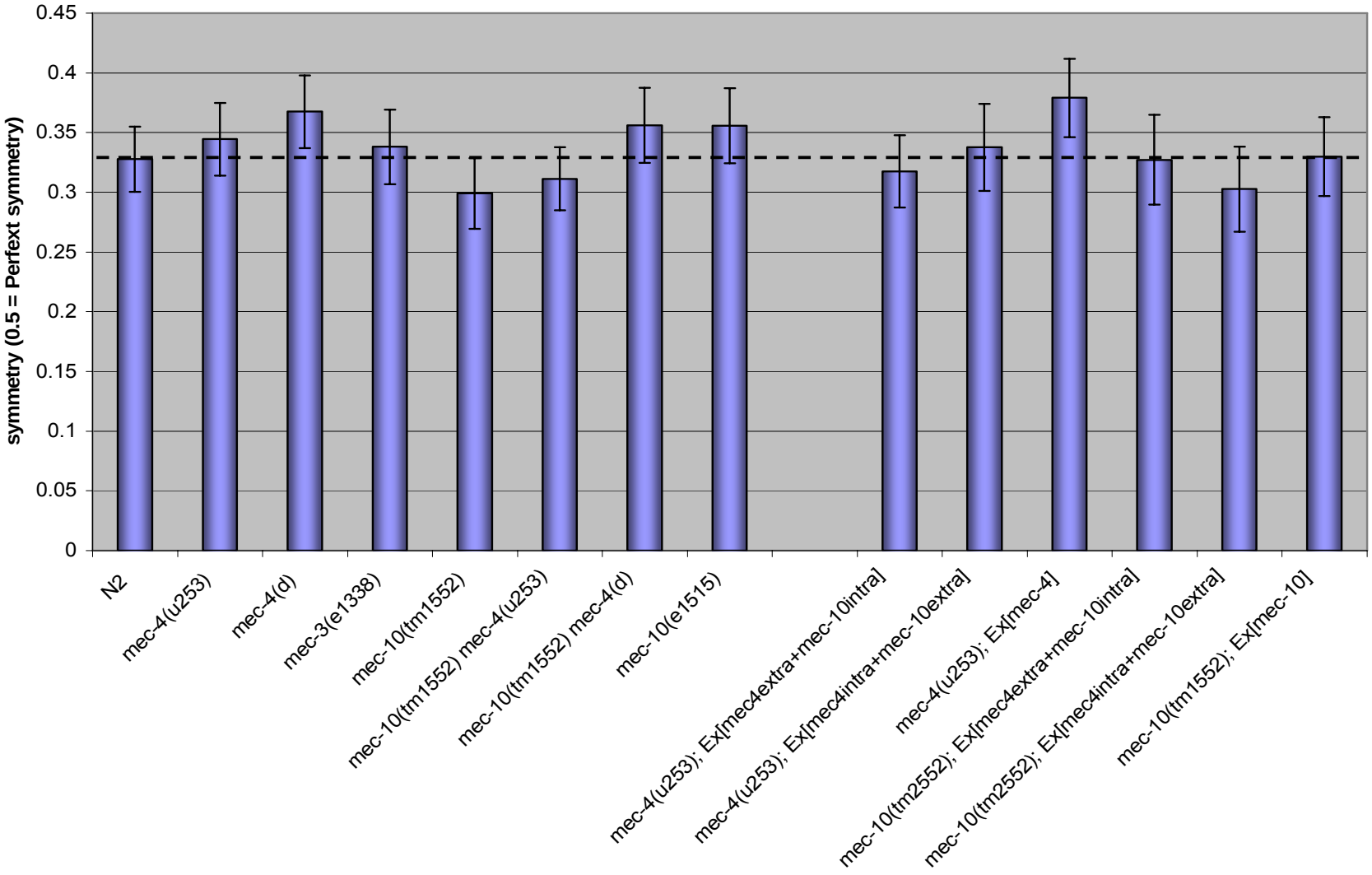
symmetry (0.5 = Perfext symmetry)
0.45
0.4
0.35
0.3
0.25
0.2
0.15
0.1
0.05
0
N2
mec-4(u253)
mec-4(d)
mec-3(e1338)
mec-10(tm1552)
mec-10(tm1552) mec-4(u253)
mec-10(tm1552) mec-4(d)
mec-10(e1515)
mec-4(u253); Ex[mec4extra+mec-10intra]
mec-4(u253); Ex[mec4intra+mec-10extra]
mec-4(u253); Ex[mec-4]
mec-10(tm2552); Ex[mec4extra+mec-10intra]
mec-10(tm2552); Ex[mec4intra+mec-10extra]
mec-10(tm1552); Ex[mec-10]

Figure 11: MEC-10(d) induces a minor necrosis phenotype with or without *mec-10* wild type in the background.

a)

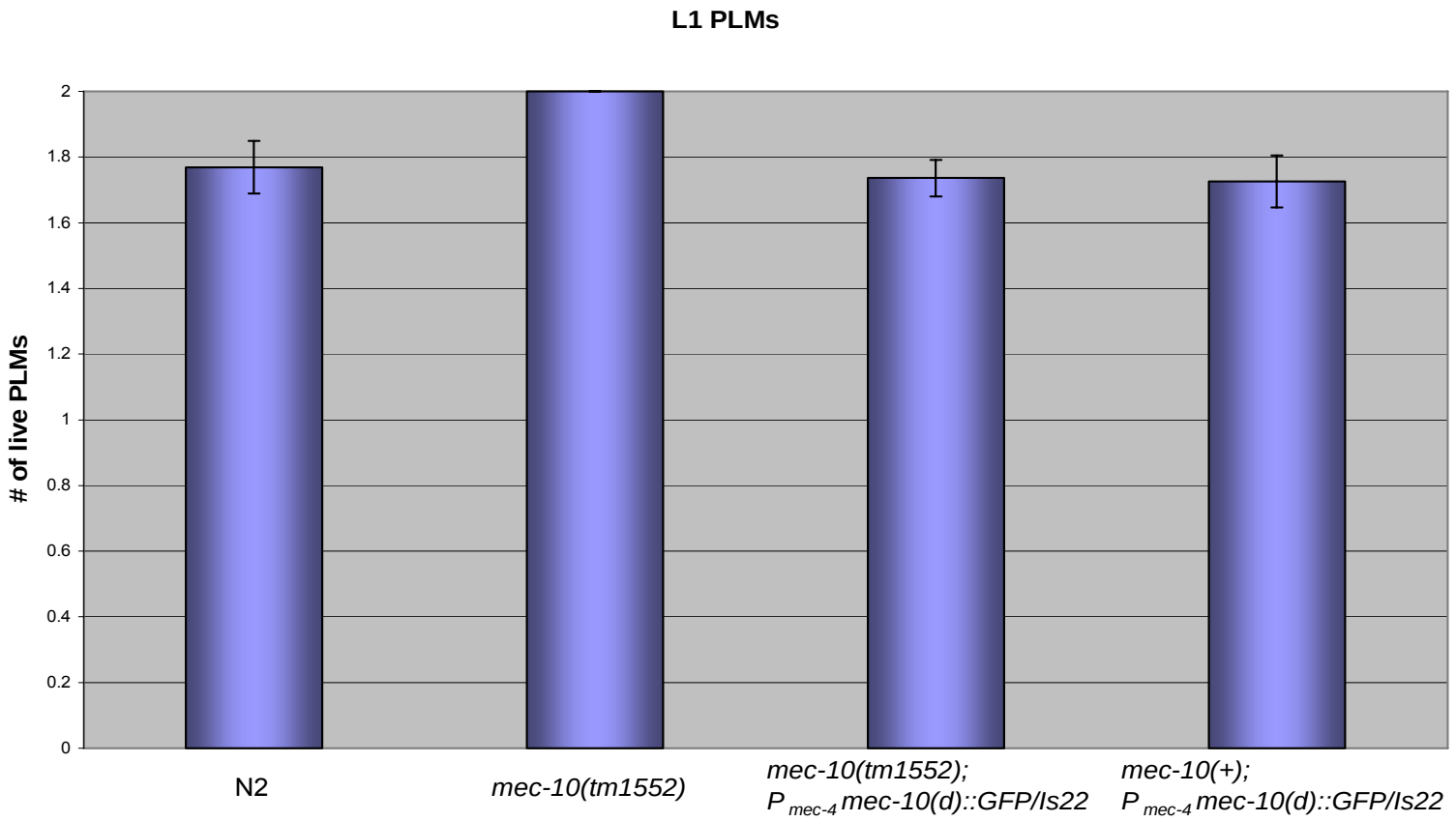

b)

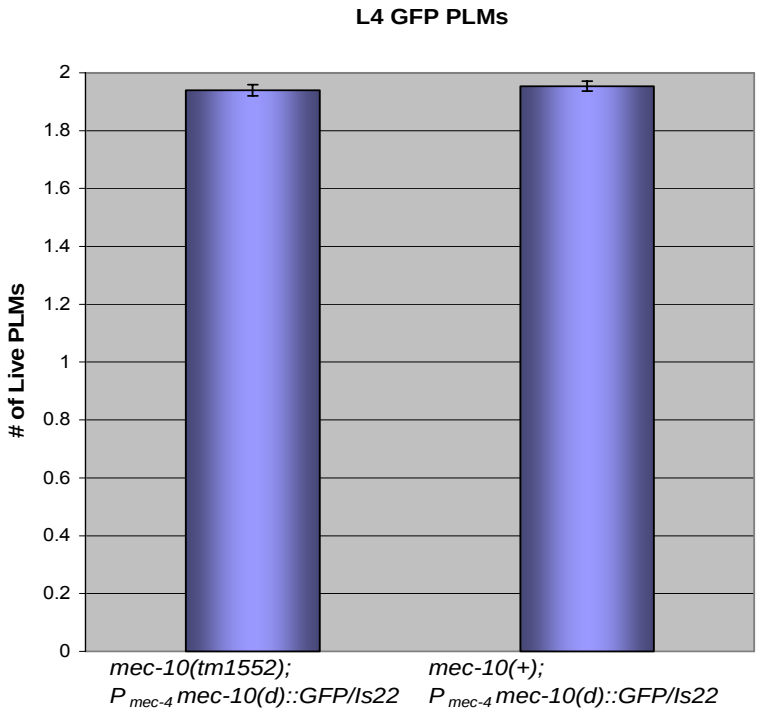
L4 GFP PLMs
# of Live PLMs
2
1.8
1.6
1.4
1.2
1
0.8
0.6
0.4
0.2
0
mec-10(tm1552); P mec-4 mec-10(d)::GFP/Is22
mec-10(+); P mec-4 mec-10(d)::GFP/Is22

c)

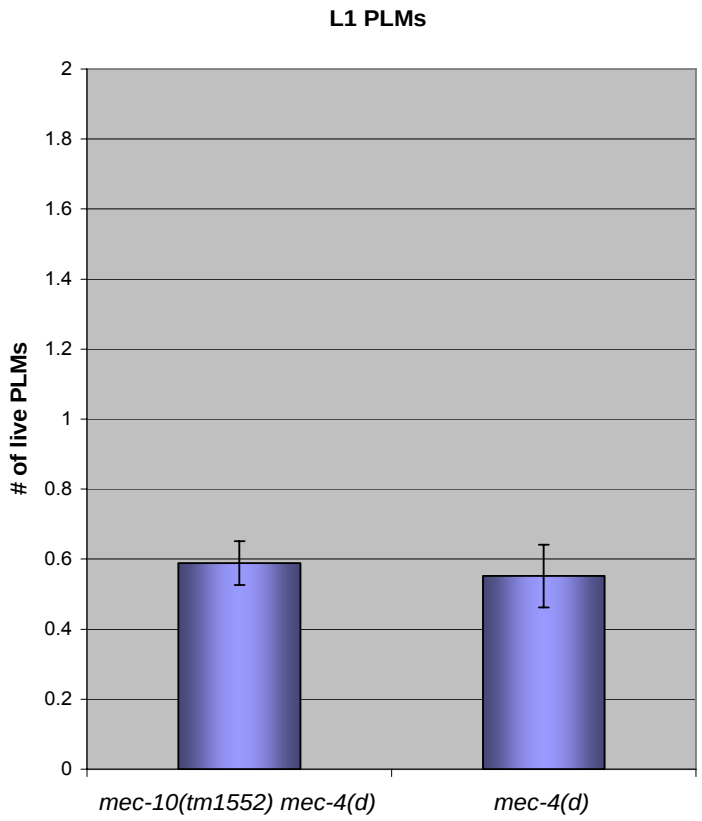
L1 PLMs
# of live PLMs
2
1.8
1.6
1.4
1.2
1
0.8
0.6
0.4
0.2
0
mec-10(tm1552) mec-4(d)
mec-4(d)

d)

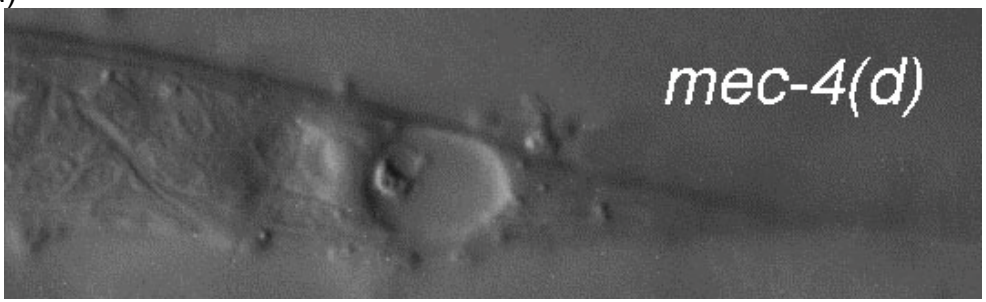

Figure 12: MEC-10 mutant subunits suppress MEC-4(d) currents more than WT.

a)

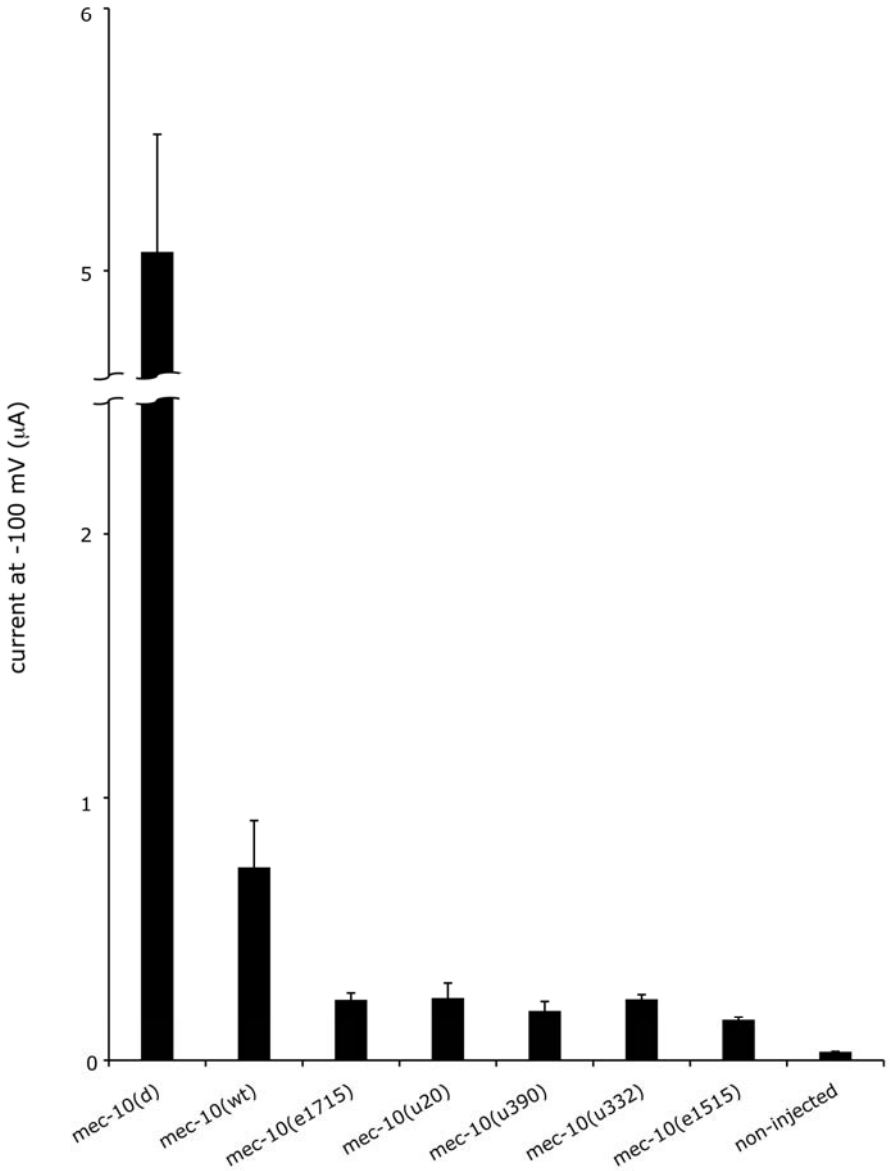

b)

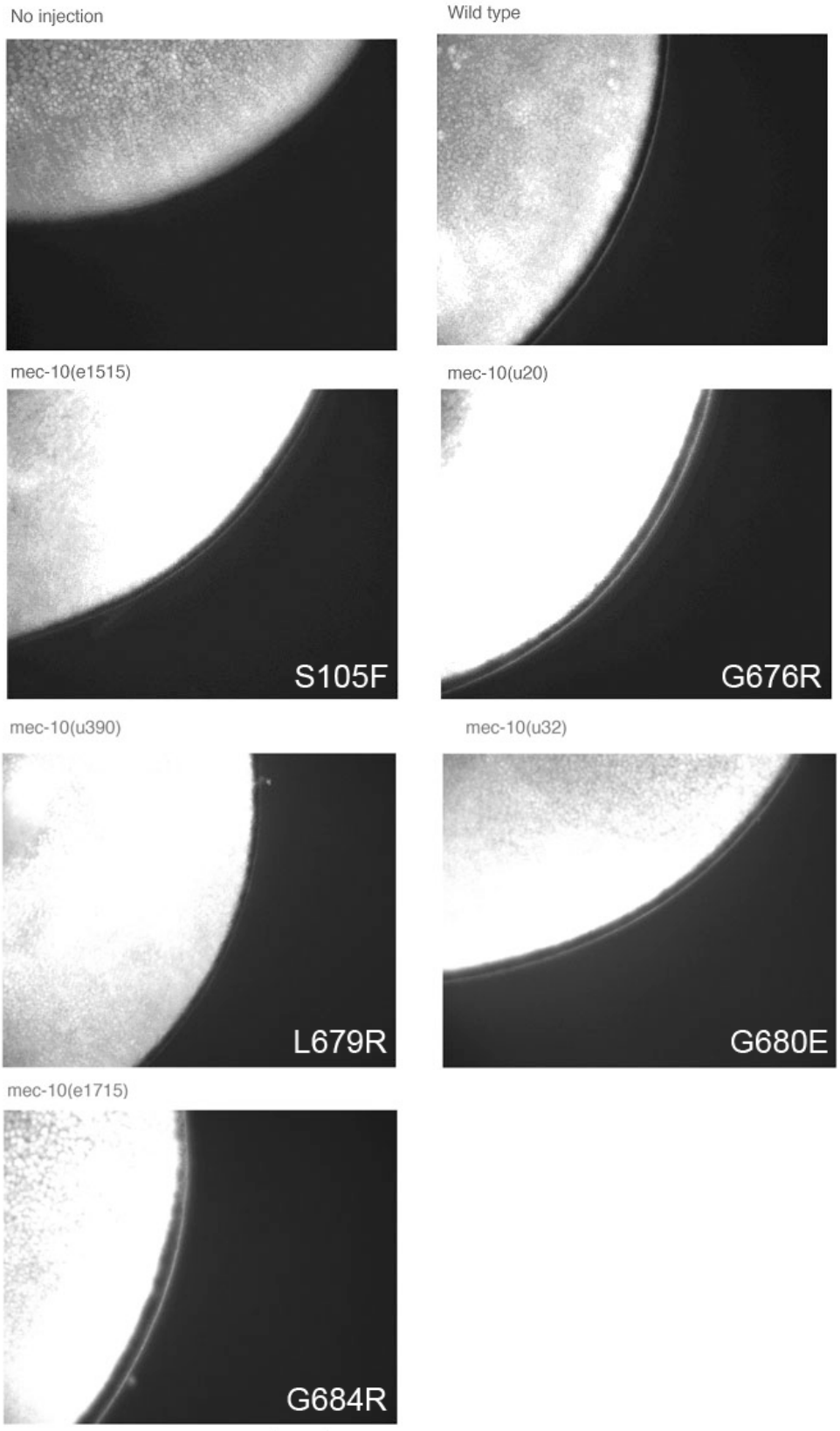
No injection
Wild type
mec-10(e1515)
S105F
mec-10(u20)
G676R
mec-10(u390)
L679R
mec-10(u32)
G680E
mec-10(e1715)
G684R

Figure 13: Sequence structures of *mec-10*, *mec-4*, and chimeric proteins.

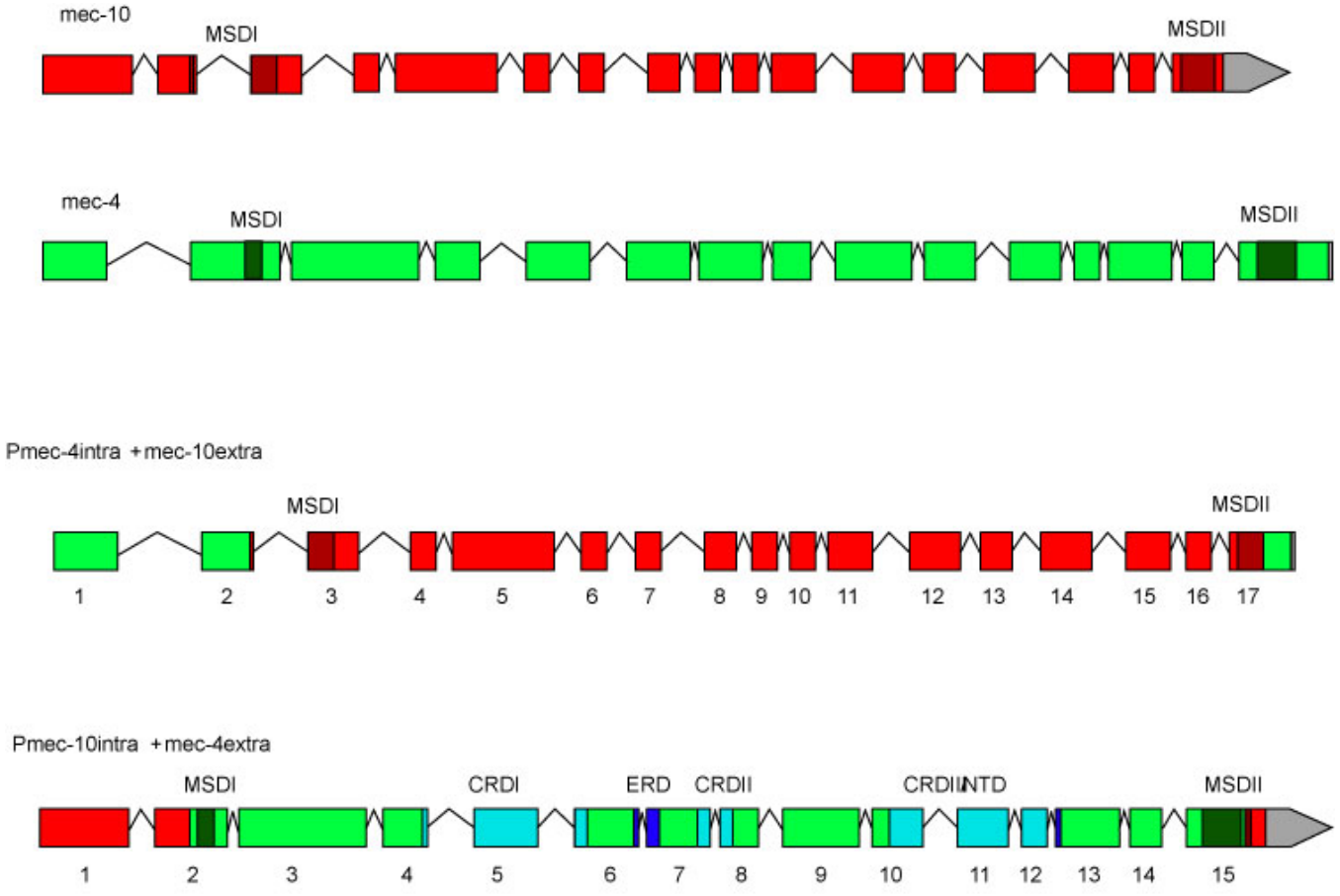

Figure 14: Figure 14: Chimeric MEC proteins do not fully restore MEC-4 or MEC-10 defects.

a)

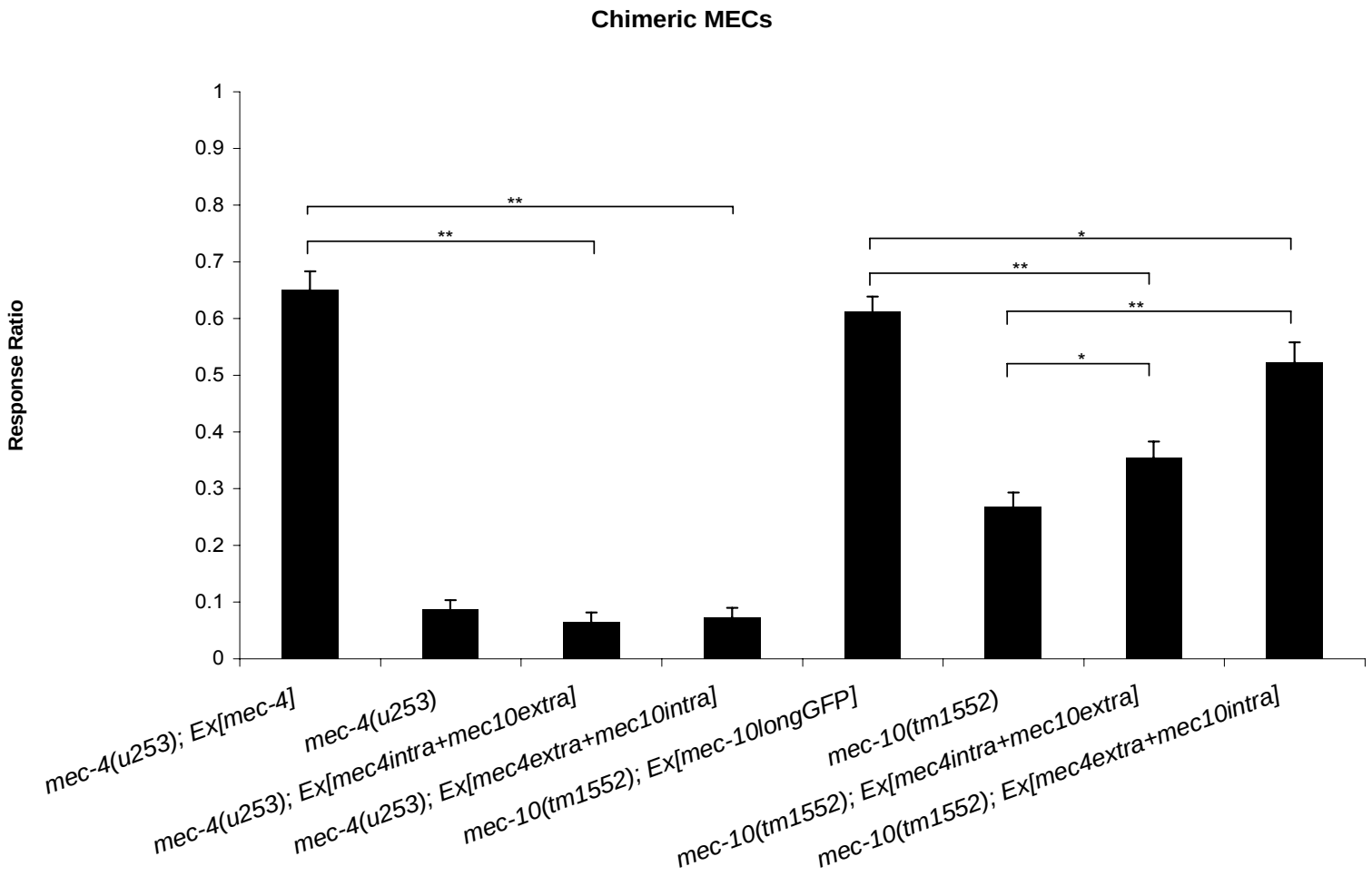

b)

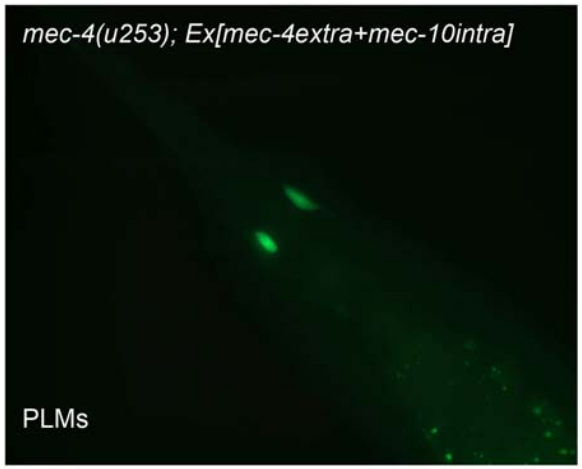
mec-4(u253); Ex[mec-4extra+mec-10intra]
PLMs

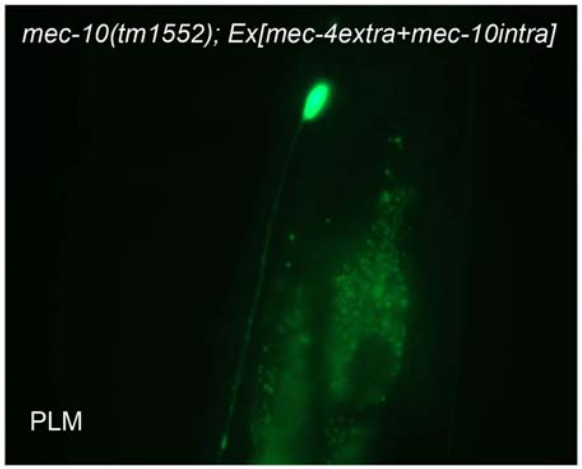
mec-10(tm1552); Ex[mec-4extra+mec-10intra]
PLM

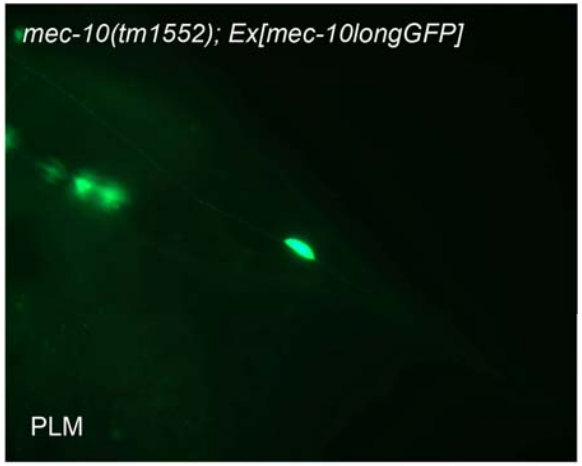
mec-10(tm1552); Ex[mec-10longGFP]
PLM

Figure 15: Protein sequence of the first 106 amino acids in MEC-4.

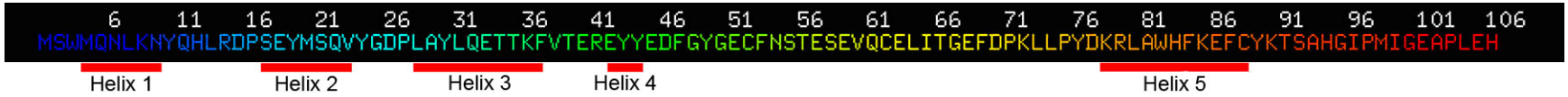

Figure 16: Ribbon diagram of MEC-4 N.

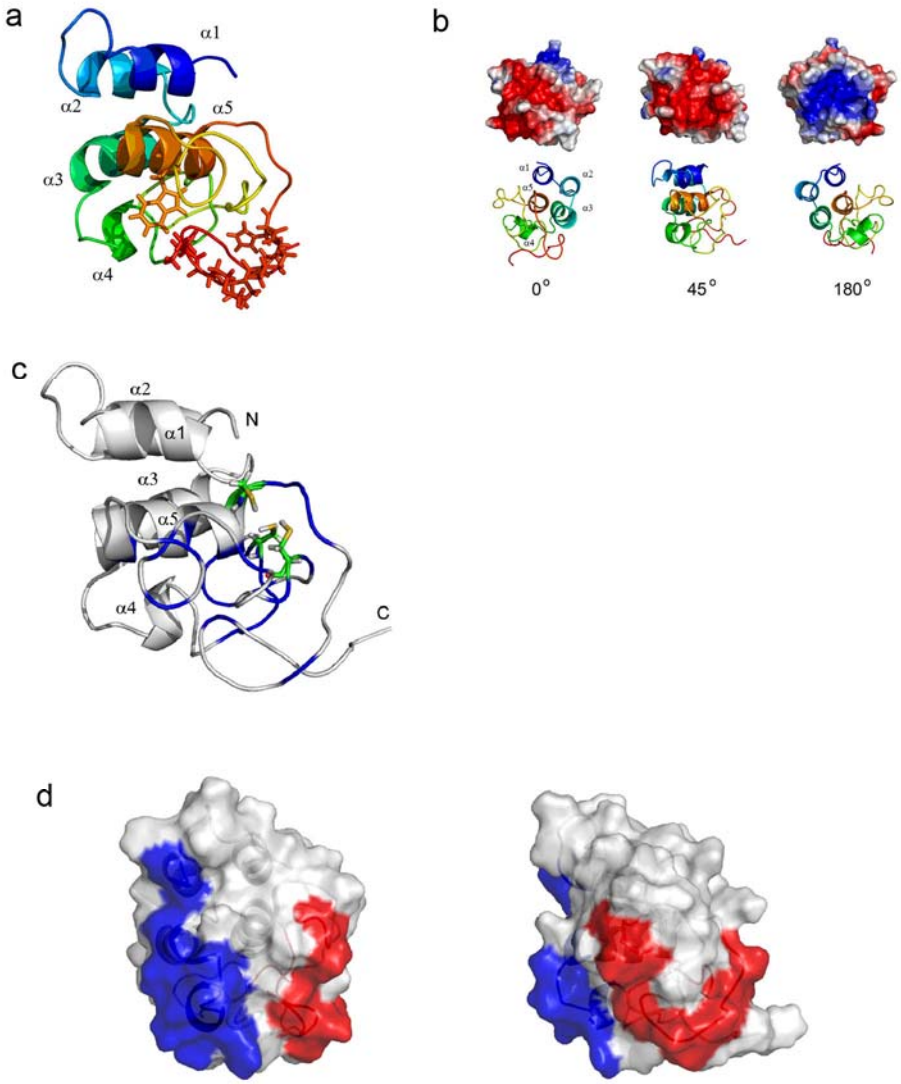

Figure 17: *in vivo* touch sensitivity assays for *mec-4* mutations that might perturb structure (and therefore function).

a)

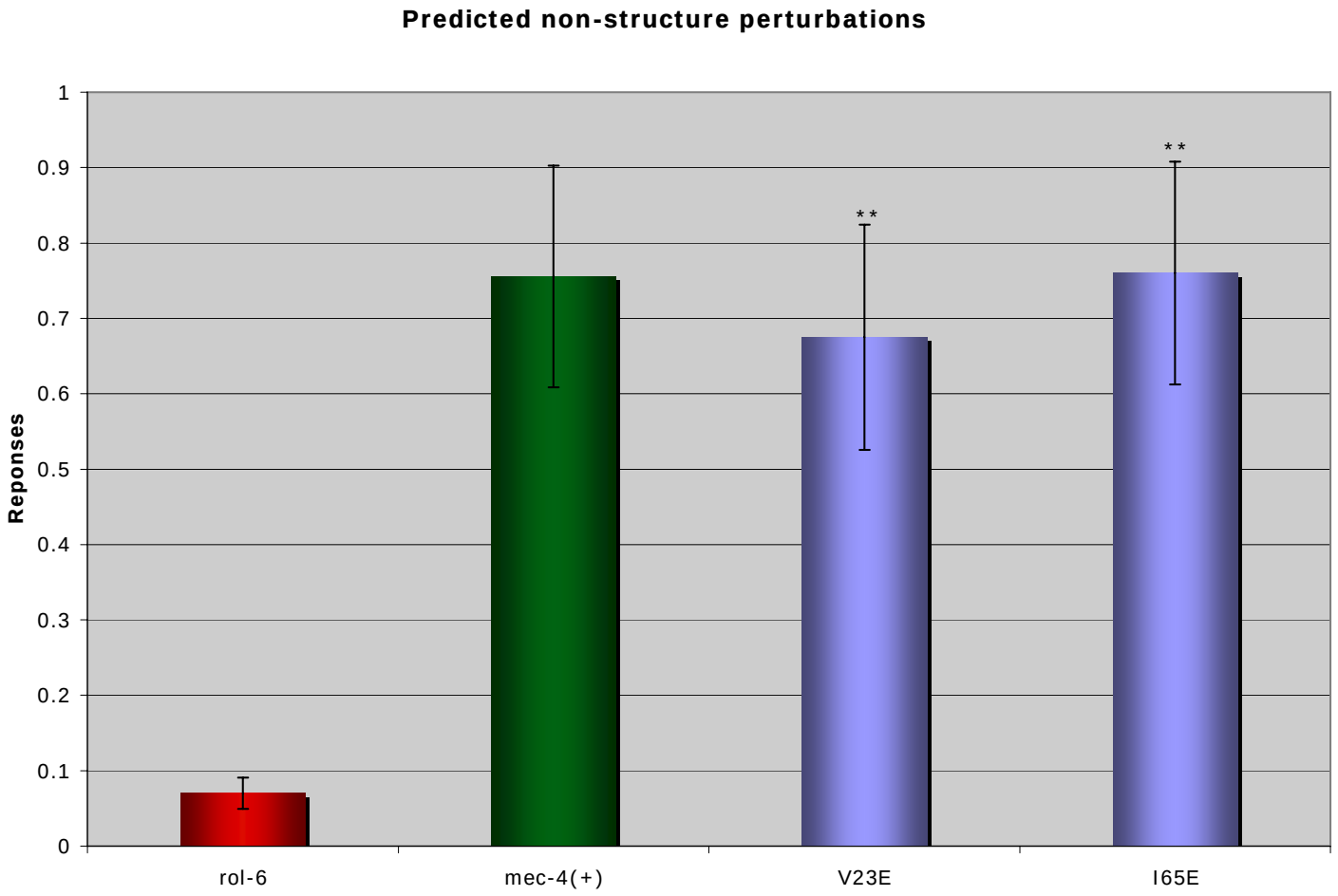

b)

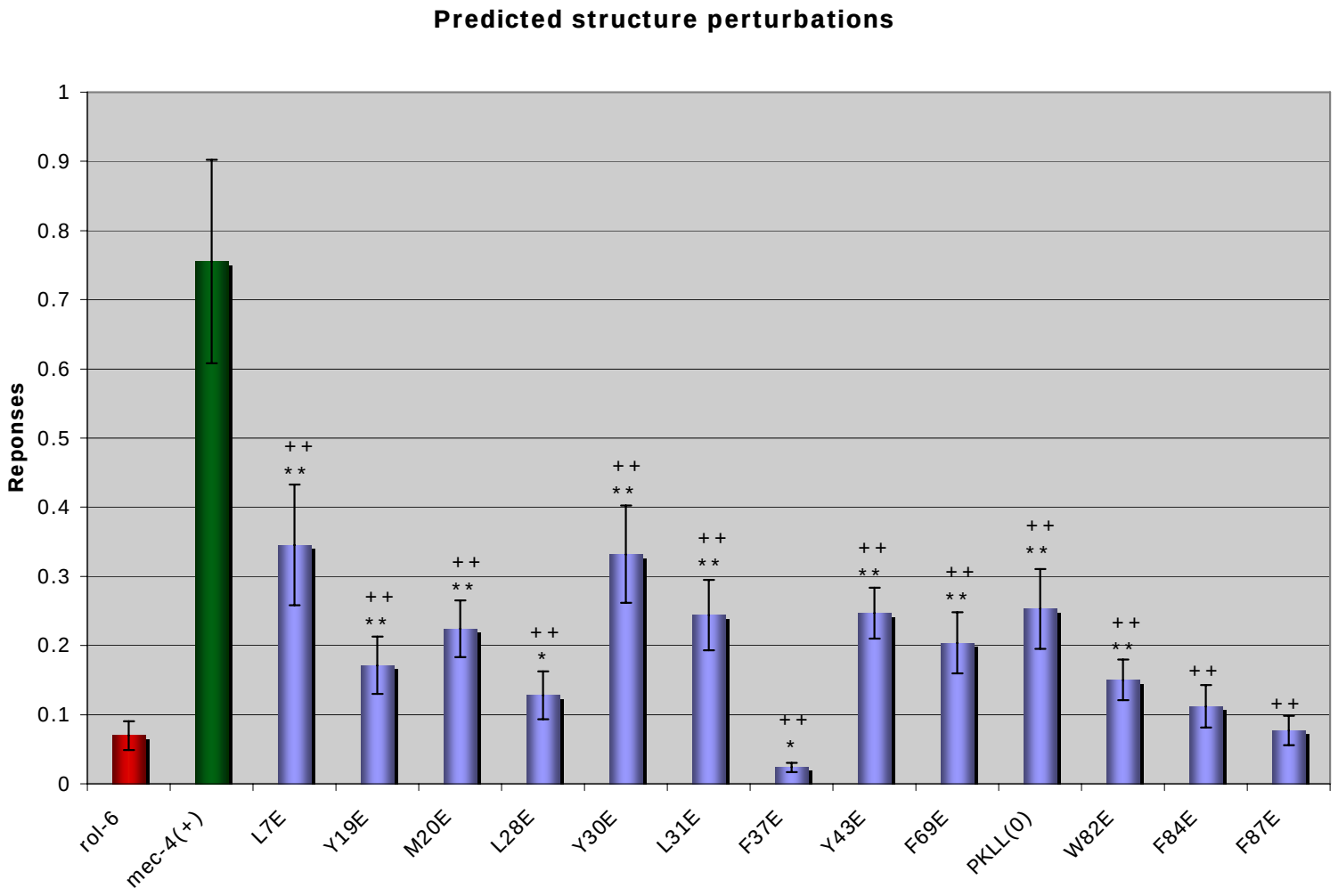
Predicted structure perturbations
Reponses
1
0.9
0.8
0.7
0.6
0.5
0.4
0.3
0.2
0.1
0
++ **
++ *
rol-6
mec-4(+)
L7E
Y19E
M20E
L28E
Y30E
L31E
F37E
Y43E
F69E
PKLL(0)
W82E
F84E
F87E

c)

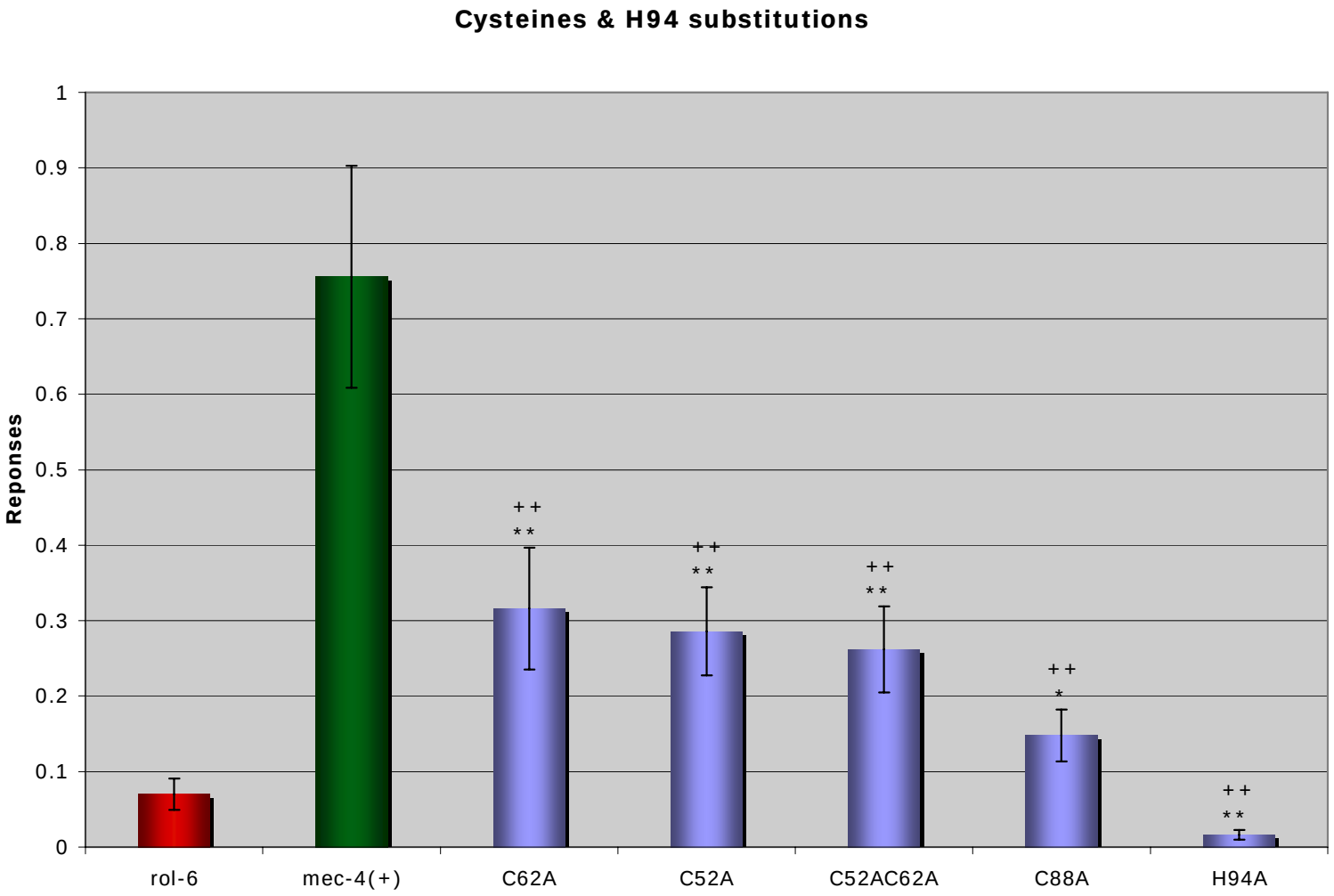
Cysteines & H94 substitutions
Reponses
1
0.9
0.8
0.7
0.6
0.5
0.4
0.3
0.2
0.1
0
++
**
++
**
++
**
++
*
++
**
rol-6
mec-4(+)
C62A
C52A
C52AC62A
C88A
H94A

Figure 18: *in vivo* touch sensitivity assays for *mec-4* mutations that might perturb structure (and therefore function).

a)

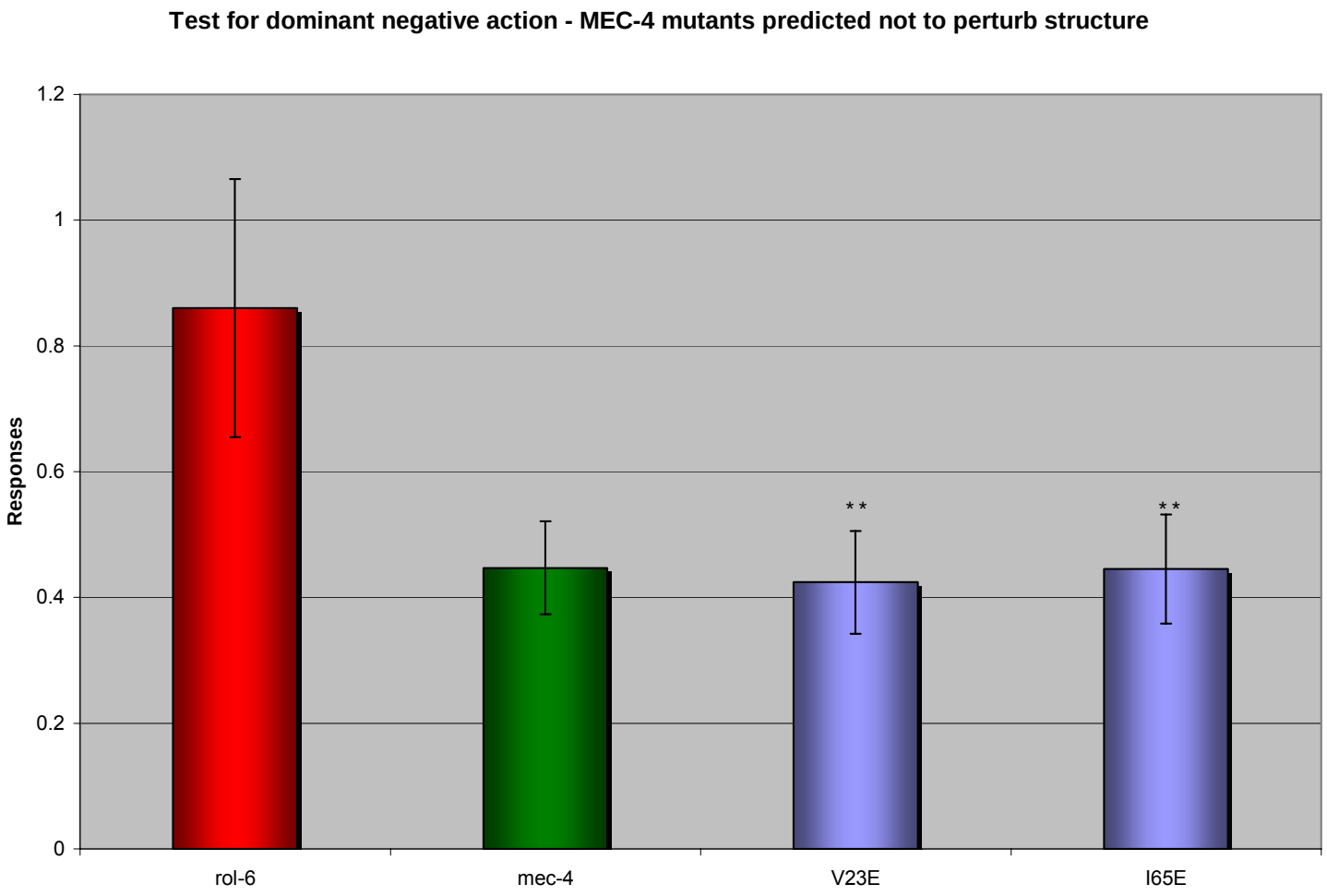

b)

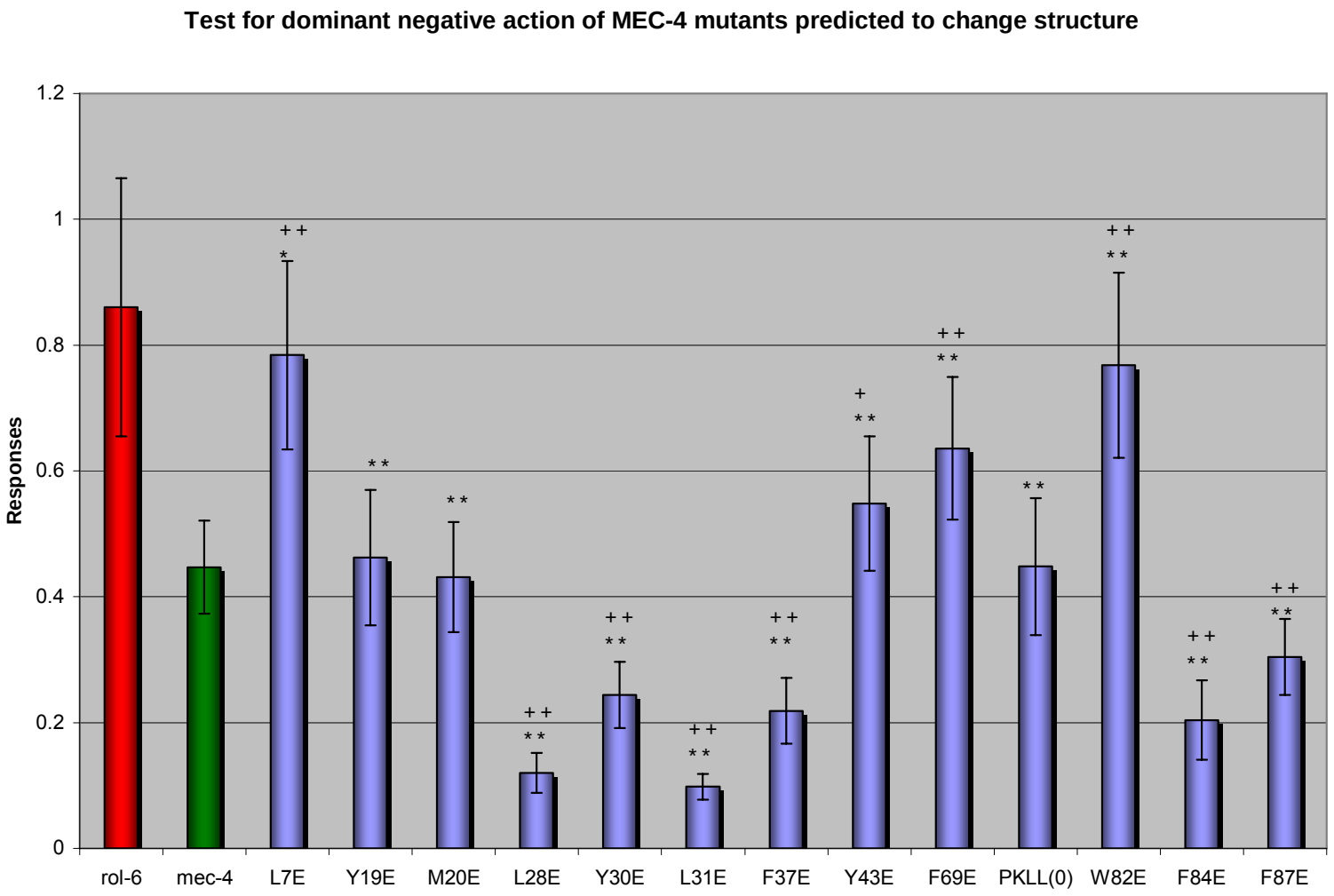
Test for dominant negative action of MEC-4 mutants predicted to change structure
Responses
1.2
1
0.8
0.6
0.4
0.2
0
rol-6
mec-4
L7E
Y19E
M20E
L28E
Y30E
L31E
F37E
Y43E
F69E
PKLL(0)
W82E
F84E
F87E

c)

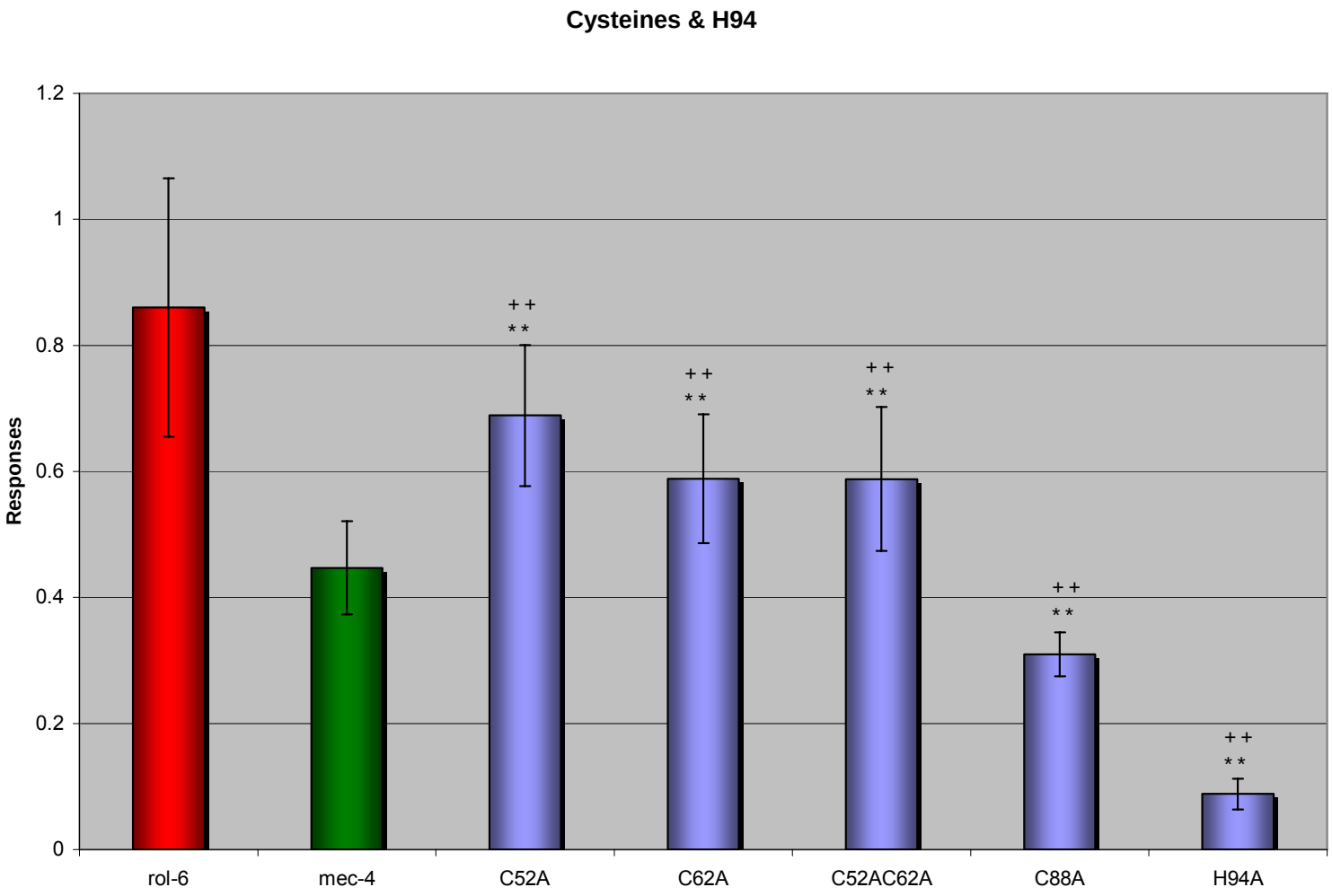
Cysteines & H94
Responses
1.2
1
0.8
0.6
0.4
0.2
0
++
**
rol-6
mec-4
C52A
C62A
C52AC62A
C88A
H94A

Figure 19: Ribbon diagram of MEC-4N(V23) and ^{15}N HSQC spectrum of MEC-4N(V23E).

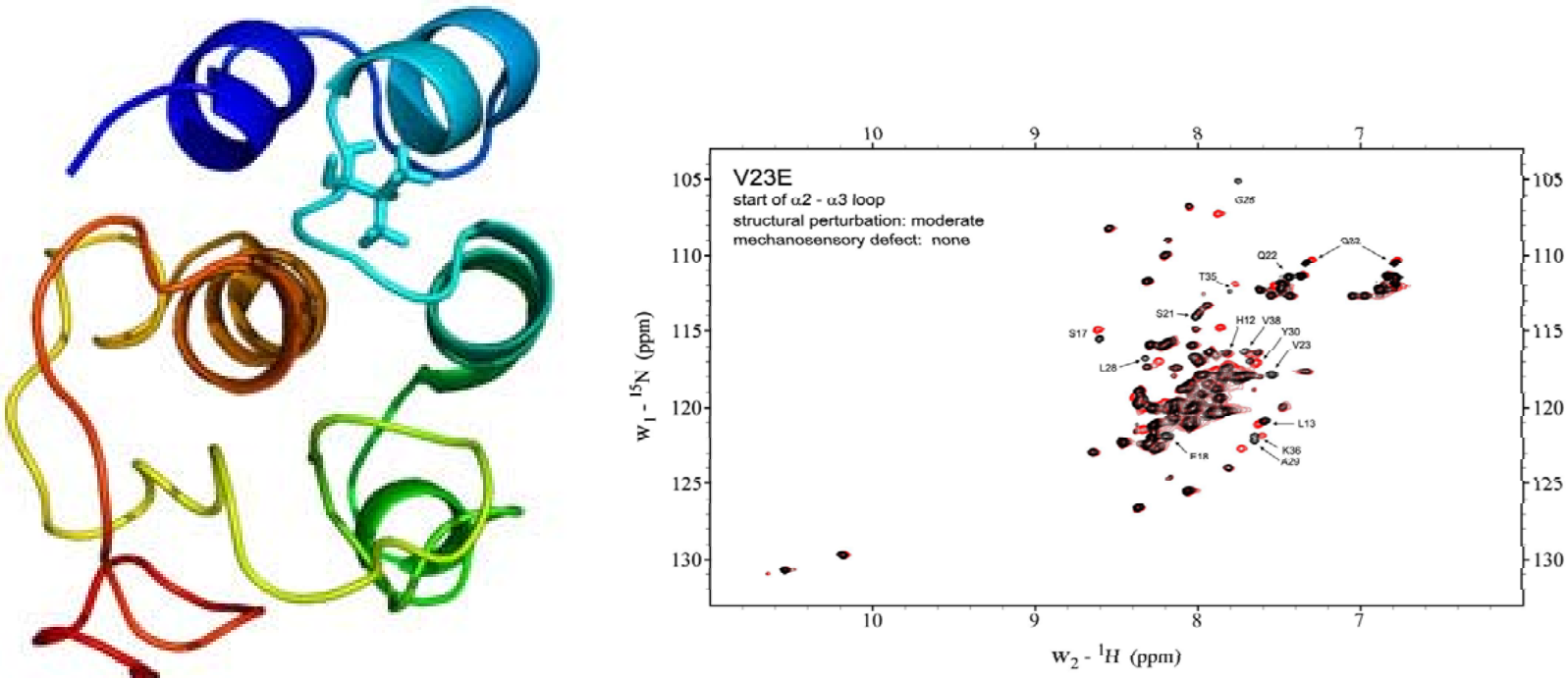

Figure 20: Ribbon diagram of MEC-4N(I65).

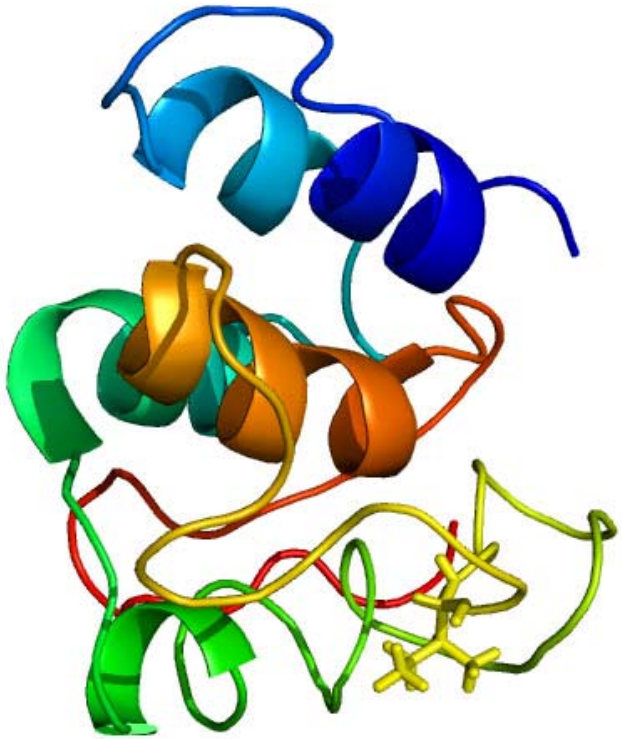

Figure 21: Ribbon diagram of MEC-4N(L7) and ^{15}N HSQC spectrum of MEC-4N(L7E).

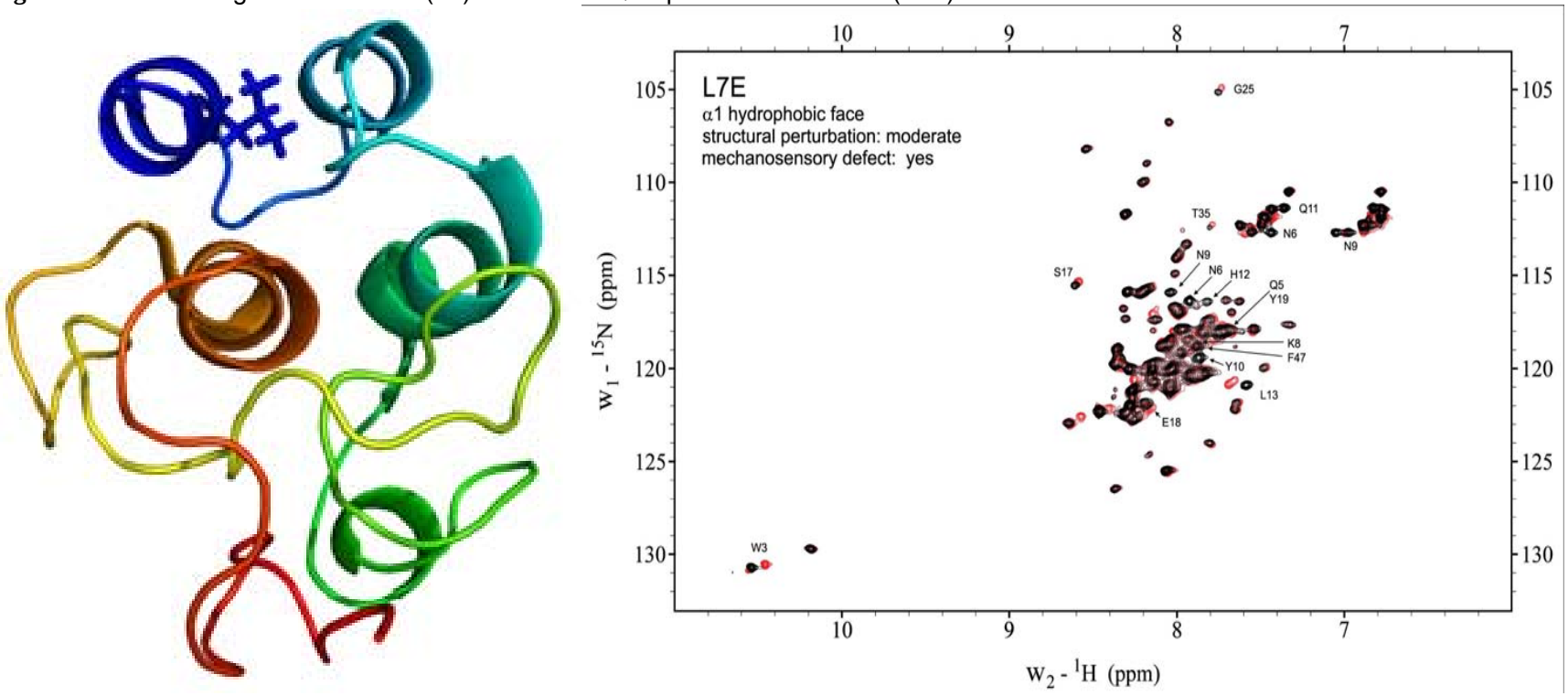

Figure 22: Ribbon diagram of MEC-4N(Y19) and ^{15}N HSQC spectrum of MEC-4N(Y19E).

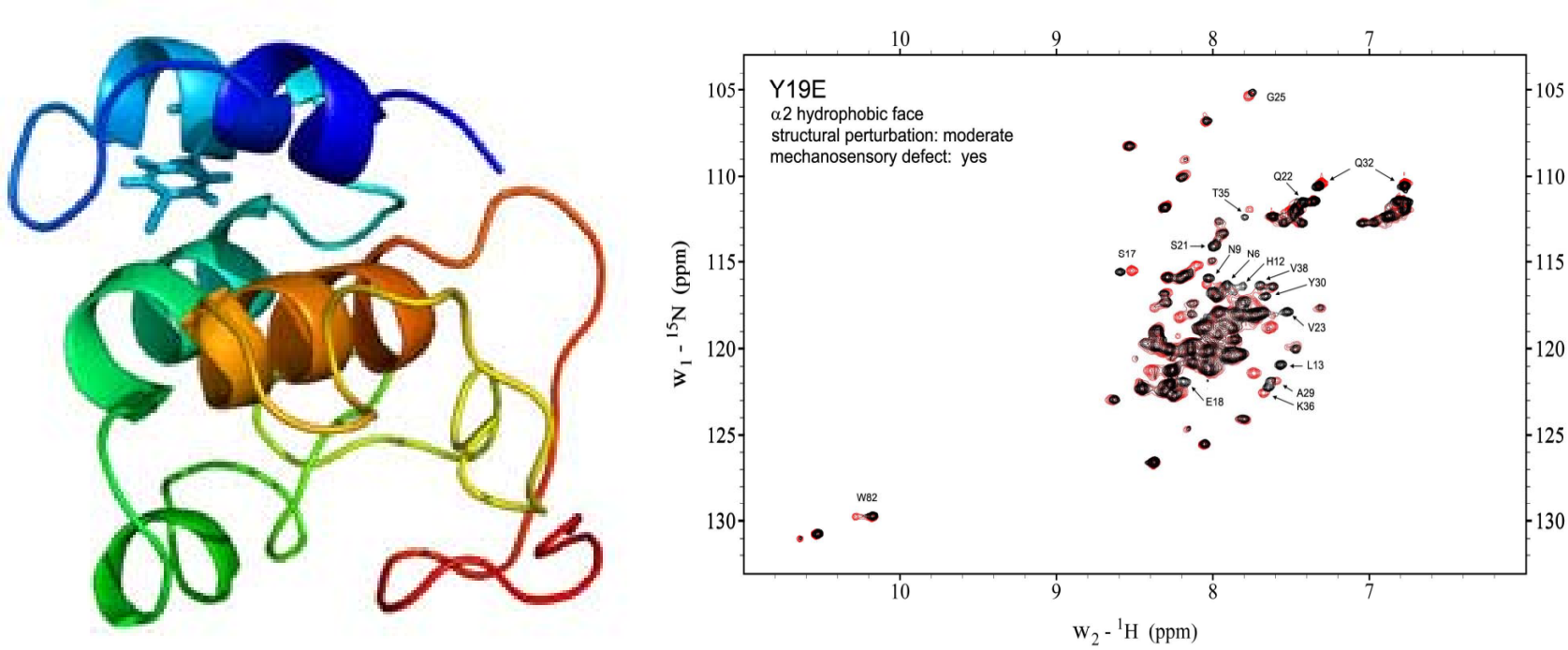

Figure 23: Ribbon diagram of MEC-4N(M20).

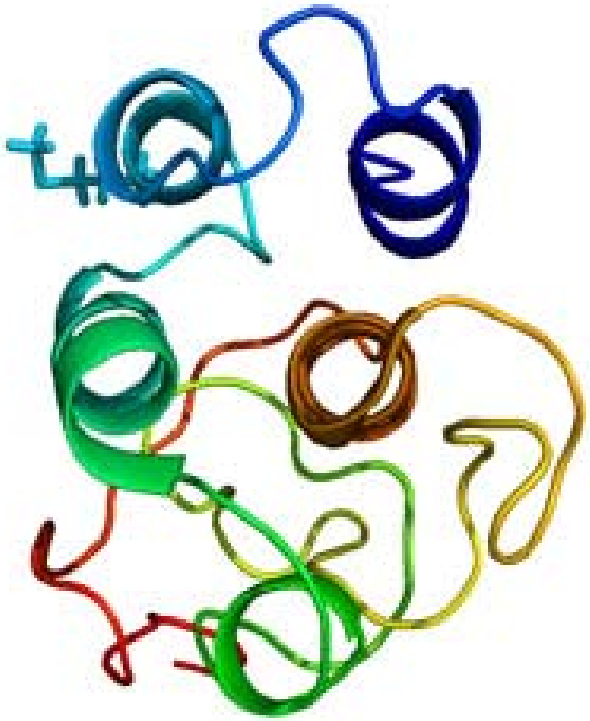

Figure 24: Ribbon diagram of MEC-4N(L28).

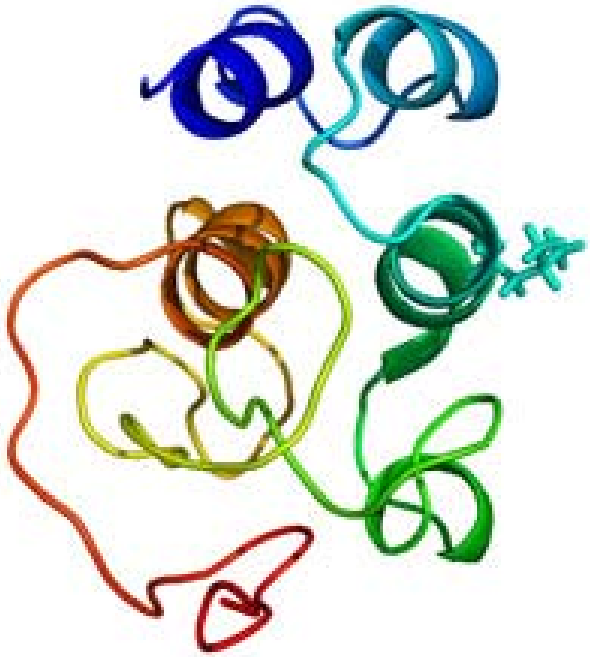

Figure 25: Ribbon diagram of MEC-4N(Y30) and ^{15}N HSQC spectrum of MEC-4N(Y30E).

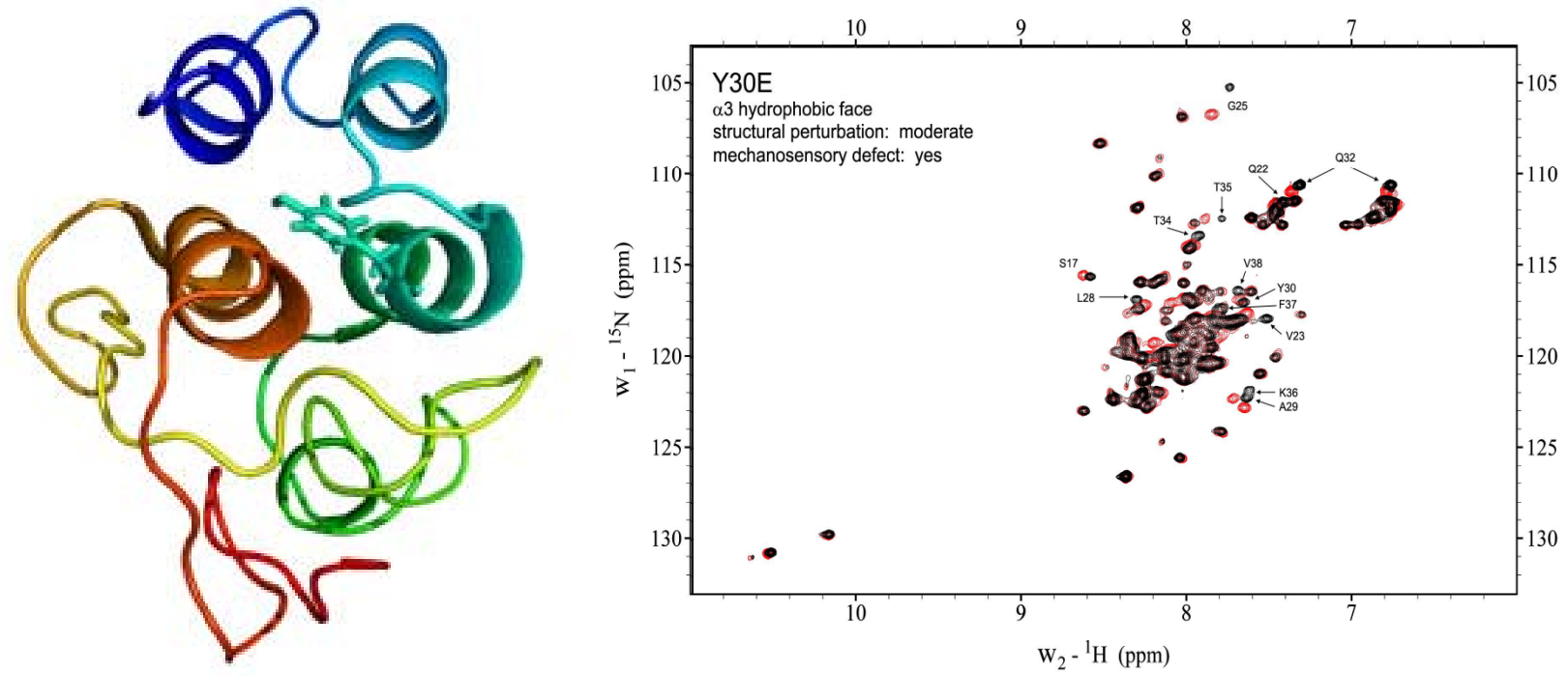

Figure 26: Ribbon diagram of MEC-4N(L31) and ^{15}N HSQC spectrum of MEC-4N(L31E).

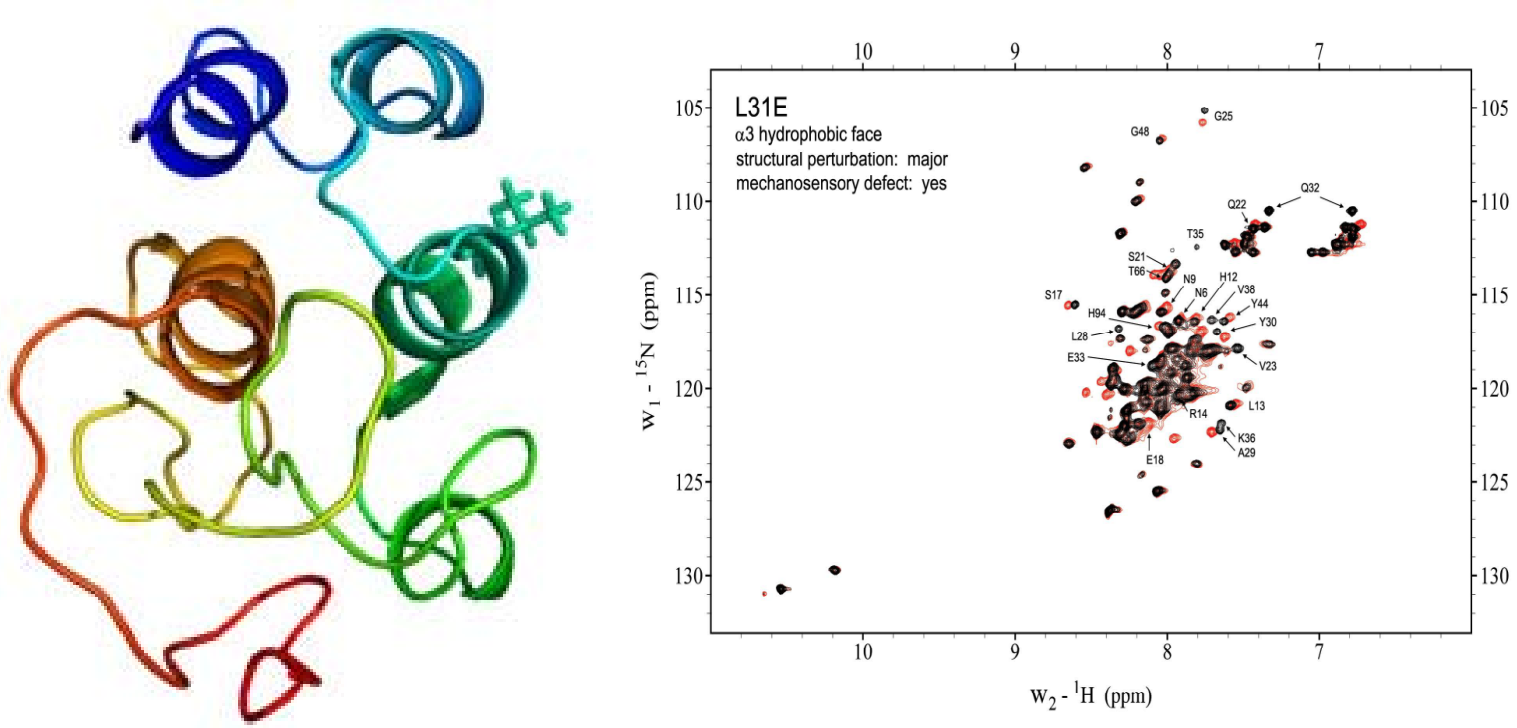

Figure 27: Ribbon diagram of MEC-4N(F37).

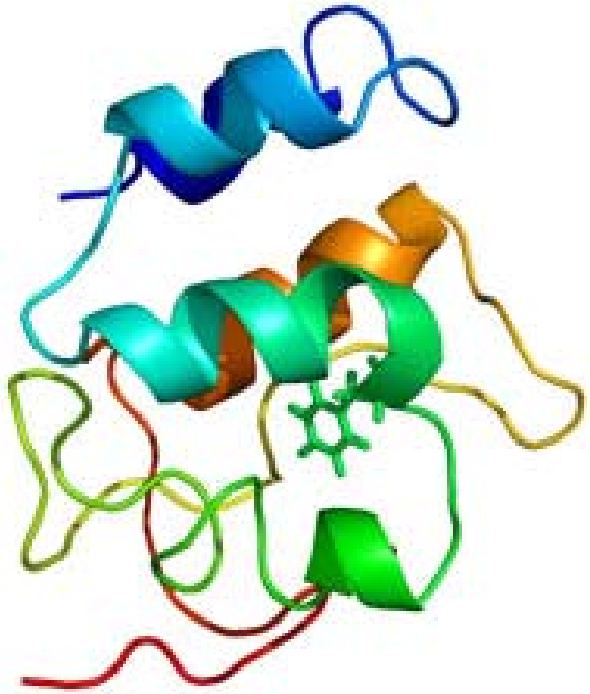

Figure 28: Ribbon diagram of MEC-4N(Y43) and ^{15}N HSQC spectrum of MEC-4N(Y43E).

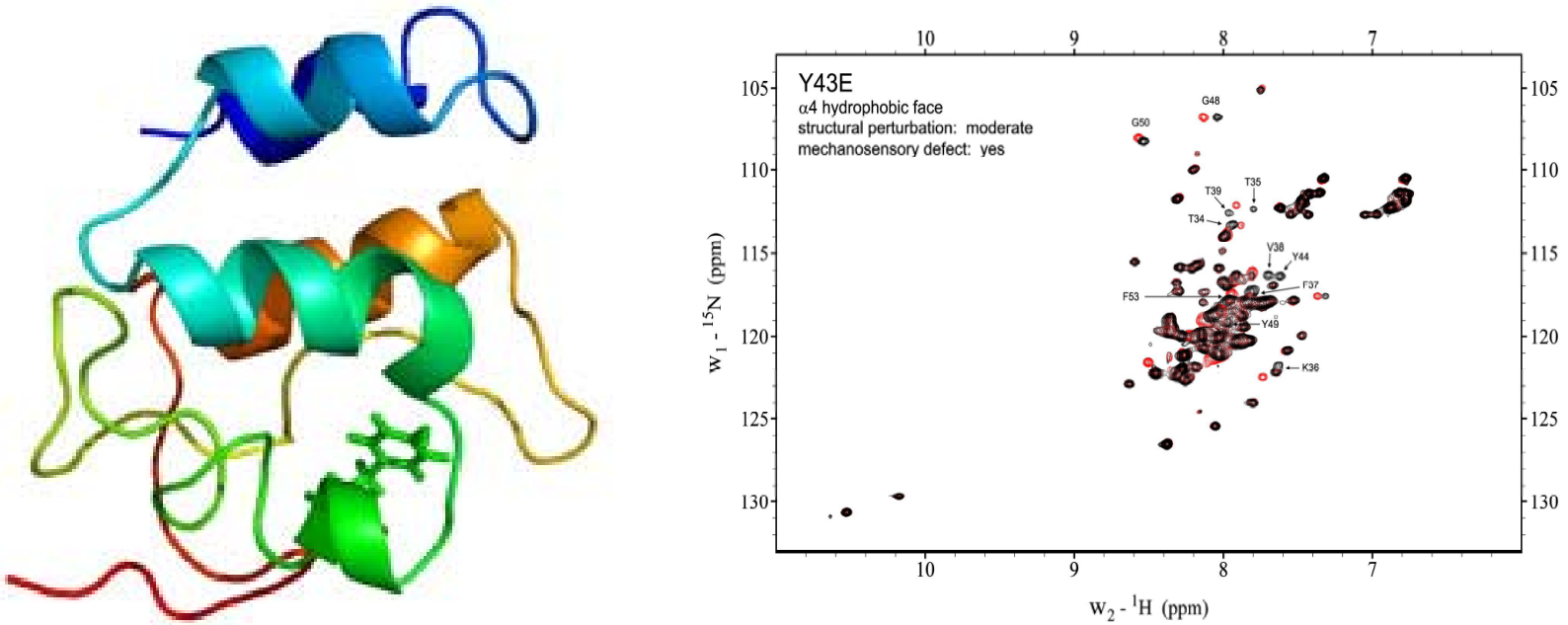

Figure 29: Ribbon diagram of MEC-4N(F69).

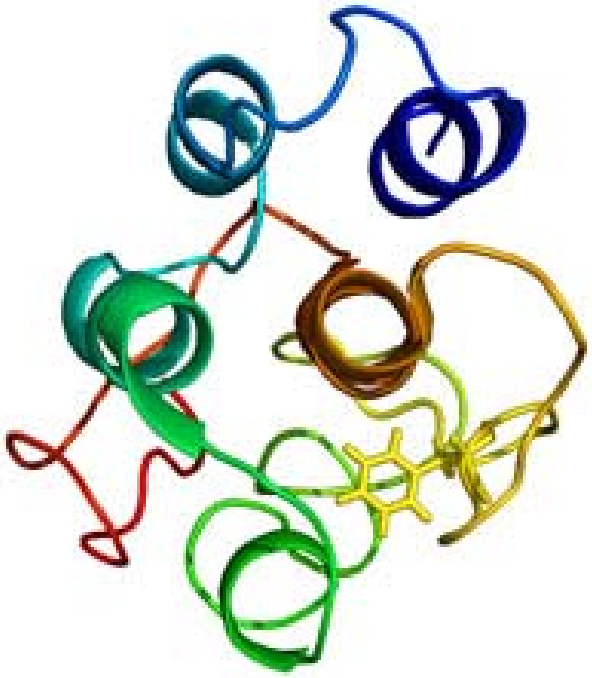

Figure 30: Ribbon diagram of MEC-4N(71PKLL74) and ^{15}N HSQC spectrum of MEC-4N(Δ71PKLL74).

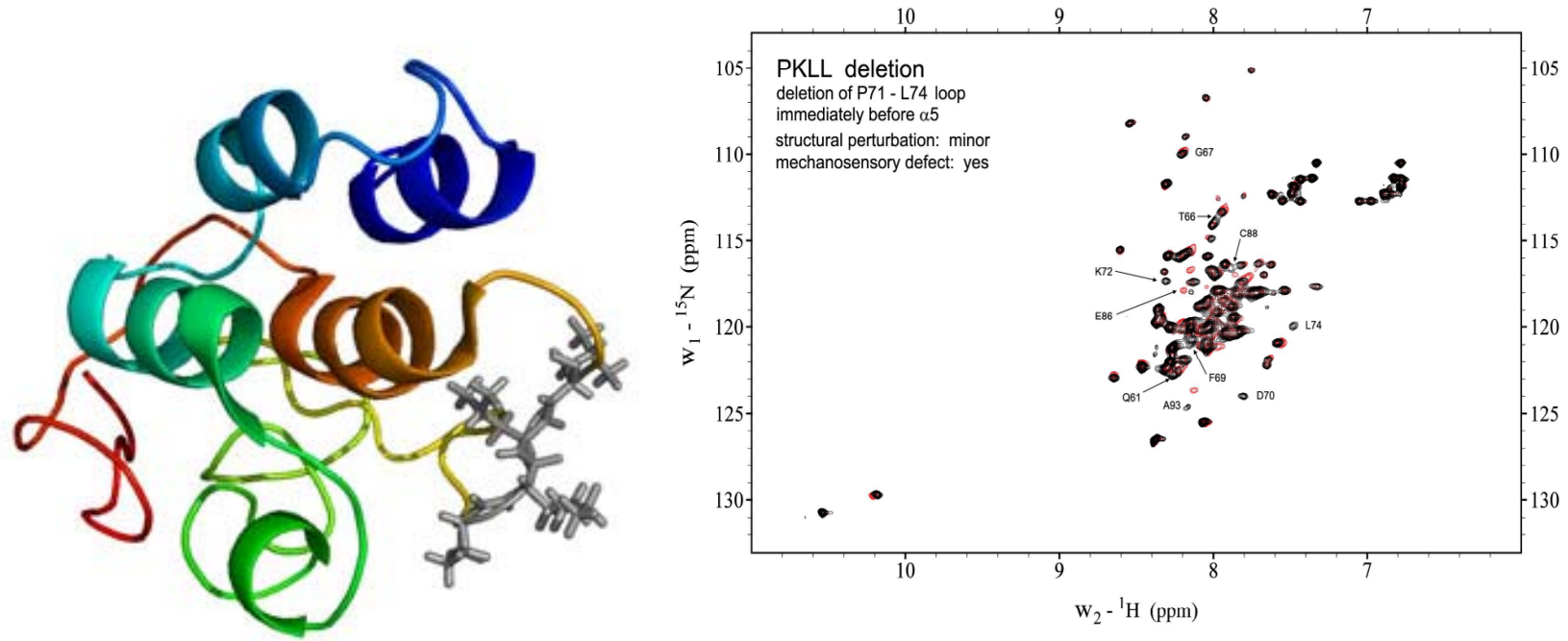

Figure 31: Ribbon diagram of MEC-4N(W82) and ^{15}N HSQC spectrum of MEC-4N(W82E).

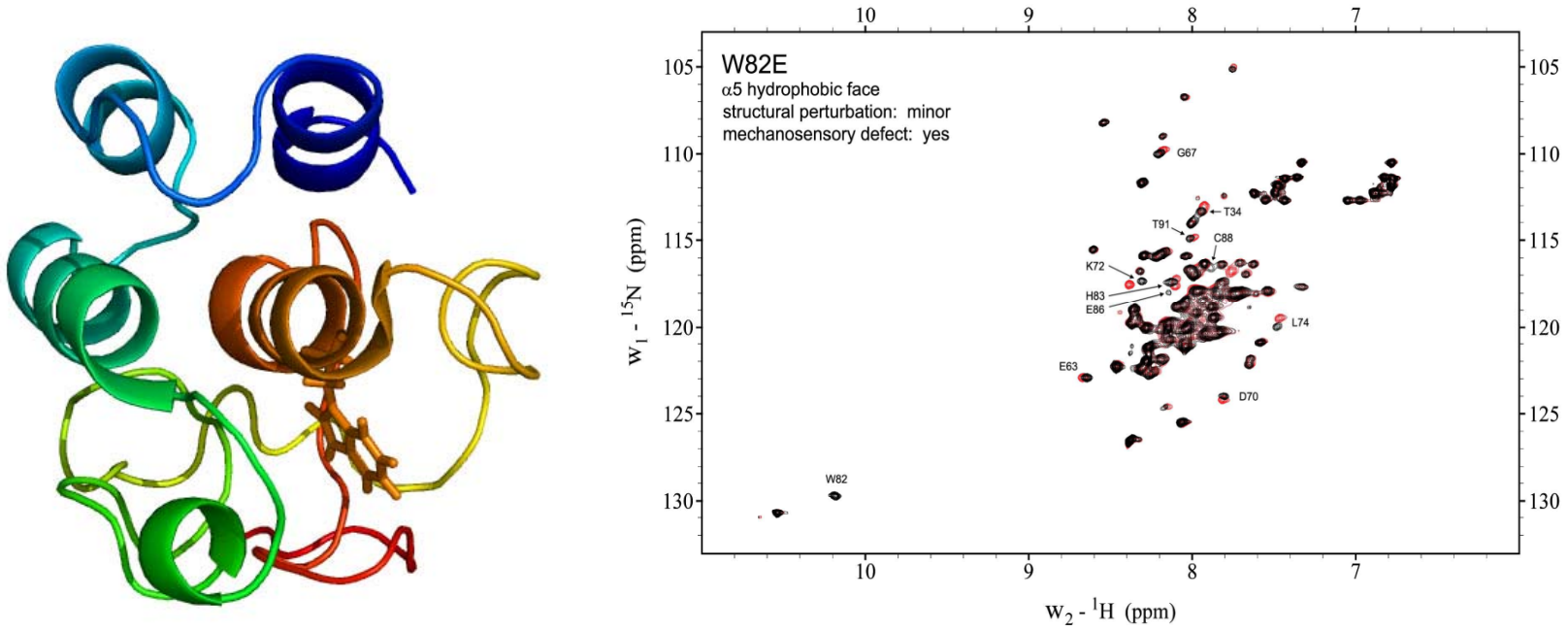

Figure 32: Ribbon diagram of MEC-4N(F84) and ^{15}N HSQC spectrum of MEC-4N(F84E).

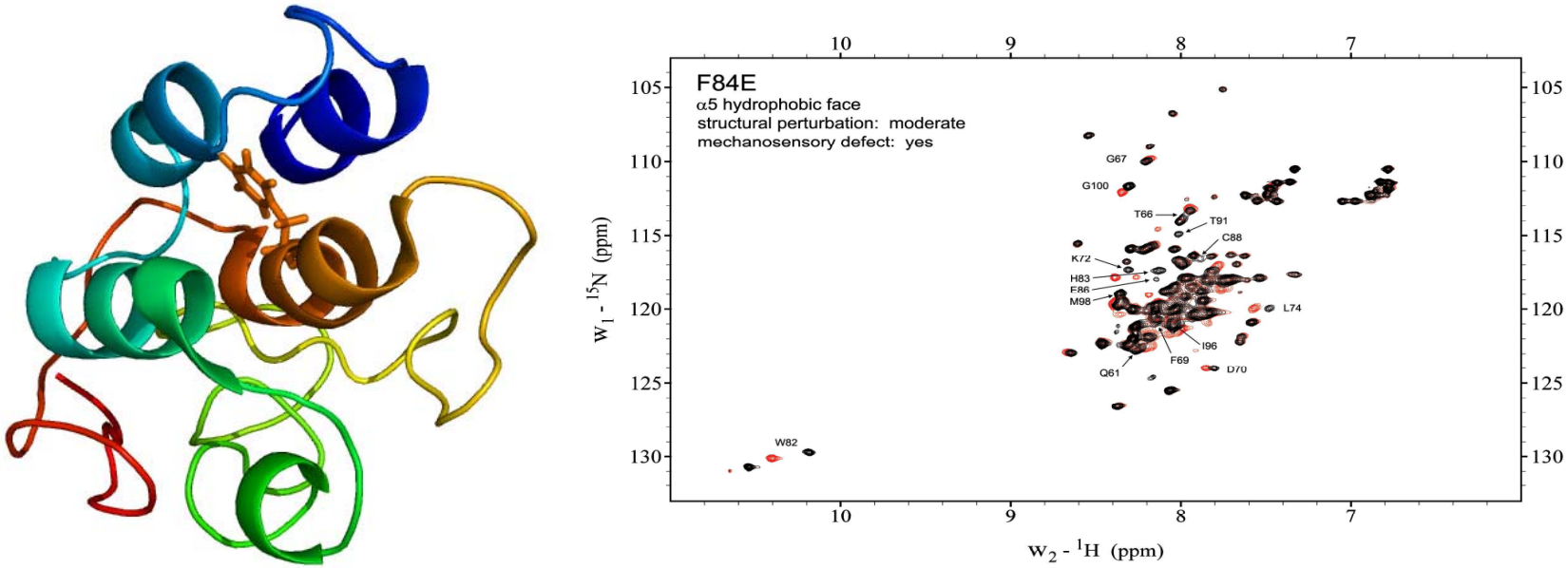

Figure 33: Ribbon diagram of MEC-4N(F87) and ^{15}N HSQC spectrum of MEC-4N(F87E).

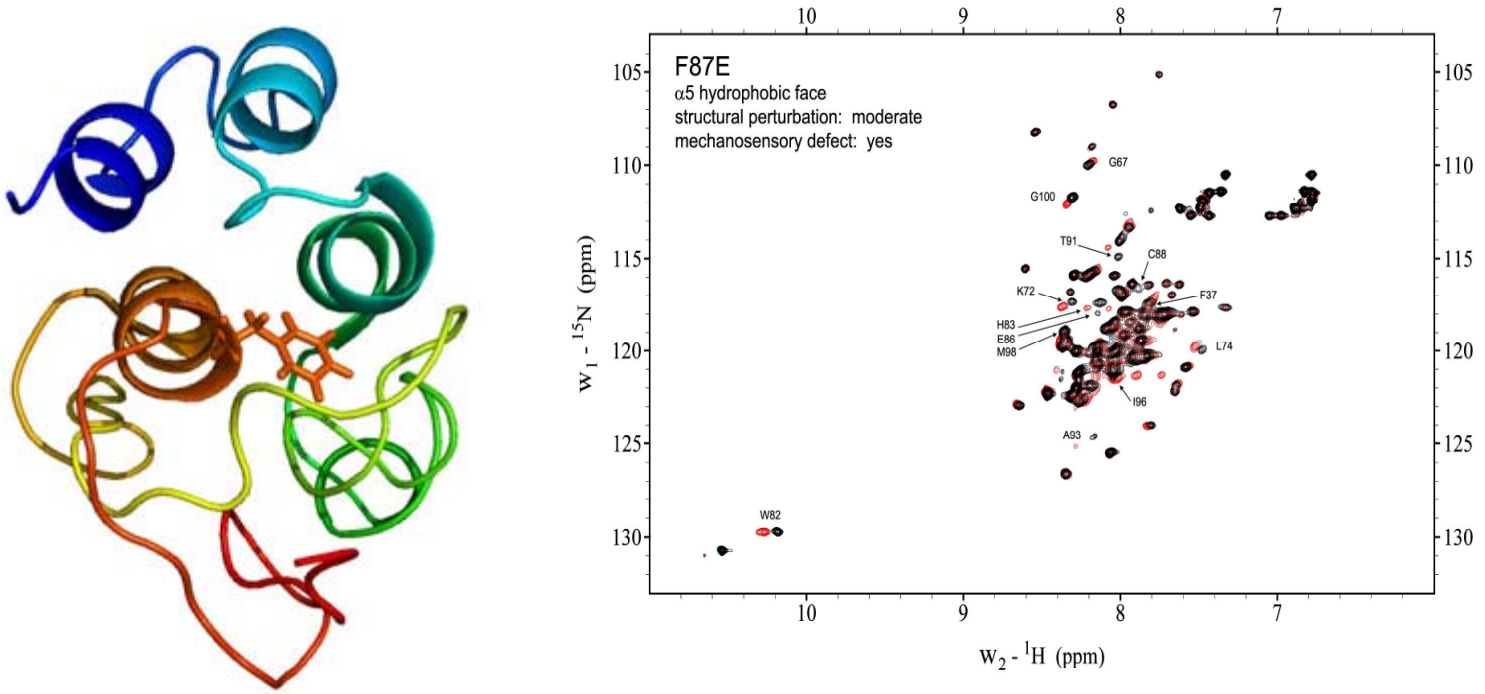

Figure 34: Ribbon diagram of MEC-4N(C52), MEC-4N(C62), and MEC-4N(C88) and ^{15}N HSQC spectrum of MEC-4N(C52A), MEC-4N(C62A), and MEC-4N(C88A).

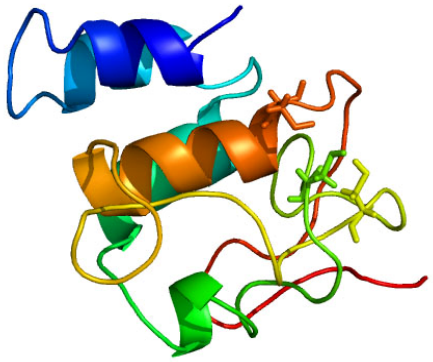

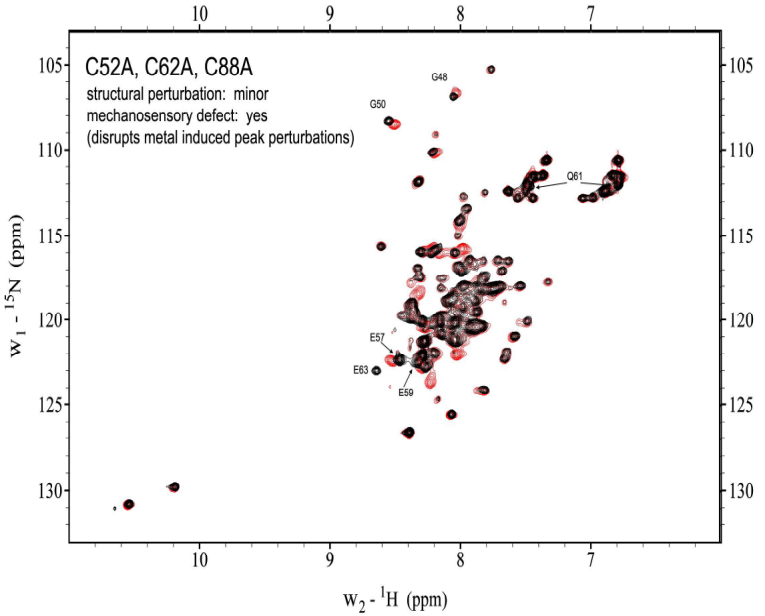

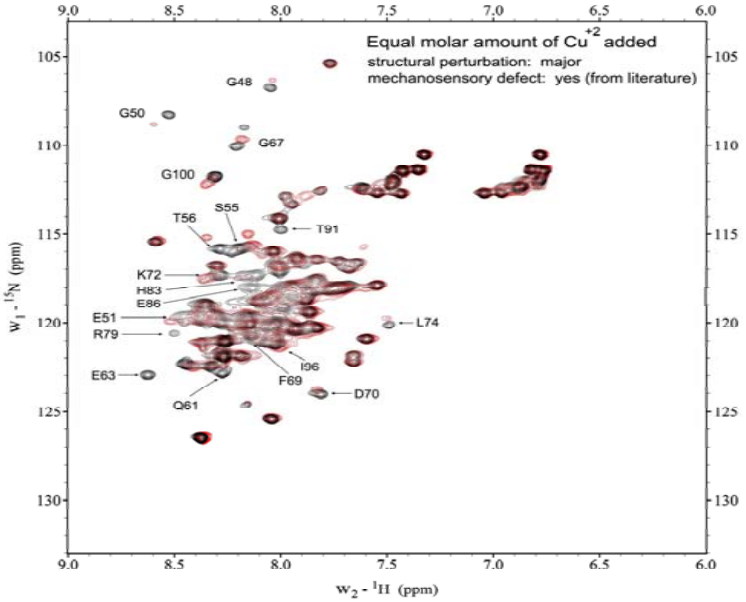

Figure 35: ^{15}N HSQC spectrum of MEC-4N(H94A).

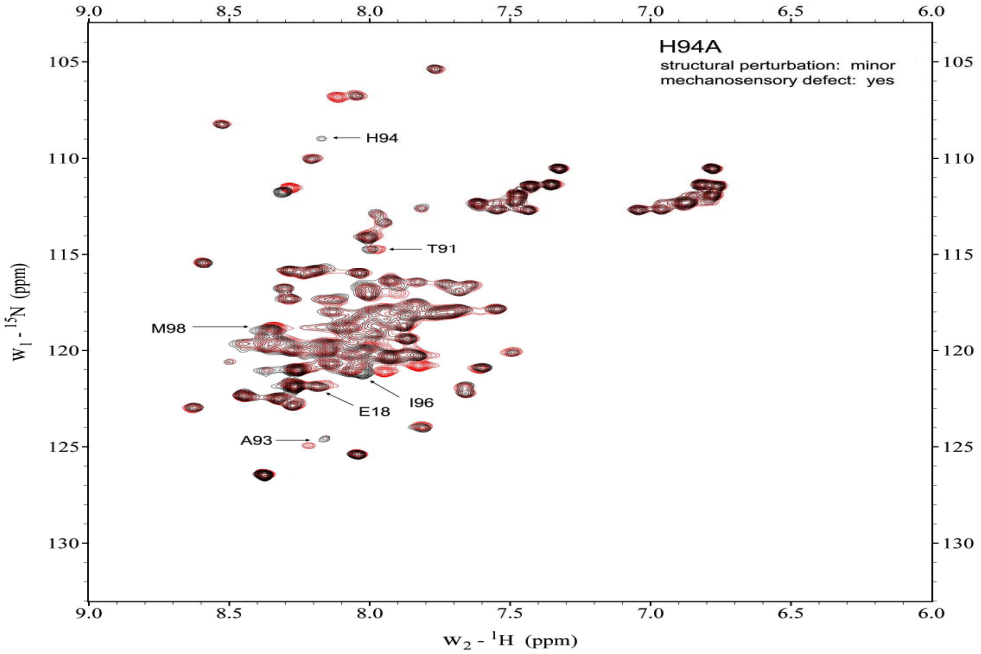

Figure 36: Puncta number and length changes in MEC-4 N-terminal mutant worms.
a)

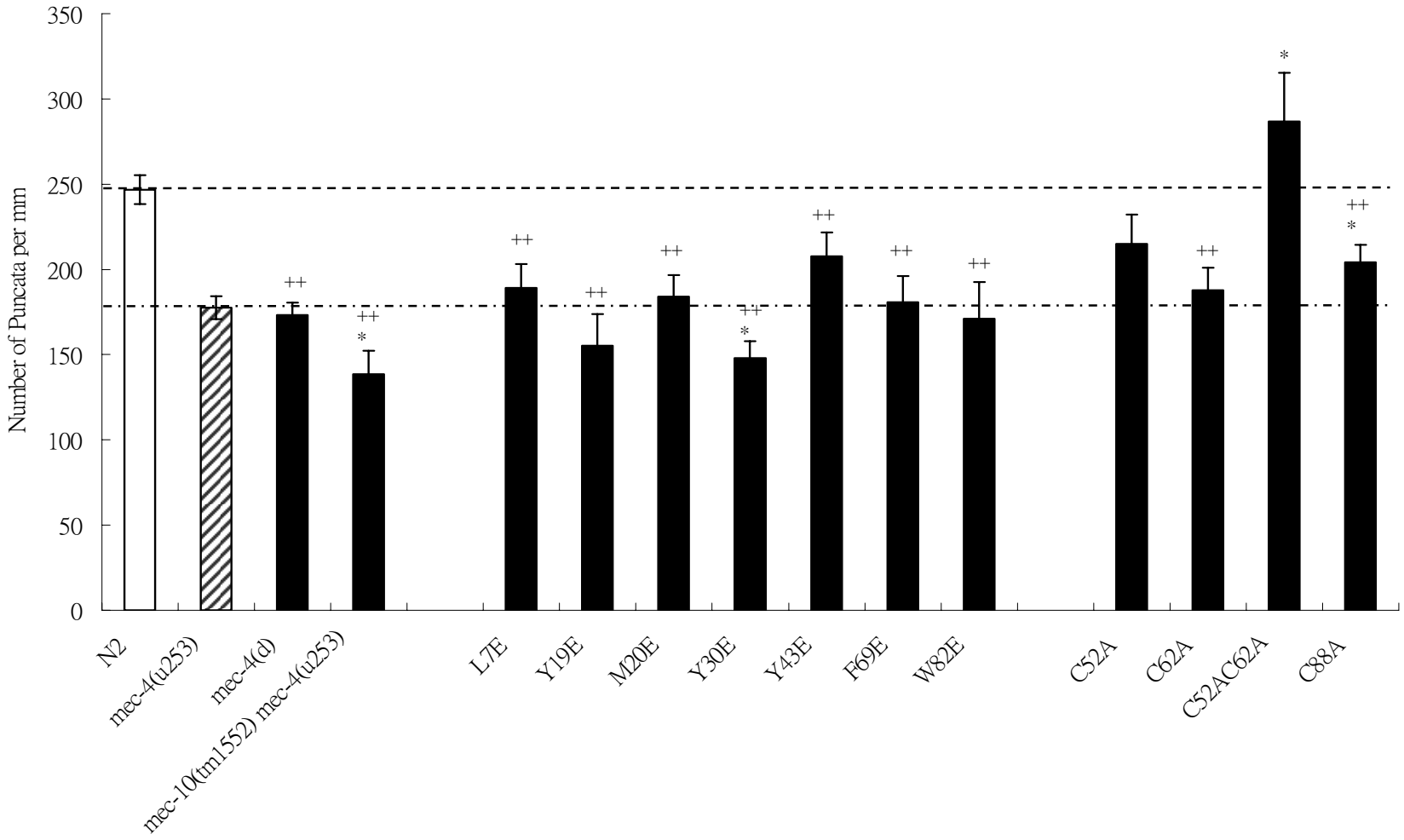

b)

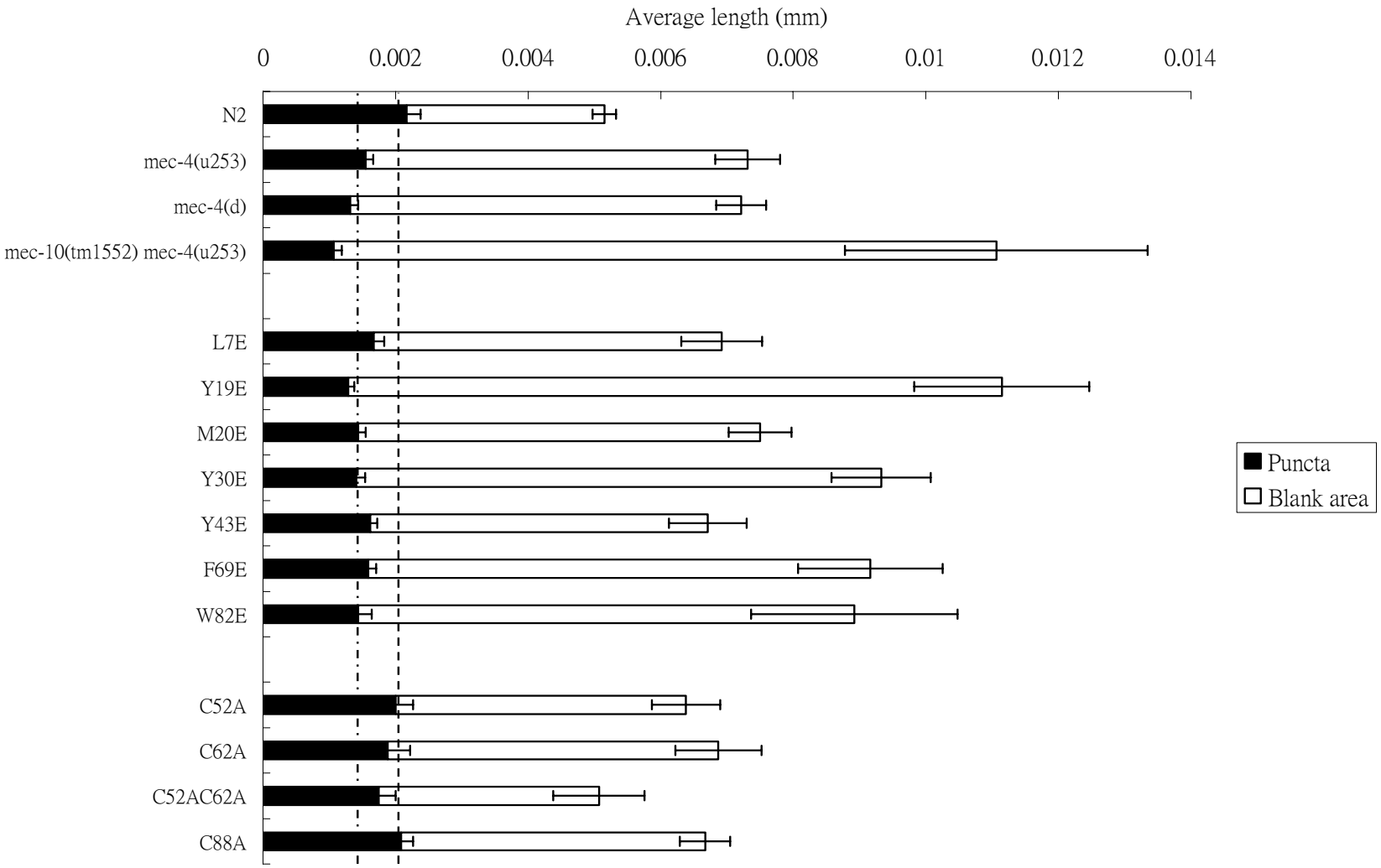
Average length (mm)
0
0.002
0.004
0.006
0.008
0.01
0.012
0.014
N2
mec-4(u253)
mec-4(d)
mec-10(tm1552) mec-4(u253)
L7E
Y19E
M20E
Y30E
Y43E
F69E
W82E
C52A
C62A
C52AC62A
C88A
Puncta
Blank area

Figure 37: Sequence alignment of 3 Cysteine regions in MEC-4 and other DEG/ENaC superfamily members.

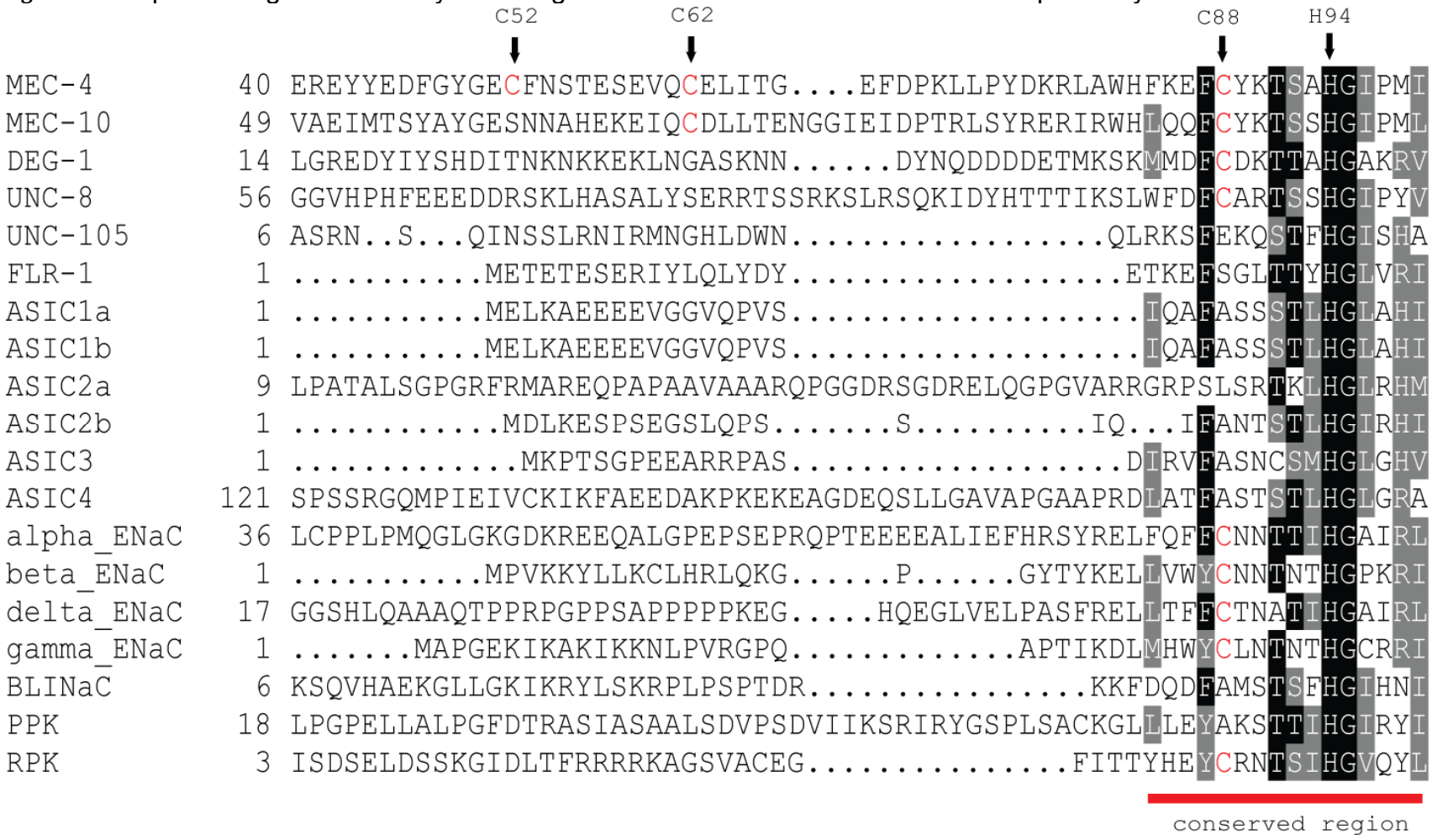

Appendix I:

The *C. elegans* DEG/ENaC channel MEC-10 functions in gentle touch and harsh touch mechanosensation

[1]Marios Chatzigeorgiou, [2]Katie S. Kindt, [3]WeiHsiang Lee, [3]Monica Driscoll, [1,2]William R. Schafer
[1]Cell Biology Division, MRC Laboratory of Molecular Biology, Hills Road, Cambridge UK
[2]Division of Biology, University of California, San Diego, La Jolla CA USA
[3] Department of Molecular Biology and Biochemistry, Nelson Biological Laboratories, Rutgers, The State University of New Jersey, Piscataway, NJ USA

SUMMARY: DEG/ENaC channels have been broadly implicated in mechanosensory transduction, yet many questions remain about how these proteins contribute to complexes that sense mechanical stimuli. In *C. elegans*, two DEG/ENaC channel subunits are thought to contribute to a gentle touch transduction complex: MEC-4, which is essential for gentle touch sensation, and MEC-10 whose importance is less well-defined. By characterizing a *mec-10* null mutant, we have found that MEC-10 is important, but not essential, for gentle touch responses in body touch neurons. Surprisingly, the requirement for MEC-10 in gentle touch neurons is spatially asymmetric; *mec-10* mutants respond well to stimulation at the distal end of touch neuron dendrites but responded poorly to stimuli applied near the neuronal cell body. MEC-10 is also expressed in touch neurons that do not express MEC-4, including the FLP neurons that sense nose touch and the PVD neurons that sense harsh touch. In FLP, we find that MEC-10 functions additively with the TRP channel OSM-9 to mediate nose touch

sensation, with MEC-10 particularly important for responses to repeated stimulation. In contrast, MEC-10 is required without OSM-9 to sense harsh touch in both PVD and FLP. These findings indicate that MEC-10 contributes to distinct harsh and gentle touch modalities in different mechanosensory neurons.

INTRODUCTION

The senses of touch, hearing, and balance depend on sensory neurons that generate receptor potentials in response to mechanical force. Most, if not all, mechanosensory neurons sense force using ion channels that are directly mechanically gated. The structural subunits of these channels appear to come primarily from one of two protein superfamilies: the TRP channels and the DEG/ENaC channels (Garcia- Anoveros and Corey, 1997; Goodman et al., 2004). TRP channels are non-specific cation channels composed of subunits with six transmembrane -helices. At least some TRP channels appear to sufficient by themselves to produce touch- or stretch-evoked currents (Christensen and Corey, 2007). In addition, TRP channels can be activated by G-protein signaling, which has been implicated in other sensory transduction processes including taste, vision and olfaction (Kahn-Kirby and Bargmann, 2006). In contrast, DEG channels have two transmembrane -helices and are permeable to sodium and in some cases calcium (Bounoutas and Chalfie, 2007). Relatively little is known about how DEG channels are activated by mechanical or other stimuli. Perhaps the best-studied case of DEG channel-mediated mechanosensation involves the gentle body touch neurons of *C. elegans*. Three gentle touch neurons (ALML, ALMR, and AVM) have processes extending from the mid-body to the pharynx and are

required for escape responses to light mechanical stimulation anterior body (Chalfie et al., 1985). Two additional neurons (PLML amd PLMR) have processes extending from the tail to the midbody and are required for escape responses to posterior gentle touch. Screens for mutants defective in gentle touch avoidance have identified over a dozen *mec* genes whose products are specifically required for the function of these neurons (Chalfie and Au, 1989). Among the *mec* genes are two that encode DEG/ENaC channel proteins, MEC-4 (Driscoll and Chalfie, 1991) and MEC-10 (Huang and Chalfie, 1994), and two DEG channel accessory subunits, MEC-2 (Huang et al., 1995) and MEC- 6 (Chelur et al., 2002). Additional *mec* genes encode extracellular or intracellular structures thought to be important for coupling external forces to channel gating; however, the mechanisms by which this might occur are not known (Bounoutas and Chalfie, 2007; Goodman and Schwarz, 2003). The importance of each of the *mec* genes for mechanosensation in the gentle touch neurons has been investigated at the cellular level through *in vivo* imaging and electrophysiology. Wild-type *C. elegans* exhibit robust calcium transients in the gentle touch neurons in response to mechanical stimulation; null mutations in *mec-4, mec-2* and *mec-6* abolish these responses (Suzuki et al., 2003). Likewise, *mec-4, mec-2*, and *mec-6* null mutant neurons lack mechanoreceptor potentials measured by electrophysiology (O'Hagan et al., 2005). Previously characterized *mec-10* alleles are missense mutations (Huang and Chalfie, 1994), which reduce but do not eliminate mechanoreceptor potentials evoked by mechanical stimulation (O'Hagan et al., 2005). Thus, determination of *mec-10*'s importance to the mechanoreceptor complex has awaited analysis of a *mec- 10* null allele. In addition to the gentle body touch neurons, MEC-10 is expressed in several additional cell types, where its function has not been established. The

PVM neurons express *mec-10*, as well as most of the other *mec* genes (Huang and Chalfie, 1994), and their overall morphology is very similar to that of the gentle touch neurons. However, unlike the gentle touch neurons, PVM is not sufficient to mediate an escape response to gentle touch, and its role in mechanosensory behaviour in general is not known (Chalfie and Sulston, 1981; Chalfie et al., 1985). Unlike the gentle touch neurons, PVM expresses another DEG channel gene, *unc-8*, which has been hypothesized to encode a stretch receptor potentially involved in proprioception (Tavernarakis et al., 1997). Another class of neurons expressing *mec-10* are the FLPs, which play a role in escape responses to nose touch. The FLPs have highly branched multidendritic arbours that surround the animal's head, which are thought to be mechanosensory (Huang and Chalfie, 1994). *mec-4* is not expressed in the FLPs, but these neurons do express the TRP channel OSM-9, which is required for nose touch responses by the polymodal ASH neurons (Colbert et al., 1997). Finally, *mec-10* is expressed in the PVD neurons, which have been implicated in responses to harsh body touch (Way and Chalfie, 1989b). Similar to the FLPs, the PVDs have multidendritic arbours that cover the animal's body. Likewise, the PVDs do not express MEC-4, but express OSM-9, a TRP channel that is involved in mechanosensation in other *C. elegans* neurons (Colbert et al., 1997). In this study, we have investigated the role of MEC-10 in three classes of *C. elegans* mechanosensory neurons, involved in sensing gentle body touch, harsh body touch, and nose touch. By analyzing a *mec-10* null mutant, we find that MEC-10 is important for responses to gentle touch applied near the mechanoreceptor neuron's cell body, but not for touch applied near the distal end of the touch receptor process. In contrast, MEC-10 is essential for harsh touch responses in two neuron types, PVD and FLP. Finally, MEC-10 functions additively with the TRP channel

OSM-9 to facilitate nose touch responses in FLP, playing a particularly important role in responses to repeated stimulation. These results suggest that MEC-10 functions in different molecular and cellular contexts to mediate distinct mechanosensory modalities.

RESULTS

mec-10 is important but not essential for gentle body touch mechanosensation

To determine the null phenotype of *mec-10*, we analyzed a deletion allele, *mec-10(tm1552)*(Zhang et al., 2008). This allele is predicted to encode only the first 189 amino acids of MEC-10, including the intracellular N terminus, the first transmembrane domain and some extracellular residues (Supplemental Figure 1). Sequences encoding most of the MEC-10 extracellular domain and part of the second transmembrane domain are absent in the mutant allele, and a frameshift would introduce new in-frame stop codons that should prevent inclusion the C-terminal domains in any truncated translation product. Attempts to detect a *mec-10(tm1552)* mutant cDNA by RT-PCR were unsuccessful, suggesting that the prematurely-terminated mRNA may be largely degraded in mutant animals. Together, these results lead us to conclude that *mec- 10(tm1552)* is a likely null allele of *mec-10*. To determine the effect of *mec-10* loss-of-function on gentle touch sensation, we scored the reversal responses of *mec-10(tm1552)* animals to a light eyelash stroke across the anterior body, which have been shown previously to depend on several of the *mec* genes. We observed that when *mec-10(tm1552)* animals were touched near the midbody, they exhibited a strong Mec phenotype comparable to that of *mec-4* null animals. Interestingly, when the animals were stimulated at locations along the ALM process that were more

distal to the cell body, we observed that *mec-10(tm1552)* animals showed significant touch sensitivity, whereas *mec-4* null animals remained touch-insensitive (Figure 1). *mec-10* point mutant animals showed a similar strong Mec phenotype at the midbody and weak Mec phenotype in more anterior locations (data not shown). Thus, *mec-10* appears to be important but not essential for gentle touch responses, particularly to stimuli received near the head. Interestingly, this spatial asymmetry in phenotypic strength resembles what was previously described for weak alleles of *mec-7* (Savage et al., 1989). We also directly measured responses of the gentle touch mechanosensory neuron ALM to mechanical stimulation using a transgenic line, *bzIs17,* expressing the calciumsensitive protein cameleon under the touch-neuron-specific *mec-4* promoter. We showed previously that wild-type animals generated calcium transients of similar size in response to gentle stimulation at various points along the anterior cell body (Suzuki et al., 2003). When we conducted similar experiments in a *mec-10(tm1552)* background, we observed that the magnitude of the touch-evoked calcium influx was significantly reduced. Moreover, as with the behavioral experiments, we observed a spatial asymmetry in the magnitude of the ALM response to touch: responses to stimulations near the head were only partially reduced relative to wild-type, while responses to stimuli applied near the ALM cell body were almost completely absent (Figure 2). These results support the conclusion that MEC-10 is important but not essential for mechanosensation in ALM, and that MEC-10 is particularly important for responses to touch in proximal regions of the dendrite. *C. elegans* also respond to gentle touch on the posterior body by accelerating forward away from the stimulus; this response is dependent on the PLM neurons. To assess the role of *mec-10* in these neurons, we applied gentle touch with an eyelash to various points within

the PLM receptive field and assayed whether the animals exhibited a forward escape response. We observed that *mec-10(tm1552)* animals were partially but not completely defective in posterior touch avoidance, similar to what we found for anterior touch. Moreover, we found that *mec-10(tm1552)* mutants were more strongly defective in responding to stimuli in areas proximal to the PLM cell body and responded better to stimuli applied in more distal areas (Supplemental Figure 2). This asymmetry in the requirement for *mec-10* in PLM was also observed in calcium imaging experiments, which showed a significantly stronger reduction in cell body calcium transients in response to proximal stimulation than to distal stimulation (Supplemental Figure 3). Thus, in PLM *mec-10* is also important but not essential for gentle touch mechanosensation, and its function appears to be more important in proximal regions of the dendrite than in distal regions. We also investigated the function of MEC-10 in the PVM neuron. PVM shares the morphology of the gentle body touch neurons ALM, AVM and PLM, and like these neurons expresses MEC-10, MEC-4, as well as other mechanosensory genes. However, unlike these other neurons, PVM is neither necessary nor sufficient for gentle touch avoidance, and its role in touch-regulated behaviors has not been characterized (Chalfie et al., 1985). To measure PVM responses to mechanosensory stimuli, we used the *bzIs17* line to image touch-induced calcium transients in PVM. We observed that in wild-type animals, PVM generated calcium transients in response to gentle touch stimuli that activated ALM and PLM (Supplemental Figure 4). In *mec-10* null mutants, the touchevoked calcium transient was reduced but not eliminated. As in ALM, neither the *mec-4* null mutant nor a *mec-10(tm1552); mec-4* double mutant had any detectable response to gentle touch. Thus, MEC-10 appears to be important but not essential for

mechanosensation in PVM.

MEC-10 and OSM-9 contribute independently to nose touch mechanosensation

In addition to the gentle body touch receptors, two other classes of *C. elegans* mechanoreceptors express MEC-10: the FLP nose touch receptors, and the PVD harsh body touch receptors. To investigate the role of MEC-10 in these neurons, we generated a transgenic line expressing the calcium-sensitive fluorescent protein YCD3 under the control of the *egl-46* promoter. These animals, designated *ljEX19*, expressed the calcium indicator in both the FLP and PVD neurons. To investigate the responses of the FLP neurons to nose touch, we immobilized *ljEX19* animals on agarose pads and applied pressure to the nose using a glass probe as described previously (Hilliard et al., 2005; Kindt et al., 2007a; Kindt et al., 2007b). We observed that in wild-type animals, a nose press stimulus evoked a robust calcium transient, indicating that FLP neurons indeed respond to nose touch. When we applied the same stimulus to animals carrying a *mec-10* null allele, we observed a partial but significant reduction in the magnitude of the touch-evoked calcium transient (Figure 3). In contrast, loss-of-function mutations in *unc-8* and *del-1*, other DEG/ENaC channel genes expressed in FLP, did not detectably affect calcium responses to touch (Supplemental Figure 5). Mutations in *mec-6*, which encodes an accessory subunit important for the activity of the MEC-4 mechanotransducer and possibly for other DEG channels (Chelur et al., 2002), reduced touch-evoked calcium transients in FLP to a similar degree as the *mec-10* null allele (Supplemental Figure 5). These results indicate that a MEC-10-containing DEG channel contributes to the nose touch response in

the FLP neurons. In addition to the MEC-10 DEG channel protein, another potential mechanotransduction channel is expressed in the FLP neurons: the TRPV channel OSM- 9. To determine whether OSM-9 could contribute to the nose touch response remaining in *mec-10(tm1552)* mutant animals, we imaged FLP responses to nose touch in *osm-9* single mutant and *osm-9; mec-10(tm1552)* double mutant animals. We observed that a null mutation in *osm-9* led to a significant reduction in touch-evoked calcium transients in FLP (Figure 3c). Furthermore, a *mec-10(tm1552); osm-9* double mutant showed virtually no significant calcium increase in response to mechanosensory stimulation in FLP (Figure 3d). These results indicate that MEC-10 and OSM-9 contributed additively to the mechanosensory response to nose touch in FLP. To investigate this possibility further, we assayed the effect of the *mec- 10(tm1552)* deletion on nose touch-related behaviour. The reversal response to nose touch depends primarily on the FLP and ASH sensory neurons. We therefore investigated whether a *mec-10(tm1552)* mutation affected this nose touch escape behaviour. We observed that the *mec-10* null mutant responded to nose touch 73% of the time, compared to 90% for wild-type. Since the responsiveness of ASH to nose touch has been shown to depend on *osm-9,* we also investigated whether *mec-10* loss-offunction could enhance the nose-touch behavioural phenotype of *osm-9*. We observed (Figure 3e) that *osm-9* single mutants responded to nose touch 66% of the time, while *mec-10(tm1552)*; *osm-9* double mutants responded 34% of the time. These results further indicate that MEC-10 and OSM-9 function together in the FLP neurons to mediate nose touch mechanosensation.

Effect of *mec-10* on nose touch desensitization

Many sensory modalities adapt or desensitize upon repeated stimulation. To investigate desensitization to nose touch, we applied a series of up to 30 nose touch stimuli, separated by an interstimulus interval of 15 seconds. We observed that in wildtype *C. elegans*, animals remained quite responsive to nose touch even after 30 nose touches. However, when we tested *mec-10* null animals, we found that their responsiveness to nose touch, which was initially nearly 80% of wild-type, desensitized almost completely after 20 touches (Figure 4a). This result suggested that the *mec-10* mutants were particularly defective in responding to repeated nose touch stimulation. To investigate this further, we imaged calcium responses in FLP to a series of four nose touch stimuli separated by 300 second interstimulus intervals. Again, whereas wild-type responses in FLP showed little diminution between the first and fourth stimulus, in *mec- 10* animals the response rapidly desensitized (Figure 4b-c). These findings indicate that MEC-10 mediates a slowly-adapting nose touch modality in the FLP neurons that is particularly important in maintaining responsiveness to repeated touch stimulation.

MEC-10 is required for harsh touch mechanosensation in PVD and FLP

Finally, we investigated the importance of MEC-10 in harsh touch mechanosensation. The PVD neuron has been shown to be important for escape responses to harsh body touch; however, the gentle body touch neurons are also capable of generating harsh touch responses. Therefore, to assess the importance of *mec-10* for mechanosensation in PVD, we assayed harsh touch phenotypes of *mec-10(tm1552)* mutants alone as well as in a genetic background in which the gentle touch neurons were absent due to a necrosis-inducing *mec-4* dominant allele. We observed that in a *mec- 10(tm1552)* single

mutant, harsh touch responses were only slightly reduced compared to wild-type (Figure 5a). However, the *mec-10(tm1552); mec-4(u231)* double mutant was significantly less sensitive to harsh touch than the *mec-4(u231)* single mutant. These results are consistent with the possibility that *mec-10* is important for the mechanosensory responses of PVD to harsh touch. To test this possibility directly, we imaged harsh touch-induced calcium transients in PVD using the *ljEX19* line described above. We observed that calcium transients could be evoked in wild-type cameleon-expressing animals using a mechanical stimulus of large displacement and high velocity (Figure 5a). In contrast, *mec-10* null mutants, showed no detectable calcium transients in response to this harsh touch stimulation (Figure 5e, g). We also tested the harsh touch responses of mutants defective in *osm-9*, which is also expressed in PVD. In contrast to what we had observed for nose touch in FLP, we found that *osm-9* loss-of-function mutants had essentially normal calcium responses to harsh touch stimulation of PVD (Figure 5c, g). Thus, MEC-10 appears to be essential for harsh touch mechanosensation in PVD, while OSM-9 has no detectable effect on this process. FLP has a multidendritic morphology similar to that of PVD; thus we reasoned it might also respond to harsh touch. We applied a harsh touch stimulus similar to that used in PVD imaging experiments to the side of the head in the region of the FLP dendritic lattice, and we imaged calcium transients evoked in the FLP cell body. We observed large calcium transients in wild-type animals that resembled harsh touch responses in PVD in size and temporal kinetics (Figure 5b). When we performed similar experiments in *mec-10* null mutant animals, the calcium response was nearly absent (Figure 5f, h). In contrast, mutations in *osm-9* had little effect on FLP harsh touch responses Figure 5d, h). Thus, FLP, like PVD, appears to contain a harsh head touch

modality that is dependent on MEC-10 but not OSM-9.

DISCUSSION

MEC-10 is important for mechanosensation in specific regions of the gentle touch neurons

We have found that although *mec-10* null mutations impair the responsiveness of the gentle body touch mechanoreceptors, they do not completely abolish touch responses in these neurons. This phenotype contrasts with that of *mec-4*, *mec-2,* and *mec-6* null mutants, whose body touch mechanoreceptors have no detectable response to gentle touch. Standard models hypothesize that the mechanosensory complex in the gentle touch neurons consists of a core channel composed of MEC-4 and MEC-10, along with MEC-2 and MEC-6 as accessory subunits. Our results suggest that MEC-10 is not an essential component of this complex. Homomeric complexes containing only MEC-4 channel subunits may be capable of functioning as touch receptors. In support of this hypothesis, coexpression of dominantly active MEC-4 with MEC-2 and MEC-6 yields functional channels in *Xenopus* oocytes, and the addition of MEC-10 actually reduces expressed currents in this heterologous system (Goodman et al., 2002). We observed an unexpected asymmetry in the requirement for MEC-10 in the ALM anterior touch neuron. Specifically, in both behavioural and calcium imaging experiments, we observed that *mec-10* null animals were significantly more defective in responding to touch stimuli administered near the mid-body than to stimuli administered at the neck. Since the imaging experiments measured calcium transients in the cell body, the fact that *mec-10* disproportionately affected responses to stimuli near the cell body is unlikely to reflect a defect in propagation

of the mechanoreceptor potential along the process. Rather, MEC-10 may contribute differentially to mechanoreceptor complexes in different regions of the dendrite. Specifically, mechanoreceptor complexes in the cell body-proximal region of the dendrite may require both MEC-4 and MEC-10 subunits, while mechanoreceptor complexes in the distal region may require MEC-4 but not MEC- 10. Consistent with this model, a previous study (O'Hagan et al., 2005) reported that strong defects in mechanoreceptor potentials recorded from *mec-10* point mutants measured receptor potentials in response to stimuli applied near the PLM cell body, a region in which MEC-10 appears to have particular functional importance.

MEC-10 functions without MEC-4 in harsh touch mechanosensation

We also identified a functional role for MEC-10 in the PVD neurons, putative harsh touch mechanoreceptors that do not appear to express MEC-4. We observed that strong mechanical stimuli evoked calcium transients in PVD that were absent in *mec-10* null mutants. Likewise, in *mec-4(u231)* animals lacking the gentle touch neurons, behavioural responses to harsh touch were highly dependent on *mec-10*. In contrast, *osm-9*, a TRP channel that is expressed in PVD and is important for nose touch mechanosensation in the ASH neurons, had no measurable effects on PVD-mediated harsh touch responses. Thus, the harsh touch modality of PVD appeared to be largely mediated by a DEG channel containing MEC-10, but not MEC-4. We note that a previous study reported that *mec-10* mutants retained sensitivity to harsh touch (Way and Chalfie, 1989a); this result might reflect the residual gentle touch modality remaining in the ALM and AVM neurons of *mec-10* point mutants, which is eliminated in the *mec- 4(u231)* background. MEC-10

thus represents an essential component of the harsh touch mechanotransducer in PVD. The FLP neurons have many similarities with the PVDs: they have a similar multidendritic morphology, and they express both DEG (*mec-10*) and TRP (*osm-9*) channels implicated in mechanosensation. Indeed, calcium transients were evoked in FLP by harsh touch to the side of the head, indicating that FLP, like PVD, is a harsh touch mechanosensory neuron. As in PVD, *mec-10* null mutant animals lacked harsh touch –evoked calcium transients, while *osm-9* mutants showed normal repsonses. Thus, the harsh touch modality of FLP also appears to be specifically dependent on MEC-10- containing DEG channels. What other proteins might contribute to the harsh touch mechanoreceptor complex? In contrast to the gentle touch modality, which has been subjected to intense genetic and physiological study, relatively little is known about the molecular basis of the harsh touch modality of PVD or FLP. Potentially, DEG channels consisting only of MEC-10 (plus accessory subunits) might participate in harsh touch sensation. However, since expression of MEC-10(d) without MEC-4 has not been reported to produce functional channels in oocytes, MEC-10 may not be able to form homomeric channels. *C. elegans* contains at least 28 DEG channel genes, most of whose expression domains have not been characterized; thus, it is reasonable to speculate that another DEG channel protein may complex with MEC-10 in harsh touch mechanoreceptors. In addition, the harsh touch mechanoreceptors are also likely to contain at least some accessory subunits not found in the gentle touch receptors. Since harsh touch receptor function can be straightforwardly assayed in *mec-4(u231)* mutant background (in which the gentle touch neurons are absent), it should be possible to identify additional components of the harsh touch mechanoreceptor by assaying candidate gene knockouts or by conducting forward mutant

screens.

DEG and TRP channels function independently in nose touch mechanosensation

In addition to responding to harsh touch to the side of the head, FLP also responds to gentler mechanical stimuli applied to the tip of the nose. Unexpectedly, the roles of the MEC-10 and OSM-9 channels in this nose touch modality of FLP appear to be somewhat different from their roles in harsh touch. Whereas MEC-10 was absolutely required for harsh touch-evoked calcium transients in both FLP and PVD, *mec- 10(tm1552)* mutations only partially reduced the magnitude of nose touch-evoked calcium transients in FLP. Moreover, the component of the FLP touch response remaining in *mec-10(tm1552)* animals was dependent on *osm-9*, which had no effect on harsh touch mechanosensation in FLP or PVD. The MEC-10-dependent and OSM-9 dependent components of the nose touch modality themselves appear to have distinct properties: the OSM-9 component appears to desensitize rapidly, and most of the response to repeated nose touch stimulation is therefore dependent on MEC-10. Taken together, there appear to be several distinct mechanosensory modalities in FLP, one (involved in harsh head touch) mediated by MEC-10-containing DEG channels and others (involved in gentle nose touch) mediated by the combined action of MEC-10- containing DEG channels and OSM-9-containing TRP channels. Together, our findings indicate that a single DEG channel protein, MEC-10, makes distinct contributions to several touch sensory modalities in *C. elegans* (Figure 6). In gentle body touch neurons, MEC-10 appears to function in association with the DEG protein MEC-4 in a mechanotransduction complex critical for gentle touch sensation in the

anterior midbody and tail. In PVD and FLP, MEC-10 contributes to a MEC-4- independent mechanosensor that responds to much stronger harsh touch stimuli. Since MEC-4 is not expressed in these neurons, we hypothesize that the harsh touch mechanosensory complex may involve an association between MEC-10 and a different DEG channel protein. In FLP, there may be a third MEC-10-dependent mechanosensor, which functions together with OSM-9-containing TRP channels to sense gentle nose touch. Since the stimulus/response properties of this nose touch modality appear to differ significantly from those of the harsh touch mechanosensor, it is reasonable to suppose that the nose touch mechanosensory complex may contain yet another complement of accessory and/or degenerin subunits. Future genetic analysis of *C. elegans* touch modalities should make it possible to better characterize the subunit composition of these mechanosensory complexes and to learn how their molecular structure affects their responsiveness to distinct mechanical stimuli.

EXPERIMENTAL PROCEDURES *C. elegans* Strains

Wild type *C. elegans* (strain N2) were grown at 21 C using standard methods. Strains used: AQ2145 *ljEx19*, AQ 2124 *mec-10 (tm1552); mec-4(u231); ljEx19[Pegl-46::YC2.3, lin-15(+)]* , AQ 2146 *mec-10(tm1552) mec-4(u253); ljEx19*, AQ2126 *mec- 10(tm1552); ljEx19*, AQ2148 *osm-9(ky10); ljEx19*, AQ2149 *osm-9(ky10); mec- 10(tm1552); ljEx19,* AQ2143 *del-1(ok1500); ljEx19]*, AQ2144 *unc-8(n491n1192); ljEx19*, NC279 *del-1(ok150), MT2611 unc-8(n491n1192*), AQ906 *bzis17[pmec- 4::YC2.12; lin-15(+)]*, AQ908 *mec-4(u253); bzIs17* , AQ1413 *mec-10(tm1552); bzIs17*, AQ2150 *mec10(tm1552) mec-4(u253) bzIs17*, AQ990 *glr-1(n2461)*, AQ2151 *mec- 6(e1342); ljEx19.*

Generation of FLP/PVD cameleon line *ljEX19*

The *egl-46* promoter region was obtained from plasmid TU#307 (Wu et al., 2001), a gift from the lab of Martin Chalfie. A 3 kb HinDIII/NotI fragment was fused to cameleon YC2.3 in the vector pPD95.75 (A. Fire). Transgenic lines were obtained by germline injection of a *lin-15(n765)* mutant strain with the *egl-46::YC2.3* plasmid at a concentration of 50 ng/ l along with *lin-15(+)* genomic DNA (30 ng/ l) as a coinjection marker. Once a stable transgenic line was obtained, the *lin-15(n765)* allele was then removed by backcrossing to wild-type (N2) animals.

Calcium Imaging

Optical recordings were performed essentially as described (Kerr et al., 2000; Kerr, 2006) on a Zeiss Axioskop 2 upright compound microscope equipped with a Dual View beam splitter and a Uniblitz Shutter. Fluorescence images were acquired using MetaVue 6.2. Filter-dichroic pairs were excitation, 400–440; excitation dichroic 455; CFP emission, 465–495; emission dichroic 505; YFP emission, 520–550. Individual adult worms (~24h past L4) were glued with Nexaband S/C cyanoacrylate glue to pads composed of 2% agarose in extracellular saline (145 mM NaCl, 5 mM KCl, 1 mM CaCl2, 5 mM MgCl2,20 mM D-glucose, 10 mM HEPES buffer, pH 7.2). Worms used for calcium imaging had similar levels of cameleon expression in sensory neurons as inferred from initial fluorescence intensity. Acquisitions were taken at 28Hz (35ms exposure time) with 4x4 or 2x2 binning, using a 63x Zeiss Achroplan water immersion objective.

Nose touch stimulation

The nose-touch stimulator was a needle with a 50- m diameter made of a drawn glass capillary with the tip rounded to ~10 m on a flame. We positioned the stimulator using a motorized stage (Polytec/PI M-111.1DG microtranslation stage with C-862 Mercury II controller). The needle was placed perpendicular to the worm's body at a distance of 150 m from the side of the nose. In the 'on' phase, the glass tip was moved toward the worm so that it could probe ~8 m into the side of the worm's nose on the cilia and held on the cilia for 1 second, and in the 'off ' phase the needle was returned to its original position.

Harsh head touch stimulation

To visualize the harsh head touch response in FLP, the same nose touch setup was used but the probe was aligned in a more posterior position between the two bulbs of the pharynx. The probe was displaced ~24 m at a raised speed of 2.8mm/s. The stimulus was a buzz (i.e., the probe was displaced 2.5 m in and out for the duration of the stimulus) lasting ~1 second.

Gentle body touch stimulation

Gentle body touch stimulation was performed as described (Suzuki et al., 2003), with a standard probe displacement of ~10 m. Positions for anterior body touch stimulation were defined as follows: 3=behind terminal bulb, 2= mid-way between the ALM cell body and terminal bulb, 1= within 10 m from ALM cell body, -1= more than 10 m posterior of the ALM cell body. For posterior body touch the points of stimulation were 3= within 10 m from the vulva, 2= midway between the vulva and the tip of the tail, 1= within 10 m of

PLM cell body. For PVM imaging, 3= 200 m anterior of the ALM cell body, 2= 10 m anterior of the vulva, 1= within 10 m of the PVM cell body, -1= more than 10 m posterior of PVM cell body. Individual worms were stimulated at all sites of interest, with a 5 minute interval between each stimulation. Some animals were stimulated at more proximal positions first and then at more distal positions, while others were stimulated in the converse order. Some worms were probed only once at one location to exclude a potential artifact due to desensitization of the neuron.

Harsh body touch stimulation

Harsh stimuli were delivered using a glass needle with a sharp end (the outcome of these experiments was the same if a piece of platinum wire was used) which was driven into the worm ~30 to 50 m at speed of 2.8mm/s. The stimulus was instantaneous and the probe was driven out after ~50ms.

Behavioral Assays

Nose touch

For nose touch, assay plates were prepared fresh within 4 h of use by spreading one drop of saturated *E. coli* strain OP50 onto nematode growth medium plates. For each strain, two plates of ten worms each per genotype were allowed to move forward into an eyelash in the path of the worm. We recorded either a reversal response or null response. We scored the assay blinded and repeated it on at least five independent days. The nose-touch insensitive mutant *glr-1(n2461)* was used as a control.

Gentle body touch

For gentle body touch assays, animals were touched by stroking an eyelash hair across the worm's body at different positions. The stimulus was applied at the following positions: anterior body position 3= behind the terminal bulb of the pharynx, position 2= between the pharynx and the midbody, and position 1= at the midbody, -1= control outside the receptive field; posterior body position 3= near the anus position, 2=half-way between the anus and the vulva, and position 1 near the vulva. Animals were stimulated in each position, and were scored for whether they reversed direction, with a 3 minute interval between each stimulus. In some animals, stimuli were applied in a proximal-todistal direction, and in other animals in a distal-to-proximal direction. 100 animals were assayed from each genotype.

Harsh body touch

For harsh body touch, animals were touched at the midsection of the body with a platinum wire. Reversal responses were scored as described for gentle body touch.

REFERENCES

Bounoutas, A., and Chalfie, M. (2007). Touch sensitivity in Caenorhabditis elegans. Pflugers Arch *454*, 691-702.

Chalfie, M., and Au, M. (1989). Genetic control of differentiation of the *Caenorhabditis elegans* touch receptor neurons. Science *243*, 1027-1033.

Chalfie, M., and Sulston, J. (1981). Developmental genetics of the mechanosensory neurons of *Caenorhabditis elegans*. Dev Biol *82*, 358-370.

Chalfie, M., Sulston, J. E., White, J. G., Southgate, E., Thomson, J. N., and Brenner, S. (1985). The neural circuit for touch sensitivity in Caenorhabditis elegans. J Neurosci *5*, 956-964.

Chelur, D. S., Ernstrom, G. G., Goodman, M. B., Yao, C. A., Chen, L., R, O. H., and Chalfie, M. (2002). The mechanosensory protein MEC-6 is a subunit of the C. elegans touch-cell degenerin channel. Nature *420*, 669-673.

Christensen, A. P., and Corey, D. P. (2007). TRP channels in mechanosensation: direct or indirect activation? Nat Rev Neurosci *8*, 510-521.

Colbert, H. A., Smith, T. L., and Bargmann, C. I. (1997). OSM-9, a novel protein with structural similarity to channels, is required for olfaction, mechanosensation, and olfactory adaptation in *C. elegans*. J Neurosci *17*, 8259-8269.

Driscoll, M., and Chalfie, M. (1991). The *mec-4* gene is a member of a family of *Caenorhabditis elegans* genes that can mutate to induce neuronal degeneration. Nature *349*, 588-593.

Garcia-Anoveros, J., and Corey, D. P. (1997). The molecules of mechanosensation. Annu Rev Neurosci *20*, 567-594.

Goodman, M. B., Ernstrom, G. G., Chelur, D. S., O'Hagan, R., Yao, C. A., and Chalfie, M. (2002). MEC-2 regulates C. elegans DEG/ENaC channels needed for mechanosensation. Nature *415*, 1039-1042.

Goodman, M. B., Lumpkin, E. A., Ricci, A., Tracey, W. D., Kernan, M., and Nicolson, T. (2004). Molecules and mechanisms of mechanotransduction. J Neurosci *24*, 9220- 9222.

Goodman, M. B., and Schwarz, E. M. (2003). Transducing touch in Caenorhabditis elegans. Annu Rev Physiol *65*, 429-452.

Hilliard, M. A., Apicella, A. J., Kerr, R., Suzuki, H., Bazzicalupo, P., and Schafer, W. R. (2005). In vivo imaging of C. elegans ASH neurons: cellular response and adaptation to chemical repellents. Embo J *24*, 63-72.

Huang, M., and Chalfie, M. (1994). Gene interactions affecting mechanosensory transduction in *Caenorhabditis elegans*. Nature *367*, 467-470.

Huang, M., Gu, G., Ferguson, E. L., and Chalfie, M. (1995). A stomatin-like protein necessary for mechanosensation in *C. elegans*. Nature *378*, 292-295.

Kahn-Kirby, A. H., and Bargmann, C. I. (2006). TRP channels in C. elegans. Annu Rev Physiol *68*, 719-736.

Kerr, R., Lev-Ram, V., Baird, G., Vincent, P., Tsien, R. Y., and Schafer, W. R. (2000). Optical imaging of calcium transients in neurons and pharyngeal muscle of C. elegans. Neuron *26*, 583-594.

Kerr, R. A. (2006). Imaging the activity of neurons and muscles. WormBook, 1-13.

Kindt, K. S., Quast, K. B., Giles, A. C., De, S., Hendrey, D., Nicastro, I., Rankin, C. H., and Schafer, W. R. (2007a). Dopamine mediates context-dependent modulation of sensory plasticity in C. elegans. Neuron *55*, 662-676.

Kindt, K. S., Viswanath, V., Macpherson, L., Quast, K., Hu, H., Patapoutian, A., and Schafer, W. R. (2007b). Caenorhabditis elegans TRPA-1 functions in mechanosensation. Nat Neurosci *10*, 568-577.
O'Hagan, R., Chalfie, M., and Goodman, M. B. (2005). The MEC-4 DEG/ENaC channel of Caenorhabditis elegans touch receptor neurons transduces mechanical signals. Nat Neurosci *8*, 43-50.
Savage, C., Hamelin, M., Culotti, J. G., Coulson, A., Albertson, D. G., and Chalfie, M. (1989). mec-7 is a beta-tubulin gene required for the production of 15-protofilament microtubules in Caenorhabditis elegans. Genes Dev *3*, 870-881.
Suzuki, H., Kerr, R., Bianchi, L., Frokjaer-Jensen, C., Slone, D., Xue, J., Gerstbrein, B., Driscoll, M., and Schafer, W. R. (2003). In vivo imaging of C. elegans mechanosensory neurons demonstrates a specific role for the MEC-4 channel in the process of gentle touch sensation. Neuron *39*, 1005-1017.
Tavernarakis, N., Shreffler, W., Wang, S., and Driscoll, M. (1997). unc-8, a DEG/ENaC family member, encodes a subunit of a candidate mechanically-gated channel that modulates *C. elegans* locomotion. Neuron *18*, 107-119.
Way, J. C., and Chalfie, M. (1989a). The mec-3 gene of Caenorhabditis elegans requires its own product for maintained expression and is expressed in three neuronal cell types. Genes Dev *3*, 1823-1833.
Way, J. C., and Chalfie, M. (1989b). The mec-3 gene of Caenorhabditis elegans requires its own product for maintained expression and is expressed in three neuronal cell types. Genes & Development *3*, 1823-1833.
Wu, J., Duggan, A., and Chalfie, M. (2001). Inhibition of touch cell fate by egl-44 and egl-46 in C. elegans. Genes Dev *15*, 789-802.
Zhang, W., Bianchi, L., Lee, W. H., Wang, Y., Israel, S., and Driscoll, M. (2008). Intersubunit interactions between mutant DEG/ENaCs induce synthetic neurotoxicity. Cell Death Differ *15*, 1794-1803.

FIGURE LEGENDS:

Figure 1: *mec-10* is important but not essential for gentle touch avoidance. Animals were touched with an eyelash at the indicated positions; escape responses (reversals) were scored as described. *mec-10(tm1552)* animals responded significantly better when the stimulus was applied more distal to the ALM cell body ($p<.01$ between positions 2 and 3; $p<.05$ between positions 1 and 2) according to the Mann-Whitney rank sum test (n= 100 for each genotype over five different days).

Figure 2: *mec-10* mutants have reduced touch-evoked calcium transients in ALM touch neurons. a. Stimulus positions for imaging experiments. Animals expressing cameleon in touch neurons were given a 1 second gentle (buzz) stimulus at the indicated position, as described in Experimental Procedures. **b-d. Averaged calcium responses of wild-type (b), *mec-10(tm1552)* (c), and *mec-4* (d) null mutants.** Each red trace represents the average percentage change in R/R_0, where R is the fluorescence emission ratio at a given time point and R_0 is its initial value. The number of individual recordings averaged for each trace were n=27, 23, 22, and 12 (wild-type, positions 3,2,1 and –1 respectively), n=20, 25, 25, and 8 (*mec-10*, positions 3, 2, 1, and –1 respectively), and n=10, 10, 8, and 8 (*mec-4*, positions 3, 2, 1, and –1 respectively). Gray shading indicates SEM of the mean response. Scale bars are indicated in upper left. The green bar indicates the time of the stimulus. **e. Scatter plot of peak calcium responses for each genotype.** Statistical significance (*** $p < .001$; ** $P< .01$) is according to the Mann- Whitney rank sum test.

Figure 3: *mec-10* and *osm-9* contribute additively to nose touch responses in FLP. a. Stimulus positions for nose touch and harsh head touch imaging experiments. Nose touch protocol is cartooned in black dashed lines; harsh head touch is cartooned in green. **b. Effects of *mec-10* and *osm-9* on nose touch avoidance behaviour.** Animals (n≥60 over three independent days) were touched on the nose with an eyelash as described; escape responses (reversals) were scored as described. Statistical significance (*** p < .001; ** P< .01) is according to the Student's t test. **c-f. Averaged responses of wild-type (a), *mec-10(tm1552)* (b), *osm-9* (c), and *osm-9; mec-10(tm1552)* double mutants to nose touch stimulation.** Each red trace represents the average percentage change in R/R_0 for 24 (wild-type), 22 (mec-10), 22 (osm-9 individual recordings. Gray shading indicates SEM of the mean response. Scale bars are indicated in upper left. The green bar indicates the time of the stimulus. **g. Scatter plot of peak calcium responses for each genotype.** Statistical significance (*** p < .001; ** P< .01) is according to the Mann-Whitney rank sum test.

Figure 4: *mec-10* is critical for responses to repeated nose touch stimuli a. Behavioral responses to repeated nose touch stimulation. Animals (n≥30 over three independent days) were touched on the nose with an eyelash as described; escape responses (reversals) were scored as described. Statistical significance of differences between *mec-10* and wild-type (*** p < .001; ** P< .01) is according to the Student's t test. **b. Averaged calcium responses of wild-type and *mec-10(tm1552)* to repeated nose touch stimulation.** Each red trace represents the average percentage

change in R/R_0 for 18 individual recordings. Gray shading indicates SEM of the mean response. Scale bars are indicated in upper left. The green bar indicates the time of the stimulus. **c. c. Scatter plot of peak calcium responses for each genotype.** Statistical significance (*** $p < .001$; ** $P < .01$) is according to the Mann-Whitney rank sum test.

Figure 5: *mec-10* but not *osm-9* is required for harsh touch responses in FLP and PVD. a. Effects of *mec-10* and *osm-9* on harsh body touch avoidance behaviour. Animals were touched on the body with an platinum wire as described; escape responses (reversals) were scored as described. Statistical significance (*** $p < .001$; ** $P < .01$) is according to the Mann-Whitney rank sum test. **b-d. Averaged responses of wild-type (a), *mec-10(tm1552)* (b), *osm-9* (c) mutants to harsh body touch stimulation in PVD.** Each red trace represents the average percentage change in R/R_0 for 17 (wild-type), 16 (*osm-9*), or 14 (*mec-10*) individual recordings. Gray shading indicates SEM of the mean response. Scale bars are indicated in upper left. The green bar indicates the time of the stimulus. **e-g. Averaged responses of wild-type (a), *mec-10(tm1552)* (b), *osm-9* (c) mutants to harsh head touch stimulation in FLP.** Each red trace represents the average percentage change in R/R_0 for 21 (wild-type and *osm-9*), or 14 (*mec-10*) individual recordings. **h. Scatter plot of peak calcium responses for each genotype.** Statistical significance (*** $p < .001$; ** $P < .01$) is according to the Mann-Whitney rank sum test.

Figure 6: Hypothesized roles for DEG channels in *C. elegans*

mechanosensory neurons. a-b. In gentle touch neurons (ALM and PLM), MEC-4 and MEC-10 comprise core subunits of a mechanosensory complex critical for touch responses proximal to the neuronal cell body. In distal regions of the dendrite, MEC-4 homomeric channels are sufficient for touch sensitivity. **c.** In harsh touch neurons (PVD and FLP), MEC-10 forms a mechanosensory complex with a different, unidentified DEG protein. **d.** In FLP, MEC-10-containing channels (possibly of different composition from the harsh touch receptor) function additively with OSM-9-containing TRP channels to detect gentle nose touch. Upon repeated stimulation, the OSM-9 channel desensitizes and most of the response is mediated by MEC-10 .

SUPPLEMENTAL FIGURES

Supplemental Figure 1: Structure of the *mec-10(tm1552)* null allele. a. Most of the extracellular loop and the 2nd transmembrane domain of MEC-10 are predicted to be missing in the *mec-10(tm1552)* deletion strain. *mec-10(tm1552)* has a deletion that removes sequences of exon 5 and part of exon 6. The deletion is 448 bp and impacts the extracellular part of MEC-10. The predicted sequence would induce a frameshift with three premature stop codons (the first one is TAA at the end of the sequence below) very close to the deletion site (…tctattcatattttt-deletion-TTTATGCAGCAAAAAAAGCTAA). This suggests that, if the transcript were translated, most of the extracellular domain and the pore-forming 2nd transmembrane domain of MEC-10 would be missing in this mutant strain. Red arrows indicate the coding region corresponding to site for the primer pair for RT-PCR. Primers were designed to avoid the homologous sequences between mec-4 and

mec-10. The purple arrow shows the region corresponding to one of the primers used to identify the deletion, another primer is inside the intron 2. Blue underline indicates the protein region corresponding to deleted sequence. Black boxes indicate the 1st and 2nd transmembrane domains. **b.** A pair of primers with sequence 5'-GTAGGGTCTGCAACTAGCTC-3' and 5'-TGGGAGGGAGCTTCATCTTA-3' were used to identify the deleted gene from the wild type. Blue arrows indicate the position of primers. Blue rectangle shows the deleted sequence. **c.** Primer pair with sequence 5'-AAATTATCTCGCAAGTGACACTAACTTTCT-3' and 5'-CCAAAGTATTCCCATAAATTCAATACCATT-3' were used for RT-PCR to amplify the mRNA isolated from wild type N2. No specific cDNA RT/PCR could be recovered from the *mec-10(tm1552)* mutant strain; the wild type strain produces a detectable band of 936 bps.

Supplemental Figure 2: Responses of *mec-10* null mutants to posterior touch. Animals were touched at the indicated positions; forward accelerations were scored as escape responses. *mec-10(tm1552)* animals responded better at anterior positions more distal to the PLM cell bodies (position 2 response stronger than position 3, $p < .05$; position 1 response stronger than position 2, $p < .01$). All *mec-10(tm1552)* responses were significantly lower than wild-type ($p < .001$).

Supplemental Figure 3: *mec-10(tm1552)* mutants have reduced touch-evoked calcium transients in PLM touch neurons. a. Stimulus positions for imaging experiments. Animals were given a 1 second gentle (buzz)

stimulus at the indicated position, as described in Experimental Procedures. **b-d. Averaged calcium responses of wild-type (b), *mec-10(tm1552)* (c), and *mec-4* (d) null mutants.** Each red trace represents the average percentage change in R/R_0. The number of individual recordings averaged for each trace were n=20, 23, and 24 (wild-type, positions 3,2, and 1 respectively), n=16, 14 and 17 (*mec-10*, positions 3, 2, and 1 respectively), and n=10, 10, 8, and 8 (*mec-4*, positions 3, 2, and 1 respectively). Gray shading indicates SEM of the mean response. Scale bars are indicated in upper left. The green bar indicates the time of the stimulus. **e. Scatter plot of peak calcium responses for each genotype.** Statistical significance (*** $p < .001$; ** $P < .01$) is according to the Mann-Whitney rank sum test.

Supplemental Figure 4: *mec-10* mutants have reduced touch-evoked calcium transients in PVM touch neurons. a. Stimulus positions for imaging experiments. Animals were given a 1 second gentle (buzz) stimulus at the indicated position, as described in Experimental Procedures. **b-d. Averaged calcium responses of (b) wildtype, (c) *mec-10(tm1552)*, and (d) *mec-4(u253)* mutants.** Each red trace represents the average percentage change in R/R_0, where R is the fluorescence emission ratio at a given time point and R_0 is its initial value. The number of individual recordings averaged for each trace were n=24, 20, 26, and 11 (wild-type, positions 3,2,1 and –1 respectively), n=19, 18, 17, and 11 (*mec-10*, positions 3, 2, 1, and –1 respectively), and n=10, 10, 8, and 8 (*mec-10; mec-4*, positions 3, 2, 1, and –1 respectively. Gray shading indicates SEM of the mean response. Scale bars are indicated in upper left. The green bar indicates the time of the stimulus. **e. Scatter plot of peak**

calcium responses for each genotype. Statistical significance (*** p < .001; ** P< .01) is according to the Mann-Whitney rank sum test.

Supplemental Figure 5: Effects of other DEG/ENac genes on nose touch a-d. Averaged calcium responses of (a) *del-1(ok150))* (b), *unc-8(n491n1192),* (c) *del- 1(ok150); osm-9(ky10)*, and (d) *mec-6(e1342)* mutants. Each red trace represents the average percentage change in R/R_0, where R is the fluorescence emission ratio at a given time point and R_0 is its initial value. The number of individual recordings averaged for each trace are 21 (*del-1*), 19 (*unc-8*), 19 (*del-1; osm-9*), and 22 (*mec-6*). Gray shading indicates SEM of the mean response. Scale bars are indicated in upper left. The dark bar indicates the time of the stimulus. **e. Scatter plot of peak calcium responses for each genotype.** Statistical significance (*** p < .001; ** P< .01) is according to the Mann- Whitney rank sum test. **f. Effects of other DEG/ENac genes on nose touch avoidance behaviour.** Animals ($n \geq 60$ over three independent days) were touched on the nose with an eyelash as described; escape responses (reversals) were scored as described. Statistical significance (*** p < .001; ** P< .01) is according to the Student's t test.

Figure 1

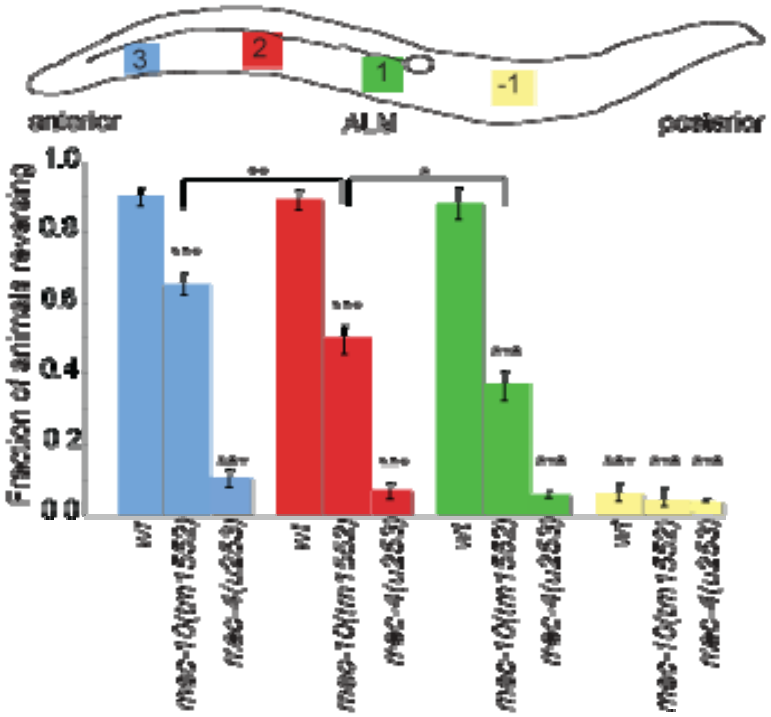
3
2
1
-1
anterior
ALM
posterior
Fraction of animals reversing
1.0
0.8
0.6
0.4
0.2
0.0
**
*
***
***
***
n.s.
n.s.
n.s.
n.s.
n.s.
wt
mec-10(tm1552)
mec-4(u253)
wt
mec-10(tm1552)
mec-4(u253)
wt
mec-10(tm1552)
mec-4(u253)
wt
mec-10(tm1552)
mec-4(u253)

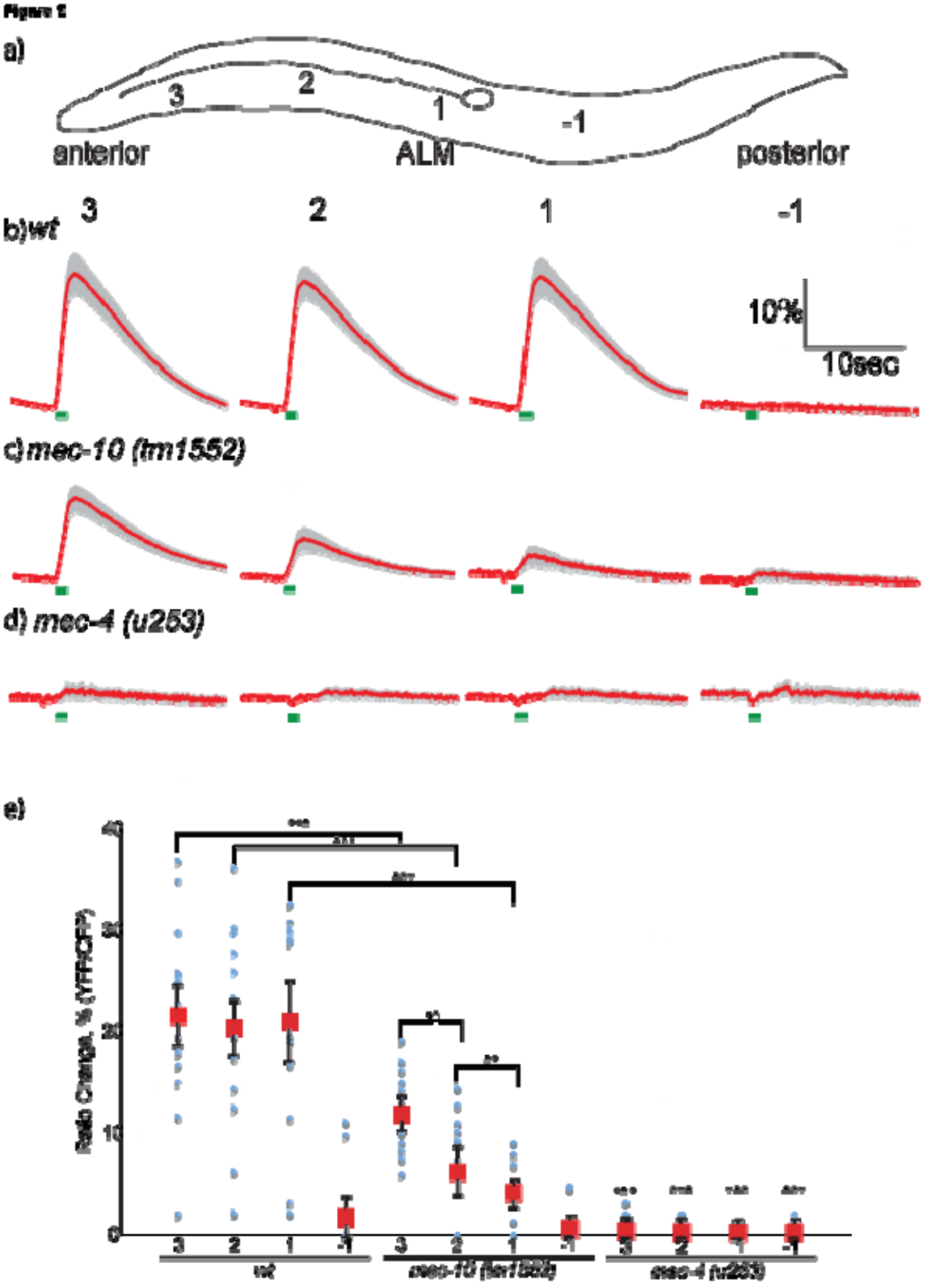
a)
3
2
1
-1
anterior
ALM
posterior
b) wt
3
2
1
-1
10%
10sec
c) mec-10 (tm1552)
d) mec-4 (u253)
e)
Ratio Change, % (YFP/CFP)
wt
mec-10 (tm1552)
mec-4 (u253)

Figure 3

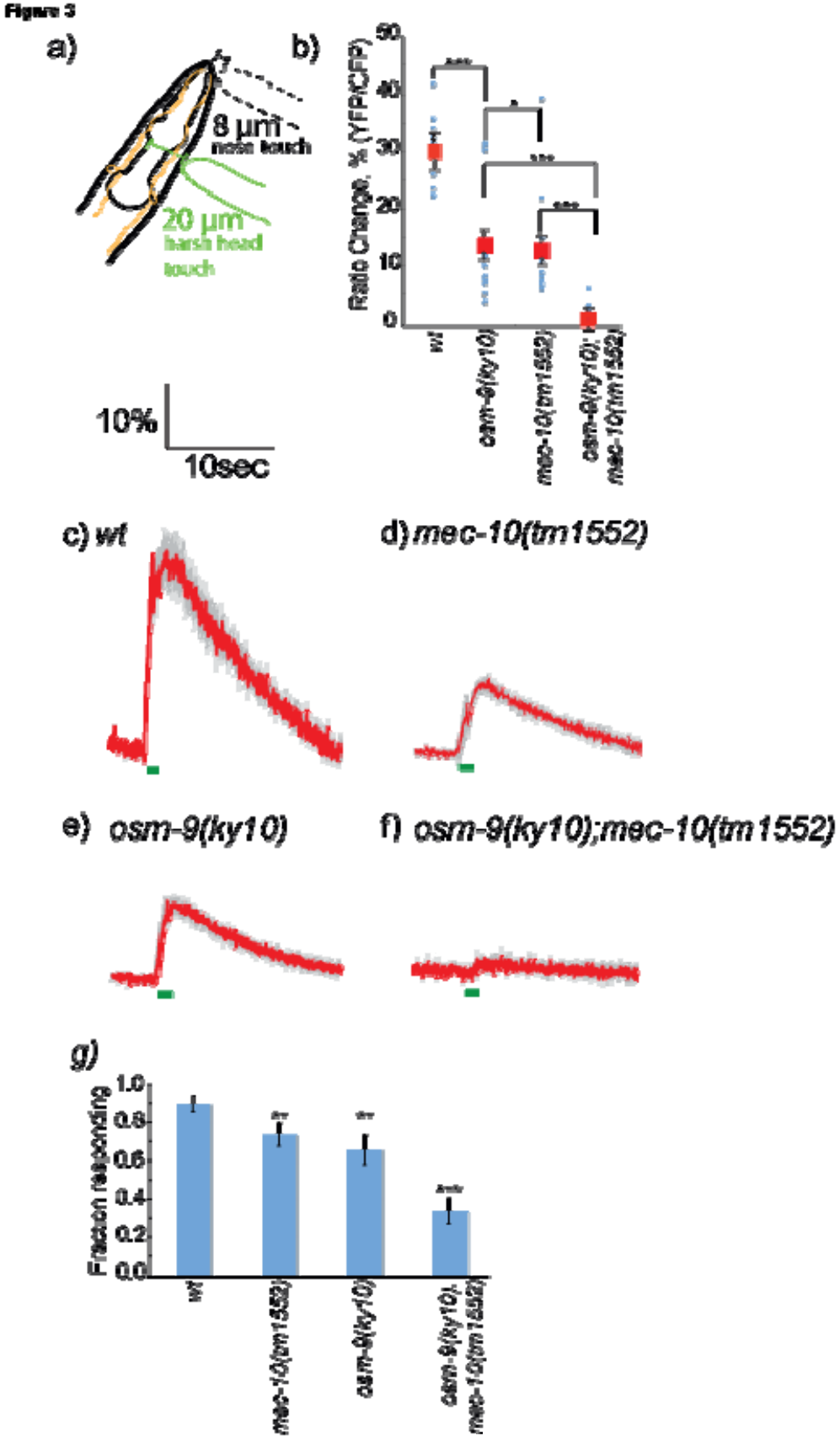
a)
b)
8 µm
nose touch
20 µm
harsh head
touch
10%
10sec
Ratio Change, % (YFP/CFP)
wt
osm-9(ky10)
mec-10(tm1552)
osm-9(ky10);
mec-10(tm1552)
c) wt
d) mec-10(tm1552)
e) osm-9(ky10)
f) osm-9(ky10);mec-10(tm1552)
g)
Fraction responding

Figure 4

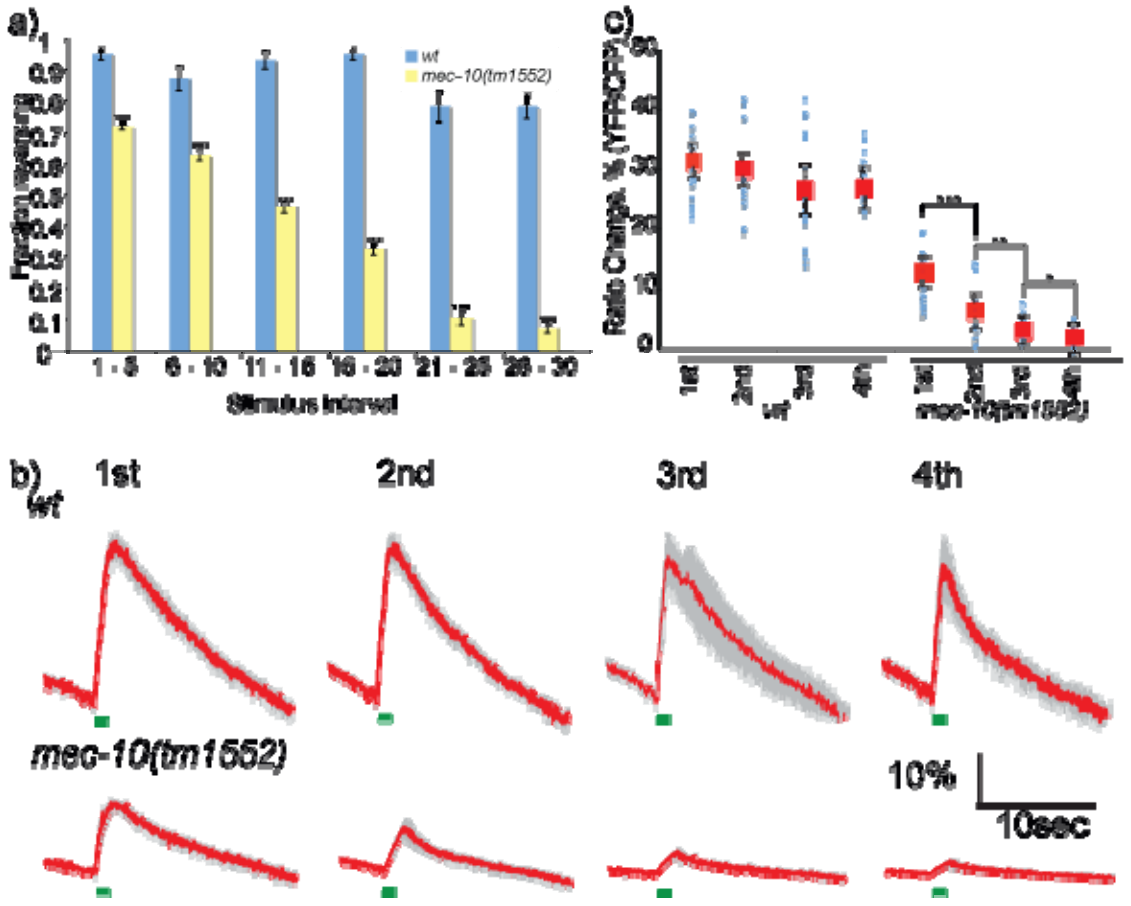
a)
wt
mec-10(tm1552)
Stimulus Interval
1 - 5
6 - 10
11 - 15
16 - 20
21 - 25
26 - 30
c)
Ratio Change % (YFP/CFP)
wt
mec-10(tm1552)
b)
wt
1st
2nd
3rd
4th
mec-10(tm1552)
10%
10sec

Figure 6

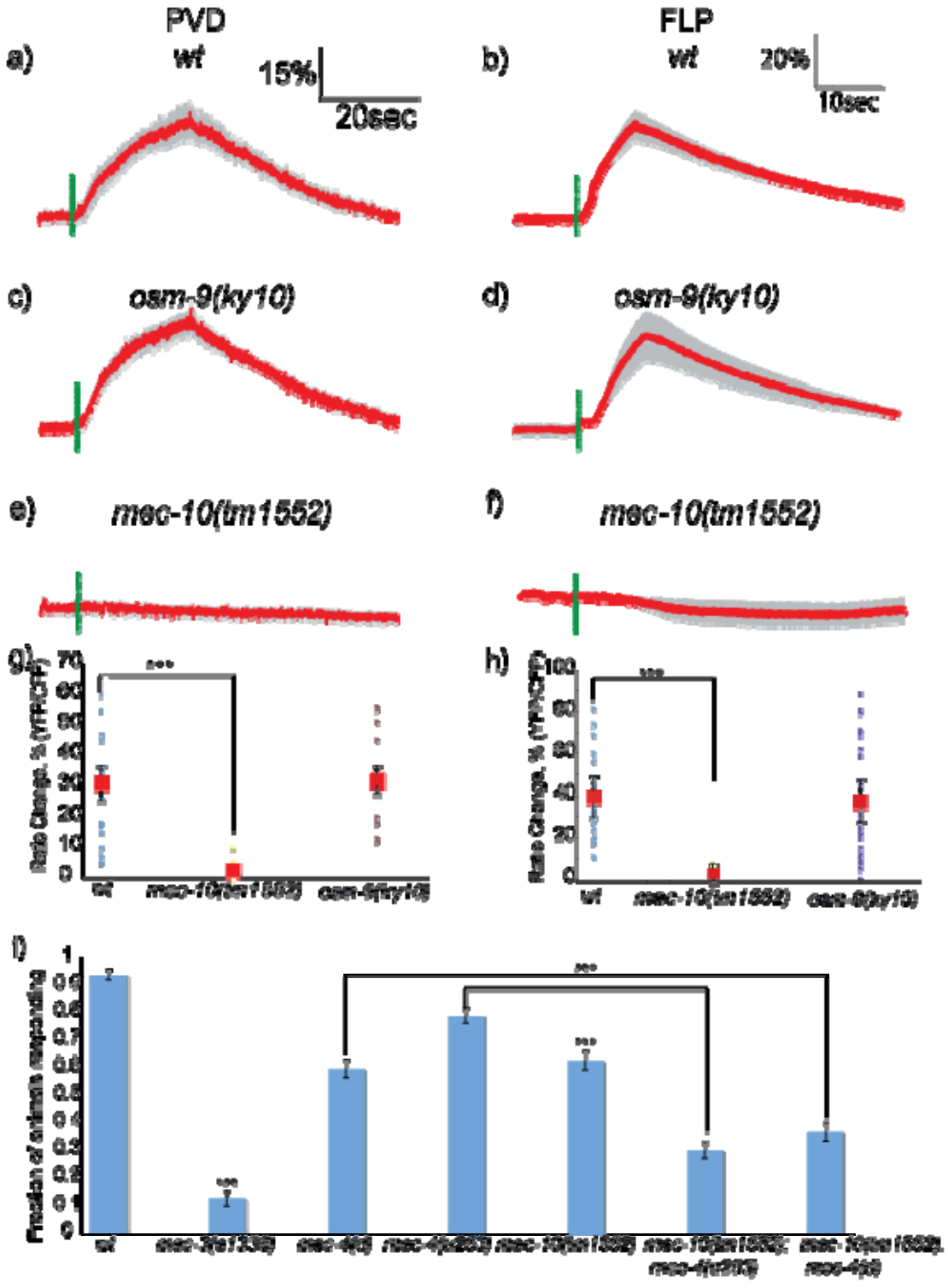
PVD
a)
wt
15%
20sec
FLP
b)
wt
20%
10sec
c)
osm-9(ky10)
d)
osm-9(ky10)
e)
mec-10(tm1552)
f)
mec-10(tm1552)
g)
h)
wt
mec-10(tm1552)
osm-9(ky10)
i)
wt
osm-3(p1309)
mec-4(d)
mec-4(d)
mec-10(tm1552)
mec-10(tm1552);
mec-4(u231)
mec-10(tm1552)
mec-4(d)

Figure 6

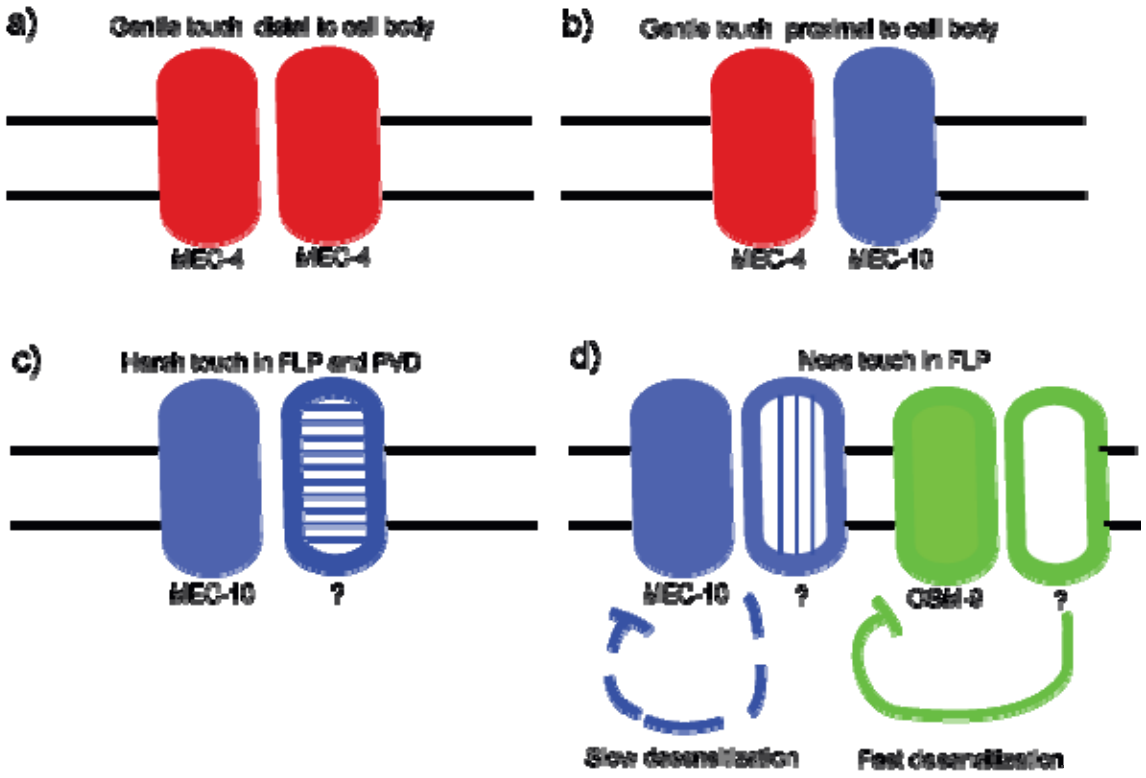
a)
Gentle touch distal to cell body
MEC-4
MEC-4
b)
Gentle touch proximal to cell body
MEC-4
MEC-10
c)
Harsh touch in FLP and PVD
MEC-10
?
d)
Nose touch in FLP
MEC-10
?
OSM-9
?
Slow desensitization
Fast desensitization

Supplemental Figure 1

a)

```
  1 MNRNPRMSKFQPNPRSRSRFQDETDLRSLRSFKTDFSNYLASDTNFLNVA
 51 EIMTSYAYGESNNAHEKEIQCDLLTENGGIEIDPTRLSYRERIRWHLQQF
101 CYKTSSHGIPMLGQAPNSIYRAAWVFLLLICAIQFINQAVAVIQKYQKMD
151 KITDIQLKFDTAPFPAITLCNLNPYKDSVIRSHDSISKILGVFKSVMKKA
201 GDSSSEALEEEEETEYDMNGITIQAKRKKRGAGEKGTFEPANSACECDEE
251 DGSNECEERSTEKPSGDNDMCICAFDRQTNDAWPCHRKEQWTNTTCQTCD
301 EHYLCSKKAKKGTKRSELKKEPCICESKGLPCIKHEHAAMVLNLWEYFGD
351 SEDFSEISTEEREALGFGNMTDEVAIVTKAKENIIFAMSALSEEQRILMS
401 QAKHNLIHKCSFNGKPCDIDQDFELVADPTFGNCFVFNHDREIFKSSVRA
451 GPQYGLRVMLFVNASDYLPTSEAVGIRLTIHDKDDFPFPDTFGYSAPTGY
501 ISSFGMRMKKMSRLPAPYGDCVEDGATSNYIYKGYAYSTEGCYRTCFQEL
551 IIDRCGCSDPRFPSIGGVQPCQVFNKNHRECLEKHTHQIGEIHGSFKCRC
601 QQPCNQTIYTTSYSEAIWPSQALNISLGQCEKEAEECNEEYKENAAMLEV
651 FYEALNFEVLSESEAYGIVKMMADFGGHLGLWSGVSVMTCCEFVCLAFEL
701 IYMAIAHHINQQRIRRRENAANEY
```

b) *exo-10* (F18F9.2)

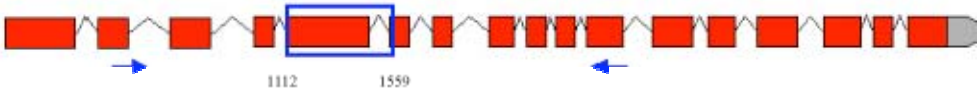

c)

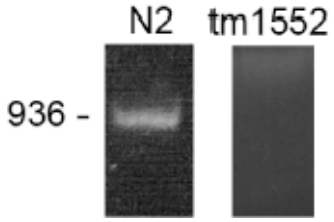

Supplemental Figure 2

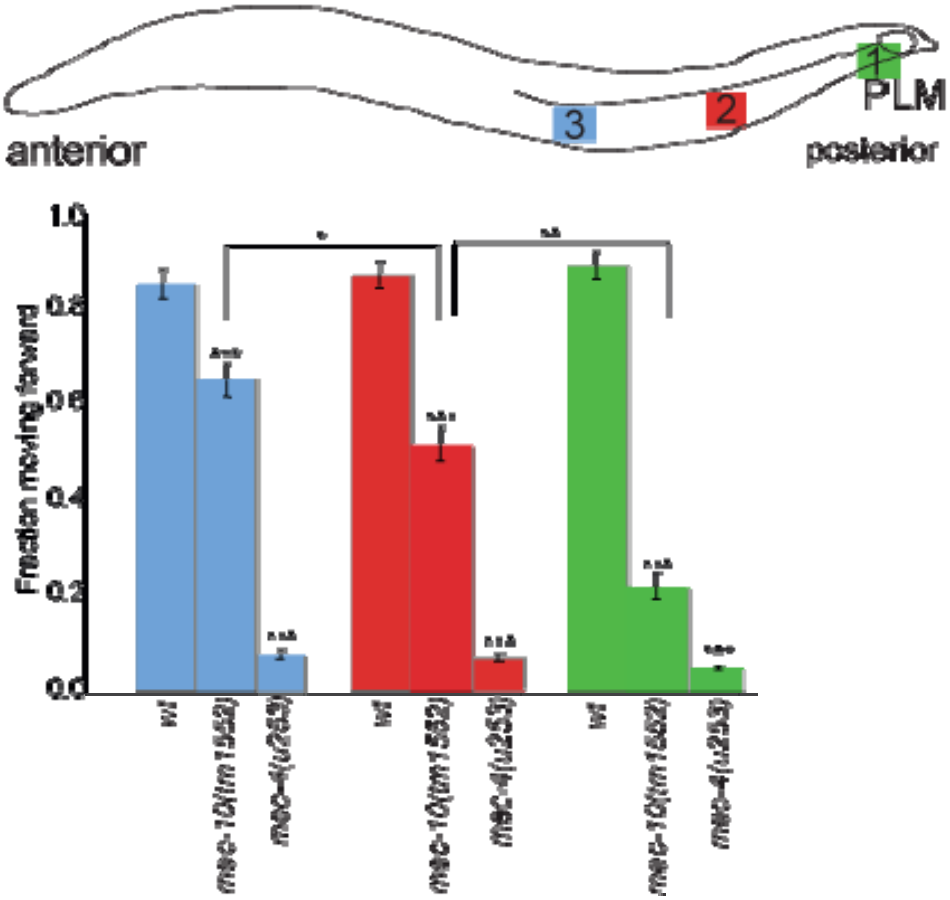

Supplemental Figure 3

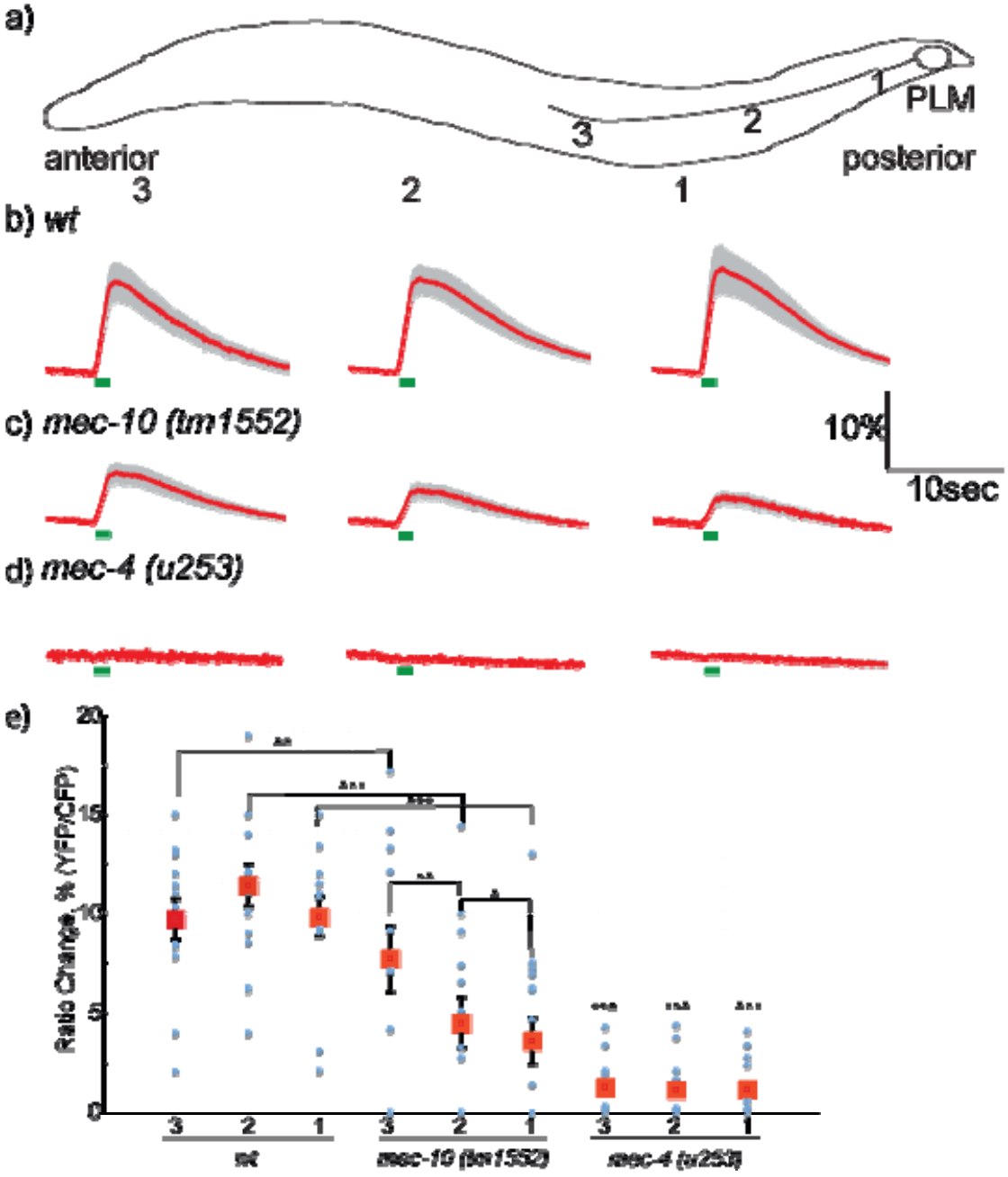

Supplemental Figure 4

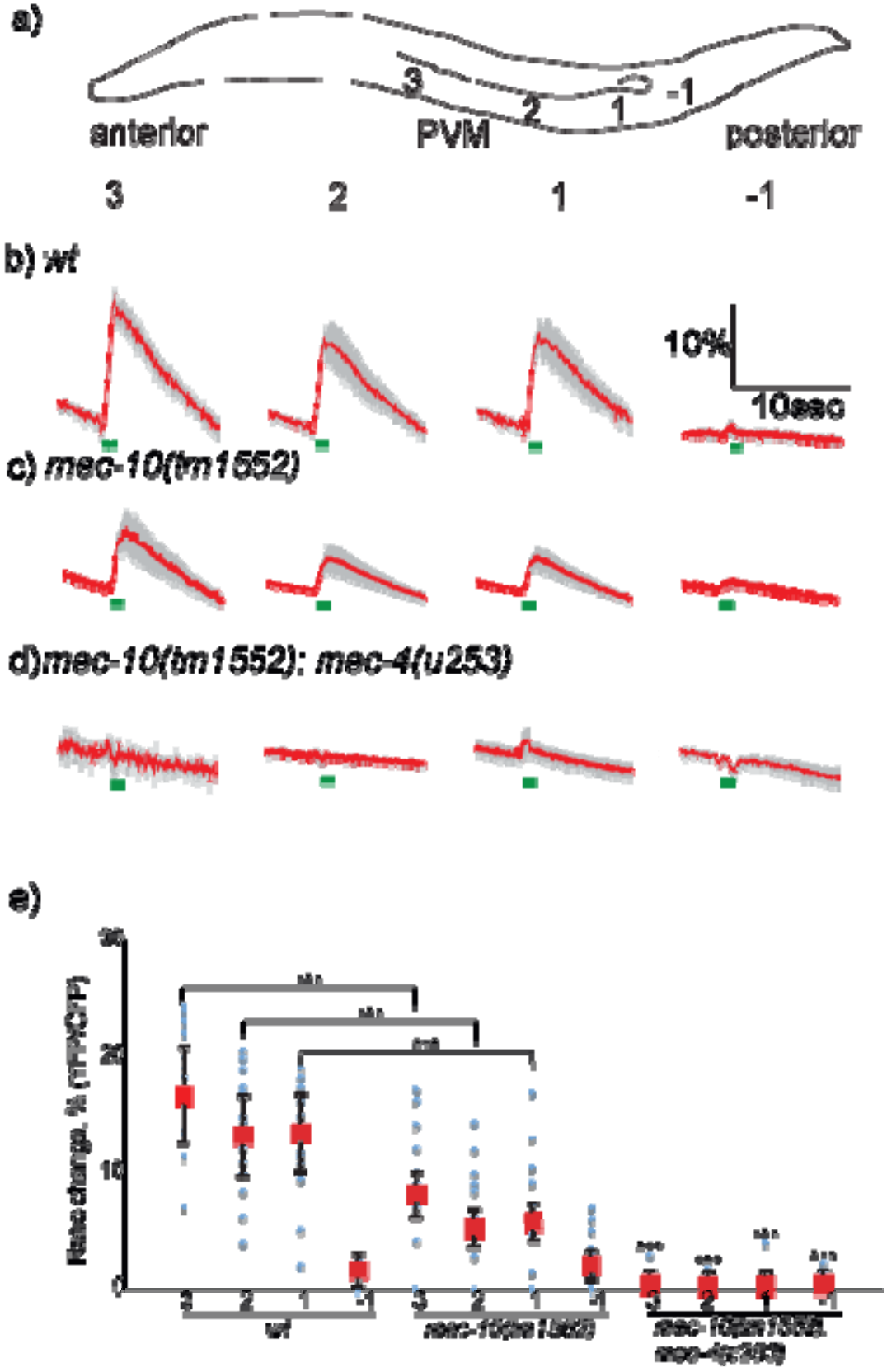

Supplemental Figure 5

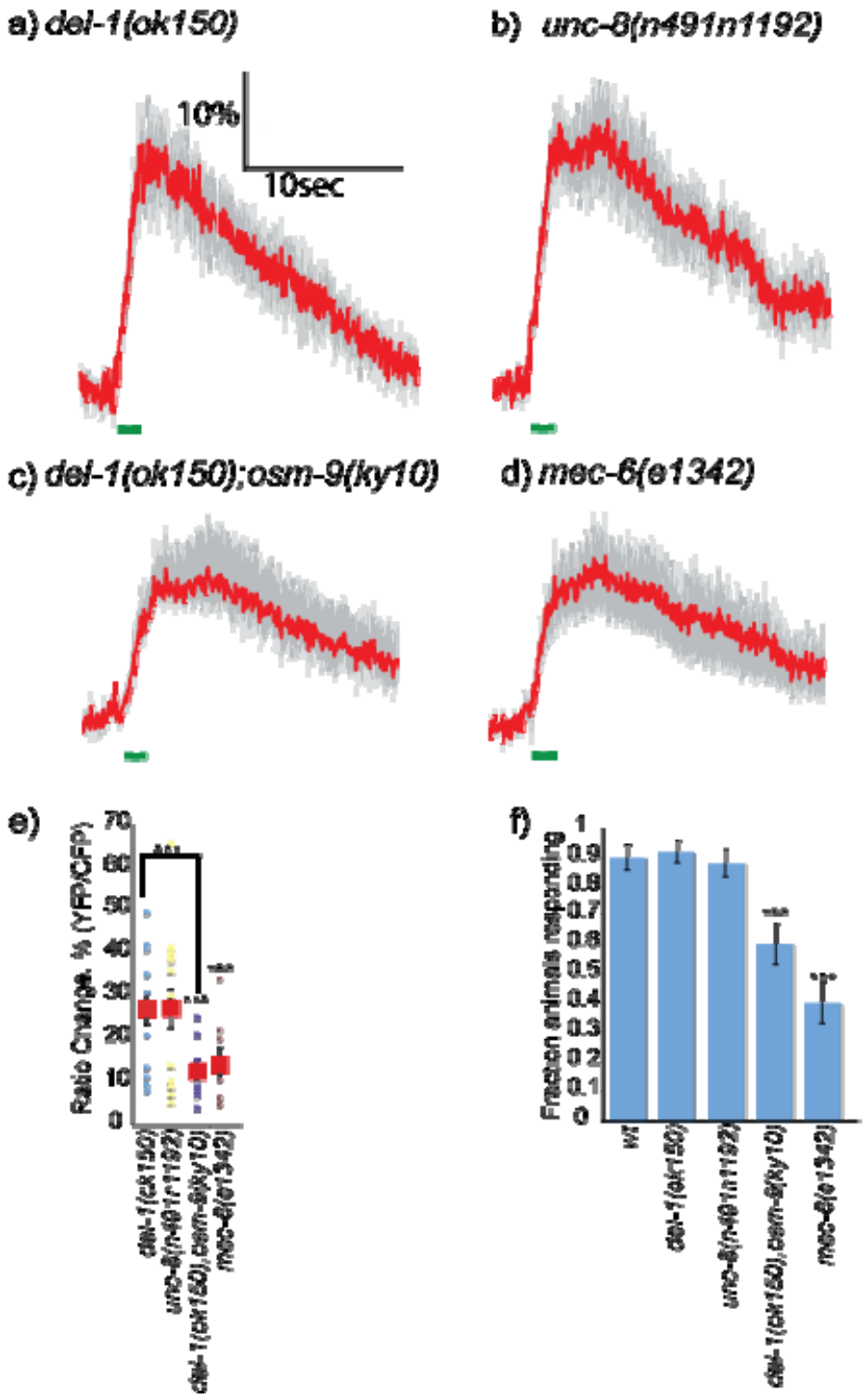

Appendix II:

Stomatins can regulate the Na^+ channel conductance and play an important in touch sensation channels

Stomatin is a 32-kDa integral membrane protein first found in human red blood cells. A rare human hemolytic anemia “stomatocytosis” is a dominantly inherited disease (Fricke et al., 2003). The morphology in these red blood cells is a mouth-like shape distinguished from spherocytosis, thus stomatocytosis, from “stoma” is Greek for mouth. Overhydrated hereditary stomatocytosis (OHSt) shows 2 major features: a leak across the plasma membrane to the univalent cations Na^+ and K^+, and the 32-kDa stomatin or erythrocyte membrane protein 7.2b, was absent from the membrane (Zhu et al., 1999). Due to the accumulation of intracellular Na^+ and the loss of intracellular K^+, the net effect is an increase in intracellular cations accompanied by a movement of water into the cell. Thus there is cell swelling, stomatocytic shape change, increased osmotic fragility, and shortened life span in the red blood cells.

Stomatins are widely distributed in human tissues and in nature. Mutations in one homologue, *mec-2*, cause a defect in gentle touch sensation in *C. elegans.* MEC-2 can increase the ion permeability of the mechanosensory ion channel (MEC-4(d) and MEC-10 in oocyte expression experiment) (Goodman et al., 2002). Stomatin might therefore be deleted from the stomatocytosis red cell in an attempt to down-regulate ion channel leakage. Stomatin also has been postulated to

participate in the formation of lipid rafts, which are membrane microdomains associated with protein complexes, cholesterol, and sphingolipids (Salzer et al., 2001). Other *C. elegans* homologues, UNC-1 and UNC-24, were also shown to affect anesthetic sensitivity and interact genetically with another subunit of the degenerin-type Na^+ channel, UNC-8, and have been implicated in lipid raft.

There are 10 stomatin proteins in *C. elegans*, including UNC-1 and UNC-24. UNC-1, expressed primarily in the nervous system, has an important role in locomotion and in determining volatile anesthetic sensitivity in *C. elegans* and it is thought to interact with the DEG/ENaC ion channel subunit UNC-8. UNC-24 affects anesthetic sensitivity and is genetically epistatic to *unc-1* (Sedensky et al., 2001). UNC-1 is almost totally restricted to the lipid rafts. The UNC-8 protein is also found in rafts and co-immunoprecipitates UNC-1. Mutations in the *unc-24* gene alter the distribution of UNC-1 in lipid rafts (Sedensky et al., 2004). UNC-24 is expressed in many neurons including the six gentle touch cells and the two pairs of neurons PVDL/R and FLPL/R. All the stomatins in *C. elegans* share very similar structures (Figure 1 shows the alignment of some *C. elegans* stomatin proteins) , it could be possible they interact with other DEG/ENaC proteins to influence these channels.

I checked 7 stomatin or stomatin-like proteins in *C. elegans,* STO-1, STO-2, STO-3, STO-4, STO-5, STO-6, and STL-1. Upstream promoters were cloned and introduced into Fire lab *C. elegans* vector, pPD95.75. Primers used to amplify

promoters are listed in Table 1. Worms with GFP expression were checked under fluorescent microscope. *sto-4* and *sto-5* did not came out any successful transgenic strains. Other stomatin promoter transgenic worms show different expression pattern including neurons near head and pharynx. However, none of them seems expressing in any mechanosensory neurons like ASH. Figure 2 shows the stomatin GFP (green) and DiO-labeled ASH (red) pictures of all stomatin strains except *sto-4* and *sto-5*.

Table 1:

Gene	Primer
sto-1	gc TCT AGA TGT GCA TTC CAG TAA TAA TAA CGA CTG GTG
	cg GGA TCC CAT AAG AGA CGG ACG GTA CGG G
sto-2	gc TCT AGA CTA GGC ACG ATA ATC GCG CTG
	cg GGA TCC AGA CGC TCG CTC TCG TTT GAC
sto-3	gc TCT AGA GAT CTA GAA TTT CCG CGC CGT
	cg GGA TCC AAG CCA AAC CAA GTG AGA AGA AGT ATT CAA
sto-4	gc TCT AGA TCG CTG CTG TAG CTC AAT TTG ATG
	cg GGA TCC ATC TCA AGG TGG ACA CTT AGA CCT
sto-4 short	gc TCT AGA CAC CAC ACC TTC TGT CCT TCT TCT
	cg GGA TCC ATC TCA AGG TGG ACA CTT AGA CCT
sto-5	aaaa CTG CAG AAC GTT TCA CCG ACG CAT CT
	cg GGA TCC TTT GTG CAT TGC TCG CCG
sto-6	gc TCT AGA CGT GAT ACC TTC GTA AAG CAA GCT
	cg GGA TCC GTT TTG TCG GCT CCT AAA ACG ACG
stl-1	gc TCT AGA ACT CAA TAG ACT ATC CAC CAT TTT GGA GAG
	cg GGA TCC TTT CTG TAA AAT CAT TTT TAA TGA TGC AAT

Figure 1:

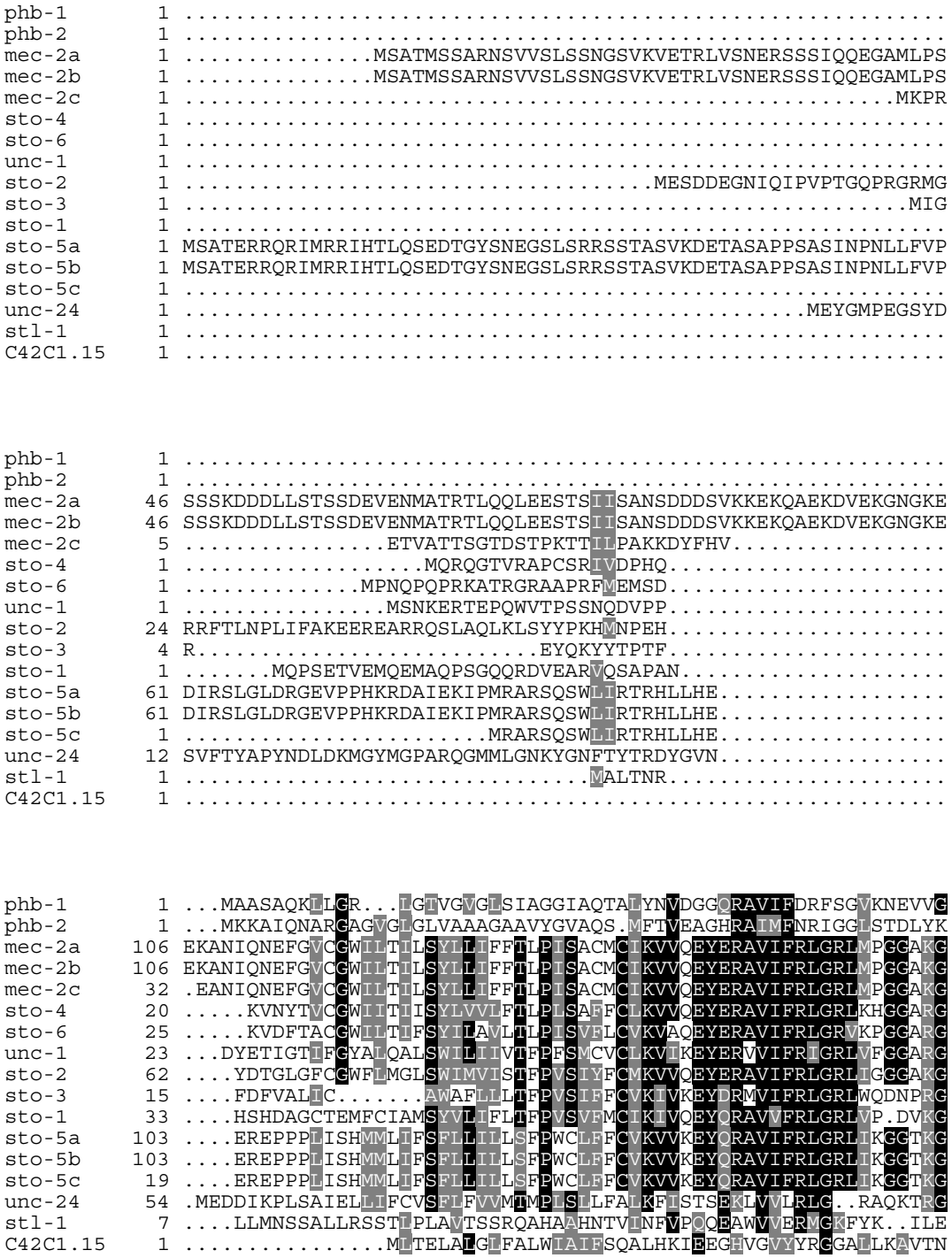
phb-1
phb-2
mec-2a
mec-2b
mec-2c
sto-4
sto-6
unc-1
sto-2
sto-3
sto-1
sto-5a
sto-5b
sto-5c
unc-24
stl-1
C42C1.15

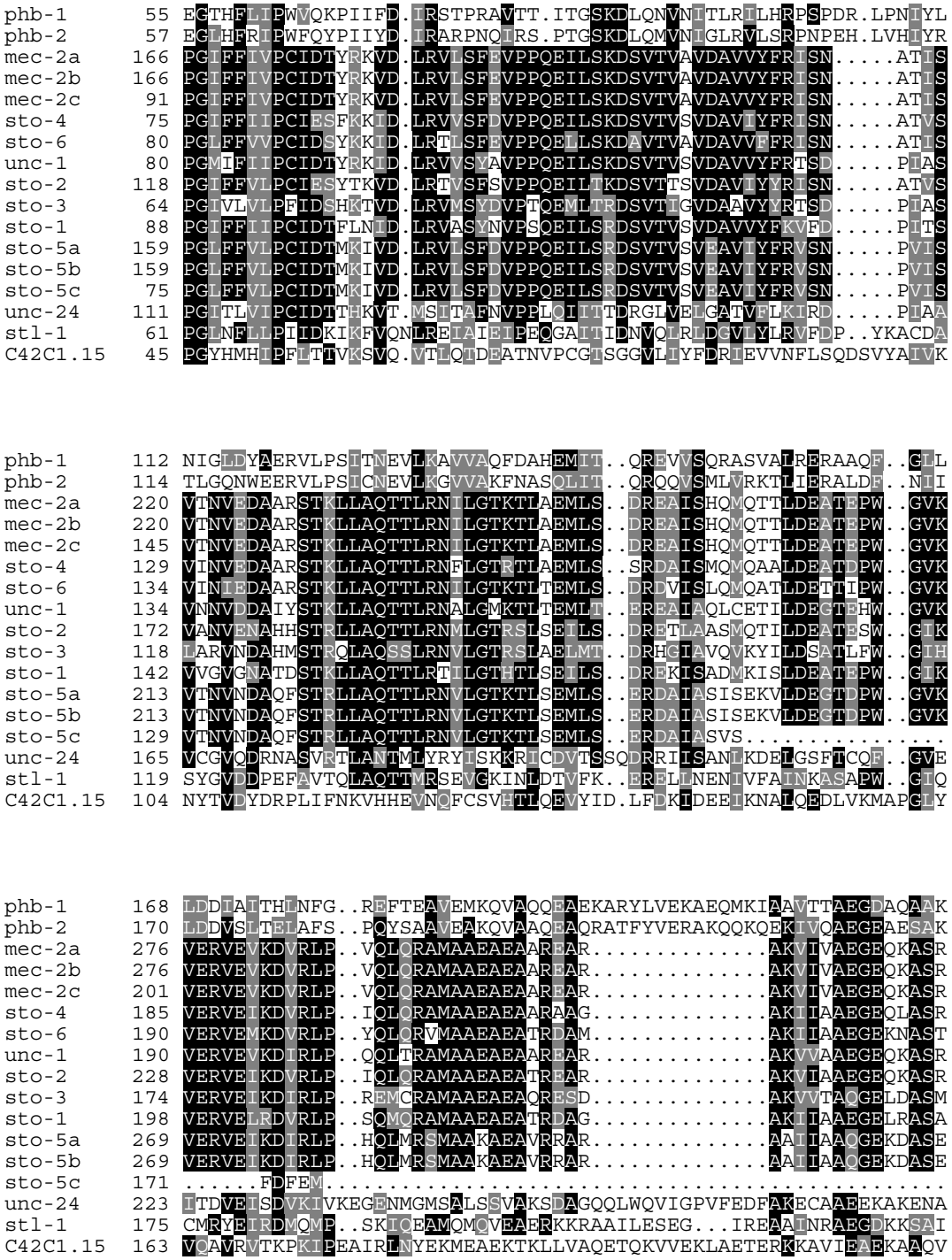
phb-1 55 EGTHFLIPWVQKPIIFD.IRSTPRAVTT.ITGSKDLQNVNITLRILHRPSPDR.LPNIYL
phb-2 57 EGLHFRIPWFQYPIIYD.IRARPNQIRS.PTGSKDLQMVNIGLRVLSRPNPEH.LVHIYR
mec-2a 166 PGIFFIVPCIDTYRKVD.LRVLSFEVPPQEILSKDSVTVAVDAVVYFRISN.....ATIS
mec-2b 166 PGIFFIVPCIDTYRKVD.LRVLSFEVPPQEILSKDSVTVAVDAVVYFRISN.....ATIS
mec-2c 91 PGIFFIVPCIDTYRKVD.LRVLSFEVPPQEILSKDSVTVAVDAVVYFRISN.....ATIS
sto-4 75 PGIFFIIPCIESFKKID.LRVVSFDVPPQEILSKDSVTVSVDAVIYFRISN.....ATVS
sto-6 80 PGLFFVVPCIDSYKKID.LRTLSFEVPPQELLSKDAVTVAVDAVVFFRISN.....ATIS
unc-1 80 PGMIFIIPCIDTYRKID.LRVVSYAVPPQEILSKDSVTVSVDAVVYFRTSD.....PIAS
sto-2 118 PGIFFVLPCIESYTKVD.LRTVSFSVPPQEILTKDSVTTSVDAVIYYRISN.....ATVS
sto-3 64 PGIVLVLPFIDSHKTVD.LRVMSYDVPTQEMLTRDSVTIGVDAAVYYRTSD.....PIAS
sto-1 88 PGIFFIIPCIDTFLNID.LRVASYNVPSQEILSRDSVTVSVDAVVYFKVFD.....PITS
sto-5a 159 PGLFFVLPCIDTMKIVD.LRVLSFDVPPQEILSRDSVTVSVEAVIYFRVSN.....PVIS
sto-5b 159 PGLFFVLPCIDTMKIVD.LRVLSFDVPPQEILSRDSVTVSVEAVIYFRVSN.....PVIS
sto-5c 75 PGLFFVLPCIDTMKIVD.LRVLSFDVPPQEILSRDSVTVSVEAVIYFRVSN.....PVIS
unc-24 111 PGITLVIPCIDTTHKVT.MSITAFNVPPLQIITTDRGLVELGATVFLKIRD.....PIAA
stl-1 61 PGLNFLLPIIDKIKFVQNLREIAIEIPEQGAITIDNVQLRLDGVLYLRVFDP..YKACDA
C42C1.15 45 PGYHMHIPFLTIVKSVQ.VTLQIDEATNVPCGTSGGVLIYFDRIEVVNFLSQDSVYAIVK
phb-1 112 NIGLDYAERVLPSITNEVLKAVVAQFDAHEMIT..QREVVSQRASVAIRERAAQF..GLL
phb-2 114 TLGQNWEERVLPSICNEVLKGVVAKFNASQLIT..QRQQVSMLVRKTLIERALDF..NII
mec-2a 220 VTNVEDAARSTKLLAQTTLRNILGTKTLAEMLS..DREAISHQMQTTLDEATEPW..GVK
mec-2b 220 VTNVEDAARSTKLLAQTTLRNILGTKTLAEMLS..DREAISHQMQTTLDEATEPW..GVK
mec-2c 145 VTNVEDAARSTKLLAQTTLRNILGTKTLAEMLS..DREAISHQMQTTLDEATEPW..GVK
sto-4 129 VINVEDAARSTKLLAQTTLRNFLGTRTLAEMLS..SRDAISMQMQAALDEATDPW..GVK
sto-6 134 VINIEDAARSTKLLAQTTLRNILGTKTLTEMLS..DRDVISLQMQATLDETTIPW..GVK
unc-1 134 VNNVDDAIYSTKLLAQTTLRNALGMKTLTEMLT..EREAIAQLCETILDEGTEHW..GVK
sto-2 172 VANVENAHHSTRLLAQTTLRNMLGTRSLSEILS..DRETLAASMQTILDEATESW..GIK
sto-3 118 LARVNDAHMSTRQLAQSSLRNVLGTRSLAELMT..DRHGIAVQVKYILDSATLFW..GIH
sto-1 142 VVGVGNATDSTKLLAQTTLRTILGTHTLSEILS..DREKISADMKISLDEATEPW..GIK
sto-5a 213 VTNVNDAQFSTRLLAQTTLRNVLGTKTLSEMLS..ERDAIASISEKVLDEGTDPW..GVK
sto-5b 213 VTNVNDAQFSTRLLAQTTLRNVLGTKTLSEMLS..ERDAIASISEKVLDEGTDPW..GVK
sto-5c 129 VTNVNDAQFSTRLLAQTTLRNVLGTKTLSEMLS..ERDAIASVS.....
unc-24 165 VCGVQDRNASVRTLANTMLYRYISKKRICDVTSSQDRRIISANLKDELGSFTCQF..GVE
stl-1 119 SYGVDDPEFAVTQLAQTTMRSEVGKINLDTVFK..ERELLNENIVFAINKASAPW..GIQ
C42C1.15 104 NYTVDYDRPLIFNKVHHEVNQFCSVHTLQEVYID.LFDKIDEEIKNALQEDLVKMAPGLY
phb-1 168 LDDIAITHLNFG..REFTEAVEMKQVAQQEAEKARYLVEKAEQMKIAAVTTAEGDAQAAK
phb-2 170 LDDVSLTELAFS..PQYSAAVEAKQVAAQEAQRATFYVERAKQQKQEKIVQAEGEAESAK
mec-2a 276 VERVEVKDVRLP..VQLQRAMAAEAEAAREAR.....AKVIVAEGEQKASR
mec-2b 276 VERVEVKDVRLP..VQLQRAMAAEAEAAREAR.....AKVIVAEGEQKASR
mec-2c 201 VERVEVKDVRLP..VQLQRAMAAEAEAAREAR.....AKVIVAEGEQKASR
sto-4 185 VERVEIKDVRLP..IQLQRAMAAEAEAARAAG.....AKIIAAEGEQLASR
sto-6 190 VERVEMKDVRLP..YQLQRVMAAEAEATRDAM.....AKIIAAEGEKNAST
unc-1 190 VERVEVKDIRLP..QQLTRAMAAEAEAAREAR.....AKVVAAEGEQKASR
sto-2 228 VERVEIKDVRLP..IQLQRAMAAEAEATREAR.....AKVIAAEGEQKASR
sto-3 174 VERVEIKDIRLP..REMCRAMAAEAEAQRESD.....AKVVTAQGELDASM
sto-1 198 VERVELRDVRLP..SQMQRAMAAEAEATRDAG.....AKIIAAEGELRASA
sto-5a 269 VERVEIKDIRLP..HQLMRSMAAKAEAVRRAR.....AAIIAAQGEKDASE
sto-5b 269 VERVEIKDIRLP..HQLMRSMAAKAEAVRRAR.....AAIIAAQGEKDASE
sto-5c 171 .....FDFEM.....
unc-24 223 ITDVEISDVKIVKEGENMGMSALSSVAKSDAGQQLWQVIGPVFEDFAKECAAEEKAKENA
stl-1 175 CMRYEIRDMQMP..SKICEAMQMQVEAERKKRAAILESEG...IREAAINRAEGDKKSAI
C42C1.15 163 VQAVRVTKPKIPEAIRLNYEKMEAEKTKLLVAQETQKVVEKLAETERKKAVIEAEKAAQV

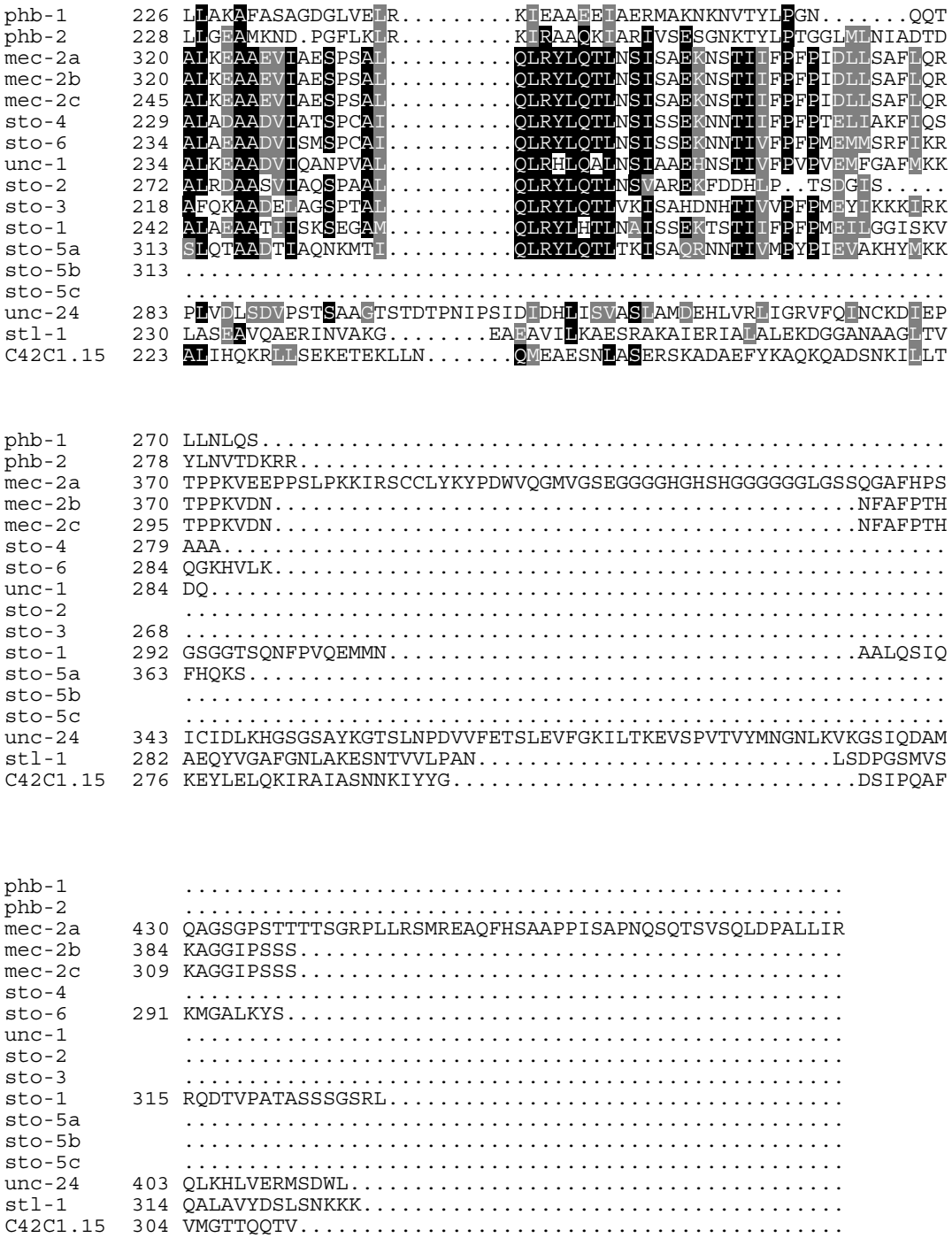
phb-1 226 LLAKAFASAGDGLVELR.....KIEAAEEIAERMAKNKNVTYLPGN.....QQT
phb-2 228 LLGEAMKND.PGFLKLR.....KIRAAQKIARIVSESGNKTYLPTGGLMLNIADTD
mec-2a 320 ALKEAAEVIAESPSAL.....QLRYLQTLNSISAEKNSTIIFPFPIDLLSAFLQR
mec-2b 320 ALKEAAEVIAESPSAL.....QLRYLQTLNSISAEKNSTIIFPFPIDLLSAFLQR
mec-2c 245 ALKEAAEVIAESPSAL.....QLRYLQTLNSISAEKNSTIIFPFPIDLLSAFLQR
sto-4 229 ALADAADVIATSPCAI.....QLRYLQTLNSISSEKNNTIIFPFPTELIAKFIQS
sto-6 234 ALAEAADVISMSPCAI.....QLRYLQTLNSISSEKNNTIVFPFPMEMMSRFIKR
unc-1 234 ALKEAADVIQANPVAL.....QLRHLQALNSIAAEHNSTIVFPVPVEMFGAFMKK
sto-2 272 ALRDAASVIAQSPAAL.....QLRYLQTLNSVAREKFDDHLP..TSDGISS.....
sto-3 218 AFQKAADELAGSPTAL.....QLRYLQTLVKISAHDNHTIVVPFPMEYIKKKIRK
sto-1 242 ALAEAATIISKSEGAM.....QLRYLHTLNAISSEKTSTIIFPFPMEILGGISKV
sto-5a 313 SLQTAADTIAQNKMTI.....QLRYLQTLTKISAQRNNTIVMEYPIEVAKHYMKK
sto-5b 313 .....
sto-5c .....
unc-24 283 PLVDLSDVPSTSAAGTSTDTPNIPSIDIDHLISVASLAMDEHLVRLIGRVFQINCKDTEP
stl-1 230 LASEAVQAERINVAKG.....EAEAVILKAESRAKAIERIALALEKDGGANAAGLTV
C42C1.15 223 ALIHQKRLLSEKETEKLLN.....QMEAESNLASERSKADAEFYKAQKQADSNKILLT
phb-1 270 LLNLQS.....
phb-2 278 YLNVTDKRR.....
mec-2a 370 TPPKVEEPPSLPKKIRSCCLYKYPDWVQGMVGSEGGGGHGHSHGGGGGGLGSSQGAFHPS
mec-2b 370 TPPKVDN.....NFAFPTH
mec-2c 295 TPPKVDN.....NFAFPTH
sto-4 279 AAA.....
sto-6 284 QGKHVLK.....
unc-1 284 DQ.....
sto-2 .....
sto-3 268 .....
sto-1 292 GSGGTSQNFPVQEMMN.....AALQSIQ
sto-5a 363 FHQKS.....
sto-5b .....
sto-5c .....
unc-24 343 ICIDLKHGSGSAYKGTSLNPDVVFETSLEVFGKILTKEVSPVTVYMNGNLKVKGSIQDAM
stl-1 282 AEQYVGAFGNLAKESNTVVLPAN.....LSDPGSMVS
C42C1.15 276 KEYLELQKIRAIASNNKIYYG.....DSIPQAF
phb-1 .....
phb-2 .....
mec-2a 430 QAGSGPSTTTTSGRPLLRSMREAQFHSAAPPISAPNQSQTSVSQLDPALLIR
mec-2b 384 KAGGIPSSS.....
mec-2c 309 KAGGIPSSS.....
sto-4 .....
sto-6 291 KMGALKYS.....
unc-1 .....
sto-2 .....
sto-3 .....
sto-1 315 RQDTVPATASSSGSRL.....
sto-5a .....
sto-5b .....
sto-5c .....
unc-24 403 QLKHLVERMSDWL.....
stl-1 314 QALAVYDSLSNKKK.....
C42C1.15 304 VMGTTQQTV.....

Figure 2:

a) stl-1

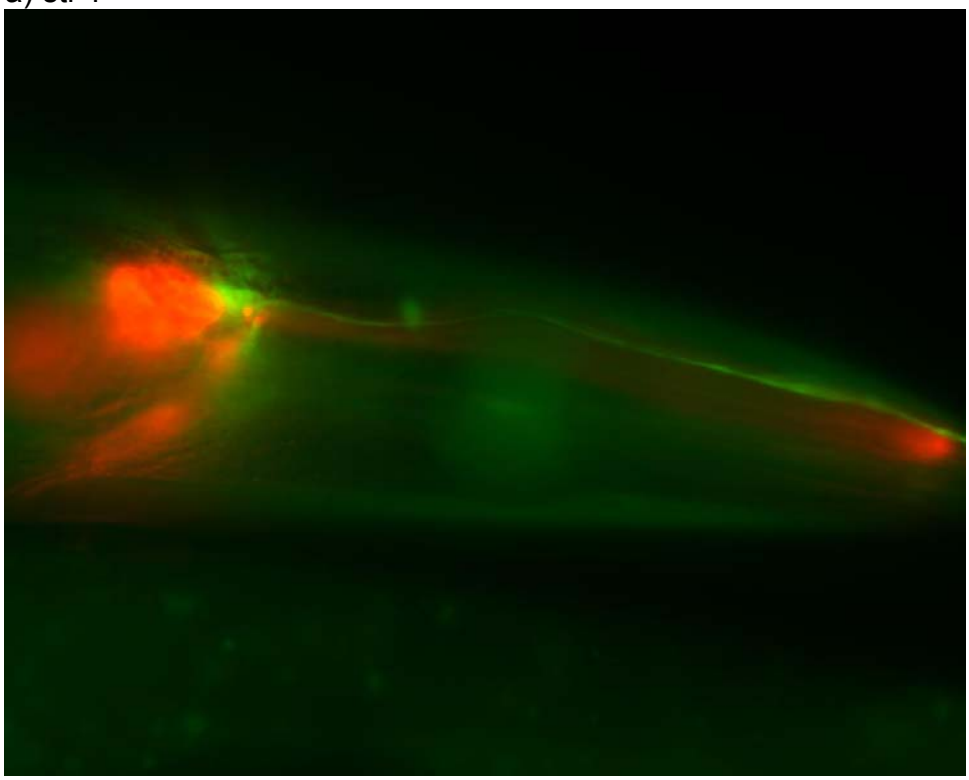

b) sto-1

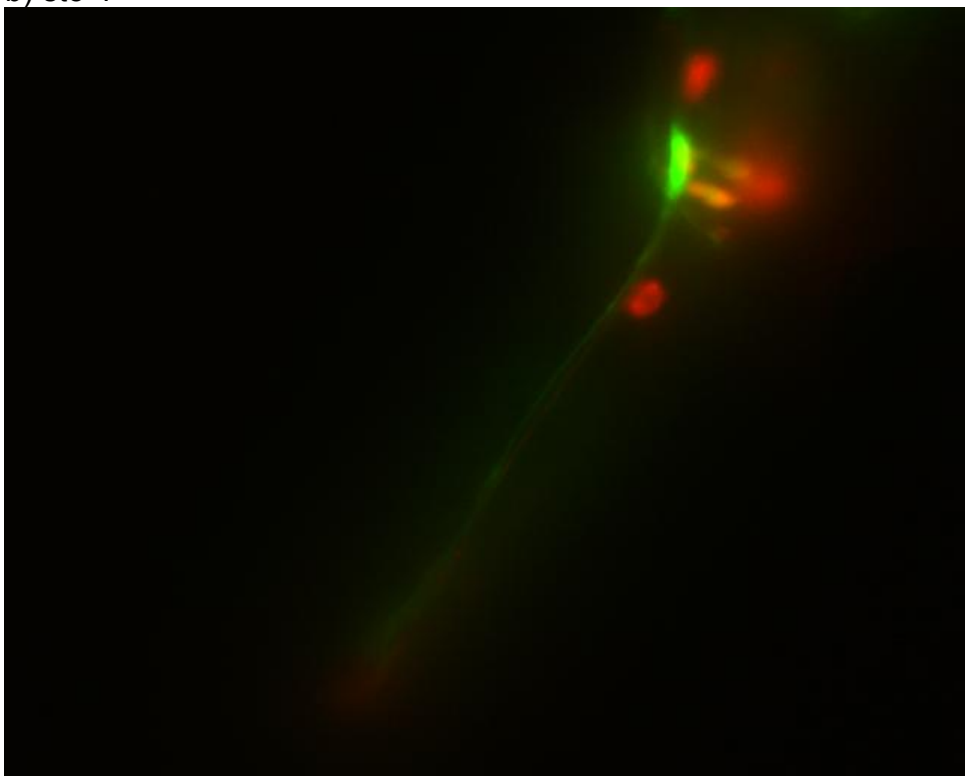

c) sto-2

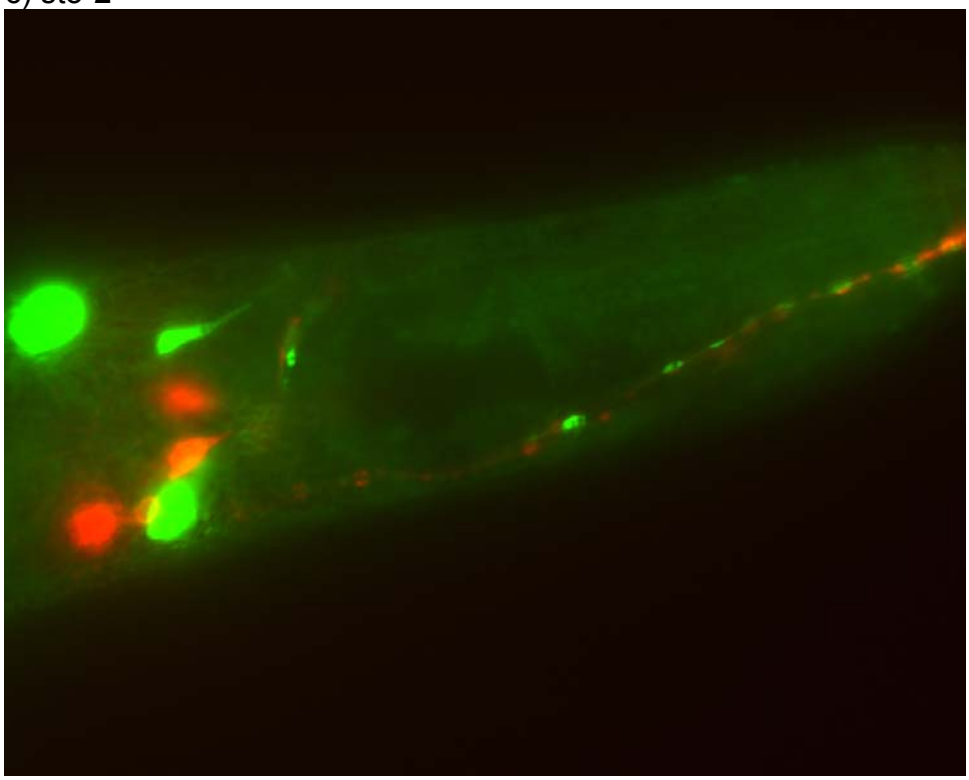

d) sto-3

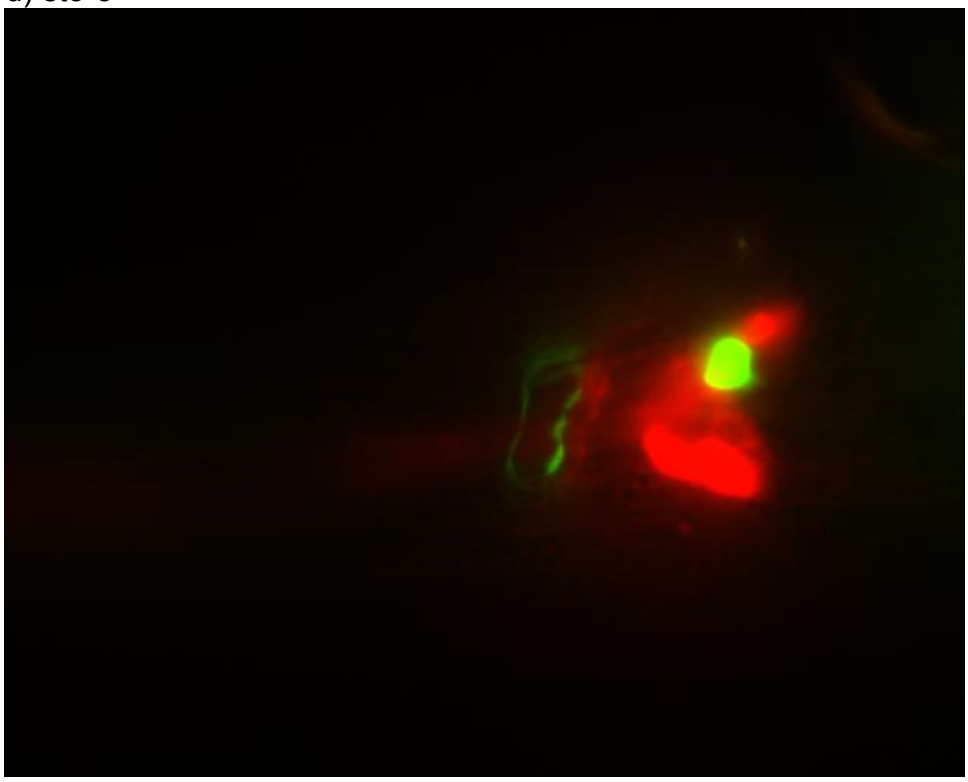

e) sto-6

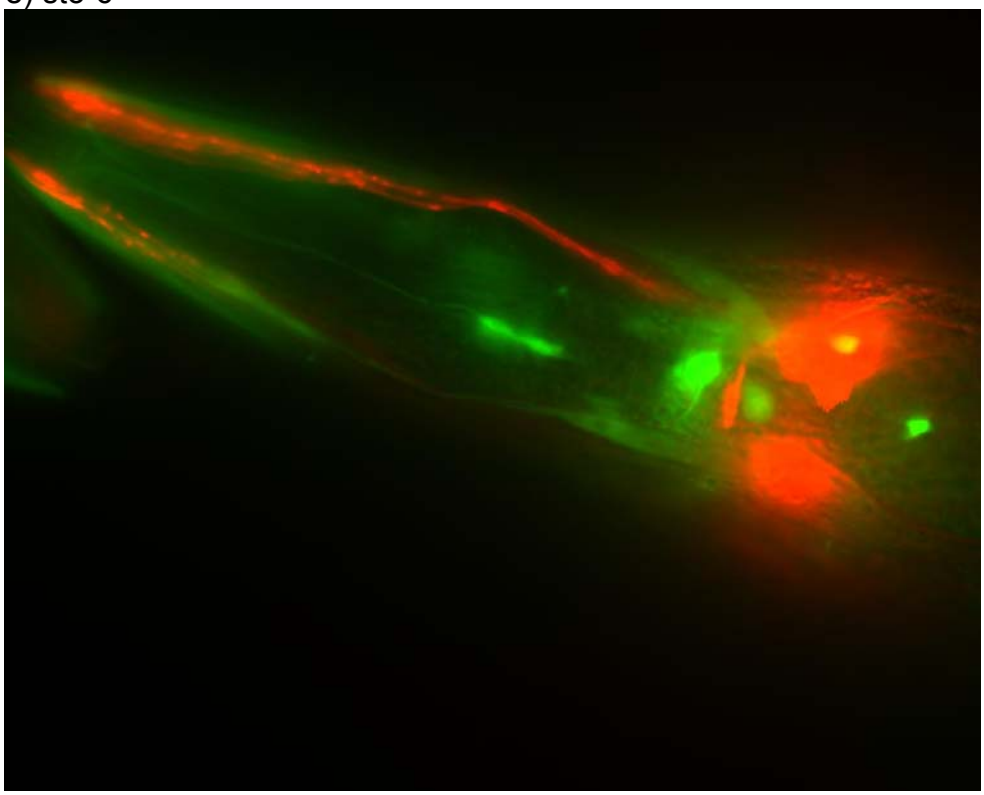

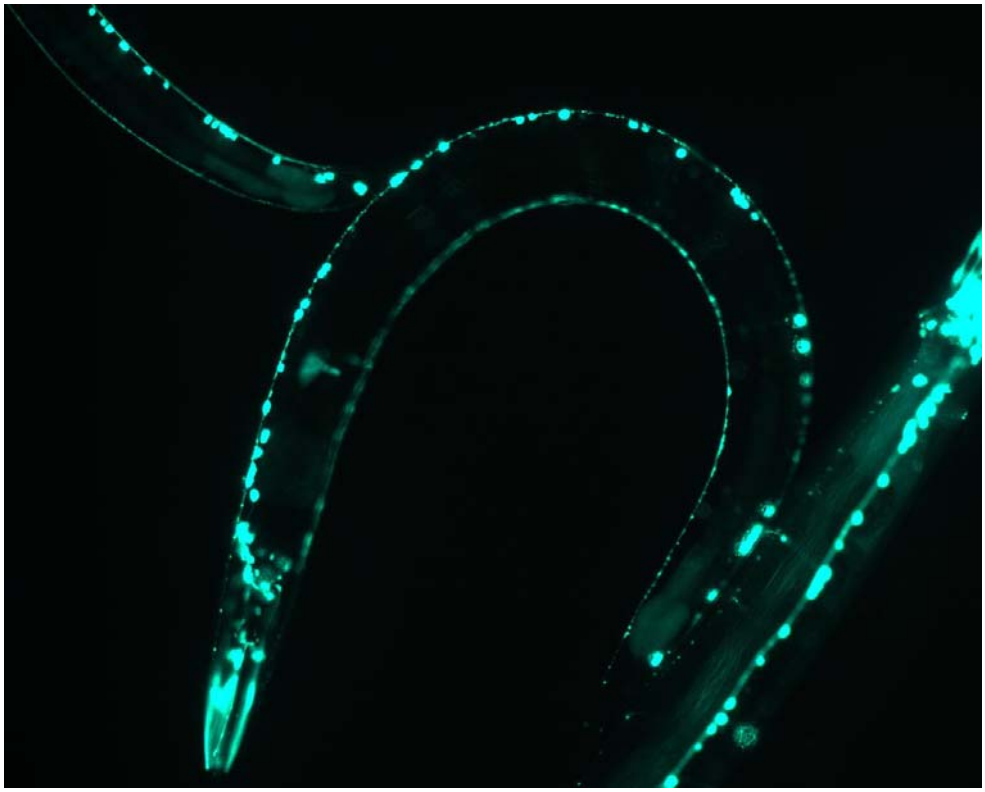

CURRICULUM VITAE

WeiHsiang Lee

Education:

09/2001~05/2009
Doctor of Philosophy, Neuroscience Program, Rutgers University & UMDNJ, Piscataway NJ
Thesis Advisor: Monica Driscoll, Ph.D.

09/1995~07/1997
Master of Science, Department of Life Science, National TsingHua University, HsinChu, Taiwan
Thesis Advisor: Ann-Shyn Chiang, Ph. D.

09/1991~06/1995
Bachelor of Science, Department of Physics, National TsingHua University, HsinChu Taiwan

Grants and Awards:

2005 Leathem / Steinetz / Stauber Summer Fellowship. Rutgers University
2003 Leathem / Steinetz / Stauber Summer Fellowship. Rutgers University

Work Experiences:

09/1999~07/2000
National Taiwan University Hospital, Department of Pathology, Taipei Taiwan
Position: Research Assistant
Supervisor: Chung-Wu Lin, M.D, Ph. D.

02/1994~06/1995
National Tsing Hua University, Department of Physics, HsinChu Taiwan
General Physics Laboratory
Position: Part-time Assistant

Publications:

Marios Chatzigeorgiou, Katie S. Kindt, **WeiHsiang Lee**, Monica Driscoll, William R. Schafer. The *C. elegans* DEG/ENaC channel MEC-10 functions in gentle touch and harsh touch mechanosensation (submitted)

John K. Everett, **WeiHsiang Lee** , Monica M. Driscoll, Gaetano T. Montelione. The NMR Structure of the N-terminal Domain of the MEC-4 Ion Channel Subunit in

Detergent Micelles Provides Novel Insights into Structure-Function Relationships (in preparation)

ZHANG, W., BIANCHI, L., **LEE, W.**, WANG, Y., ISRAEL, S., DRISCOLL, M. Inter-subunit interactions between mutant DEG/ENaCs induce synthetic neurotoxocity. Cell Death and Differentiation, 2008 15(11):1794-803.

Lin CW, Chang CL, Li CC, Chen YH, **Lee WH**, Hsu SM. Spontaneous regression of Kikuchi lymphadenopathy with oligoclonal T-cell populations favors a benign immune reaction over a T-cell lymphoma. Am J Clin Pathol. 2002 Apr;117(4):627-35

Lin CW, **Lee WH**, Chang CL, Yang JY, Hsu SM. Restricted killer cell immunoglobulin-like receptor repertoire without T-cell receptor gamma rearrangement supports a true natural killer-cell lineage in a subset of sinonasal lymphomas. Am J Pathol. 2001 Nov;159(5):1671-9.

Maciej A. Pszczolkowski, **Wei-Shiang Lee**, Hsin-Ping Liu, Ann-Shyn Chiang. Glutamate-induced rise in cytosolic calcium concentration stimulates in vitro rates of juvenile hormone biosynthesis in corpus allatum of *Diploptera punctata*. Molecular and Cellular Endocrinology 158(1999) 163-171.

Abstracts:

John Everett, **WeiHsiang Lee**, Monica Driscoll, Gaetano T. Montelione. The NMR Structure of the N-terminal Domain of the MEC-4 Ion Channel in Detergent Micelles Provides Novel Insights into Structure-Function Relationships. International Worm Meeting .2007

Monica Driscoll, Dewey Royal, Jian Xue, Beate Gerstbrein, Laura Bianchi, Gargi Mukherjee, Maryanne Royal, **Wei-Hsiang Lee**. Calcium permeability of death-inducing DEG/ENaC ion channel MEC-4(d). East Coast Worm Meeting 27. 2004

Laura Bianchi, **Wei-Hsiang Lee**, Dan Slone, Julie Y Koh, David M Miller III, Monica Driscoll. Towards understanding the role of the stomatin-like protein UNC-24 in the process of gentle touch sensation: evidence for functional interaction with the mechanosensory ion channel complex MEC-4/MEC-10. East Coast Worm Meeting 77. 2004

Laura Bianchi, **Wei-Hsiang Lee**, Julie Y Koh, Jian Xue, David M Miller, Monica Driscoll. Cellular localization of MEC-10, but not MEC-4, depends on the stomatin-like protein UNC-24. International Worm Meeting 466. 2003